EMPIRICAL STOPE DESIGN
AT THE
RUTTAN MINE, SHERRITT GORDON MINES LTD.

by

RIMAS THOMAS PAKALNIS

B. Engineering, McGill University, 1979
MASc, University of British Columbia, 1982

A THESIS SUBMITTED IN PARTIAL FULFILLMENT OF
THE REQUIREMENTS FOR THE DEGREE OF
DOCTOR OF PHILOSOPHY
IN
THE FACULTY OF GRADUATE STUDIES

DEPARTMENT OF MINING AND MINERAL PROCESS ENGINEERING

We accept this thesis as conforming
to the required standard

THE UNIVERSITY OF BRITISH COLUMBIA
August, 1986

In presenting this thesis in partial fulfilment of the requirements for an advanced degree at the University of British Columbia, I agree that the Library shall make it freely available for reference and study. I further agree that permission for extensive copying of this thesis for scholarly purposes may be granted by the head of my department or by his or her representatives. It is understood that copying or publication of this thesis for financial gain shall not be allowed without my written permission.

Department of MINING & MINERAL PROCESS ENGR.

The University of British Columbia
1956 Main Mall
Vancouver, Canada
V6T 1Y3

Date Sept 20 /86

ABSTRACT

This thesis evaluates the factors that influence the stability of large, open stopes for an existing mining operation. The Ruttan mine, a 6000 tpd base metal operation has mined by open stoping methods since 1979. This has resulted in a large data base of information which includes forty-three (43) stopes at various stages of extraction, thereby yielding 133 observations of:

Rock Mass Rating (footwall, hanging wall, ore)
Stope Dimensions (height, width, length)
Observed Dilution
Excavation Rates
Stope Configuration (isolated, rib, echelon)
Mining Sequence/Method

In addition, the observations were supplemented with in-situ measurements, structural mapping, stress and deformation monitoring and historical observation. It was concluded through numerical modelling, observation and measurement that the hanging wall and footwall of the individual stopes are in a state of relaxation, thereby enabling structural blocks to be released. This would generally be the case for most stope geometries whose major in-situ stress direction lies perpendicular to the long dimension of the opening. Consequently the critical parameters were quantified in terms

of their effect on dilution by employing multivariate analysis. The relationships derived were entirely confined to the Ruttan operation as they were empirically delineated and quantified.

The Ruttan operation is a multi-lensed orebody with individual stopes dipping at 70°. The following empirically derived relationships were found to correlate strongly with the observed dilution:

ISOLATED STOPES (61 observations) Figure 8.7a

$$Dil. = 8.6 - 0.09(RMR) - 13.2(Exp.Rate) + 0.0038(Area\ Exp.)$$

$r = 0.79$ $\hat{s} = \pm 3\%$

ECHELON STOPES (44 obs.) Figure 8.7b

$$Dil. = 10.3 - 0.13(RMR) - 14.8(Exp.Rate) + 0.003(Area\ Exp.)$$

$r = 0.83$ $\hat{s} = \pm 2\%$

RIB STOPES (28 obs.) Figure 8.7c

$$Dil. = 15.8 - 0.18(RMR) - 7.7(Exp.Rate) + 0.0026(Area\ Exp.)$$

$r = 0.80$ $\hat{s} = \pm 4\%$

where:

DIL(%) - refers to predicted stope dilution (tons waste/tons reserves)

RMR(%) - Rock Mass Rating of the critical wall contact, generally the hanging wall

Exp. Rate($'1000m^2$/mth) - refers to the rate at which the hanging wall is exposed (excavation rate/stope width)

Area(m^2) - refers to the exposed surface area of the hanging wall

r,s - refers to the correlation coefficient and the unbiased standard error of estimate respectively

The empirical relationships were related to stopes mined subsequent to the study and yielded errors of estimate ($\hat{s}$) of predicted dilution to within 2 - 4% of the observed dilution. The blast induced dilution was subsequently added to the predicted dilution. This value is difficult to estimate and is presently recorded as the dilution that is observed as the slot (initial cut) is being excavated. The design equations were based on a relatively large data base, considering, that the works of Bieniawski (1973) and Barton (1974) were based on 49 and 200 case histories respectively. It is suggested that the empirical methods of design outlined in this thesis be attempted at other operations where structural failure is the main factor contributing to stope dilution. This would augment the data base and extend its applicability. Parameters unique to Ruttan that were employed in establishing the data base are as follows:

hanging wall and footwall of all stopes are in relaxation
groundwater is not a factor
mean stope inclination = $68^{\circ} \pm 9^{\circ}$
mean stope dilution = 10% ± 6%
mean RMR = 56% ± 20%
mean exposure rate = $0.18m^2 \pm .09m^2$ (x1000)/mth
mean excavation rate = $2700m^3 \pm 1300m^3$/mth
mean span = 31m ± 13m
mean stope width = 15m ± 8m
mean stope height = 68m ± 20m
mean exposed surface area = $2250m^2 \pm 1120m^2$
mean stope depth = 360m ± 48m below surface
mean blast correction factor = 3% ± 6%

TABLE OF CONTENTS

CHAPTER FOUR

STRESS

CHAPTER FIVE

ROCK MASS CHARACTERIZATION

CHAPTER SIX

DILUTION

CHAPTER SEVEN

DATA BASE

CHAPTER EIGHT

STOPE DESIGN

CHAPTER NINE

APPLICATION

CHAPTER TEN

CONCLUDING REMARKS

LIST OF TABLES

LIST OF ILLUSTRATIONS

ACKNOWLEDGEMENTS

The author would like to express his appreciation to the management of Ruttan Mine for providing assistance, data, access to its mining facilities, financial support and review of the manuscript. Special gratitude is extended to Todd Madill and Bernie Haystead of the Geology Department at Ruttan for providing guidance and direction.

The author would like to thank Professor H.D.S. Miller for providing the atmosphere of learning, that he has helped create in the field of underground rock mechanics at the University of British Columbia. His guidance, encouragement and constructive criticism throughout the study was greatly appreciated.

The author is indebted to his committee members , Mr. Allan Moss, Dr. Ross Hammett, Professor C.O. Brawner and Dr. George Polling for providing invaluable guidance throughout the study.

Thanks is extended to Mr. Yves Potvin for assistance in conducting parts of the study.

The writer wishes to acknowledge the devoted support of his wife, Anna, particularly during the final two months. This thesis is dedicated to Mrs. Helen Pakalnis.

CHAPTER ONE

INTRODUCTION

1.0 Introduction

This thesis is the culmination of three years of study both on site at the Ruttan Mine of Sherritt Gordon Mines Ltd. and at the University of British Columbia . The objective of this thesis is to delineate and to quantify the factors that influence the stability of large, open stopes for an existing mining operation. This thesis will assess the governing hypothesis that the "Optimum Stope Geometry" can be quantified in terms of the rock quality, the extraction rate and the exposed surface area. Optimum is defined as that stope geometry that would yield a minimal acceptable dilution. Dilution is a measure of the quality of the design since it records the amount of hanging wall and/or footwall slough with respect to the stope reserves expected to be removed.

The Ruttan Mine, a 6000 tpd underground operation, is located in Northern Manitoba, 760 km. north of Winnipeg and 20 km east of the town of Leaf Rapids. The Ruttan copper-zinc orebody is a multi-lensed, steeply dipping (70) en echelon deposit. Individual lenses have a maximum strike length of 350m with widths varying from 7 to 61m. The mining method is open stoping with delayed backfilling which extends from surface to

860 m below surface. Stope spans at the Ruttan Mine were initially designed employing classical beam theory. Failures at the mine were found to be controlled primarily by structure, and this could not be explained by the previous homogeneous model. There exists no accepted design method of predicting stope spans in jointed materials. Beam theories, numerical models and empirical criteria have been employed in the past with some degree of success, however, the major drawback is that many of our classical design approaches have been based on the assumption that homogeneous, isotropic, elastic conditions do exist.

Forty-three (43) stopes at the Ruttan operation were analyzed in terms of the hypothesis stated previously. This data base represents 432 stope geometries and resultant dilutions as recorded by the mine. The prevailing stress conditions at Ruttan cause the hanging wall(HW) and footwall(FW) to be in a relaxed state. This is an important addendum to the above statement of hypothesis, since the effect on dilution from stress induced failure and the confinement of individual structural blocks is eliminated. It has been shown by Brady and Brown (1985) that a confining stress will retain blocks that would otherwise slough into an opening. It is not attempted in this thesis to quantify the critical confinement since stope walls at Ruttan will be shown to be within a zone of relaxation. The governing hypothesis will be empirically developed given the Ruttan data base.

The cases involved at Ruttan are for that particular stress regime which causes the rock mass in the vicinity of the ore contacts to be in a state of relaxation. The term "zone of relaxation" is employed rather than a zone of tension. While it is true that this region is unconfined, it may not be in pure tension. The reason being that in order for tensile stresses to be sustained in the rock mass , the rock mass must have a tensile strength which is generally assumed to be non existent. An ore contact that is in a high state of shear or compression will result in entirely different failure modes. The deviations that may occur from the Ruttan data base will be addressed and discussed, however, the thesis will generally be applicable only to a Ruttan type situation whereby:

- hanging wall and footwall of an individual stope is in a relaxed state
- stope plunge ranges between 60-70 degrees
- stope is not choke blasted ie. stope is voided prior to blasting next cut

This thesis is divided into relevant chapters which by themselves can stand alone, however, they are ultimately incorporated into a cohesive unit in formulating the solution to accept or reject the stated hypothesis. The chapters are as follows:

A) The Ruttan Orebody: This is a general chapter

summarizing the ore geometry, lithology, stope configuration, mining method and history.

B) Stope Design Methodology: This chapter outlines the complexity of the Ruttan deposit with respect to arriving at a methodology for stope design. It also summarizes a literature search that assesses the state of the art of a)stope design in jointed materials and b)of existing rock mass classification systems. A survey conducted by the author which reviews the present state of stope design as is practiced by open stope operators throughout Canada is summarized. This questionnaire was sent to all Canadian base metal open stope and room and pillar operators whose production exceeded 1000 tpd. A 58% response was achieved which represented twenty-two (22) mines, fifteen (15) of which practised open stoping methods. This survey was conducted in order to assess the present state of stope design in Canadian operations.

C) Stress : This chapter assesses the influence of stress on the stope geometries at Ruttan. Individual stopes are modelled by employing a two dimensional "boundary element" numerical code and a post-processor developed for this study. Nomograms are employed in estimating the stresses given a particular stope length/width dimension. A two dimensional analysis is employed and compared to observational and quantifiable measurements made throughout the mine. A three

dimensional boundary element program, modified for the Ruttan operation, compares the validity of modelling stopes at Ruttan by the 2D process. This chapter describes a methodical approach to the estimation of the in-situ stresses at Ruttan. The results were subsequently verified by conducting CSIRO hollow inclusion overcoring measurements.

D) Rock Mass Assessment: The Ruttan operation, including all forty-three (43) stopes, has been assessed in terms of a suitable rock mass descriptor. A selection of the most suitable classification was chosen upon identifying the relevant rock quality parameters with respect to the Ruttan data base. The most critical parameters were evaluated in terms of resultant dilution. This is the **"control"** parameter that will enable the hypothesis to be quantifiably assessed. All development areas, mined stopes and future mining areas were assessed a Rock Mass Rating.

E) Dilution: This parameter is a measure of the quality of the stope design. It is a parameter that is recorded by most open stope operators in Canada (Questionnaire, 1985). It is a measure of the degree of wall slough with respect to the expected stope reserves mined. Various definitions exist and are summarized in this chapter. These definitions are derived from the survey conducted previously. Dilution is recorded for all mined stopes at Ruttan at various stages of extraction.

These are statistically correlated to the rock quality parameters identified as critical. It will form the test for hypothesis acceptance or rejection. Dilution is a quantifiable assessment of stope design,however it is assessed in most instances by observation.

F) Data Base: Upon the assessment of the significant factors affecting dilution, a data base is derived for the individual mined stopes at Ruttan. The data base is comprised of stope dimensions (span, height, width), stope configuration, stope depth, inclination, extraction rate, resultant recorded dilution, rock mass rating of the critical wall contact, and observed damage due to blasting. This data base is comprised of 43 mined stopes yielding 432 recorded stope geometries which were subsequently averaged into 133 case histories.

G) Stope Design Assessment: The best fit parameters are incorporated through single/multiple correlation testing. Linear,planar,linear hyper-surface, and quadratic curved lines and surfaces are fitted to the relevant parameters in order to assess the level of acceptance of the proposed hypothesis. Statistical assessment in terms of multiple and partial correlation coefficients, levels of significance, and confidence limits are determined for the best fit surface. It is concluded at this stage that stress is not significant in terms of dilution since numerical modelling indicated that the

hanging and foot wall of individual stopes at Ruttan are in a state of relaxation, thus resulting in structurally controlled failures. This statement will be further reinforced through measurement and observational approaches.

H) Application: This chapter analyzes the relationships derived from the existing data base to stopes subsequently mined. A brief comparative analysis is made between the most prospective existing methods of stope design and the empirical method proposed in this thesis.

I) Conclusions: The acceptance or rejection of the following hypothesis is made:

Optimum Stope Geometry = f(Rock Quality, Extraction Rate, Exposed Surface Area)

CHAPTER TWO

THE RUTTAN MINE

2.1 Introduction

In order to understand the parameters involved in developing a method of stope design for the Ruttan orebody, it is important to know the history, geology, mining practice and the mine geometry. Studying the influencing factors requires that the methodology be integrated into the overall mine regime. This involves, in addition to numerical and analytical analyses, a coordinated field effort drawing from all the available information and re-analyzing that information from a different perspective. This chapter describes the first stage of developing a data base which will outline the associated geometric complexities associated with the Ruttan orebody.

The Ruttan mine is located in northern Manitoba, 760km north of Winnipeg and 20km east of the town of Leaf Rapids, Figure 1.1. The Ruttan copper-zinc orebody is a multi-lensed, steeply dipping (70°) en echelon deposit. Individual lenses have a maximum strike length of 350m and widths varying from 7 to 61m. The mining method practiced is blasthole open stoping with delayed fill. Production, Figure 1.2, commenced by open pit in April of 1973 and continued until Dec, 1980. The pit at this time was 1000m long, 600m wide and 200m deep. The Ruttan

orebody is considered to be open at the 860m level (below surface). The underground operation was developed to 430m below surface and is commonly referred to as the "Upper Mine". Production from the Upper Mine commenced in March, 1979 and is presently at 6000tpd. The removal of the entire surface crown pillar in the summer of 1988 will complete the mining of the Upper Mine. Delineated reserves exist to the 860m level yielding tonnages sufficient for mining until 1992 at a production rate of 8000tpd. The "Lower Mine" is defined as that portion of the operation that exists between the 430m level and the 860m level. In October of 1985 mining of the Lower Mine commenced while the Upper Mine was phasing down.

A significantly large data base of information is available from the Upper Mine, containing approximately 56 stopes of which 48 have been mined at the time of the completion of this study. It was decided to terminate the data gathering stage in February 1985 with the subsequently mined stopes (8) serving to reinforce or disprove the proposed formulated hypothesis.

2.2 Geology of the Ruttan Deposit

The Ruttan Orebody is a copper-zinc rich, exhalative, massive sulphide deposit contained within a sequence of Proterozoic volcanic rocks and their derived sediments. Ruttan is located within the Churchill Geologic Province of Manitoba,

Figure 2.3. This geologic province is characterized by two east-west trending volcanic arc belts, the Wasekwan Group to the north and the Amisk Group to the south, separated by a wide sedimentary basin termed the Burntwood River Suite, Figure 2.3. This is particularly important in relating the orogeny of the deposit to its present configuration and stress regime. The Ruttan deposit is Aphebian in age and is interpreted to be a synclinal deposit associated with island arc development. This is graphically shown in the subsequent section concerning the tectonic history of Ruttan. The Wasekwan Group consists of a conformable sequence of volcanic flows, tuffs, agglomerates, breccias and volcaniclastic sediments. Overlying this package of rocks are the shallow water sediments of the Sickle group. Archean basement borders the Wasekwan and Sickle Groups to the north.

The volcanic rocks of the Wasekwan and Sickle Groups have been considerably altered during regional metamorphism to lower amphibolite, amphibolite and greenschist facies. Basic volcanic rocks and sediments have been converted to schists and banded gneisses locally characterized by epidote, hornblende, biotite, chlorite, garnet, staurolite, cordierite and andalusite alteration.

2.2.1. Local Geology

The Ruttan mine is thought to be a geosynclinal deposit associated with island arc development. This is where a plate of lithosphere is slowly plunging downwards into the mantle. The volcanism that builds the volcanic mountains is presumably caused by the melting of the downgoing plate, Figure 2.4. Therefore, the Ruttan deposit is assumed to have been formed along a flank of a large volcano. This volcanic arc trends east-west as shown in Figure 2.3. A schematic section, drawn perpendicular to the trend of the island arc, is employed to describe the sequence of events leading to the formation of the Ruttan deposit, Figure 2.5. It is best summarized as follows:

- Ruttan was formed beneath sea level as a result of magma being vented within a granitic host.
- Basalt flows were deposited then subsequently overlain by a sequence of volcanically derived sediments. Pillow structures are found within the basalt unit indicating that this unit was emplaced at a rock-water interface. The footwall volcaniclastics are as a result of acid volcanism and its subsequent erosion. The rock is quite uniform, thinly to thickly bedded, relatively unaltered and composed of fine grained, intermediate, clastic fragments. This unit grades into the footwall altered volcaniclastics which is characterized by increased alteration and the presence of cordierite, staurolite

and magnetite.

- The mine rhyolites (quartzites) follow in sequence. They are the products of erosion from the flanks of the volcano. These rhyolites were interbedded with channelways of mud deposits. This is a felsic rock which was subsequently replaced by copper and zinc rich solutions originating from the mineralized vent. The mud zones were hydrothermally altered to chlorite and chlorite-talc schist on both the footwall and hanging wall contacts of the ore lenses.

- Overlying the mine rhyolite is the exhalite horizon which was formed as a precipitate resulting from the mixing of the hydrothermal fluids and seawater on the sea floor. The zinc rich lenses of the Ruttan deposit are found in the Exhalite unit and are characterized by pyrite-sphalerite-silicate and chert banding. Well bedded detrital sediments dominate the upper portions of this horizon. The sulphide lenses formed are sedimentary in formation unlike the igneous origin of the lenses within the mine rhyolites.

- Finally, low (sediments) and high energy (turbidites) volcanically derived deposits settled over the exhalative horizon. It (PM unit) consists of interbedded graywackes and volcanic(erosion) derived conglomerates. Subsequent deformation was in the form of shearing of the weaker sulphide deposits and the further intrusion of a system of dykes throughout the above horizons.

The above sequence of events are sedimentary in nature

resulting in flatly dipping deposits. It is postulated that, after the deposition of the Ruttan deposit, the Churchill province had subducted underneath the Superior province. This tectonic activity resulted in the inclination of the ore body to that shown in Figure 2.6. The combined tectonic activity of the initial island arc development and the subsequent subduction resulted in a late phase of regional metamorphism to influence the Ruttan deposit. This late phase of metamorphism converted the basic volcanic rocks to hornblende, plagioclase schists and banded gneises with variable amounts of epidote, biotite and chlorite. The sediments were converted to biotite, muscovite,quartz schists and gneisses. An alteration zone is associated with the Ruttan deposit which is dominated by a bifurcating shear zone. The shear zone at Ruttan is oriented at N70° E dipping at 68° SE. It is up to 30m wide and bifuricates into three main shear zones: Art's Fault, North Wall Shear and East Shear, Figure 2.7. The overall effect of the shearing was to significantly change the geometry of the ore lenses and alteration zones. The individual mine rock units will be further described in the context of "rock masss characterization", Chapter 5. Figure 2.8 is a geologic plan of the Ruttan area.

2.3 Orebody Geometry

The Ruttan orebody comprises nine ore lenses all

subparallel in attitude and echelon in nature,Figure 2.7. The orebody strikes N70°E, dips 70°SE and plunges 70°to the east. The maximum dimensions of the ore zone are 120 metres wide by 700 metres long. An open pit lies immediately above the underground workings to a depth of 210 metres.

The geometry of the lenses is such that to the west of the east shear, five major lenses form a zone with a strike length of 350m at the 260m level (below surface) which narrows to 200m at the 430m level. These are known as the "west lenses" and the width of the individual lenses range from 7 to 35m. The west lenses bottom out at the 660m level whereas the "east lenses" continue to a yet unknown depth. These lenses lie east of the east shear and are comprised of four lenses. Generally, the ore contacts are irregular both in plan and section and pinch and swell down dip, thereby enclosing narrow bands of waste,Figure 2.9,2.10. Consequently, in order to properly delineate the stope geometry , diamond drilling is conducted on a 15m by 15m pattern along the ore contact, Figure 2.11. The complexity of the ore geometry is indicated by Figure 2.12. Individual stopes are defined by draw level, a letter designating the lens and a number defining the stope within that lens. An example is 320-11B. This stope is drawn off the 320m level, is a "B" lens as defined in Figure 2.9 and is stope number "11" within that lens. Generally, a stope having a similar number is located either in the footwall or hanging wall of the preceding stope. The "B" lenses are located in the

footwall of the "C" which are located in the footwall of the "D" lenses. This terminology will be useful in identifying areas of the mine. Stope numbers increase from west(7 to 16) to east(17 to 22).

2.4 Mining Practice

The Ruttan orebody is a complex arrangement of ore lenses. These lenses are located in close proximity to each other and join in certain locations. Such complexity and irregularity of ore outlines require that mining of the individual lenses be carried out in a predetermined sequence in order to ensure maximum ground stability. The stoping method is blasthole open stoping with delayed fill. Two variations of open stoping are used. In one, conventional small diameter (51mm) holes are drilled from levels spaced at 30m vertical intervals. In the second, large diameter (165mm) holes are drilled from levels spaced at 60m vertical intervals. The blasting sequence in these "large diameter stopes" is a combination of vertical crater retreat and slash.

Stopes and pillars are laid out on a regular pattern and resemble the dimensions outlined in Figure 2.13. In general, stopes and pillars are approximately 30m and 15m in length respectively. Pillar recovery is an integral part of the normal stoping progression. When a stope is mined out, it is planned to be backfilled using classified mill tails. The adjacent

stope is mined back to the predetermined pillar line, then the remaining pillar is blasted into the open stope leaving a 6m remnant of ore to retain the fill. In practice, this is generally not the case since the filling cycle is well behind schedule, thereby not enabling the filling of stopes prior to the mining of the adjacent stope. Consequently, the rib pillar is blasted to the 6m remnant without the benefit of fill. After removal of the broken pillar ore, the stope and pillar void is then backfilled with mill tails. The fill forms the draw level for the next mining lift.

Drawpoint levels are established at 60m vertical intervals. Active draw levels are currently the 260m, 320m, 370m and 430m levels. Due to the irregularity of the ore lenses, it is sometimes necessary to locate additional drawpoints on levels other than the main levels. This consequently results in stope heights being less than 60m. Intermediate drill levels are driven between the main levels creating a 30m level interval in stoping areas where small diameter blastholes are utilized. All production blasting is with ANFO and packaged water gels. Non-electric delays are used to effect proper sequencing of initiation.

2.4.1 Stoping Method

Generally, transverse open stoping is employed at Ruttan leaving a remnant pillar as shown in Figure 2.13. Mine practice

dictates that where the ore width exceeds 30m, a longitudinal pillar is left, thereby ensuring that the stope width does not exceed 30m. These values have been determined empirically through trial and error.

As previously indicated, the Ruttan operation employs two variations of open stoping. Figure 2.14 depicts the conventional method of open stoping employing 51mm diameter holes. Initially, the undercut is silled out for a vertical height of 12m from footwall to hanging wall and remnant to remnant pillar. The 2m x 2m slot is mined either conventionally or raise bored to a 12m height above the upper drill level. In addition to slot development, it is required to develop a footwall and hanging wall drive which are normally located at the ore contact. It is the practice at Ruttan that a single drill drive be driven through the centre of the stope if the ore width does not exceed 15m. Similar development occurs on the intermediate level. The 2m x 2m slot raise is subsequently slashed to 3.7m x 3.7m for the full stope height. Subsequently the slot is slashed full width from hanging wall to footwall. Rings are then slashed into the void for the full stope width on either side of the slot, assuming access exists on either side. Normally, the rings that are blasted from the intermediate level correspond to a similar set of rings on the upper drill level, thereby ensuring that a continuous void extends from the draw level to 12.2m above the upper drill drive. The stope is generally drilled off prior to the

commencement of slot blasting. The upholes on the intermediate and draw level are required to ensure that proper "inter-leaf" coverage between drill holes occurs between levels. Normally, the rings are spaced at a spacing of 1.5m and a toe burden of 2.1m, and only a sufficient number of holes are drilled for that particular blast.

The second method, Figure 2.14, involves a modified form of "vertical crater retreat" and slash. Large 151mm diameter holes are employed, thereby allowing longer holes to be drilled by using in the hole hammer type of drill equipment. This enables the deletion of intermediate levels. Similarly, an undercut is taken as with the conventional method. The "vcr slot" is drop raised from the upper drill level to a 3.7 x 3.7m raise. The slot is not necessarily taken through to the upper level prior to production blasting. The production blasting requires the widening of the slot to 6.1 x6.1m and subsequently slashing full stope width from hanging wall to footwall. The main tonnage is achieved through slashing decked charges into the void. The decked rings are blasted full stope width as in the conventional method described previously. The rings are spaced 3m apart with a toe burden of 4.2m. The slot, therefore, is the only part of the stope that is advanced employing the "vertical crater retreat" method of mining, which is characterized by spherical charges (6:1=L/D).

Deviations of the above methods lie in the following:

- The initial slot is bored by machine from the draw

level to the upper drill level.

- The VCR-Slash method may have the slot entirely complete prior to commencement of slashing. Subsequently, long parallel rings will be blasted for the full height of the stope.

The stope is ultimately filled to 12.2m above the upper drill level. Upon fill consolidation, the previous upper drill drive will form the draw level for the next lift. The draw cones are formed out of the fill. The sequence of extraction for an individual stope is as summarized by Figures 2.15,2.16. The extraction sequence for an individual lens is generallly from the hanging wall lens to the footwall and from the center of an individual lens to the extremities. This again is not generally followed since production requirements necessitated changes to individual mining areas. The significance of mining sequence will be analyzed in Chapter 4 (Stress)

2.5 Observations/ Conclusions

This section was included to document the difficulties that will present themselves in trying to categorize the individual stopes into a data base, or to even commence analyzing by a suitable numerical code. The following categories of stopes generally occur at Ruttan, Figure 2.17:

- isolated
- rib: stopes exist along strike
- echelon: stopes exist along dip

The variance in mining sequence, Figures 2.15,2.16 is not systematic or methodical but is primarily a function of production requirements. This is the case in most mining operations in Canada. The controlled experiment that one would like to achieve for a thesis now is starting to accumulate many variables. An experimental stope would yield quantitative and qualitative observations. The difficulty arises in extrapolating the results to other areas of the mine exhibiting different rock qualities, stope configurations and mining practices. The data base would have to be enlarged, which would mean an "experimental mine" rather than an individual stope would have to be instrumented. At the time of the study, the Upper Mine was in an advanced stage of extraction and had reserves for only three more years. A test stope, that would be isolated from adjacent workings, was not available. A further restriction was that it takes approximately ten (10) months for a stope to be completely excavated and another seven months to fill. The approach taken was to analyze the existing data base and to derive, if possible, critical parameters and areas to be further studied. A rock mechanics program at Ruttan had been implemented from inception which basically included stress gauges and extensometers. Stopes, as they have been extracted, were evaluated in these terms with minor success. A program has

now been implemented at Ruttan where an isolated stope is being monitored in the Lower Mine to prove or disprove the theories and ideas brought forth in this thesis. The stope will be mined from October 1985 to October 1986 and the results will be analysed. This thesis is the first phase of the development of a methodical approach to assessing the parameters that are of particular significance to stope design at Ruttan.

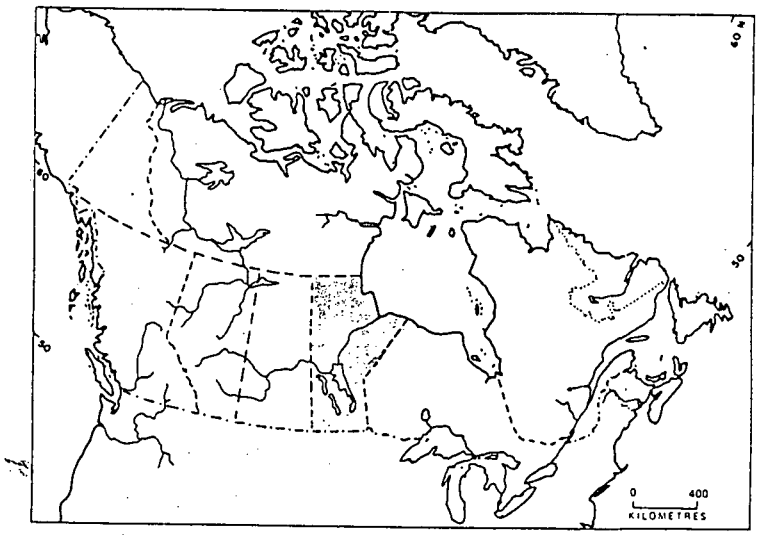

Map of Canada

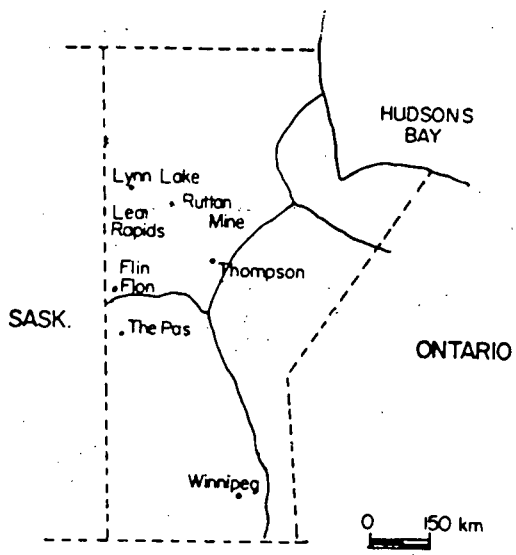

Map of Manitoba

Figure 2.1: Location Map

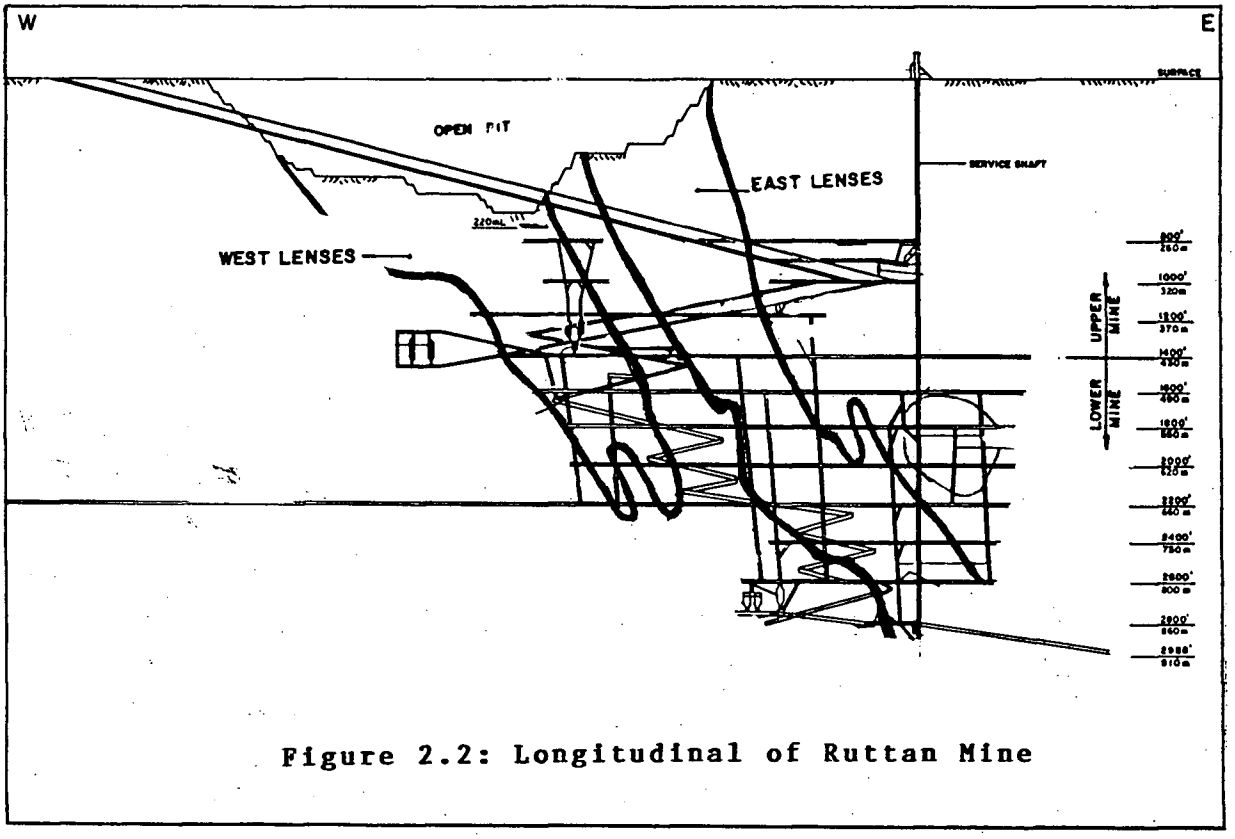

Figure 2.2: Longitudinal of Ruttan Mine

(Speakman et al, 1976)

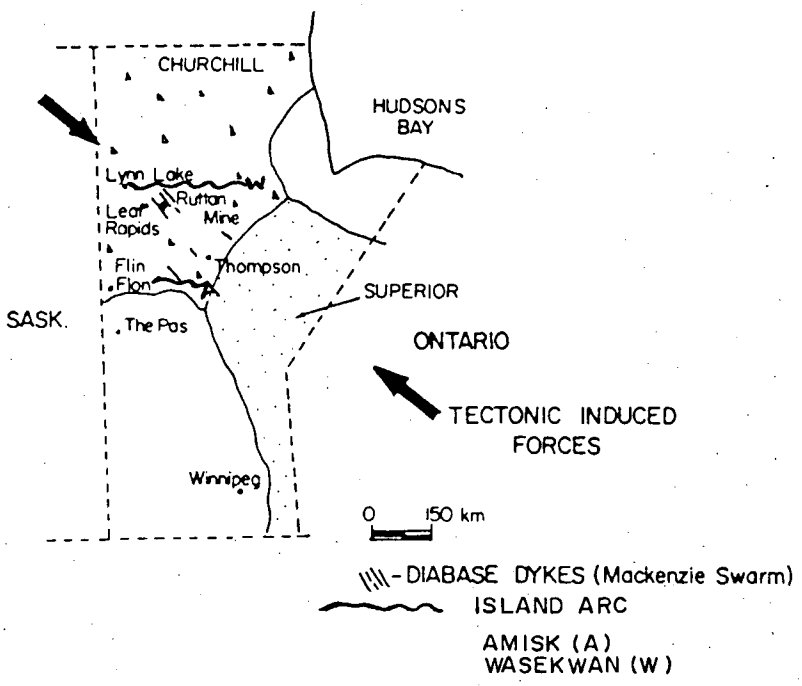

Figure 2.3: Regional Geology

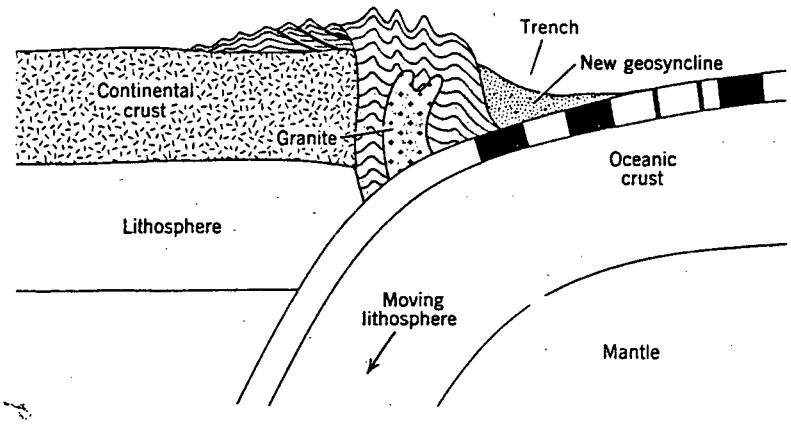

Figure 2.4: Island Arc Development

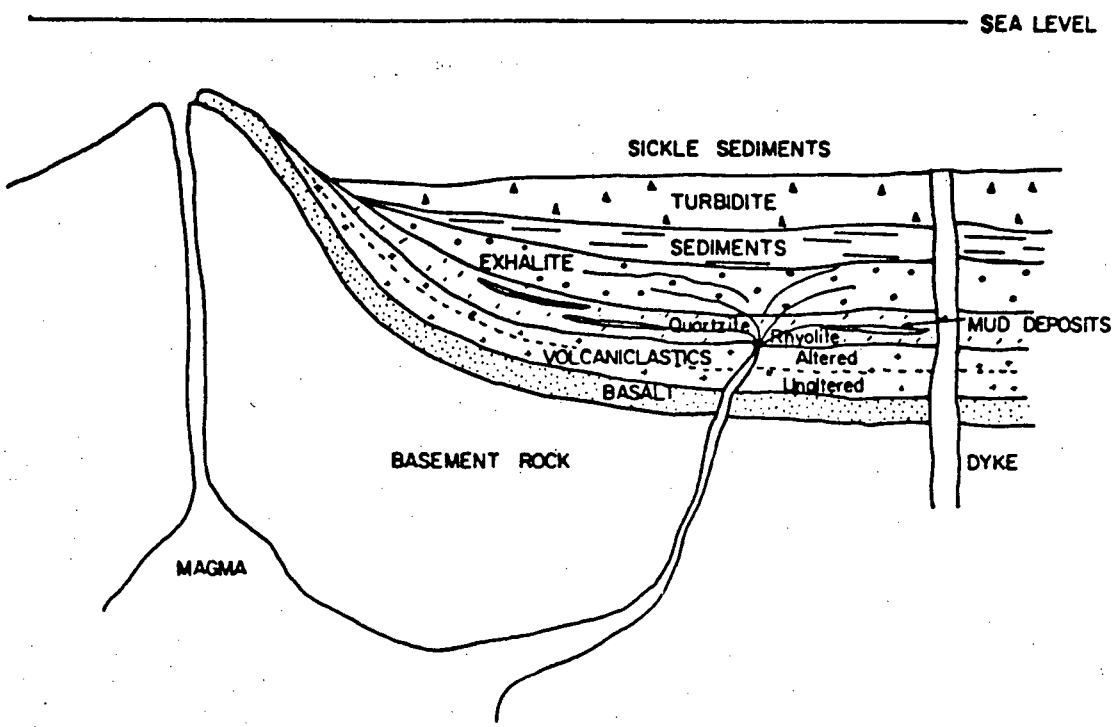

Figure 2.5: Schematic Section Showing the Formation of the Ruttan Deposit

(Speakman et al, 1976)

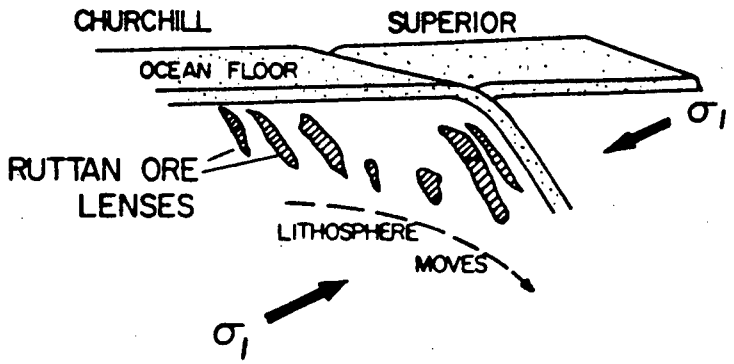

Figure 2.6: Tectonic Evolution

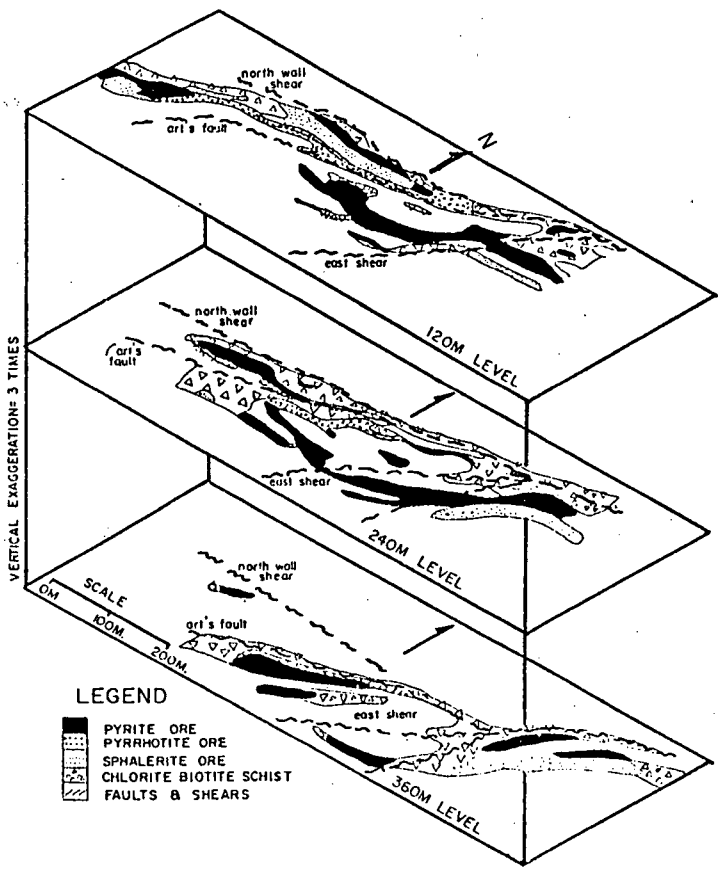

Figure 2.7: Isometric Diagram - Ruttan Deposit

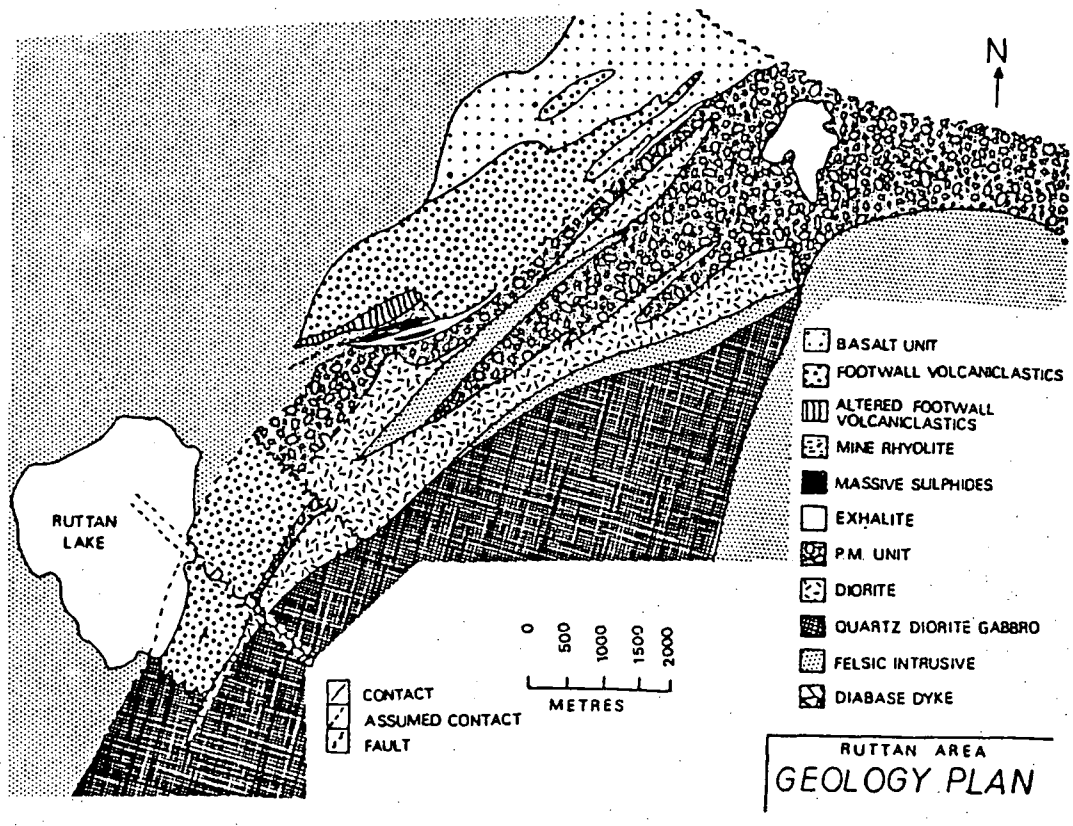

Figure 2.8: Local Geology

(Speakman et al, 1976)

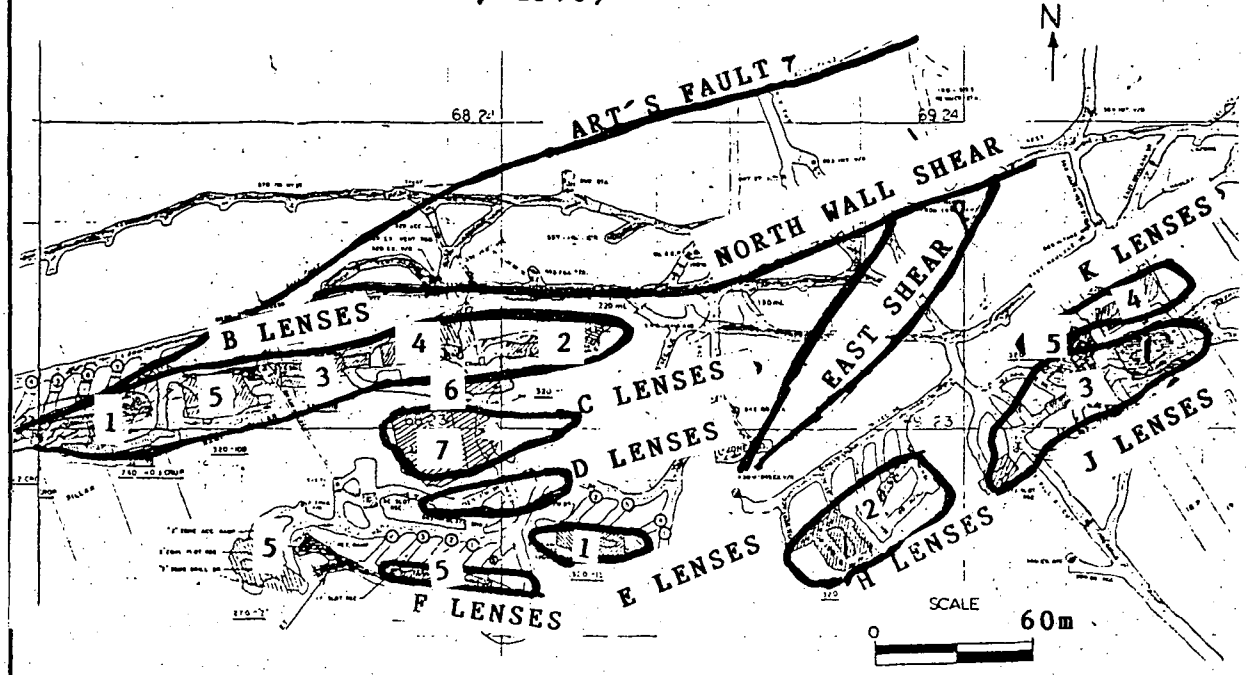

Figure 2.9: Plan of Ore Lenses - 260m Level

- Numbers Refer to Sequence of Extraction

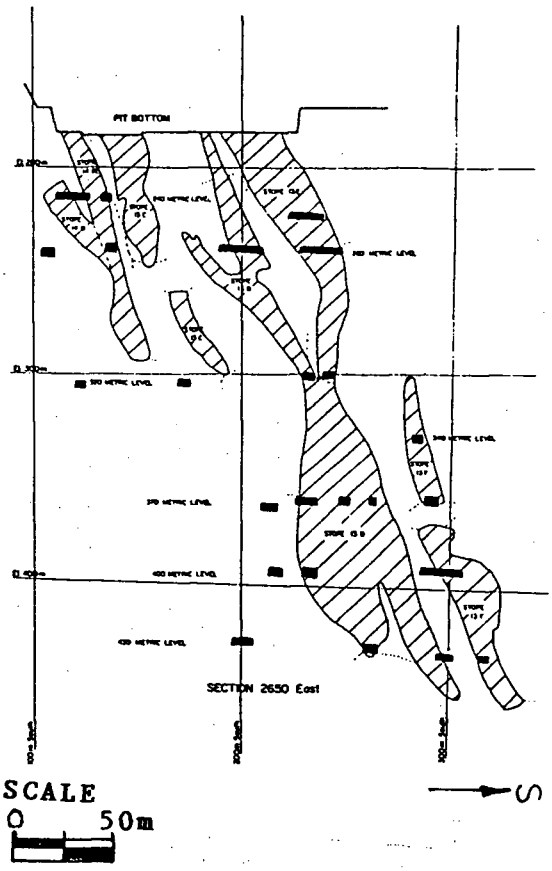

Figure 2.10: Typical Section - 2650E

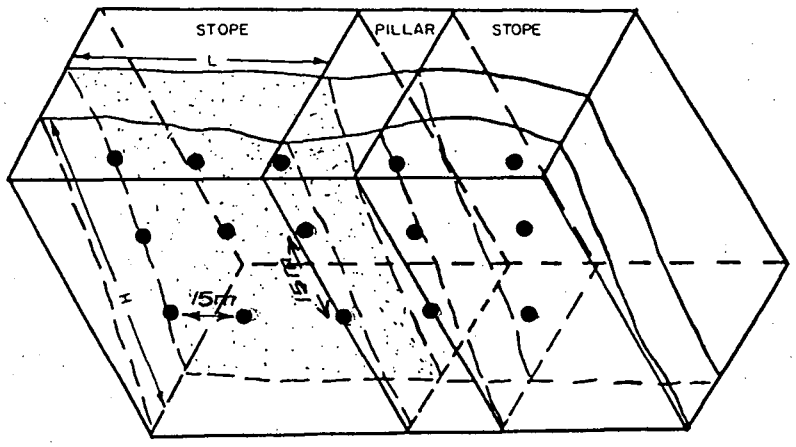

Figure 2.11: Ore Delineation Pattern

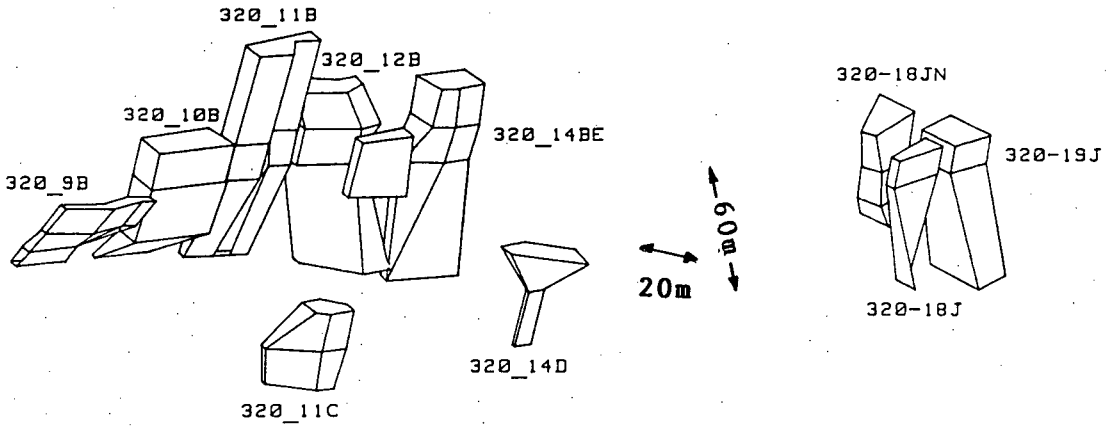

Figure 2.12: Isometric - 320m Level

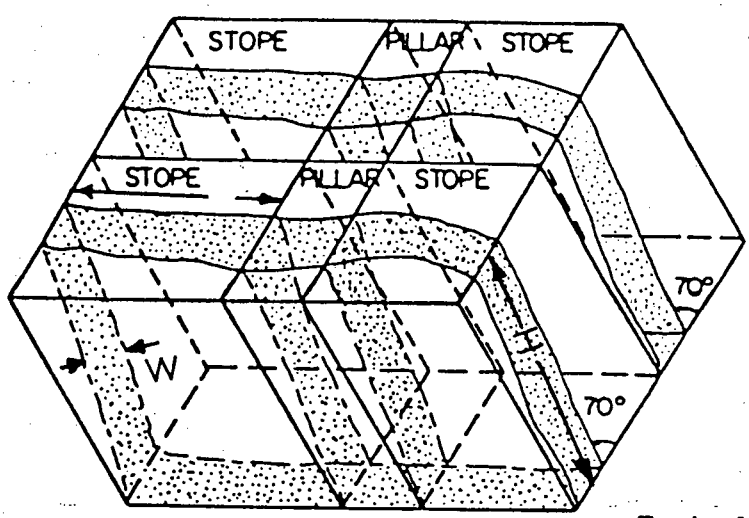

Typical Stope Dimensions

Stope Height (H) = 40-100 m
Stope Length (L) = 40-50 m
Stope Width (W) = 6-30 m
Rib Pillar Length = 6 m

Figure 2.13: Typical Stope Dimensions

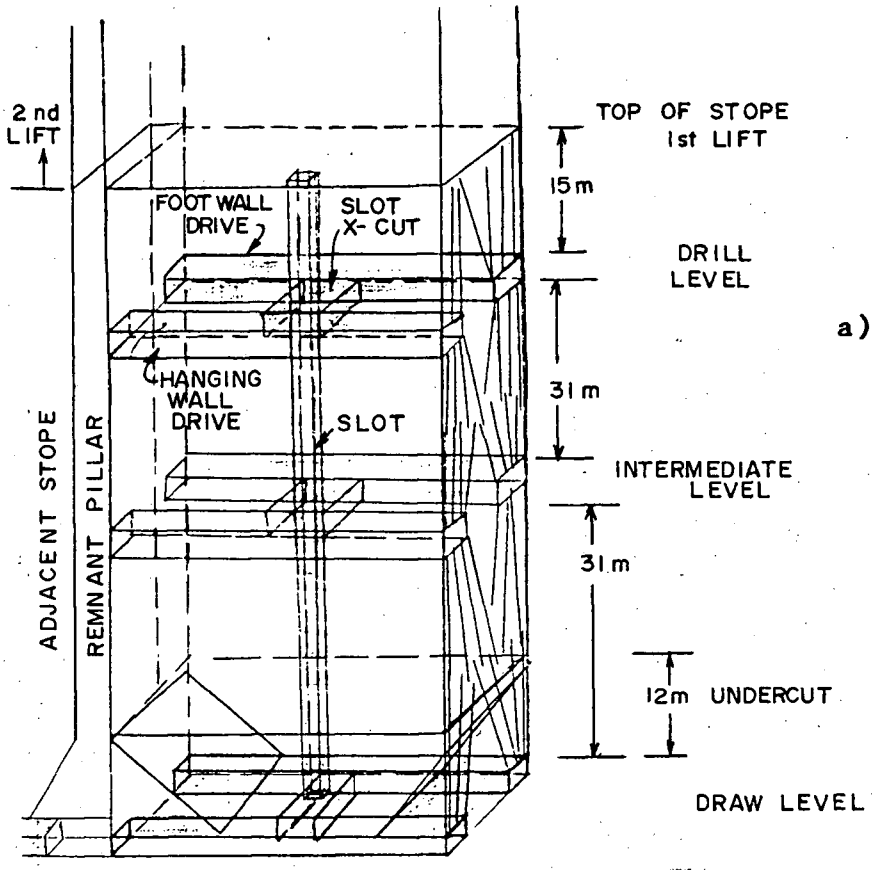

a) SUB-LEVEL (51mm)

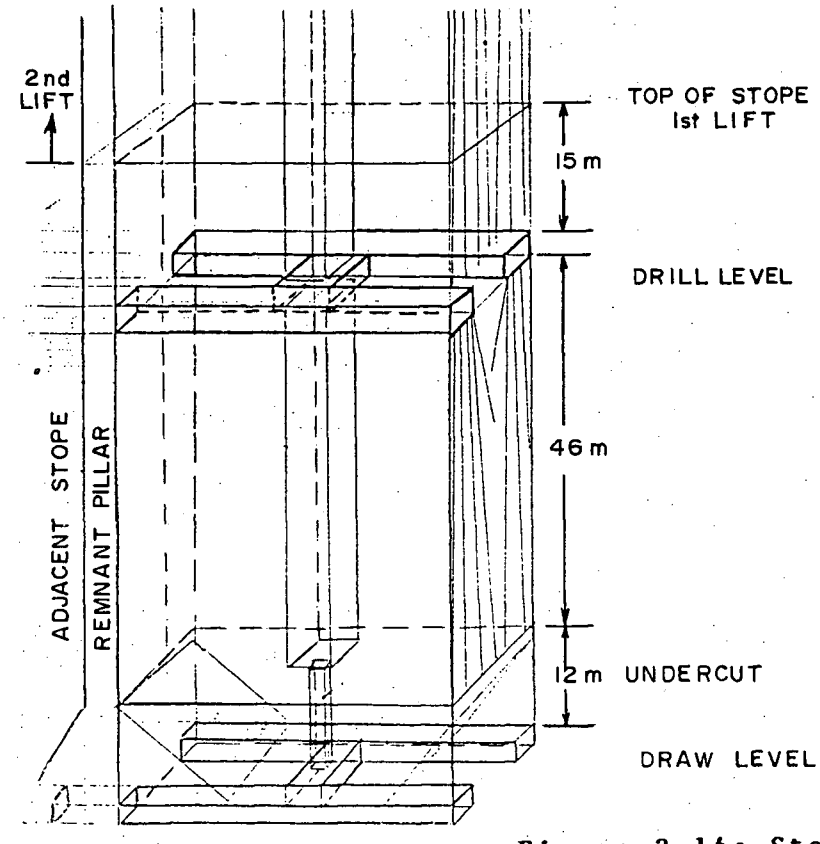

b) VCR-SLASH (165mm)

Figure 2.14: Stoping Method

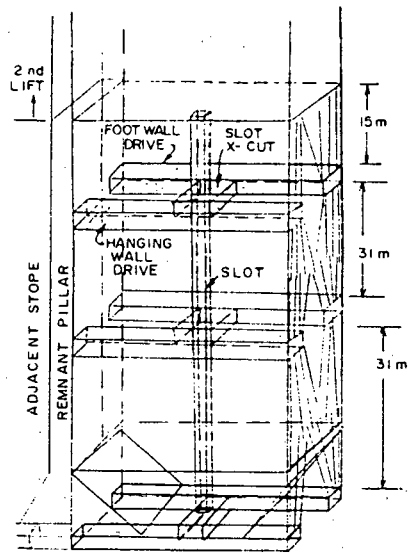

1) Initial Development
- Drill Drives
- Slot X-Cut
- Slot Raise

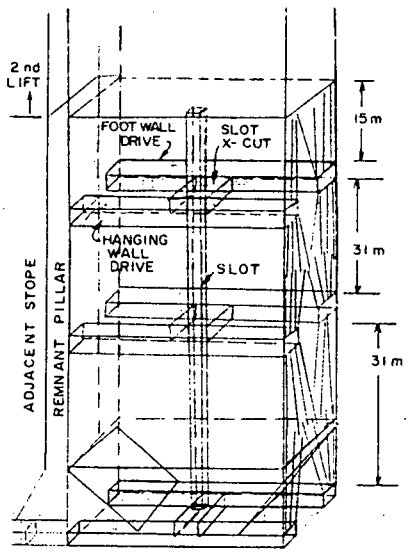

2) Stope Silled Out

Alternative

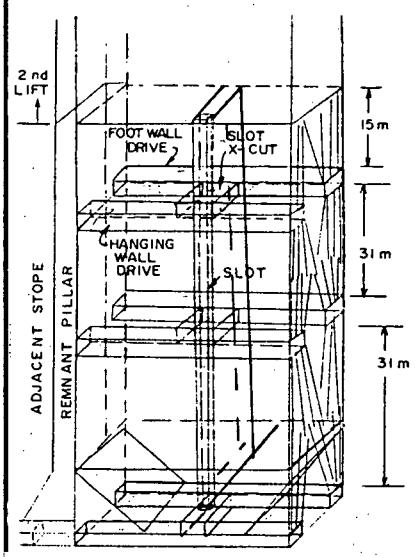

3) Slot Taken Full Stope Width (HW to FW). Rings Blasted on Either Side of Slot and Retreat to Pillar Access

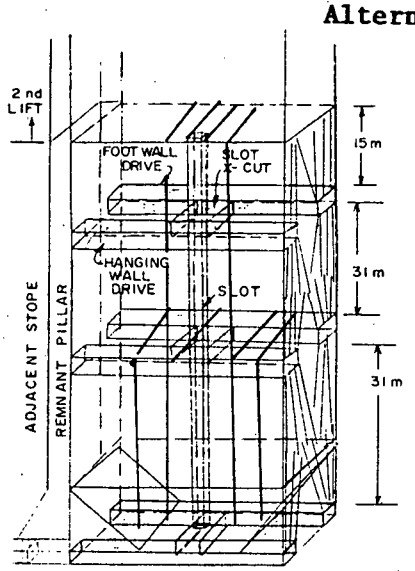

3a) Blasted Rings on Upper Levels Not Duplicated Below.

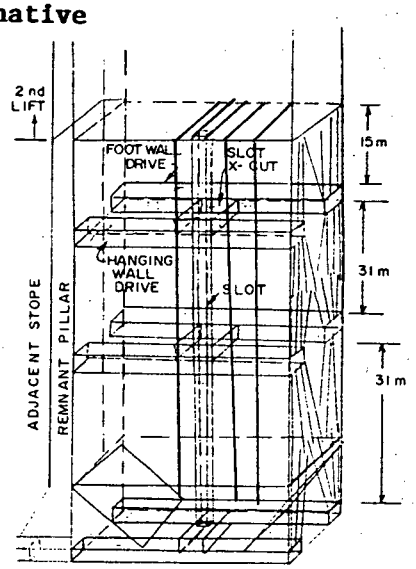

3b) Blasted Rings Coinciding on Each Level

Figure 2.15: Sequence of Extraction - Conventional

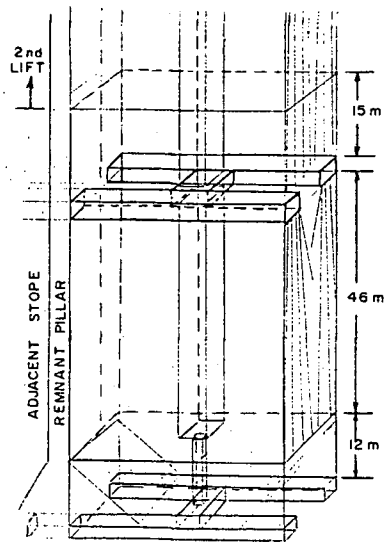

1) Initial Development

- Drill Drives
- Slot X-Cut
- Slot Raise

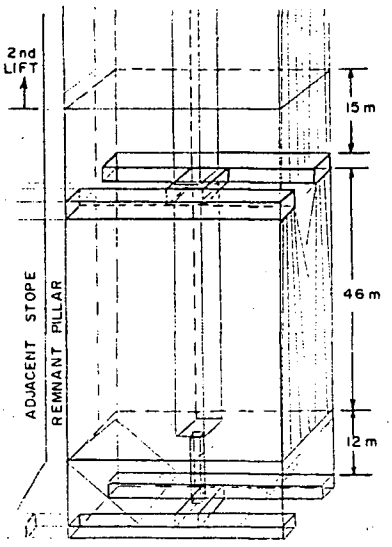

2) Stope Silled Out

Alternative

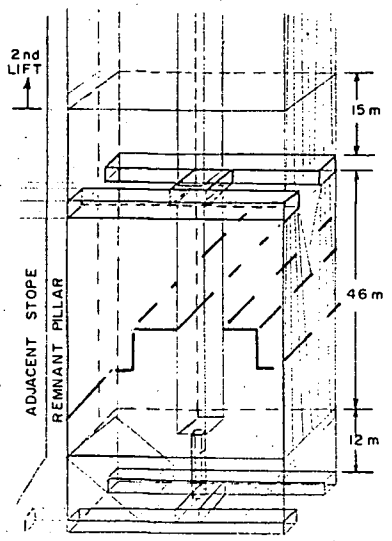

3) Slot Blasted and Stope Benched for Full Stope Width

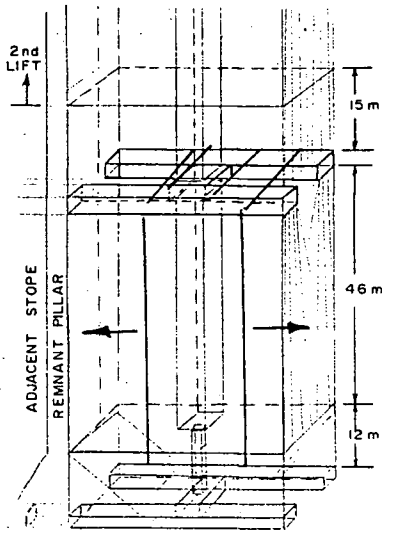

3a) Slot Taken Through to Upper Level and Slashed for the Full Stope Width. Production Slashing on Either Side of Slot.

Figure 2.16: Sequence of Extraction - VCR + Slash

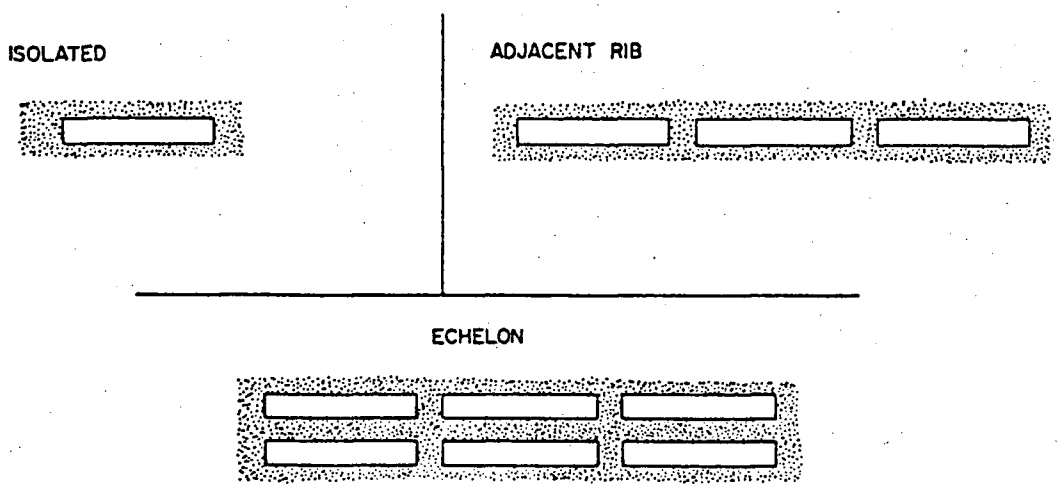

Figure 2.17: Categorization of Stopes - Plan View

The term "echelon" is synonomous with "parallel" for the context that it is employed in this thesis.

CHAPTER THREE

STOPE DESIGN METHODOLOGY

3.1 Introduction

A thesis is defined by the "Oxford English Dictionary" as "a theory put forward and supported by arguments". This chapter will identify the problem, setting forth the objectives, delineating the input requirements and formulating whether to accept or reject the governing hypothesis. The first part of the chapter will summarize a literature search of methods in stope design and "Rock Mass Classification" systems currently available. A section is included on the design methods employed at Ruttan prior to this study and a discussion on why the previous theory was not applicable. The final part of the chapter will review a questionnaire that examines the state of rock mechanics design and, in particular, opening design in Canada today. This questionnaire was included to show that the problem of stope design is universal and not a "Ruttan" problem.

3.2 Literature Review

There exists no accepted comprehensive design methods of predicting stope spans in jointed materials

(Kersten,1985). Beam theories, numerical models and empirical criteria have been employed in the past with some degree of success. The major drawback is that most of our classical design approaches have been based on assuming that homogeneous, isotropic elastic conditions exist.

Stope design practice has ranged from solutions involving trial and errror, rule of thumb, beam theories, to numerical modelling. Rule of thumb approaches such as the stope span should equal one-half the stope height (Morrison, 1976), have evolved from field trials. The elastic beam and plate solutions are based on concepts derived from solid mechanics (Evans, 1940). They assume that the rock above the excavation behaves as a series of elastic beams or plates loaded by self-weight and the roof span is designed on the tensile strength of the beam. A further modification (Beer and Meek, 1982) to beam theory is the "Voussoir" beam which recognizes that cross joints may exist within the beam and consequently, may not allow any tensile stresses to develop. In addition, the Voussoir beam theory assumes that the beam carries its weight by arching, resulting in a confined situation. The basic assumptions common to beam and Voussoir theory are that:

- The ground above the hanging wall is completely destressed in the direction normal to the plate;

- The rock mass has parted along smooth bedding plane breaks, forming a series of beams or plates.

Horizontal confining stresses may also be incorporated in

the above analysis. It is believed that the "Voussoir Beam " theory has definite possibilities in predicting stope spans at Ruttan. The major limitation may be the assumption of evenly distributed cross-joints, well defined bedding planes and the use of elastic, homogeneous, isotropic theory. Possibly a combination of mass predicted strengths and "Voussoir Theory" may result in a more realistic solution, Figures 3.1,3.2. This will be further evaluated in Chapter 9, "Applications".

Numerical modelling (Mathews et al, 1983) of mine openings would outline the state of stress present around the excavation. Relating the induced stress to the rock mass strength would outline possible failure areas. Figure 3.3 outlines typical failure modes that may result. A combination of structural and stress controlled failure is also a possible mode of instability.

This method of analysis requires accurate input into the model, in terms of the numerous parameters affecting the stability of the opening. The designer is offered an invaluable tool in comparing the stability of one opening relative to another configuration. In order to employ the results quantifiably, computer verification through field observation and measurements must be conducted. This, however, is not always a possibility especially in the preliminary design stages of a proposed operation. The use of analytical methods in stope design can best be summarized by Mathews et al (1981) whereby " in general, the number of variables to be considered

is too high to permit other than empirical approaches to stope design. However, analytical methods are often used to identify excessive stress conditions or excessive deformations."

Input parameters, such as the rock mass moduli, are generally derived from performing a rock mass evaluation. Rock mass classification systems have evolved from the need to relate rock substance properties to those of the jointed rock mass. Rock mass classifications provide a common language and consequently, improve communications among all personnel concerned with the safe extraction of ore. It seems to overcome the problem caused by the complexity of the rock masses in terms of quantifying their properties.

Several rock mass classification systems have been developed since Terzaghi (1946) proposed his classification for the prediction of rock load on steel arch design. Several rock mass classification systems have been developed and the following are the most widely used:

Deere (1971), RQD
Wickham (1974), RSR
Barton (1976), Q
Bieniawski (1973), RMR

A summary of the comparison of the application of the rock mass classification systems reviewed is shown in Table 3.1, with limitations highlighted in Table 3.2. A review of the critical parameters used for the major systems is outlined in Table 3.3.

Rock mass classifications have been successfully employed in the overall design of civil engineering structures since the late 1940's. It is only recently that this success is being transferred to mining related problems. Laubscher (1976) has devised a modified rock mass rating patterned after the Bieniawski system, which has been successfully employed in the design of bulk mining layouts. Nicholas (1981) employs a classification system in order to aid in the selection of an optimum mining method by characterizing the footwall, ore and hanging wall. Kendorski et al (1981) has proposed a method of classification for caving operations.

Recently, studies have been undertaken by Mathews et al (1981) whereby a modified NGI system has been employed to predict empirically the dimensions of isolated open stopes at depths below 1000 metres. Conclusions as stated by Mathews et al (1981), are as follows: " Results obtained from the limited data available were considered sufficient to develop the concepts presented, but insufficient to confirm them". The classification combines selected geotechnical factors into a "stability number" and plots, Figure 3.4, these values against a "shape factor" which accounts for the size and shape of the surface of the open stope to be investigated. These values are empirically calibrated against open stope data obtained from mine visits and literature (55 points) and assessed in terms of stable, potentially unstable, and potentially caving regions. The stability number used accounts for the rock mass quality

(Q), the state of stress and the orientation of exposed surfaces. It is envisioned to incorporate the concepts and expand on the study since it strongly parallels the studies proposed to be conducted at Ruttan. The major criticism of this method is the limited number of case studies actually incorporating stope walls, since only seven (7) cases involved stope walls, the remainder were horizontal stope backs. The following parameters were discussed:

- relaxation effect on the HW or FW is not fully assessed
- blasting effects
- excavation rate
- quantitative assessment of instability
- stope configurations other than "isolated".
- effects of fill

The methods of design particularly relevant to the Ruttan orebody will be discussed in subsequent chapters on "Rock Mass Assessment", Chapter 5 and "Application", Chapter 9.

3.3 Design Philosophy

Stope spans at Ruttan had been based on the assumption that the hanging wall acts as a simply supported beam that can bend only to the point that the strength of the intact rock will allow, Figure 3.5. The tensile stresses created at the centre of the beam, due to bending, must be less than the existing in-situ tangential compressive stress, in order to

ensure that the beam is in confinement (Smith,1976). Smith's design was based on experience and theory available at the time of the study. Subsequent research has shown that the resultant stress at mid-span is tensile under the prevailing stress regime. The balancing of bending stresses to the induced tangential stresses must take into account the three dimensional state of stress and resultant geometry of the opening.

The beam approach to analysis, as described above, recommended two stope lengths, the longer stope length being in areas having a higher in-situ tangential stress. Figure 2.13 outlines the typical stope and rib dimensions employed at Ruttan. The above method of design was employed in all rock types irrespective of the rock mass conditions. The above analysis was not able to explain local instabilities that occurred, which generally were due to the release of blocks along existing structures.

A different approach to stope design was incorporated in 1983 by the author whereby numerical modelling techniques were augmented by a large empirical data base. This forms the basis for the development of a solution to the governing hypothesis stated in Chapter One. Figure 3.6 is a plot of stress trajectories for the mined out stopes on the 320m level. Tensile zones are evident adjacent to most hanging and footwall contacts. The size of the zone is dependent upon the excavation geometry and the prevailing stresses. Visual observations at the mine indicated that the hanging wall and footwall contacts

are more foliated in certain areas than others. The result was sloughing along preferential planes that were not restrained by a confining stress, Figure 3.7.

The absence of a confining stress, coupled with a foliated wall contact, enables one to arrive at a relationship showing that a higher dilution results in mining a stope having a poorer "Rock Mass Rating".

The Ruttan orebody is a multi-lensed echelon type deposit which requires one to determine the influence of mining geometry. Sufficiently large pillars separating individual stopes would limit this effort. Mathews (1981) suggests that pillar dimensions along strike should exceed the stope span by at least 25%. Pillars separating adjacent stopes at Ruttan are only 6m. in length with stope spans varying from 40 to 50m. Employing tributary theory, it had been shown that the rib pillars would exhibit factors of safety much less than one. This indicates that the pillars are in a state of post-failure, Figure 3.8. The remnant pillar exhibits sufficient rock mass strength to remain standing. The pillar separating adjacent stopes may be considered as crushed, however, it will influence the stability of adjacent stopes by increasing the effective stope dimensions. Pillars at Ruttan were observed to fail in this manner rather than by an uncontrolled violent release of energy.

Other factors affecting stope span that must be investigated are:

- Blasting
- Rate of Excavation
- Geometrical Configuration of Stopes
- Excavation Sequence
- Depth Below Surface

and, as previously discussed:

- Rock Quality; parameters as defined as in Table 3.3
- Adverse Structure
- Stress Regime; sequence of mining, fill

Artificial support methods will not be addressed in this thesis, since Ruttan does not employ any method of stope support other than fill.

Groundwater is not considered to be a problem at this stage at Ruttan, since the deposit has been delineated on 15m x 15m centers, thus providing adequate depressurization, Figure 2.11. This will be further discussed in Chapter 5, "Rock Mass Assessment".

The above will be incorporated to determine empirical stope design guidelines based on a stability assessment for each individual volume of excavation.

Dilution at the Ruttan operation is recorded for each individual stope at various stages of excavation. It is envisioned to employ this value as an indicator of the stability of the opening. Dilution is an indirect indicator of the quantity of slough originating from the stope walls. The data base is comprised of forty-three (43) stopes at various stages of extraction, thereby yielding 432 stope geometries.

3.4 Survey of Open Stope Operators

A questionnaire (Pakalnis, 1985) was distributed to thirty-eight(38) underground base metal mine operations throughout Canada. It was designed to assess the present state of knowledge with respect to stope design amongst mine operators. The selection criteria for this study were as follows:

- only Canadian underground base metal operations were surveyed
- the extraction method had to include either open stoping and/or room and pillar
- the daily production from underground had to exceed 1000 tonnes per day

All underground operations satisfying the above requirements were contacted. The questionnaire was sent out in March of 1985. Twenty-two(22) operations had responded representing a 58% response rate.

The following areas were investigated by the questionnaire:

a) Mine Profile:

-Production rate
-Maximum depth of mining
-Ore dip, type
-Mining Method

b) Geomechanical data base that is available at each

operation :

-Rock strength parameters
-Stress investigations
-Rock mass parameters
-Monitoring
-Instrumentation

c) Stope and Pillar design, evaluated in terms of:

-methods employed
-success of design
-stope characterization
-resultant dilution

A copy of the questionnaire is enclosed in Appendix I. Table 3.4 identifies the individual operators that responded to the questionnaire. Parameters that are particularly relevant to the scope of this thesis are summarized within this section.

3.4.1 Mine Profile

Twenty-two mining operations completed and returned the enclosed questionnaire (Appendix I). The size distribution of participating operations is shown in Figure 3.9. The smallest tonnage producer responding was equivalent to 800 tpd. Distribution of mining method in terms of percentage of total tonnage attributed to that method is shown in Figure 3.10. The classification of individual mining methods for the purposes of this study are as follows:

a) Open Stoping Mining Methods:

- blasthole, longhole (I.T.H.)
- sub-level stoping
- vertical crater retreat

b) Room & Pillar Mining Methods

c) Backfill Mining Methods

-overhand cut & fill
-underhand cut & fill
-mechanized cut & fill

d) Other Mining Methods

-shrinkage
-pillar recovery
-development mining

Figure 3.10 indicates that under the selection criteria stated previously, approximately 50% of the data base is composed of "open stope operators" . This compares favourably to a survey conducted by the Ontario Ministry of Labour (1985) that indicated that 51% of all ore production by underground metal mines in Canada is derived directly from open stoping operations.

Mining depth distribution is shown in Figure 3.11. The shallowest operation is at 240 m, and the deepest at 1250 m. Mining depth is a critical factor in determining the in-situ stress that may be encountered during mining. In addition, at each depth interval the distribution of production, in terms of tonnage attributed to each method divided by the total tonnage for that particular method, was determined (ie. between 300-600 m depth, 17% of the total open stope production is mined).

3.4.2 Rock Mechanics

Significant advances have occurred in the science of rock mechanics throughout the past twenty years. These have included the development of comprehensive failure critera for intact and fractured rock, sophisticated computer codes for modelling rock structures, and in determination of rock properties. In addition, advances in instrumentation have enabled the operator to more precisely determine the prevailing in-situ stress. In terms of monitoring, advanced early warning systems have been developed, and are, in addition, being used in the calibration of the design process.

The level of rock mechanics activity in this area has been investigated through the questionnaire.

Figure 3.12 shows the different intact rock strength properties that have been investigated by the participating mines. The following parameters have been referred to :

-unit weight (UW)

-elastic modulus (E), Poisson´s ratio (V)

-unconfined compressive strength (UCS), tensile strength (TS), internal friction angle, triaxial testing (TR), sliding angle of friction (SS)

-employment of a failure criterion to estimate the rock strength (FC)

Figure 3.13 outlines the percent utilization of numerical modeling for mine design. In addition, it shows that in-situ stress measurement has been conducted in 85% of the mine operations. These two techniques are often associated, in that the virgin stress is a critical input parameter for numerical modelling. Photo-elastic methods of modelling were not used.

The distribution of stresses around underground openings coupled with the rock strength parameters, is an indicator of instability. Rock mass classifications have evolved from the need to relate the rock substance properties to those of the jointed rock mass. Figure 3.14 shows that structural mapping is conducted by all operations, with Deere's (1964) RQD classification being the most widely used. The following were the classification systems surveyed:

-Rock Quality Designation(RQD) - Deere(1964)
-Q system - Barton et al(1974)
-RMR system - Bieniawski (1973)
-Modified RMR system - Laubscher(1974)

The classification system coupled with the laboratory strength results enables the operator to assess the properties of the rock mass.

3.4.2.1 Stope and Pillar Design

The problems of estimating "critical stope spans" and

"pillar dimensions" are complex. This is because the rock mass behaviour is dependent upon a large number of inter-related variables such as the rock mass quality, stress distribution, and the mine geometry among others. Several pillar (Potvin, 1985) and opening design methods have been developed (Pakalnis, 1985). This report classifies the methods in the following categories:

-Empirical methods; such as those derived from a large data base, ie. Hedley pillar formula (1972)

-Analytical solutions; such as beam theory in the design of stope spans

-Practical experience; observational approaches

-Numerical modelling methods; such as boundary element, finite element codes

Figure 3.15 indicates that all mines in the data base utilize practical experience in their design followed by empirical and numerical techniques of modelling. Figure 3.15, however, shows that only 34% of the mines rely solely on practical experience as their main input to design. The most widely used combination was that employing practical and empirical experience as well as computer modelling derived results.

The term "practical" refers to trial-and-error approaches, whereas empirical refers to pillar and stope formulae as derived throughout the literature.

3.4.3 Dilution Assessment

Dilution is a measure of external waste that has sloughed into the drawpoint. Stope dilution as estimated by the participating mine operators, is a quantitative parameter that enables the operator to evaluate the quality of his design. The following are the most common methods of estimating dilution as indicated by the questionnaire:

-% Dilution = (weight of external slough x 100)/(weight of ore reserves)

-Dilution = (undiluted in place grade (DDH))/ (sample assay grade at drawpoint)

-Dilution = (undiluted in place grade reserves)/(mill head grades obtained for same tonnage)

-Dilution = (total waste tonnage)/(total tons mined)

-Dilution = (total waste mined)/(tons of ore reserves estimated)

-difference between tonnage mucked and that blasted

-difference between tonnage of backfill placed and that theoretically required to fill "ore reserves" void

-dilution is visually observed and assessed

-"x" amount of feet in the footwall plus "y" amount of feet in the hanging wall divided by the stope width

-historical average over past 10 years = actual tons drawn from stopes/calculated reserve tonnage

The level of acceptable dilution is highly dependent upon grade since a higher grade stope can be economical, whereas a

lower grade stope with the same dilution will no longer be mineable.

It is proposed that the following thresholds be employed for comparative purposes:

-less than 10% dilution
-10 - 19% dilution
-20 - 35% dilution
-greater than 35% dilution

The non-entry methods of mining, such as open stoping, can accept a certain degree of wall slough without injury to the workers. Figure 3.16 shows the amount of dilution as determined by the open stope operators. The percent occurrence was measured as the number of operations exhibiting an average dilution divided by the total number of operations in the data base. The open stope dilution statistics reveal that 47% of all open stope operations have more than 20% dilution. It was generally stated by the operators that dilutions under 5% are acceptable and were classified as low. This is considered normal due to recording accuracy, blasting effects, and variability in the ore geometry and in the rock mass strengths.

3.4.4 Stope Characterization

The individual mine operations were further categorized by "Rock Mass Rating", this is shown by Figure 3.17 and Table

3.5. The rock mass assessment was conducted as shown in the questionnaire. This categorization of the rock mass in terms of strength, RQD, spacing and joint condition were as defined by Nicholas (1981). This system was employed due to its simplicity and similarity to the RMR system which is described in subsequent chapters. Appendix I shows the relationship employed between the two systems. Nicholas had proposed a classification system for the selection of an optimal mining method given the following constraints:

- geometric considerations
- rock mechanics considerations

It was intended to delineate those mining methods that will be most effective given the above constraints. Nicholas suggested the following conditions be present if an open stope method is to be considered:

- rock substance strength in the hanging wall and the ore zone to be at least of moderate strength, wide spacing, and moderate joint condition.

The groundwater rating was assessed as dry for all operations considered. This was due to: a) the difficulty in estimating water pressures during logging of core, b) most mine workings are depressurized due to the presence of exploratory drill holes, development headings etc. Unless indicated

otherwise by the mine operator, the groundwater rating was assessed as "RMR=10". This was also found to be the case in the Ontario Ministry of Labour survey (1985) where groundwater, Figure 3.18, was found to be of little or no concern to open stope operators except in the vicinity of the crown pillar.

The rock quality of the hanging wall was assessed for open stope operators. This is due to the reasoning that most of the dilution is probably from the adjacent overhang. Cases where lower footwall RMR ratings prevailed required one to assess the stope characterization individually. This situation did not occur. The ore RMR was evaluated for characterization of pillars for open stope operations, Table 3.6. Appendix I outlines the terminology employed in identifying stope and pillar dimensions.

3.4.4.1. Stope Assessment

The exposed surface area was further analysed in terms of hydraulic radius. Mathews et al (1981) have attempted to relate the rock quality for open stopes in terms of the area of wall exposed. The term "hydraulic radius" is employed which is defined by the exposed surface area/surface perimeter. This value tends to incorporate the stope configuration as well as the size;ie. openings whose long span to short span exceed approximately four to one have minor variations in hydraulic radius with increased span and therefore represent one way spanning geometries (tunnel).

Open stope dimensions for the data base are shown in Figure 3.19. A further analysis was conducted for the larger open stope data base (24 stopes) that compared the following parameters in order to determine if a correlation existed:

a) fill/no fill vs. depth

Figure 3.2 indicates that 69% of open stope operators employ fill. There was found to be no correlation between mining depth and fill option (fill/no fill).

b) dilution vs. RMR

The average dilution was 19% $\pm$ 15%
The average RMR value was 53% $\pm$ 16%
Correlation was: r= -.74 (highly significant at the 99% level)

c) dilution vs. stope depth

The average stope depth was 388m $\pm$ 237m
Correlation was: r=+.23 (not significant at 90% level)

d) dilution vs. hydraulic radius(HR)

The average hydraulic radius was 10.5m $\pm$ 4.2m
Correlation was: r=-.26 (not significant at 90% level)

e) dilution vs. exposed surface area

The average exposed surface area was 2751 m^2 $\pm$ 2213m^2
Correlation was: r=-.29 (not significant at 90% level)

f) dilution vs. RMR,HR

Multiple correlation is: r= .8 (highly significant at the 99% level, slight improvement over b)

g) dilution vs. stope depth,RMR

Multiple correlation is: r= .75 (highly significant at the 99% level, no improvement over b)

The above linear correlation coefficients indicate that the only parameter directly correlative to dilution is the rock quality. A combination of individual parameters would be a better estimate of dilution as shown by e) RMR, hydraulic radius but not in f) stope depth, RMR.

3.4.4.2. Pillar Assessment

A further analysis was also conducted on the rib pillars as shown in Figure 3.21 for the open stoping operations (data base = 24 stopes). The following were compared:

a) RMR vs. Lp/Wp

The mean RMR=67 $\pm$ 20
The mean Lp/Wp=3.9 $\pm$ 3.4
Correlation:r= 0.08 (no correlation)

b) RMR vs. Lp/Lo

The mean Lp/Lo=.8 $\pm$ .5
Correlation:r=+.36 (not significant at 95% level)

c) Stope depth vs. Lp/Wp

Correlation:r=-.26 (not significant at 95% level)

d) Stope depth vs. Lp/Lo

Correlation:r=-.33 (not significant at 95% level)

The variables investigated were found not to be correlative at the 95% significance level. This is possibly due to the many variables involved in the estimation of pillar geometry. In

addition, it was not possible to determine the state of pillar distress whereas dilution is a quantitative measure of opening instability.

3.4.5. Observations

Historically Canadian underground mines have been designed based on experience, and optimized through a trial-and-error process. This approach in the long term can lead to an optimum mine layout, however, the real cost of such procedures can often be measured in terms of:

-injuries to the worker
-dilution
-additional artificial support requirements
-production delays and/or isolation of ore due to instability

The degree of rock mechanics data available at the individual mine operations surveyed suggested that ground control is an integral part of the mine design process. There is no single accepted method of design in jointed materials, as is shown by the variability in design methodology and the exceptionally high levels of recorded dilution.

The rock quality was found to be strongly correlated to dilution in terms of opening design and consequently, should play an important role in the design process. Values for Lp/Lo and Lp/Wp for open stope operations averaged .8 $\pm$ .5 and 3.9 $\pm$

3.4 respectively. This was determined over an average depth of 388m ± 237m. Correlations among the pillar variables were poor. This is partly due to the difficulty in estimating the state of pillar distress, whereas dilution is a quantitative parameter and more easily determined.

Figure 3.18 summarizes the ground control problems identified by the Ontario survey of Canadian operators. The Ontario Ministry of Labour sponsored a study whereby information was obtained from approximately 65 base metal underground Canadian mines. This represents most of the operating Canadian mines at the time of the survey (March 1985). The questionnaire was completed by contacting the individual mines or group of mines by telephone. The following is a breakdown of the individual mine operators:

-open stoping	31 mines	
-cut & fill		23 mines
-caving	4 mines	
-room & pillar	7 mines	
Total		65 mines

3.5 Conclusions

This survey along with the Ontario(1985) study indicated that dilution is of particular concern to open stoping operators. Neither backs nor pillars will be addressed in this thesis since:

- the observed dilution at Ruttan is solely a measure of the hanging wall and footwall slough

- deterioration of stope backs and pillars has caused only minor problems at Ruttan

It is realized that back and pillar stability is an important design requirement. The author must limit the scope of this study to the factors affecting "wall slough" at Ruttan. Mechanisms other than relaxation may prevail and consequently, may require a procedure of design different that that suggested in this study.

The design methods that are available for assessing the stability of mine openings can be categorized as follows:

a) Analytical
b) Observational
c) Empirical

Analytical methods are based on the analyses of stresses and deformations around openings. Observational methods rely on the monitoring of ground movement during mining to detect measureable instability. Empirical methods assess the stability of mines by the use of statistical analyses of underground observations. Analytical methods are primarily employed for comparative design and parametric studies. The observational approach would require a large data base and would have to be implemented in the initial stages of mine development in order to achieve some reliable measurement of opening stability. The Ruttan orebody is in an advanced stage of extraction and consequently, observational methods are of limited use in predicting hanging wall or foot wall dimensions in various rock types and stope configurations. Bieniawski(1985) states that in

order to meet the immediate needs of the mine practioner, studies should be directed to the development of empirical failure criteria. Jaeger and Cook (1979) suggest that a failure criteria has yet to be developed that describes the actual mechanism of fracture and that empirical equations fit the experimental results much better. Bieniawski suggests that such criteria can be selected by fitting a suitable equation to experimental data which do not necessarily require a theoretical basis. The empirical relation will serve to meet the requirements of adequate prediction, simplicity of use and speed of application. It is therefore proposed to employ an empirically based approach that evaluates the parameters that may have an influence on hanging and foot wall stability design and ultimately develop a relation whereby:

$$Z = A + Bx + Cy + Du + \ldots.$$

or

$$Z = A + Bx + Cy + Dx^2 + Ey^2 + Fxy + \ldots.$$

where:

Z: refers to the control variable which is quantifiable and will be for this study "Dilution"

A,B,C,...: are constants determined by regression analysis perfomed on a linear hyper-surface or quadratic surface

x: refers to the dimensions of the hanging wall or footwall

y,u,v ....: refers to the variables that are critical to the evaluation.

The best fit will be evaluated in terms of a statistical regression analysis performed on linear and quadratic equations. The correlations and probability theory will determine the acceptance or rejection of the hypothesis. A rejection of the hypothesis would not enable an empirical equation to be estimated whereas an acceptance would suggest that an empirical formulation may be possible.

Table 3.1: Rock Mass Classification Systems - Applications

	APPLICATIONS \ CLASSIFICATION	TERZAGHI	LAUFFER-PACHER	DEERE	RSR	RMR	Q	KIRSTEN	LOUIS	FRANKLIN	COATES & PARSONS	BULICHEV	LAUBSCHER	KENDORSKI	McMAHON	MATHEWS	NICHOLAS	MULLER	COAL CLASSIFIC
MINING APPLICATIONS	MINING METHOD SELECTION												X	*X	*X		X		X
	MINE SEQUENCING												X						
	STAND-UP TIME		X			X	X												X
	MAX. UNSUPPORTED SPAN		X			X	X						X			X			X
	SUPPORT DESIGN				X	X	X	X					X	*X					X
	PILLAR DESIGN					X	X						X						X
	CAVABILITY							·					X	X	X				X
	CAVE ANGLE												X						
	ROOF STABILITY					X	X						X			X			X
	FLOOR STABILITY					X	X									X			X
	OPEN STOPE DESIGN					X	X						X			X			
	ROCK LOAD	X				X	X	X								X			
	RIPPABILITY					X		X											
ROCK MASS STRENGTH INDICES	COHESION					X	X	X										X	
	FRICTION ANGLE					X	X	X										X	
	DEFORMATION MODULUS				X	X	X	X											
	STRENGTH					X	X	X					X						
CIVIL APPLICATIONS	ROCK LOAD	X		X		X	X	X	X	X									
	STAND-UP TIME		X			X	X			X									
	MAX. UNSUPPORTED SPAN		X	X		X	X	X		X		X							
	SUPPORT DESIGN	X	X	X	X	X	X	X	X	X		X							
	FOUNDATION DESIGN					X	X	X											
	SLOPE DESIGN					X	X	X											

NOTE: In order for method to be classified as having a mining application, it must have been referenced in the literature.

Table 3.2: Limitations of the Major Rock Mass Classification Systems - Mining Applied

	LIMITATIONS \ CLASSIFICATION	TERZAGHI	DEERE	RSR	RMR	Q	KIRSTEN	LAUBSCHER	KENDORSKI	McMAHON	MATHEWS	NICHOLAS
CLASSIFICATION DOES NOT CONSIDER	STRESS FIELD		X	X	X					X		
	JOINT CONDITION		X							X		
	CONTINUITY		X							X		X
	JOINT ORIENTATION	X	X			X	X			X		X
	JOINT INFILLING		X	X						X		
	SWELLING MATERIAL		X		X			X		X		
	BLASTING EFFECT	X	X	X	X	X	X			X	X	X
	UNIAXIAL COMPRESSIVE STRENGTH	X	X	X						X		
	EXCAVATION METHOD	X	X		X					X	X	X
	GROUNDWATER		X							X		X
CLASSIFICATION REQUIRES	STRESS FIELD < 30MPA			X	X			X				
	EXTENSIVE EXPERIENCE					X	X	X				
	MORE FIELD EXPERIMENTATION						X	X	X	X	X	X

Table 3.3: Summary of Parameters Used in Rock Mass Classification Systems - Hard Rock Mining

	CLASSIFICATION / ROCK MASS PROPERTIES	TERZAGHI	LAUFFER-PACHER	DEERE	RSR	RMR	Q	MODIFIED Q KIRSTEN	LOUIS	FRANKLIN	COATES AND PARSONS	BULICHEV	Mining: LAUBSCHER	KENDORSKI	McMAHON	MATHEWS	NICHOLAS	MULLER
ROCK MATERIAL	DEFORAMATIONAL CHARACTERISTICS										X							
	UNIAXIAL COMPRESSIVE STRENGTH					X	X	X	X	X	X		X	X		X	X	X
ROCK MASS JOINTING	ROCK QUALITY DESIGNATION			X		X	X	X	X	X			X	X	X	X	X	
	NUMBER OF SETS				X	X	X	X				X	X	X		X		
	SPACING				X	X				X	X		X	X			X	X
	CONTINUITY				X	X				X	X		X	X				
	CONDITION				X	X	X	X				X	X	X		X	X	
	ORIENTATION				X	X						X	X	X		X		
	OVERALL QUALITY	X	X															
ENVIRONMENT	VIRGIN STRESS						X	X		X			X	X		X	X	
	EXCAVATION STRESS	X					X						X	X		X		
	GROUNDWATER	X			X	X	X	X	X	X		X	X	X		X		
	EXCAVATION METHOD				X		X	X					X	X				
	OPENING GEOMETRY/ORIENTATION	X	X		X	X				X		X	X	X		X		
	STAND-UP TIME		X			X	X	X										
	LITHOLOGY			X		X				X	X							
	WEATHERING					X							X	X				

Table 3.4: Participating Mining Operations

No.	PROD. RATE(TPD)	MINING DEPTH(m)	ORE TYPE	ORE DIP(deg)	MINING METHOD
1	6500	1220	Ni Sulph.	65-70	36% OS,45% C&F,19% VCR
2	<1000	960	Au-Ag	90	100% OS
3	4200	520	Pb-Zn-Cu	80	100% OS
4	10500	910	Pb-Zn-Cu-Ag	65-75	100% C&F
5	800	460	Au	75-80	90% OS,10% SHR
6	2000	610	Cu-Au	55-85	54% OS,24% SHR
7	1400	850	MS	40	100% OS
8	2600	270	Pb-Zn Sulp	20	100% OS
9	10000	610	Fe-Pb-Zn-Ag	30-35	100% OS
10	11800	960	Cu-Pb-Zn	75-85	97% OS,3% SC
11	1425	240	Breccia	15-30	60% C&F,40% OS
12	<1000	400	Chert,Sulf	65-90	80% VCR,20% PR
13	1400	240	MS	55	100% C&F
14	1400	1070	MS	65	50% SC,30% OS
15	<1000	330	MS	80-85	100% VCR
16	<1000	1100	MS	42	90% C&F,10% OS
17	<1000	1000	MS	70	80% VCR,20% C&F
18	12800	910	QTZ-Cong	19	100% R&P
19	4000	1250	QTZ-Cong	9-15	100% R&P
20	5000	850	QTZ-Cong	20	100% R&P
21	3000	530	QTZ-Cong	20	100% R&P
22	3350	300	Niobium	90	100% OS

Legend

C&F: Cut and Fill
OS: Open Stope
VCR: Vertical Crater Retreat
SHR: Shrinkage
SC: Sub-Level Cave
R&P: Room and Pillar
PR: Pillar Recovery
%: Percent of Total Production

Table 3.5: Open Stope Mining Operators (Stope)

No.	MINING DEPTH(m)	RMR(%)	WIDTH(m)	SPAN/HEIGHT(m)	HYD.RAD.(m)	DIL.(%)
1	670	66	4.5-18	12/46	5	50 ?
2	137-960	63	9	61/91	18	15
3	520	68	34	30/122	12	30 ?
5a	250	80	8	13/45	5	5
5b	250	63	5	25/45	8	15
6a	160	36	2	15/61	6	32
6b	251	45	2	18/79	7	25
6c	343	45	2	18/73	7	30
6d	610	42	2	18/62	7	50
7a	823	68	46	46/61	13	10
7b	823	68	30	23/61	8	17
8a	120	60	10	101/25	10	0
8b	149	60	15	101/60	19	0
9a	107	70	61	61/41	12	12
9b	366	70	21	168/55	8	12
10a	427	57	18	46/91	15	10
10b	914	57	15	30/61	10	5
11	230	57	15	40/20	7	5
12	277	51	10	16/28	5	26
14	396	59	24	30/122	12	NA
15a	200	48	10	80/45	14	30
15b	300	60	10	80/45	14	NA
17a	640	25	10	37/43	10	50
17b(sh)	366	25	10	107/37	14	30
17c(sh)	+914	25	10	91/37	13	30
22	243	52	24	46/91	15	4

Legend

Sh: Open Stope Shrink
RMR: Rock Mass Rating of Hanging Wall
HYD RAD: f(Span,Height)

Table 3.6: Open Stope Mining Operators (Pillar)

No.	MINING DEPTH(m)	RMR(%)	Lp(m)	Wp(m)	Lp/Wp	Lo(m)	Lp/Lo
1	670	61	NA	NA	NA	12	NA
2	137-960	63	5	4	1.3	61	.4
3	520	67	27	34	.8	30	.9
5a	250	80	25	8	3.2	13	1.9
5b	250	80	25	5	5.0	25	1
6a	160	29	4	2	2.0	15	.3
6b	251	34	6	2	3.0	18	.3
6c	343	37	5	2	2.5	18	.3
6d	610	37	5	2	2.5	18	.3
7a	823	68	15	46	.3	46	.3
7b	823	68	15	30	.5	23	.7
8a	120	58	100	10	10.	101	1.
8b	149	69	100	15	6.7	100	1.
9a	107	69	122	61	2.	61	2.
9b	366	69	168	18	9.3	168	1.
10a	427	100	46	24	1.8	46	1.
10b	914	100	NA	NA	NA	30	NA
11	230	90	40	10	4.	40	1.
12	277	80	4	3	1.3	16	.3
14	396	89	6	34	.2	30	.2
15a	200	61	80	10	8.	80	1.
15b	300	61	80	10	8.	80	1.
17a	640	87	21	11	1.9	37	.6
17b(sh)	366	87	107	11	9.8	107	1.
17c(sh)	+914	87	91	11	8.3	91	1.
22	243	52	46	24	1.9	46	1.

Legend

RMR Rock Mass Rating of Pillar
Lp Length of Pillar
Wp Width of Pillar
Lo Length of Opening
NA Not Applicable - Isolated Stope

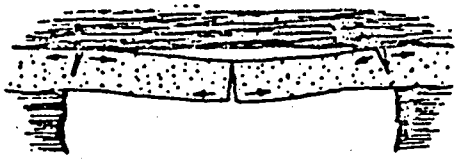

To compensate for original assumptions, a factor of safety of six is generally employed. (Wright,1980)

Figure 3.1: Beam Theory

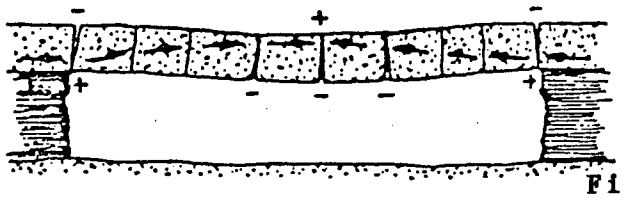

Figure 3.2: Voussoir Arch

The beam is assumed to be supported by resultant arching action. Note shear stresses (interslice forces) must be overcome for a single block to fall out.

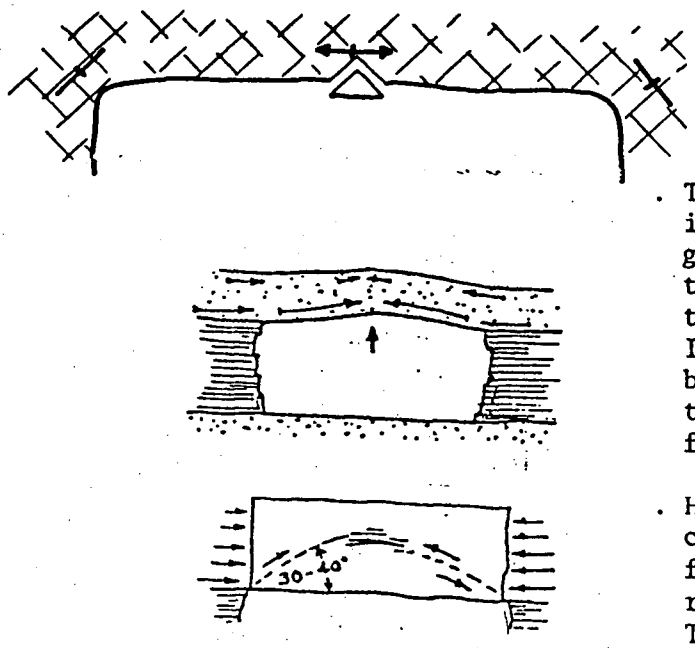

Figure 3.3: Numerical Solution

- Tensile stress in the back is an indicator that the region is in a state of relaxation and consequently, structural blocks may be released. If the back is a homogeneous beam, the tensile strength of the beam must be exceeded for failure to occur.
- High compression in the roof, coupled with low compressive forces normal to the roof may result in buckling failure. This is particularly true if structures paralleling the roof are present.
- Failure when the shear strength of the rock is exceeded.

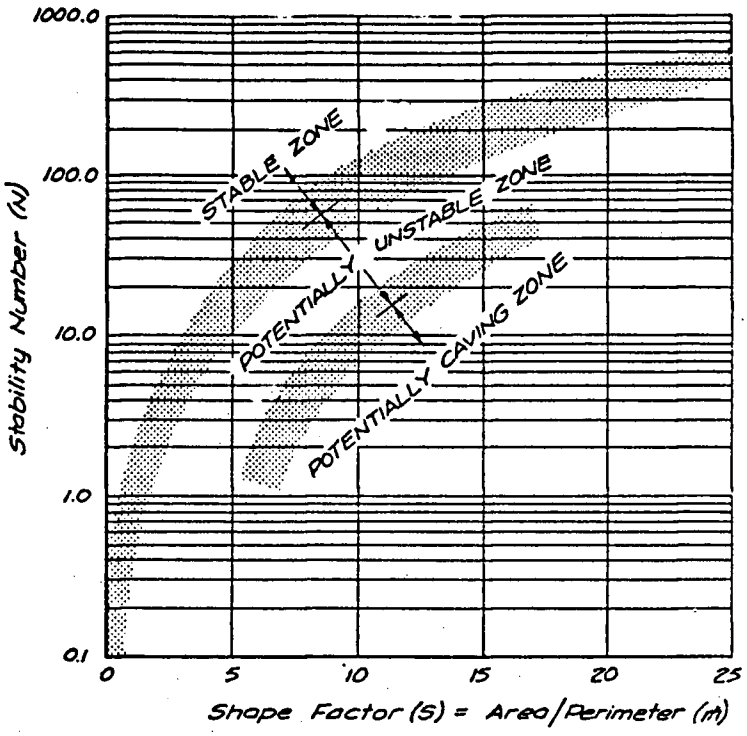

Figure 3.4: Mathews Method of Stope Design (Mathews et al, 1981)

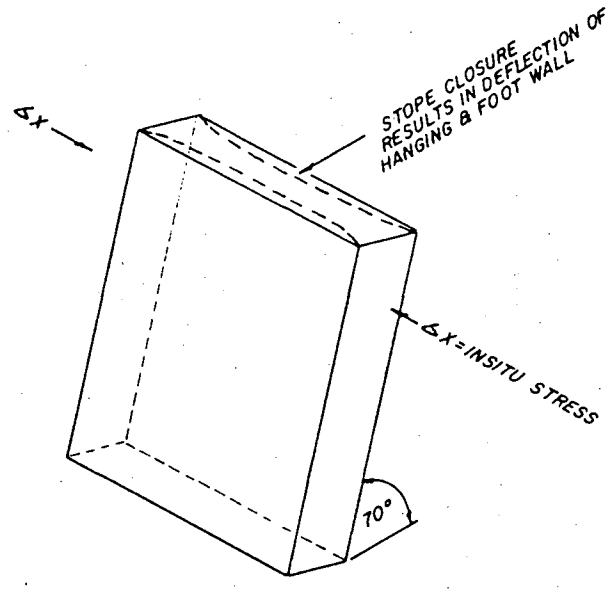

Figure 3.5: Hanging Wall and Footwall Beam Deflection

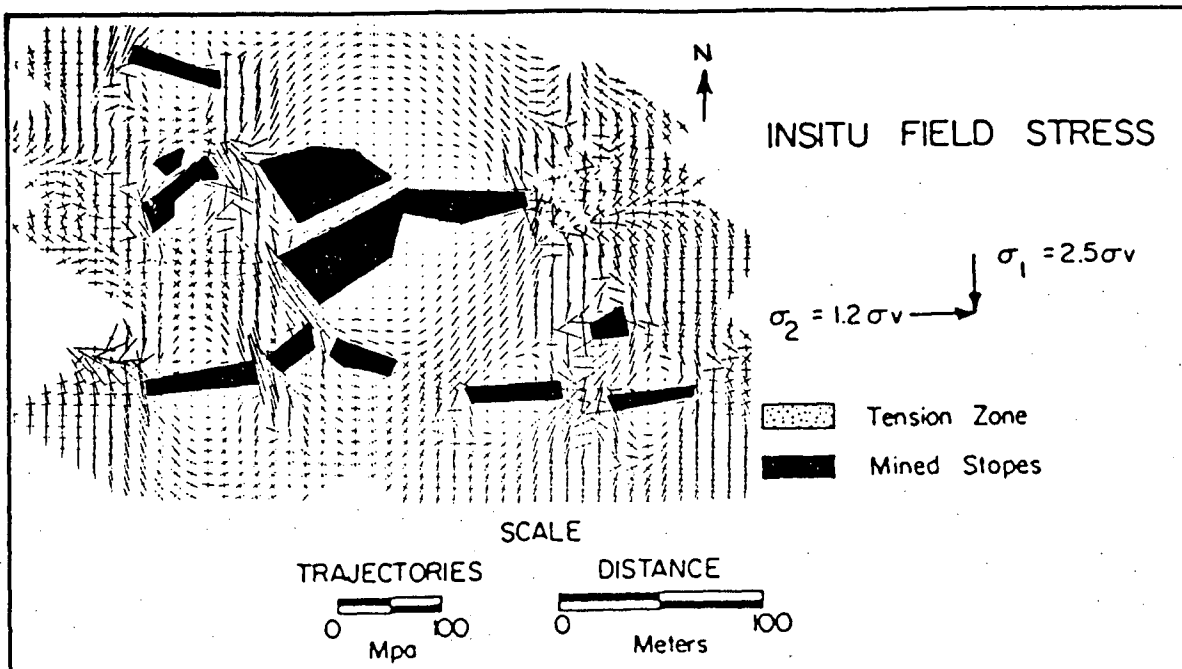

Figure 3.6: Stress Trajectories - 320m Level, Plan View

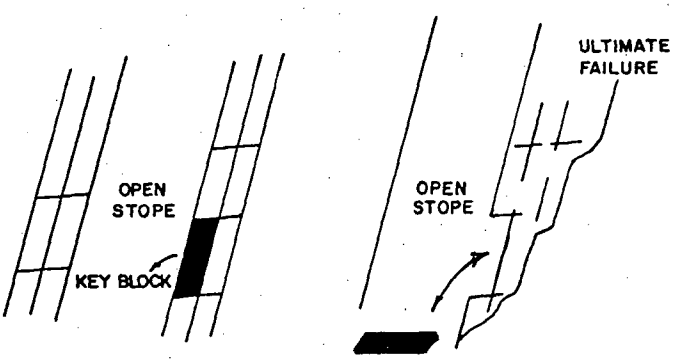

Figure 3.7: Structurally Controlled Failure - Section of Typical Stope

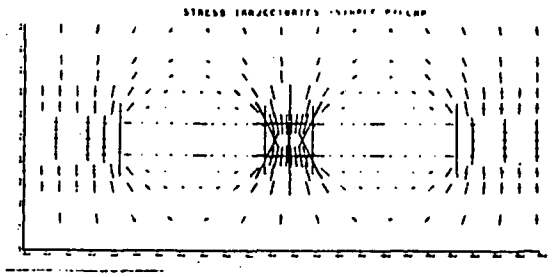

E_{pillar} = 70 GPa

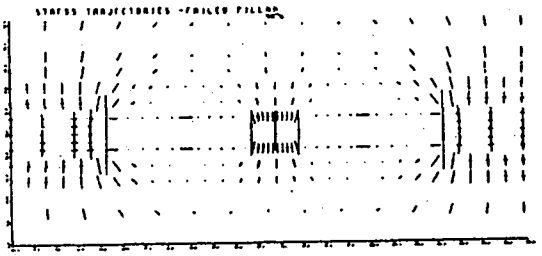

E_{pillar} = 7 GPa

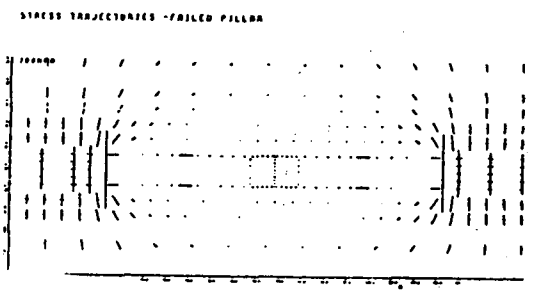

E_{pillar} = 700 MPa

E_{pillar} = 70 MPa

E_{pillar} Removed

. Load is shed to adjacent areas as pillar is wrecked. This is simulated by reducing the pillar modulus.

Figure 3.8: Plan View of Two Adjacent Stopes

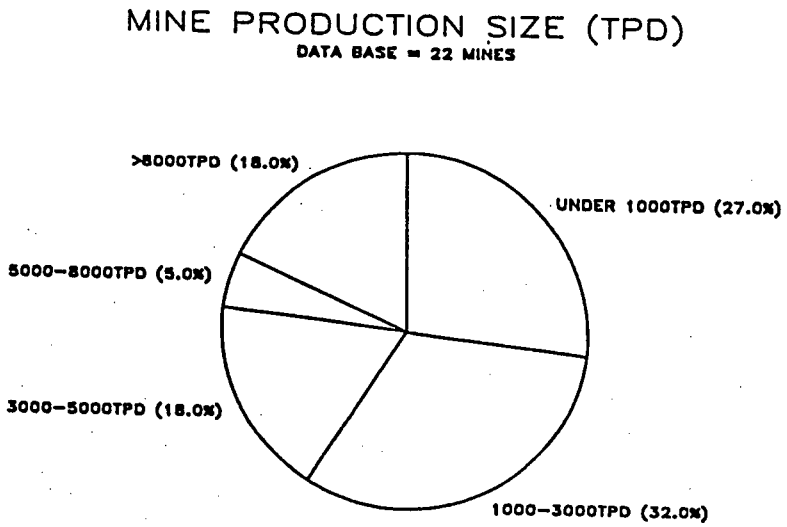

Figure 3.9: Distribution of Mine Production Size

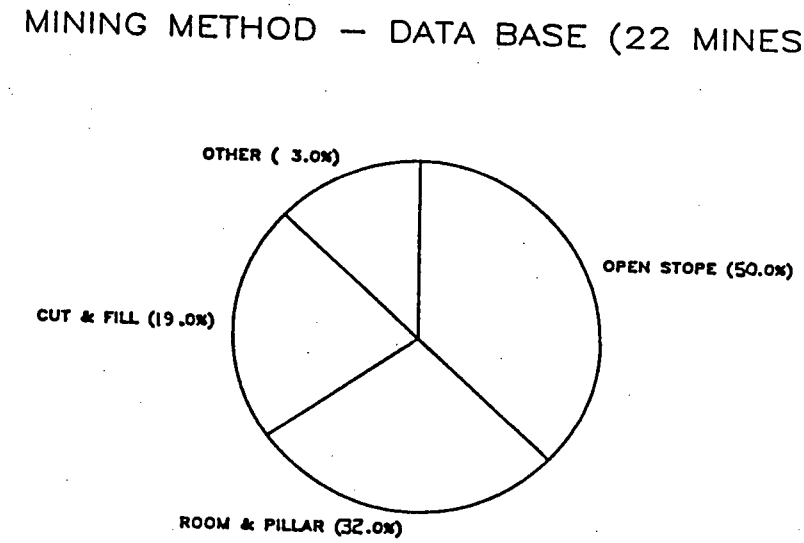

Figure 3.10: Distribution of Mining Method

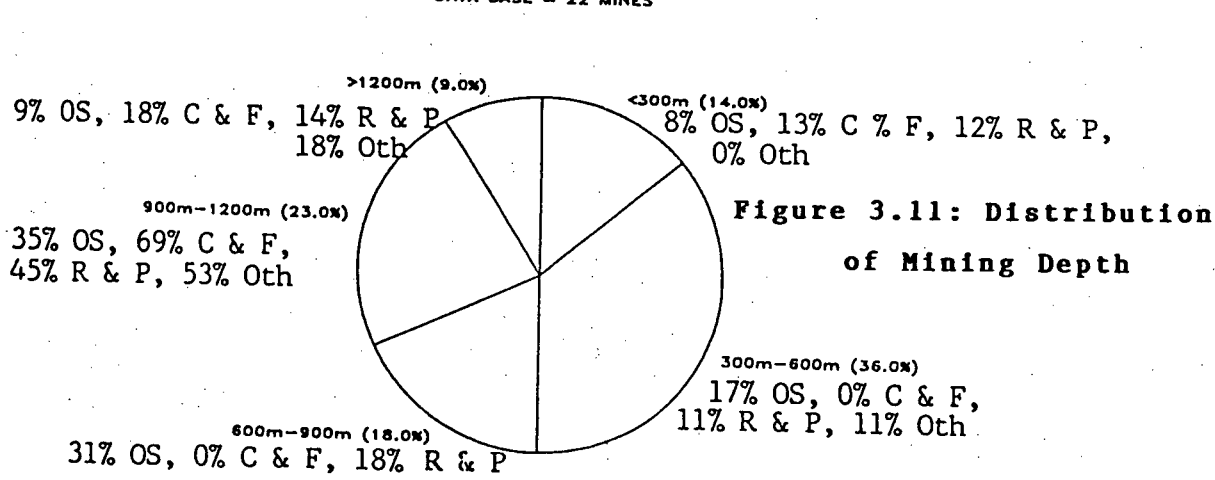

Figure 3.11: Distribution of Mining Depth

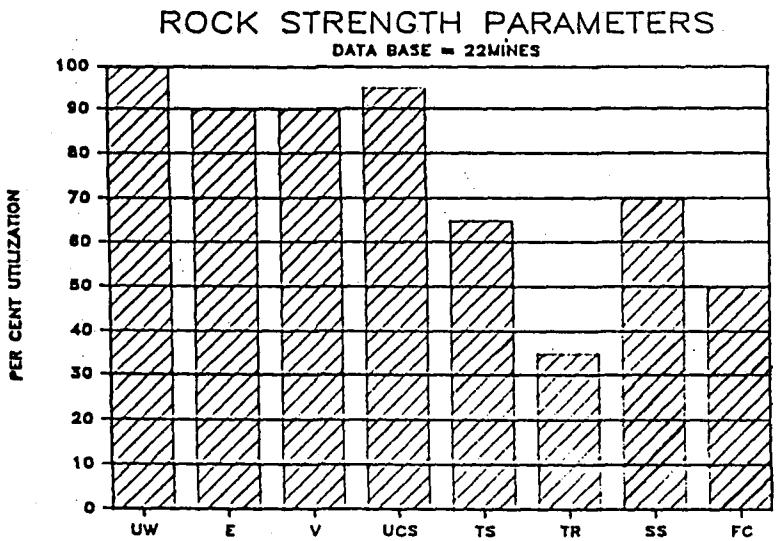

Figure 3.12: Rock Strength Parameters

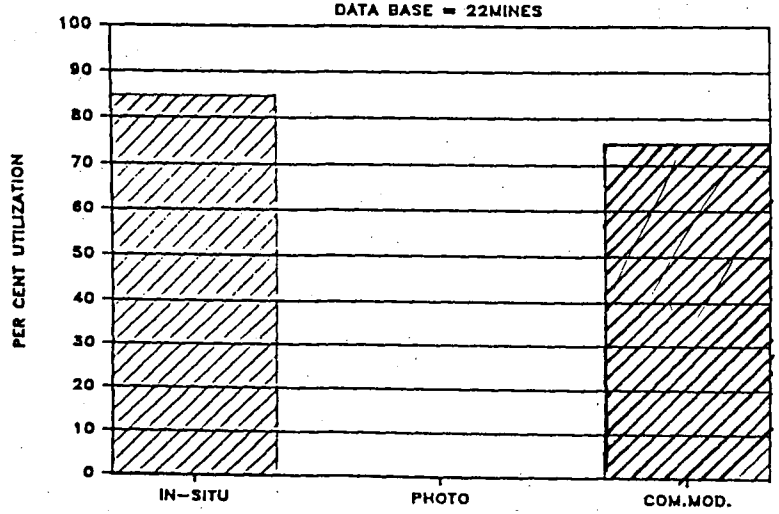

Figure 3.13: Stress Investigation

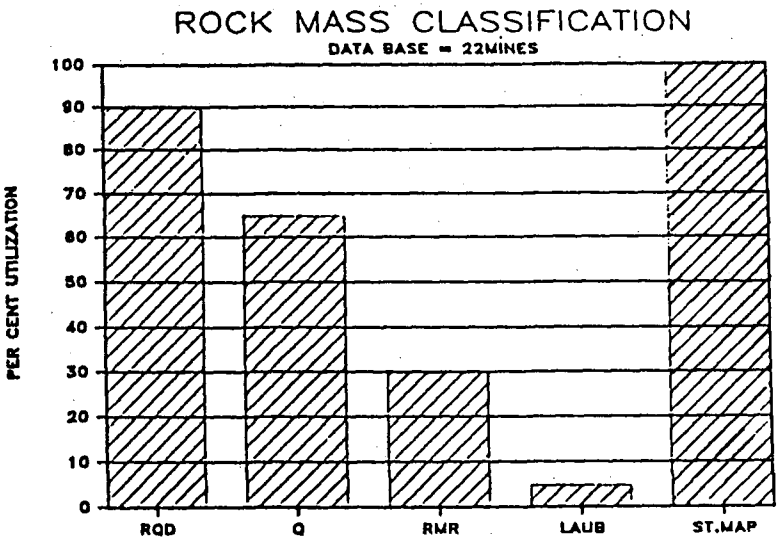

Figure 3.14: Rock Mass Investigation

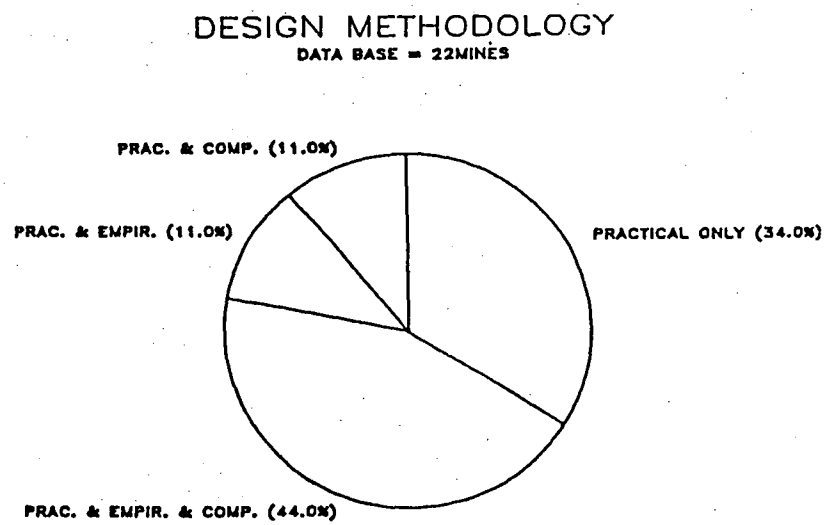

Figure 3.15: Methods of Design

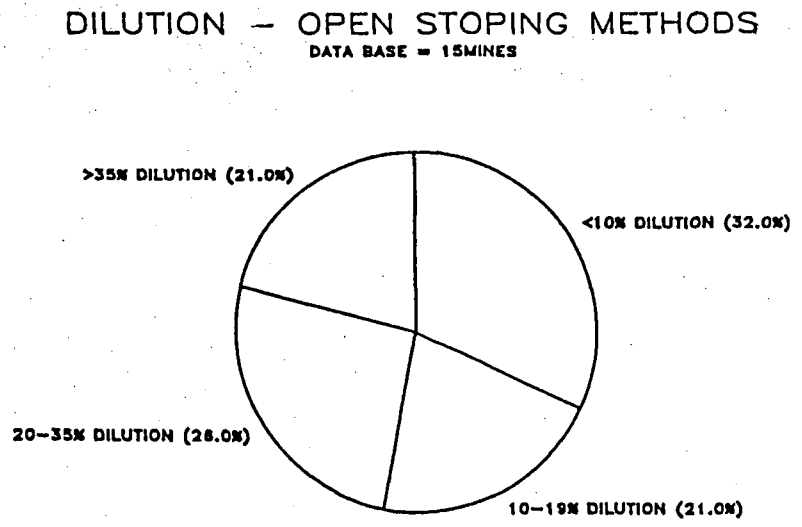

Figure 3.16: Stope Dilution

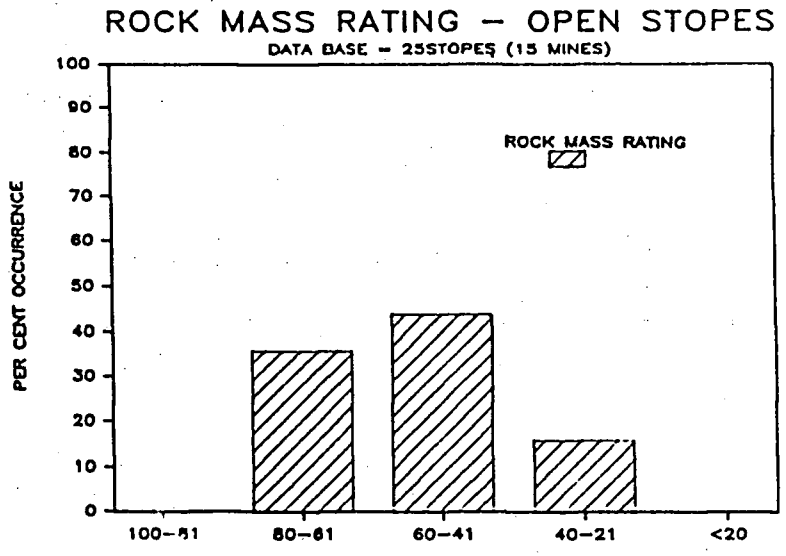

Figure 3.17: Rock Mass Rating

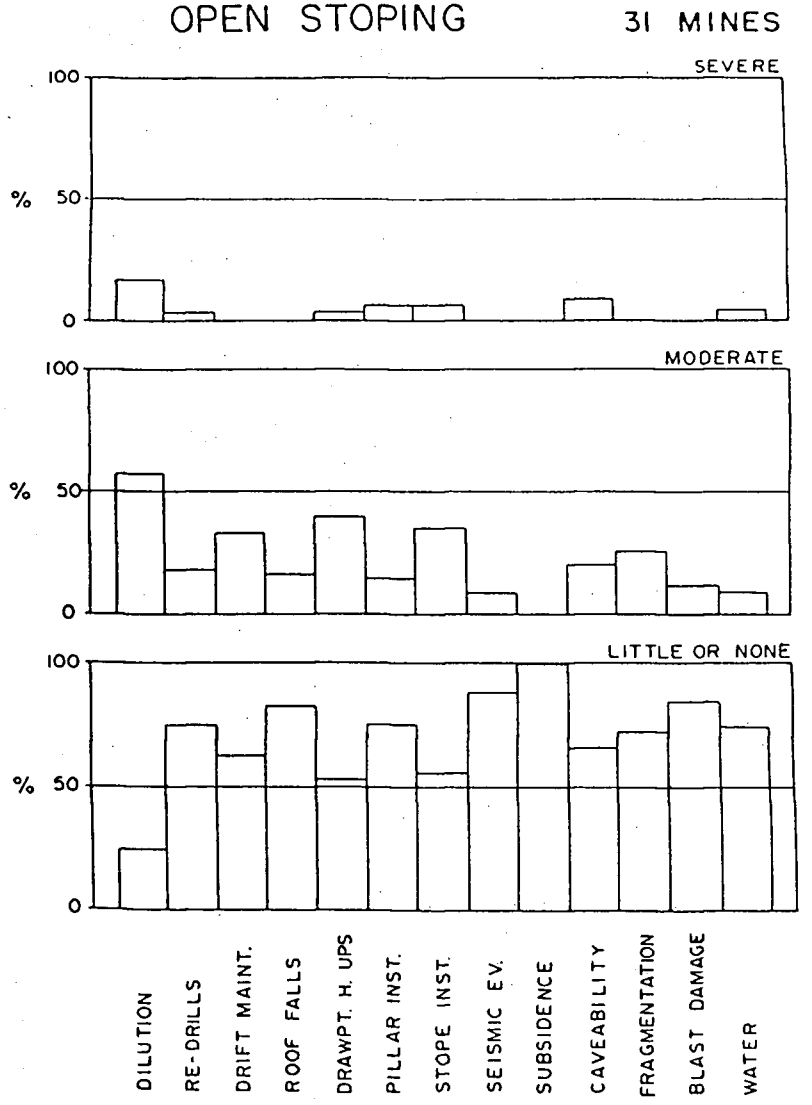

Figure 3.18: Ground Control

Problems in Open Stoping Operations

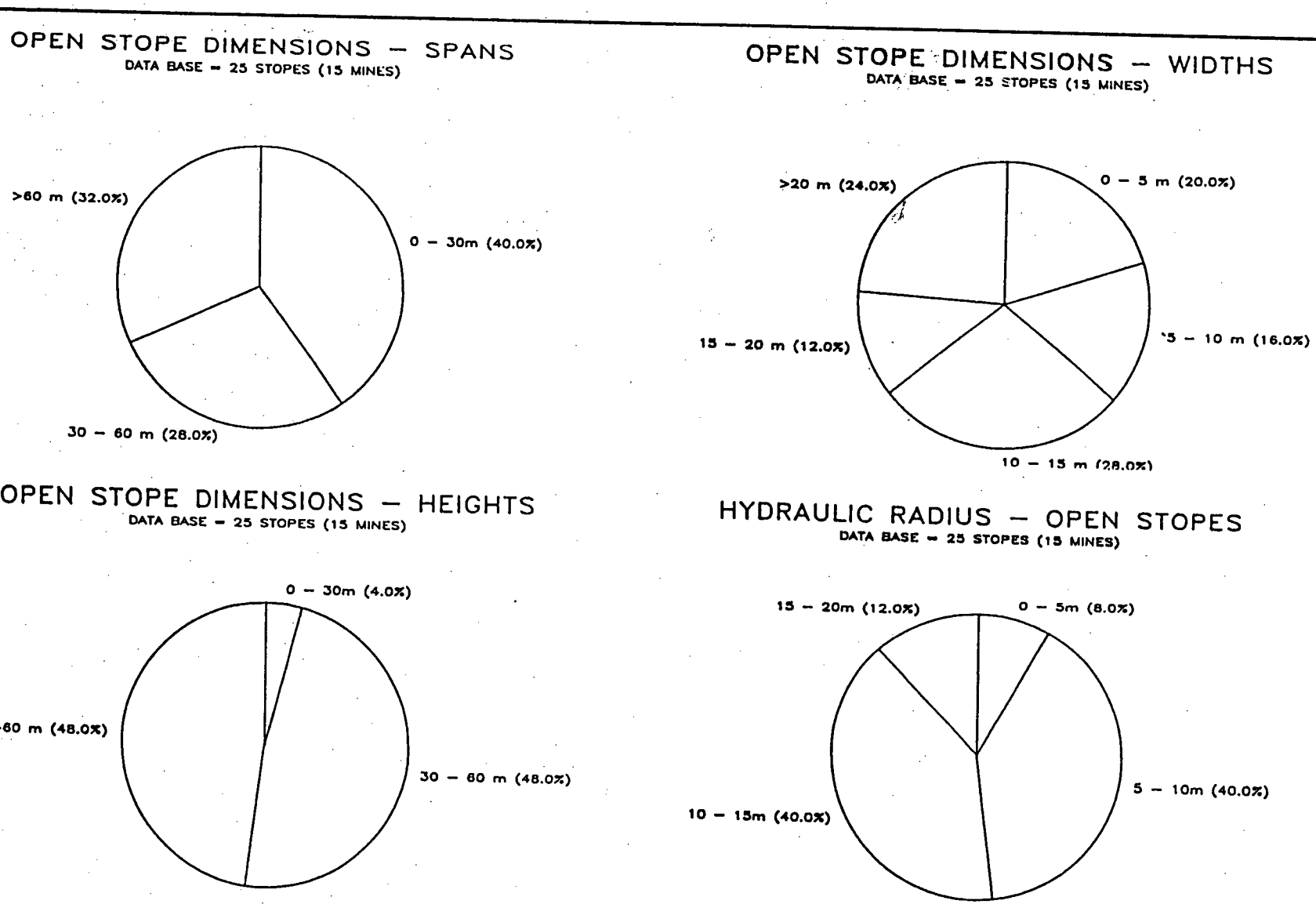

Figure 3.19: Open Stope Dimensions

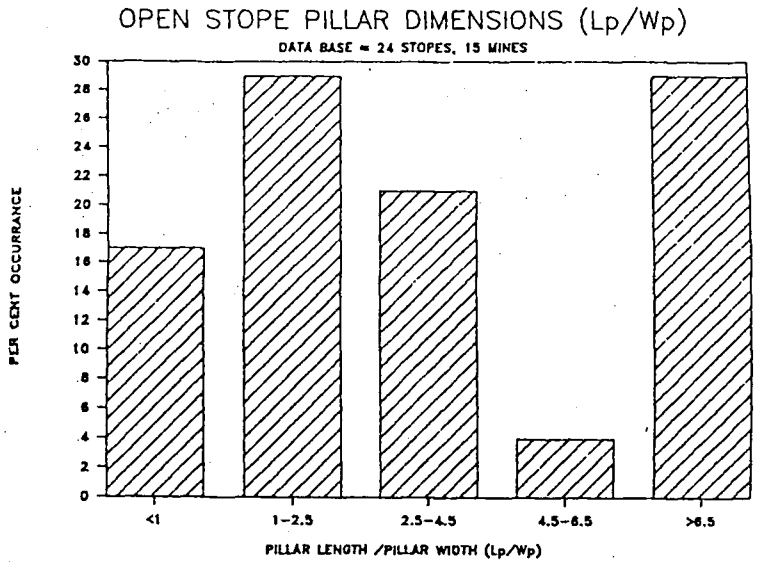

Figure 19b: B376

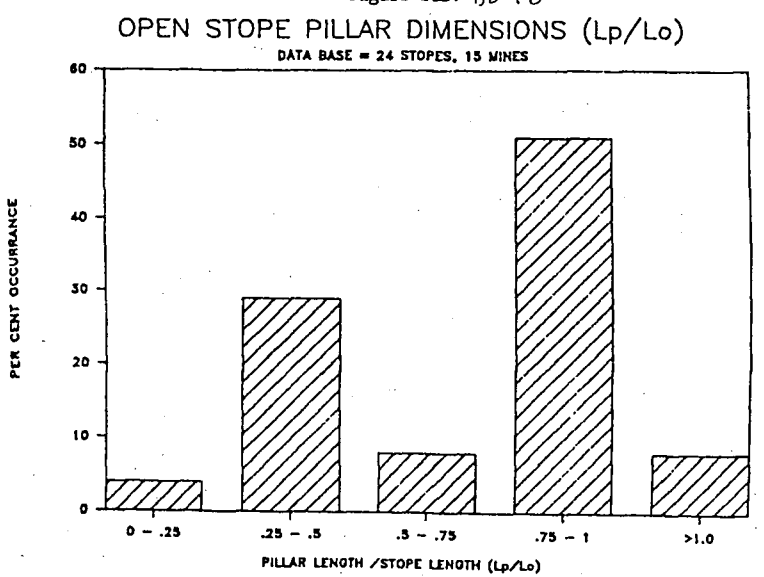

Figure 3.21: Pillar Dimensions

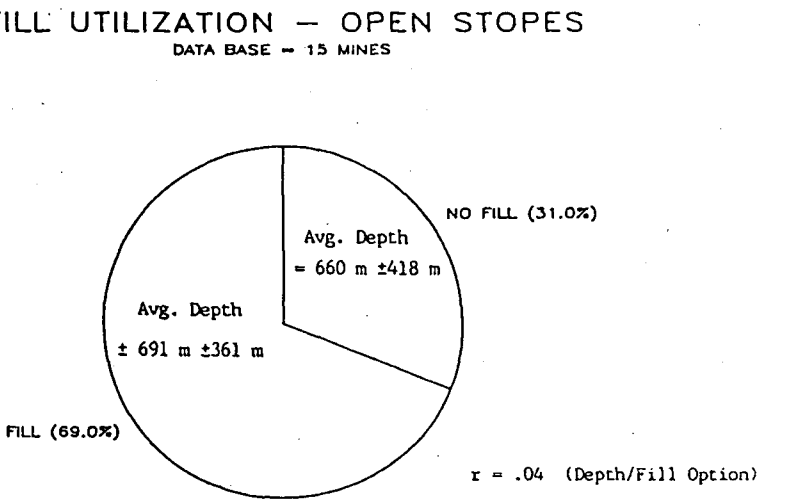

Figure 3.20: Fill Utilization

CHAPTER FOUR

STRESS

4.1 Introduction

This thesis attempts to delineate all parameters that contribute towards wall slough. Brady and Brown (1985) state that upon "identifying the feasible block collapse modes associated with joint attitudes and excavation surface geometry, it is necessary to determine the potential for block displacement under the ambient conditions which exist in the post-excavation state of the opening periphery". The contributing stress factors that would affect the stability of an individual block are gravitational, hydrostatic and confining stresses. This chapter will show that the hanging wall and footwall of stopes at Ruttan are in a state of relaxation. This dictates that all stresses (other than gravitational) acting on a particular wall segment are less than or equal to zero. Consequently that particular segment is not confined and coupled with a jointed material would result in the block to slip out under its' "own weight". This chapter will study the validity of the assumption that the hanging wall and footwall of the individual stopes are in a state of relaxation.

4.2 In-Situ Stresses at Ruttan

Prior to understanding the effect of stresses on openings at Ruttan, it is important to determine the magnitude and orientation of the in-situ rock stresses influencing the Ruttan operation. These stresses are related to the weight of the overlying strata and the geological history of the rock mass.

"Doorstopper-photoelastic" techniques have been employed in the past at Ruttan (Smith,1977). These results, while similar in orientation to the most recent measurements done at Ruttan, were concluded to be anomolous since they were recorded in too close proximity to the tunnel face (0.2 x drift diameter). This section describes a methodical approach to the estimation of the orientation and the magnitude of the in-situ stresses that exist at Ruttan. Initial estimates were made based upon:

- structural interpretation
- virgin stress measurements conducted in other areas (world wide, regional)

The verification of the prevailing stress regime was made by conducting CSIRO hollow inclusion overcoring measurements (Worotnicki and Walton, 1976). The current cost for virgin stress determination is about $7000 per measurement and the difficulty encountered in attaining a good reading is high. Three overcore

tests were performed at the 660m level in order to evaluate the in-situ stress magnitudes and orientations. The prevailing stress regime can be summarized as follows:

-Vertical stress = σv (MPa) = 0.027 x depth (m)
-Major principal stress = $\sigma 1$ = 2.5 σv (340°/ -20°)
-Intermediate principal stress = $\sigma 2$ = 1.2 σv (070°/0°)
-Minor principal stress = $\sigma 3$ = 0.8 σv (160°/-70°)

The above are expressed as azimuth from true north/plunge with individual tests performed 660m below surface.
A detailed analysis of the findings reported in this section can be found in Pakalnis and Miller (1983)

4.2.1 Structural Interpretation

The Ruttan deposit, as stated previously (Chapter 2), is located in a greenstone belt which is postulated to be an island arc. The island arc, is a product of crustal movements, whereby a plate of lithosphere is slowly plunging downward into the mantle. This tetonic activity is thought to have resulted in the inclination of the Ruttan orebody as shown in Figure 2.6. It is postulated that the Churchill province subducted underneath the Superior province and consequently induced the in-situ forces indicated in Figure 2.3.

There is great evidence to suggest that stresses in rock are related to geologic structure (Parker,1973). Figure 4.1 shows the fracture pattern that may result in the crushing of a

rock cylinder. The orientation of the fracture pattern is unique to the applied stress condition. It must be emphasized that only the most "recently formed" structures must be analyzed in order to aid in estimating the orientation of the existing stress field.

Local geological mapping outlined quartz veining and dykes having a trend of approximately N20°W. This corresponds to a major regional feature, the "Mackenzie Dyke Swarm" (Figure 2.3), which is found throughout Northern Manitoba. These structures are tensile features which parallel the major principal stress direction, Figure 2.3. In addition, local folding of quartz veins and the evidence of boudinage all predict a major stress direction, trending approximately N20°W. Foliation paralleling the deposit is the most dominant structure at the mine. It is thought to have formed during the formation of the deposit, whereby due to vertical burial forces, a preferred orientation of platelets parallel to the deposit were established, Figure 4.2.

The above geological environment influencing the Ruttan orebody suggests that the existing stress orientation may be trending N20°W to S20°E.

4.2.2 Previous Measurements

A study of virgin stress measurements conducted in other areas throughout the world will greatly aid in the

determination of the in-situ stress at the proposed location. Figure 4.3 is a plot of vertical stress with depth as compiled by Hoek and Brown (1980). Figure 4.4 is a plot of horizontal to vertical stress as a function of depth, Herget (1980), and is based on numerous measurements conducted within the Canadian Shield. Virgin stress measurements at Ruttan were confined to the 661m level below surface. This would imply the following existing stress magnitudes:

Vertical Stress = 18 Mpa
Horizontal Stress = 27 Mpa
(refer Figures 4.3,4.4)

In-situ stress measurements in the vicinity of the Ruttan orebody have been performed at the Thompson Mine (Moss and Niemi,1985), Thompson and the McLellan Mine (Rotzien and Miller,1985), Lynn Lake (Figure 2.3). The results indicate that the magnitudes of stress can be approximated by Figures 4.3,4.4. The orientations for these two operations can be summarized as follows:

- major principal stress trends N70°W, plunges 10°
- intermediate principal stress trends N30°E, plunges 10°
- minor principal stress is near vertical

4.2.3 Virgin Stress Measurements

To determine the stress at a point in the rock mass, it

is necessary to change the stress from its unknown value (in-situ) to zero, and consequently measure the associated change in strain. This change is introduced by an overcoring operation which completely relieves the stresses acting on a piece of core. Since the state of stress at any point in a body can be completely defined by its three normal stresses and three associated shear components, it is necessary to carry out six independent measurements in the rock. The elastic constants of the rock must also be determined, since strain is related to stress by a deformation modulus.

The CSIRO hollow inclusion cell was employed. The CSIRO cell contains nine gauges; two axially, three circumferencially and four angular gauges oriented relative to the borehole axis. It is installed in-situ and subsequently overcored with corresponding strains recorded. Theory and installation procedure for the CSIRO cell can be found in a paper by Worotnicki and Walton (1976).

Three measurements were carried out in a single borehole at 660m below surface, Figure 4.5. The first test was conducted at a borehole depth of 6.7m, with subsequent tests at 7.1m and 7.4m. This was required in order to ensure that the tests were performed away from any stress influences, (two tunnel diameters). The test hole was inclined at +23 from horizontal and drilled perpendicular to the trend of the orebody. A continuous recording unit was employed, capable of scanning each strain gauge every 20 seconds. Standard HX bits were

employed which produced an 86.7 mm diameter overcore.

4.2.3.1 Discussion of Results

Figure 4.6 summarizes the resultant magnitudes and directions of the principal stresses as derived for each CSIRO test. Note that for certain gauges two strain values were extrapolated since a single value could not be delineated. A modulus of deformation of 70 GPa and Poisson's ratio of 0.18 were employed. Figure 4.7 shows a plot of overcored distance versus released strain for CSIRO Test #2. Partial debonding occurred in CSIRO #1 and #3. This resulted in a considerable variation in the measured stress magnitudes. One method for checking the validity of the results is to see how the derived vertical stress deviates from the overburden stress caused by the weight of the overlying rock. CSIRO values are also compared to other measurements obtained from the literature.

The stress magnitudes, as predicted from the literature, would be as follows:

$$\sigma_v = 18 \text{ MPa}$$
$$\sigma_h = 27 \text{ MPa}$$
$$\sigma_h/\sigma_v = 1.5$$

Stress measurements conducted at Ruttan indicated a σ_h/σ_v ratio ranging from 1.3 to 1.9, which is in agreement with values obtained in other localities, Figure 4.4. Figure 4.6 also shows

that the normalized principal stresses $\sigma 1/\sigma v$, $\sigma 2/\sigma v$, $\sigma 3/\sigma v$ for all three CSIRO measurements were in general agreement:

$\sigma 1/\sigma v$ ratio varies 2.1 - 3.1
$\sigma 2/\sigma v$ ratio varies .9 - 1.2
$\sigma 3/\sigma v$ ratio varies .7 - .8

The above shows that even though the stress values for CSIRO #1 and CSIRO #3 were excessively extreme and variable, the normalized values were in general agreement. These extremes are most likely due to stress concentrations that result from air bubbles in the vicinity of the gauge.

Figure 4.8 is a plot of stress directions recorded throughout the Canadian Shield. In addition, the measured principal stress orientations at Ruttan are also indicated. The measured stress directions and magnitudes are in good agreement with:

- the orebody geometry
- geological environment
- other measurements conducted throughout the Canadian Shield

4.2.4 Observations

It is generally concluded that stress magnitudes and directions are as shown in Figure 4.8. The CSIRO technique

allows one to record the entire strain relief history as overcoring commences. This proved to be invaluable information in utilizing the results from Test #1 and Test #3. The results will be employed in modelling of the induced stress behaviour surrounding openings at Ruttan. Four successful CSIRO stress measurements have been recently conducted on the 620 and 800m level indicating similar results to those described in Figure 4.4. The recent measurements are part of a broader program of research sponsored by CANMET and Sherritt Gordon Mines on the development of stope and pillar design guidelines.

4.3 Stress Configuration

The stress magnitudes and orientations, shown in Figure 4.8, will be employed in order to determine the state of induced stress that exists at the wall contacts. Parametric studies were performed on the geometric shapes shown in Figure 2.17. The variance of axial to diametrical (span/width) dimensions were evaluated in terms of the effect on the state of induced stress. The hypothesis is based upon a "relaxed" state of stress existing in the wall contacts (HW/FW). Consequently, the analysis is more concerned with the qualitative comparisons than with absolute quantitative results. The stress induced regime is evaluated based on the assumption of two dimensional plane strain. It is then verified in the qualitative sense by a three dimensional boundary element numerical code.

4.3.1 Numerical Code

A two dimensional boundary element program was employed. The solution is used to identify and compare the state of stress resulting from different stope configurations. "Bitem", a computer program, obtained from the CSIRO (Commonwealth Scientific and Industrial Research Organization), is capable of two dimensional boundary element modelling of up to five piecewise homogeneous regions. This program was modified to run

on the U.B.C Amhdahl computer system. Further modifications were in enlarging its modelling capabilities and in developing a post-processing program that would graphically display :

- Principal Stress Contours
- Maximum Shear Stress Contours
- Stress Trajectories
- Displacements

In addition, the following failure criteria were incorporated into the program:

- Mohr Coulomb
- No Tension
- Hoek Rock Mass Failure Criterion

The failure criteria were incorporated to identify possible failure zones. This, however, does not form an integral part to the solution of the stated hypothesis. The reader is referred to a report produced by the author "Bitem Operating Manual" and "Plot-Bite" for further details. In addition ,"3DBELM", a three dimensional boundary element program was obtained through CSIRO . The program models the boundary by piecewise flat triangles over which the boundary data varies linearly. Modifications to the program are as follows:

- Modification of code to enable it to run on the U.B.C.

Amhdahl system

- Increase in problem size ie. number of elements and nodes allowed

This program can model multiple openings, however in practice, the associated costs limit its application. Unlike Bitem, it can only model a single piecewise homogeneous region. Table 4.1 summarizes the program specifications for "Bitem" and the "3DBelem" programs respectively.

4.3.2 Parametric Study

The in-situ stresses at Ruttan as shown in Figure 4.8 were employed in modelling typical stope geometries. Figure 4.9 shows that for opening geometries where the in-situ stresses are greatest, perpendicular to the longest dimension result in the immediate sidewall stresses to be tensile. The "k" value, as defined in Figure 4.9, would be greatest in the vertical plane of the orebody and least in the horizontal plane, Figure 4.10. This would yield lower tensile stresses in the horizontal plane of the orebody. For purposes of conservatism, the numerical analysis was conducted on the horizontal plane only. The magnitude and extent of the tensile zone would only be magnified in the vertical plane of the orebody. Parametric studies were conducted whereby the stope span/width ratios, as defined in Figure 4.10, were altered under a constant stress regime. It was shown that for the isolated stope case, for

stopes having a span/width ratio exceeding 0.66:1, the hanging wall and footwall commence going into tension, Figure 4.11. The stress configuration showing minor principal stresses (dashed) and major principal stress contours (solid) for the isolated cases analyzed is shown in Figure 4.12. The extent of the tensile induced zone is shown by Figure 4.13 as a function of the stope geometry. Typical stope geometries at Ruttan approach the 2:1 and 4:1 span/width ratios. This would ensure that the ore contacts (span) will always be in a state of relaxation.

A typical stope span to width of 4:1 would indicate that the extent of the tensile zone would correspond to a wall slough extending 0.55 stope widths beyond the reserve wall contact. The maximum stope dilution recorded at Ruttan is approximately 20% which if, assuming it is generated entirely from the hanging wall, would ensure that the dilution would be entirely confined within the zone of relaxation, Figure 4.14.

The zone of relaxation is more suitable a descriptor of the tensile region since in order for tensile stresses to exist, the rock mass must be able to have a tensile strength. Brady and Brown (1985) suggest that the tensile strength of the rock mass is minimal if non-existent. This may be true. The author, however, believes that a rock mass does have some tensile strength depending upon its rock quality. The reader is referred to a treatise on the subject by Hoek (1983). The term zone of relaxation is taken to mean a zone that is unconfined, consequently, enabling a structural block to be released under

its own weight.

The above analysis is based upon a "k" value of 2.1. This is the in-situ stress as determined at the 660m Level. The data base for this study is derived from stopes ranging in depth from surface to 430m below surface. It is predicted that the in-situ stress ratios will follow patterns similar to those shown in Figure 4.4. This would alter the magnitude and lateral extent of the zone of relaxation. It would be increased since the horizontal to vertical stress ratio is generally found to increase nearer to the surface, Figure 4.4. A lower stress ratio "k", as shown in Figure 4.15, would cause the sidewall stresses to be more in compression than in tension. In addition, the extent of the zone of relaxation would reduce as shown in Figure 4.16. The analysis has been based on assuming:

- that a plane strain condition exists
- opening is within an isotropic, elastic and homogeneous medium.

The first condition assumes that all displacements will occur within the plane being analyzed, consequently resulting in the third dimension being an intermediate principal plane. This assumption and its implication on the hypothesis will be further analyzed in the section on 3D modelling. The second assumption is valid to the extent of what this parametric study was intended to show. That was that the hanging wall and

footwalls of the Ruttan stopes are in a state of relaxation under the prevailing stress regime. The conditions also enable the parametric study to be reduced to stress magnitudes that are independent of the elastic constants.

The effect of rib and echelon configurations are shown by Figures 4.17,4.18. Figures 4.17,4.19 and 4.20 show the magnitude of major and minor(tensile) principal stresses surrounding two and three stopes located along strike. It differs from the base case shown in Figure 4.21 in that the hanging wall and footwall are in a greater tensile state.

The lateral extent of the zone of relaxation has not greatly increased beyond that of the base case. This is due to the integrity of the pillar that is modelled as a rigid element. In actual fact, due to the high compressive stresses in the rib pillars modelled, these pillars will ultimately crush. The final stress configuration will more closely resemble that of the isolated case with dimensions 8:1 and 12:1 (span/width).

The echelon configuration shown in Figure 4.18 as compared to the base case reveals that the wall contact forming the longitudinal pillar is not in a state of relaxation, but in a state of confinement. The stope span that forms the abutment is in a lower state of tensile stress than that found for the base case. In addition, the lateral extent of the zone of relaxation has been reduced, Figure 4.20. The echelon configuration, Figure 4.18, commences to resemble the stress

configuration for the 2:1 and 1.3:1 span/width ratios for the isolated stopes investigated in Figure 4.12. Ultimately, the tensile region surrounding the footwall and hanging wall abutments will be replaced by compressive stresses upon the addition of more echelon lenses. The echelon stopes can also be envisioned as being mined in a destressed area which is in the "stress shadow" of the previously mined stope. This results in an overall more stable stope extraction configuration assuming that the longitudinal pillar remains intact and the area to be mined has not been greatly disturbed by the extraction of the adjacent stope. The mining of the succeeding echelon stopes should therefore be facilitated in terms of the resulting stress regime.

The above parametric study enables observations made in subsequent chapters to be correlated to the state of stress encompassing the individual hanging wall and footwall contact. Further analysis on the effect of fill and stope sequencing will be discussed in following chapters.

4.3.2.1 Verification of 3D Model

Brown (1985) states that the plane strain boundary stress usually approximates the correct three-dimensional stresses to within less than ten, and sometimes five per cent at locations removed by at least two excavation "diameters" from excavation ends and intersections. The above is particularly valid for uniform excavation cross-sections ie. axial ratios are not extreme (span/width). The rule of thumb, "two excavation diameters", is not particularly valid for all in-situ stress magnitudes and orientations since it has been derived for a circular opening in a uni-directional stress field (Elissa,1980). It starts to become invalid when openings begin to resemble axis ratios as shown in Figure 4.22. Figure 4.22 shows how the "end effects" of individual stopes may come into importance in modelling individual planes. Case A of Figure 4.22 is truly a plane strain situation with resultant intermediate stresses paralleling the dimension perpendicular to the stope (z). This is a further assumption made in plane strain and is generally valid since the third dimension will not result in a stress concentration due to far removed end effects. The resultant stress will be equal to or less than in-situ stress paralleling this direction. On the other hand, the stresses modelled in the plane strain will be modified due to stress concentrations and redistributions occurring within that plane. Case B of Figure 4.22 shows that employing a "one

or two" excavation diameter zone of influence, the modelled plane will be influenced by the individual end configurations. The dimension perpendicular to the plane will also undergo stress concentrations and consequently, will not necessarily be an assumed intermediate principal stress plane upon excavation. Mathews (1981) has adopted an approach to modelling open stopes in a method discussed in Chapter 3.2 whereby stresses in the sidewall are determined employing a plane strain analysis for a horizontal and a vertical section through the midspan of the particular wall. Mathews employs the larger of the two values in subsequent analyses. The results are calibrated to empirical observations which is the method normally employed by practioners. The three dimensional codes presently in use are generally:

- difficult to apply
- expensive in terms of computer time usage
- require a high degree of experimental and theoretical skill

(Hoek,1983)

In addition, Brady (1985) states that " in the design of an underground rock structure, such as a mining structure consisting of a set of stopes and pillars, the system of openings and support members is frequently too complex to allow adequate 3D modelling of the structure and it is necessary to resort to plane strain methods of analysis". It is the author's opinion that upon undertaking a thorough literature search of

two dimensional and three dimensional comparisons that:

- minimal published works if any exist on the comparison of 2D and 3D models
- accepted practice is to employ plane strain analysis and to calibrate the model.

A similar approach was taken by Chen et al(1983) whereby multiple sub-level open stopes were modelled employing two-dimensional, non-linear elastic-plastic finite element methods. It was realized that the geometry was three-dimensional and the method employed was not entirely correct. However, due to the large computer costs incurred with 3D modelling, therefore limiting the number of cases that could be simulated, the investigators opted for a calibrated 2D plane strain analysis. Chen (1983) states that theoretical studies have shown that stress concentrations around symmetrically shaped openings in two-dimensional cases are always slightly greater than those in three-dimensional.

Figure 4.23 shows an example of five adjacent stopes that form part of a much larger mining block of the Mt. Isa mine . The extreme axial ratios and geometric irregularity required that a complete three-dimensional analysis be carried out to accurately determine the true pillar boundary stresses. The major and minor principal in-situ stresses are in the "xz" plane with $\sigma 1$ and $\sigma 3$ rotated clockwise by 25° from the x and z axes, respectively. The intermediate principal in-situ stress acts in the y direction. The three-dimensional stress analysis

carried out by Watson and Cowling (1985) gave :

- Lower maximum stress concentrations than those which were calculated by use of plane strain approximations.

- The effect of the group of openings on the stress field was found to be more localized in three-dimensional than in two-dimensional solutions.

A three dimensional solution was attempted for this study by employing "3DBELM". The objective of this portion of the study was to show that the hanging and foot wall is primarily in a state of relaxation and consequently, dilution is attributed to the release of structural blocks under gravity. The existing literature on three-dimensional modelling is minimal and too general in substance. A three-dimensional approach was applied to the base case shown in Figure 4.21. A stope 30m high,20m in span and 5m in width was generated. These dimensions are similar to the actual axis ratios that exist at Ruttan. Figure 4.24 shows the model employed with the triangular surface elements indicated. In-situ stresses as determined previously were employed:

- x direction 2.5 $\measuredangle$ v
- y direction 1.2 $\measuredangle$ v
- z direction 0.8 $\measuredangle$ v

Seventy (70) nodes and one hundred and thirty-six (136) triangular elements were employed. The cost of running this

program on the U.B.C. Amhdahl 580/5850 system was $40.00 or in terms of CPU time equal to 120 seconds. The rates are based on UBC charges of $480/hr CPU time (normal priority) and a factor of 3.2 which represents additional charges for memory usage and file input/output. Commercial bureau rates would be five times this amount.

Vertical and horizontal sections of the generated stress distributions were produced as shown in Figures 4.25,4.26. Stress magnitudes in terms of $\sigma x, \sigma y, \sigma z$ and $\sigma 1, \sigma 2, \sigma 3$ were determined at various intervals on and external to the boundary. Figure 4.25a shows that the tangential stresses at the midpoint of the horizontal plane are in tension in either direction within the "yz" plane ($\sigma y = \sigma 3 = -49$ MPa, $\sigma z = \sigma 2 = -27$ MPa). The extent of the relaxed zone has been contoured and represents the furthest extent that tension is observed. This tension is recorded within the "xy" plane. The magnitudes and relaxed zone distribution tend to be extreme when related to the base case 2D-plane strain analysis, Figure 4.21. Reasons for this are as follows:

- end effects not accounted for
- mesh is particularly coarse since each element is 5m in length

A further analysis was conducted whereby the height of the stope was extended to 300m with the remaining parameters

unchanged. The horizontal profile H-H´ is shown in Figure 4.25b for the modified geometry. A comparison is as follows between 2D and the 3D models:

Comparison	2D	3D
Tangential stress mid-span	-9MPa	-7MPa (σ_3= -9 MPa)
Extent of relaxed zone	.55W	.6W (W=stope width)

The contours drawn in Figure 4.25 refer to the tangential stresses on the boundary and the minor principal stresses off the boundary. The minor principal stress was found to be consistently located within the "xy" plane. The in-situ minor principal stress is oriented in the "z"direction prior to excavation and upon excavation becomes the intermediate stress direction. This has been discussed previously. The above comparison does indicate the importance of end effects, however, the author must caution the reader in pointing out that the magnitudes of the coarser mesh are extreme. A vertical section was also analyzed with the original stope configuration, Figure 4.26. The magnitudes again are extreme, however, the zones of relaxation can be contoured and represented as shown in Figure 4.27. Figure 4.28 shows the modelled stope outlining the elements which are in a complete state of relaxation.

Finer meshes or more complex geometries were not modelled in three-dimensions due to the high computer costs and time of preparation involved. Two stopes having similar coarse

meshes to that previously modelled would cost $200 per run. It is assumed that the results generated, however, would not alter the premise that the HW/FW are in a state of relaxation.

4.3.2.2 Observational Approach

In addition to the analytical approach discussed previously, measurements and observations were made at Ruttan to reinforce the premise that the wall contacts are in a state of relaxation. Extensometers and stress meters were installed at the inception of underground mining, March 1979, in order to monitor the first stopes mined.

Stressmeters throughout the mine were evaluated in order to understand the mechanism of stress transfer that occurs due to mining. The following areas were analysed:

- 400mL west lenses extraction, Figure 4.29
- 340mL west lenses extraction
- 340ml east lenses extraction

Vibrating wire stressmeters (Irad,1977) and extensometers (Smith,1976) were employed. The stressmeters were able to measure directional change in stress and were oriented as shown in Figure 4.29. They were located primarily in pillar cross-cuts and footwall and hanging wall drives. Orientations were either north - south(N), east - west(E) or vertical (V). The extensometers were located perpendicular to ore contacts

and within pillars. The results were analyzed as part of this study in order to establish a mechanism of stress distribution by observation. Problems that occurred with the analysis are in the:

- poor location of certain stressmeters ie. at corners of openings

- stressmeters not oriented in the direction that would yield maximum benefit for interpretation

- extensometers drilled to lengths that exceeded 100m which are excessive in terms of giving reliable and repeatable results

Upon excavation, the north/south and east/west stressmeters located in the vicinity of the hanging wall and footwall decreased, Figures 4.30,4.31. Extensometers indicated that upon extraction, the HW/FW commenced converging towards the opening, Figure 4.32.

An investigation of stope sequence, Goldbeck (1985), was analytically assessed employing the BITEM code. Figure 4.33 is a typical extraction sequence at Ruttan generally duplicating the configuration and extraction sequence of the stopes previously identified. Individual observation points were analyzed and for purposes of this thesis, only the hanging wall observations will be reproduced. A detailed analysis is found in "Analysis of Stress Changes at Ruttan Mine" by Goldbeck (1985). Location "A and C" is shown in Figure 4.34b, indicating that upon excavation in the vicinity of the

observation points, the north/south stresses decrease. Prior to excavation, a stress buildup is observed as shown in location C for cuts 1 through 5. Similarly for the east/west stresses, Figure 4.34b, a large tensile stress change is observed upon excavation. The results have been plotted in terms of change of stress from in-situ, in order to be related to the recorded stress gauges. A quantitative assessment may be made, however, for purposes of this study, it is sufficient to say that " the hanging wall and footwall are analytically shown to be in a relaxed state".

A photograph depicting the effect of stope relaxation is shown in Figure 4.35. Initially, the rock mass exhibited closed joints and upon excavation of the adjacent stope, joint separation occurred. Figure 4.35 shows joints paralleling the hanging wall of 320-12B stope on the 240m level.

4.4 Conclusion

The purpose of this chapter was to prove an important assumption in order to employ the data base under the premise that failure is kinematically controlled. Subsequent chapters will show that adversely oriented discontinuities exist and are primarily responsible for the resultant dilution. The degree of dilution will then be related to parameters that will have the greatest impact on its magnitude, stress not being one of those factors. The relaxed zone was concluded in this chapter to

encompass all isolated, rib, and echelon stopes having configurations resembling those of Ruttan. The resultant dilutions are well within the zones of relaxation and consequently are not considered to be greatly effected by geometry. This will be discussed further in Chapter 6, "Dilution".

Table 4.1: Numerical Code

Title:	Boundary Integral Technique for Multiple Materials
Program:	BITEM
Capacility:	Solves two-dimensional elasticity problems for a piecewise homogeneous, isotropic elastic solid using the boundary integral equation method with linear variation of displacements and tractions along the boundary segments, and allowing mixed displacement and traction boundary conditions. The solid may be composed of at most five homogeneous regions with differing elastic constants. Problem symmetry can be taken into account. Facilities for automatic data generation are available.
Input:	Problem geometry - node coordinates, symmetry properties. Elastic properties of each homogeneous region. Nodel boundary conditions. Points within solid at which stress and displacement solutions required.
Output:	Statement of input data, plus data generated by the problem. Tractions and displacements on all boundaries of the problem. Stress and displacement solutions for selected interior points.
Language:	ANSI FORTRAN IV
Origin:	BITEM was written at the CSIRO division of Applied Geomechanics and is based on program BITE which analyses homogeneous solids only. Refer Crotty and Wardle (1977) and Riccardella (1973). The program was converted from CDC to IBM FORTRAN by R. Pakalnis (1983), University of British Columbia.
Information:	Further information may be obtained from -

Commonwealth Scientific and Industrial Research Organization
Institute of Earth Sciences
Division of Applied Geomechanics
P.O. Box 54
Mount Waverley, Vic. 3249
Australia

Mining and Mineral Process Engineering Dpt.
6350 Stores Road
University of B.C.
Vancouver, B.C.
V6T 1W5
Canada

Documentation: CSIRO and supplemented by work of R. Pakalnis, University of British Columbia

Title:	Three Dimensional Boundary Element Program for Mining Applications
Program:	3DBELM
Capacity:	Program models a three-dimensional boundary by piecewise flat triangles over which the displacements and tractions vary linearly. The boundary may be composed of multiple openings within a single homogeneous region. Problem symmetry can be taken into account.
Input:	Problem geometry - node coordinates, symmetry properties. Elastic properties of the homogeneous region. Nodel boundary conditions. Points within solid at which stress and displacement solutions required.
Output:	Statement of input data, plus data generated by the problem. Tractions and displacements on all boundaries of the problem. $\sigma x, \sigma y, \sigma z, \sigma xy, \sigma xz, \sigma yz, \sigma oct, \sigma normal$. Stress and displacement solutions for selected interior points.
Language:	ANSI Fortran IV
Origin:	3DBELM was written at the CSIRO Division of Applied Geomechanics and is based on program Bite which analyses homogeneous solids. Refer Crotty and Wardle (1977) and Riccardella (1973). The program was converted from CDC to IBM FORTRAN by R. Pakalnis(1983), University of British Columbia.

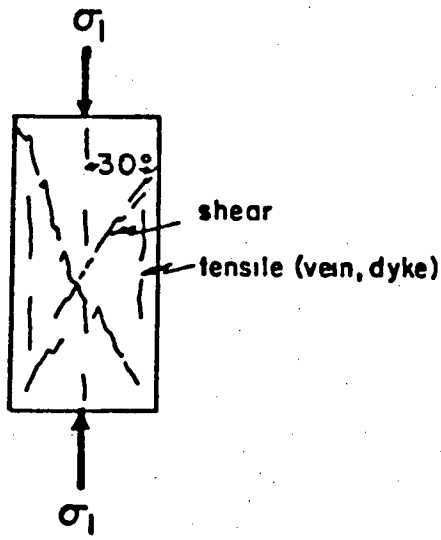

Figure 4.1: Fracture Pattern Caused by Crushing of a Cylinder

(refer to section 4.2.1)

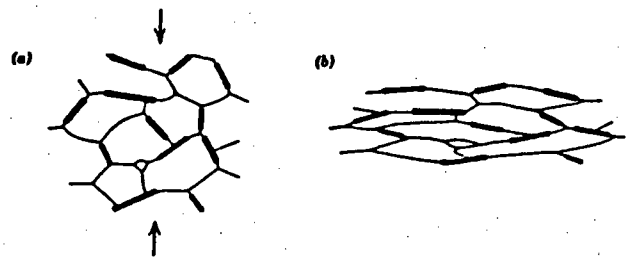

Figure 4.2: Possible Explanation for the Formation of Foliation Platelets

(refer to section 4.2.1)

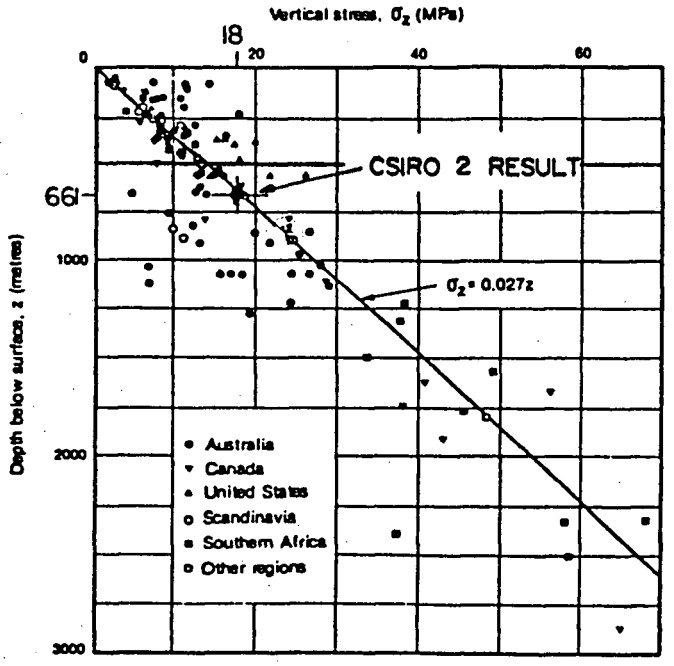

Figure 4.3: Vertical Stress Vs Depth (Hoek, 1983)

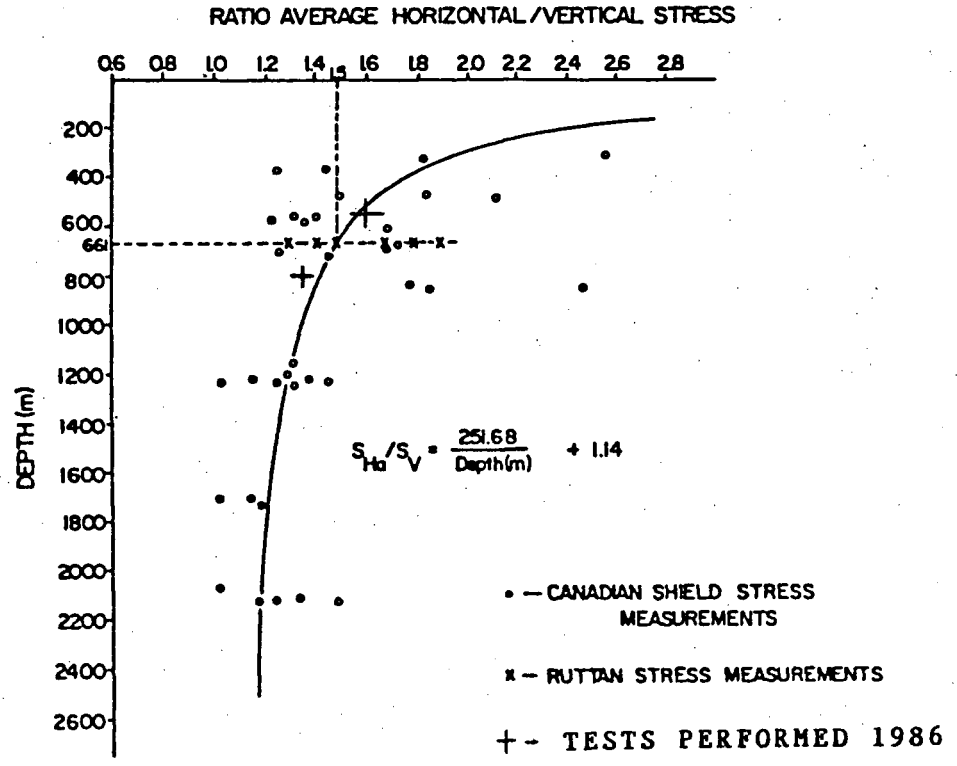

Figure 4.4: Horizontal Stress Vs Depth (Herget, 1980)

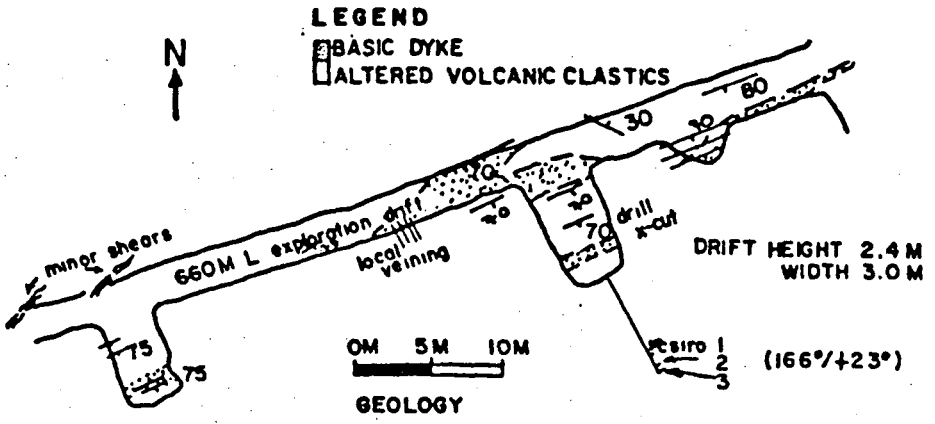

Figure 4.5: Stress Measurement Location

(E = 70 GPa, υ = 0.18, Z = 661m)

TEST NUMBER	PRINCIPAL STRESSES $\sigma 1$ MPa	$\sigma 2$ MPa	$\sigma 3$ MPa	$\sigma 1$ BRG DIP	$\sigma 2$ BRG DIP	$\sigma 3$ BRG DIP	VERT STRESS σv MPa	HORIZONTAL STRESSES $\sigma h \perp$* MPa	$\sigma h \parallel$* MPa	'K' FACTOR $\frac{\sigma h \perp}{\sigma v}$	$\frac{\sigma h \parallel}{\sigma v}$	$\frac{\sigma h \text{ avg}}{\sigma v}$	$\frac{\sigma 1}{\sigma v}$	$\frac{\sigma 2}{\sigma v}$	$\frac{\sigma 3}{\sigma v}$	*A % DIFF σv Theor	*B % DIFF $\frac{\sigma h}{\sigma v}$ Theor (Mean)
1A	96	31	27	344 -18	85 -30	226 -54	35	89	30	2.6	0.9	1.8	2.8	0.9	0.8	93%	20%
1B	121	32	28	340 -19	81 -30	221 -54	39	110	31	2.8	0.8	1.8	3.1	0.8	0.7	119%	20%
2	46	27	15	341 -24	231 -38	95 -43	25	41	22	1.7	0.9	1.3	1.8	1.0	0.5	38%	-13%
$2^{\text{Less G8}}$	45	21	14	346 -17	248 -26	106 -59	18	42	19	2.4	1.1	1.8	2.5	1.2	0.8	0%	20%
$2^{\text{G8 Avg}}$	45	20	14	347 -16	250 -23	109 -61	17	42	19	2.4	1.1	1.8	2.5	1.2	0.8	4%	20%
3A	63	28	26	342 -22	74 -4	174 -68	30	59	28	1.9	0.9	1.4	2.1	0.9	0.8	70%	-7 %
3B	65	29	25	347 -22	79 -6	185 -67	30	59	30	1.9	1.0	1.5	2.2	1.0	0.8	68%	0%

$\perp$: Horz. Stress Perpendicular to Orebody Trend 340/0°

$\parallel$: Horz. Stress Parallel to Trend 70/0°

*A σv Theoretical = 18 MPa

*B $\frac{\sigma h}{\sigma v}$ Theoretical = 1.5

Figure 4.6: CSIRO Stress Magnitudes and Orientations

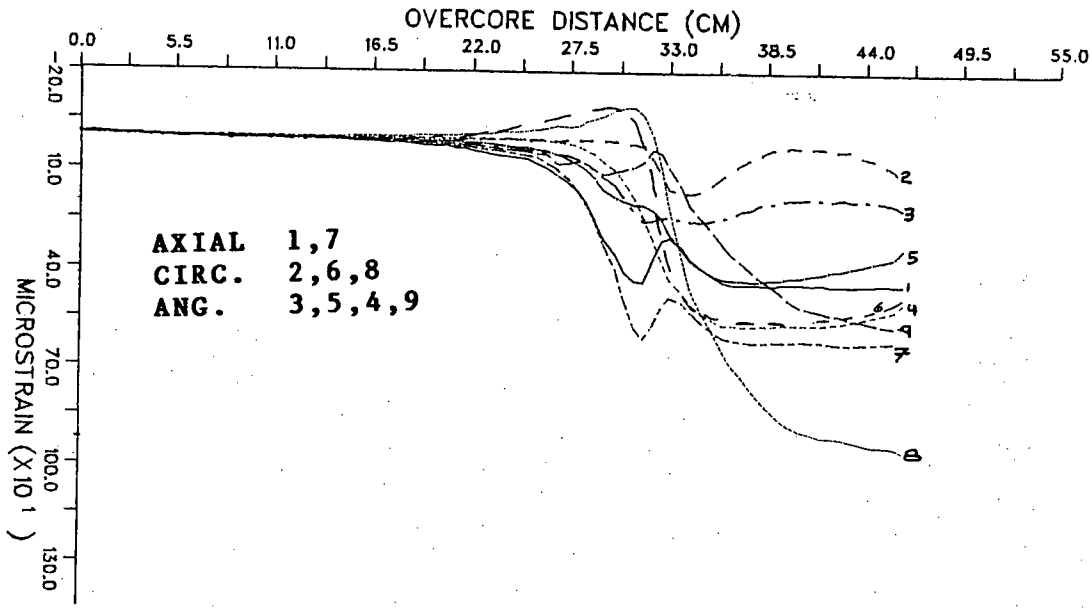

Figure 4.7: CSIRO Test #2 - Overcore Distance Vs. Released Strain

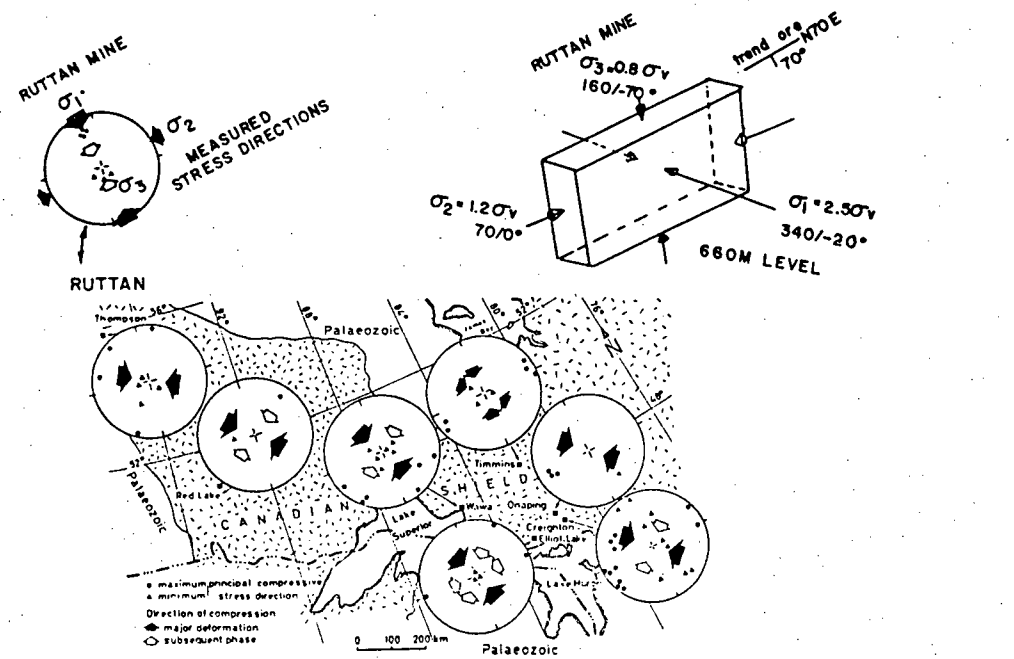

Figure 4.8: Measured Principal Stress Directions and Suggested Direction of Compression During Tectonic Deformation (Herget, 1980)

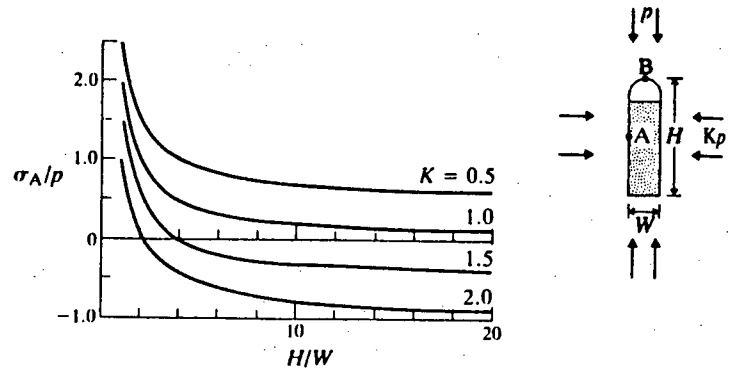

Figure 4.9: Sidewall Stresses as a Function of Opening Geometry and Applied In-Situ Stress (Bray, 1985)

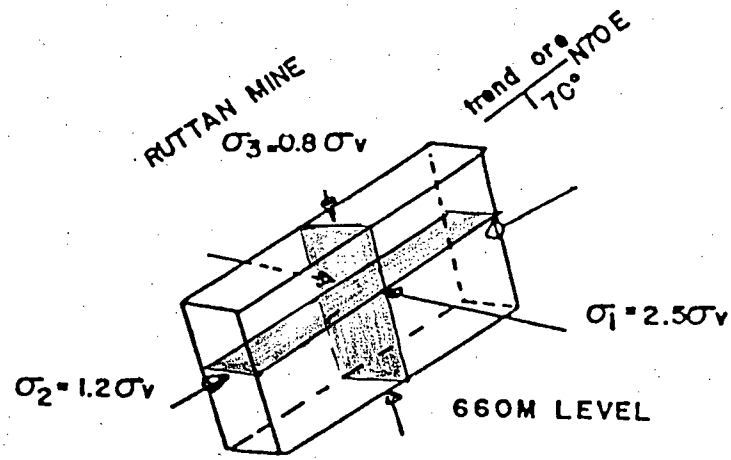

$K_{vert.\ plane} = \frac{2.5\sigma V}{0.8\sigma V} = 3.1$

$K_{horiz.\ plane} = \frac{2.5\sigma V}{1.2\sigma V} = 2.1$

Figure 4.10: Horizontal/Vertical Stress Ratio (k)

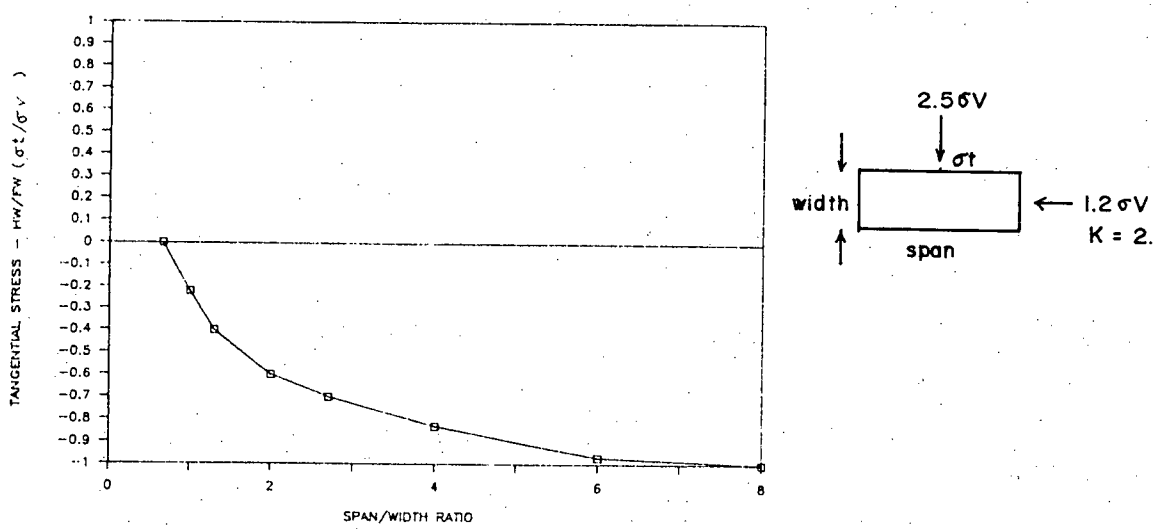

Figure 4.11: Tangential HW/FW Stress Vs Span/Width

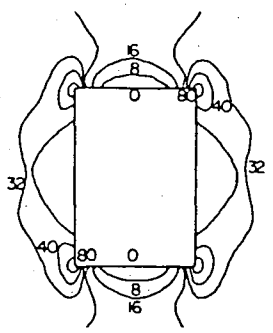

Length/Width = 0.66:1

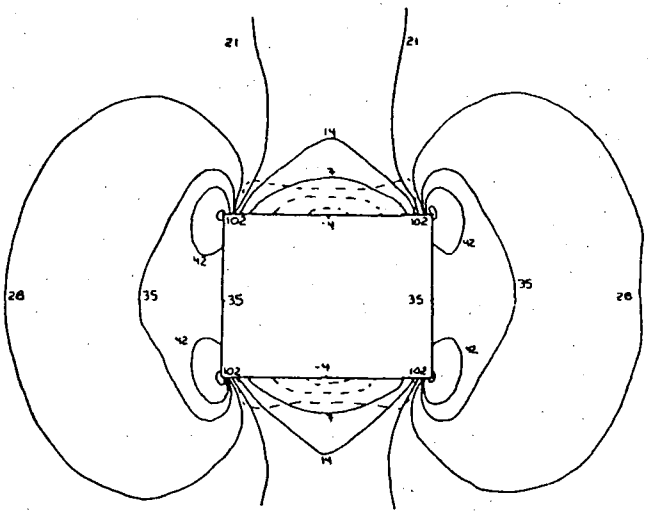

Length/Width = 1.3:1

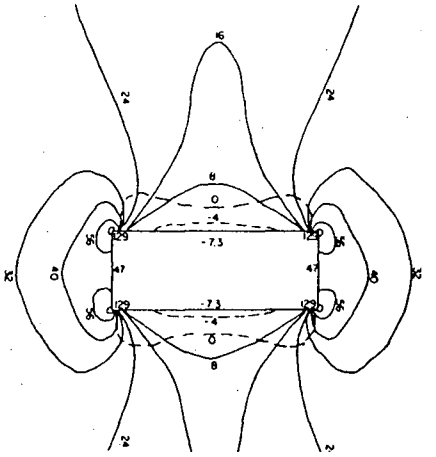

Length/Width = 2.7:1

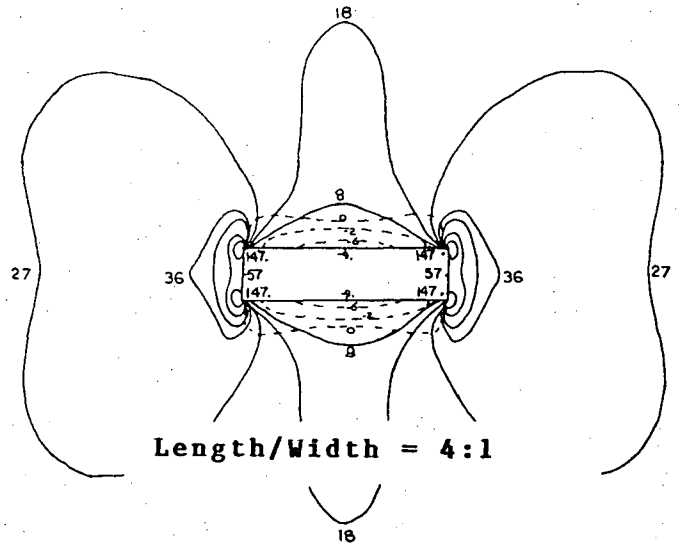

Length/Width = 4:1

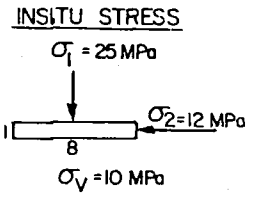

STRESS CONFIGURATION

—— MAJOR STRESS CONTOURS

----- MINOR STRESS CONTOURS (TENSION)

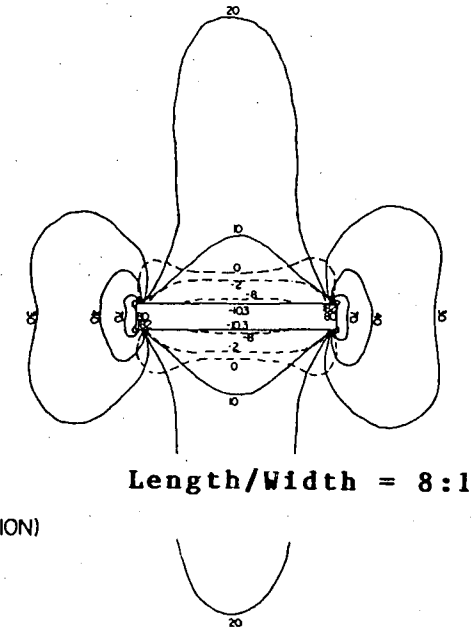

Length/Width = 8:1

Figure 4.12: Stress Configuration - Parametric Study

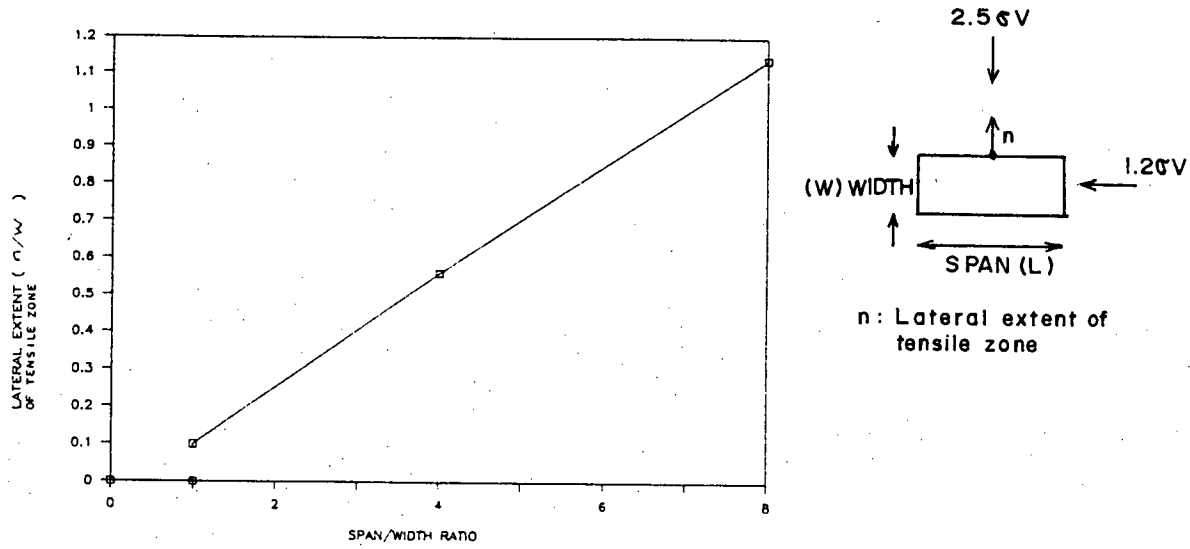

Figure 4.13: Lateral Extent of Tensile Zone

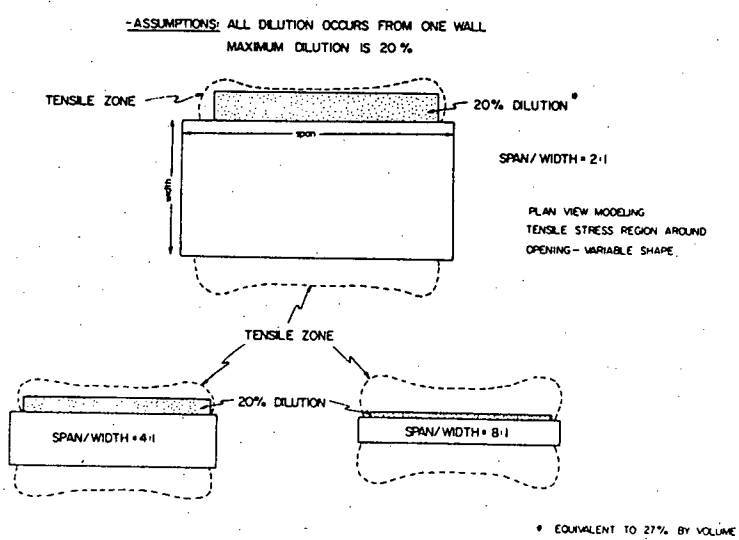

Figure 4.14: Relationship Between Dilution and Tensile Zone

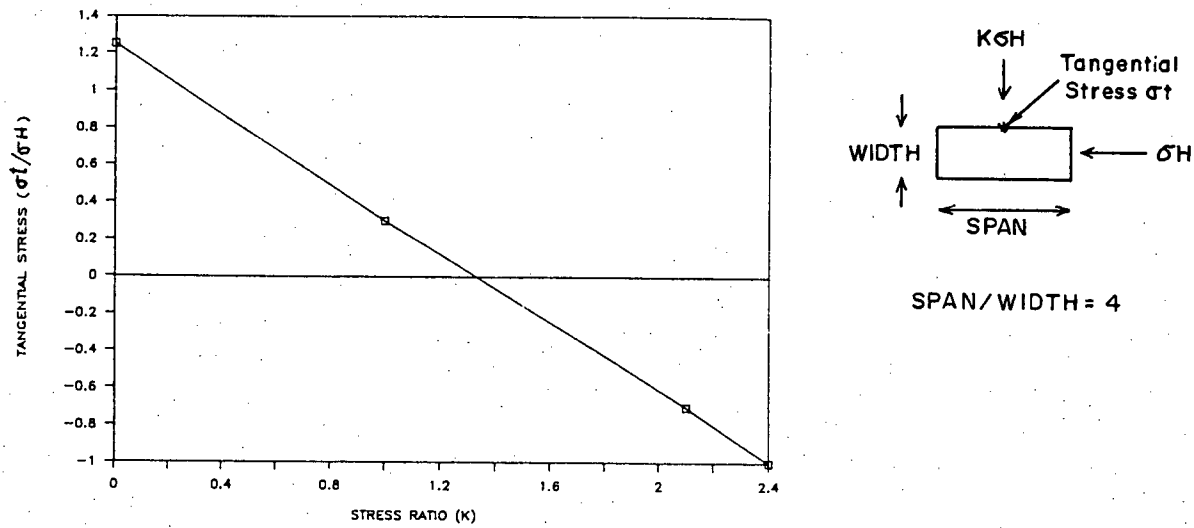

Figure 4.15: Effect of "k" on the Tangential Stress in the FW/HW

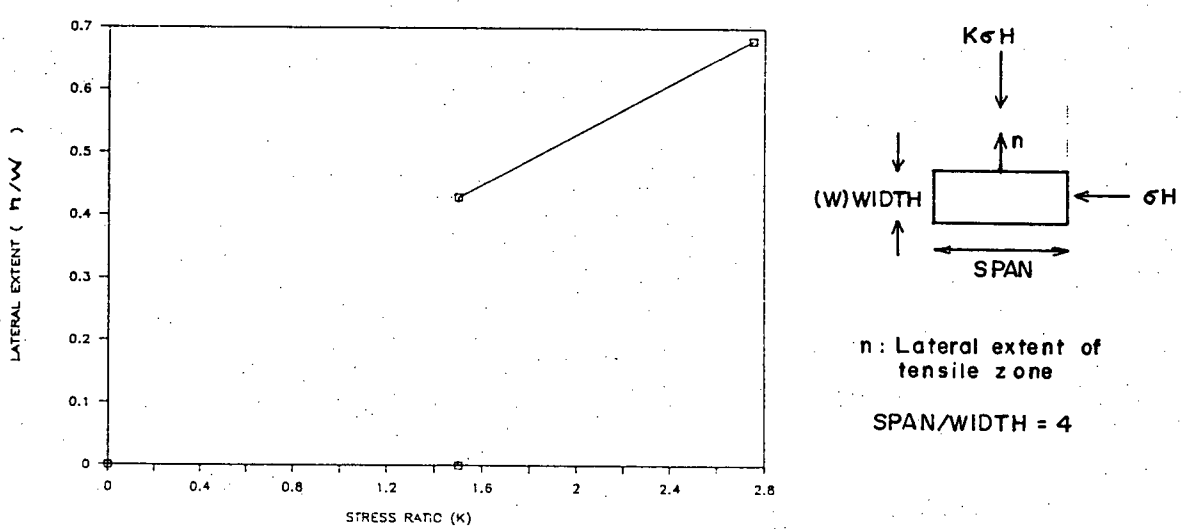

Figure 4.16: Extent of Lateral Tensile Zone with Variance in "k"

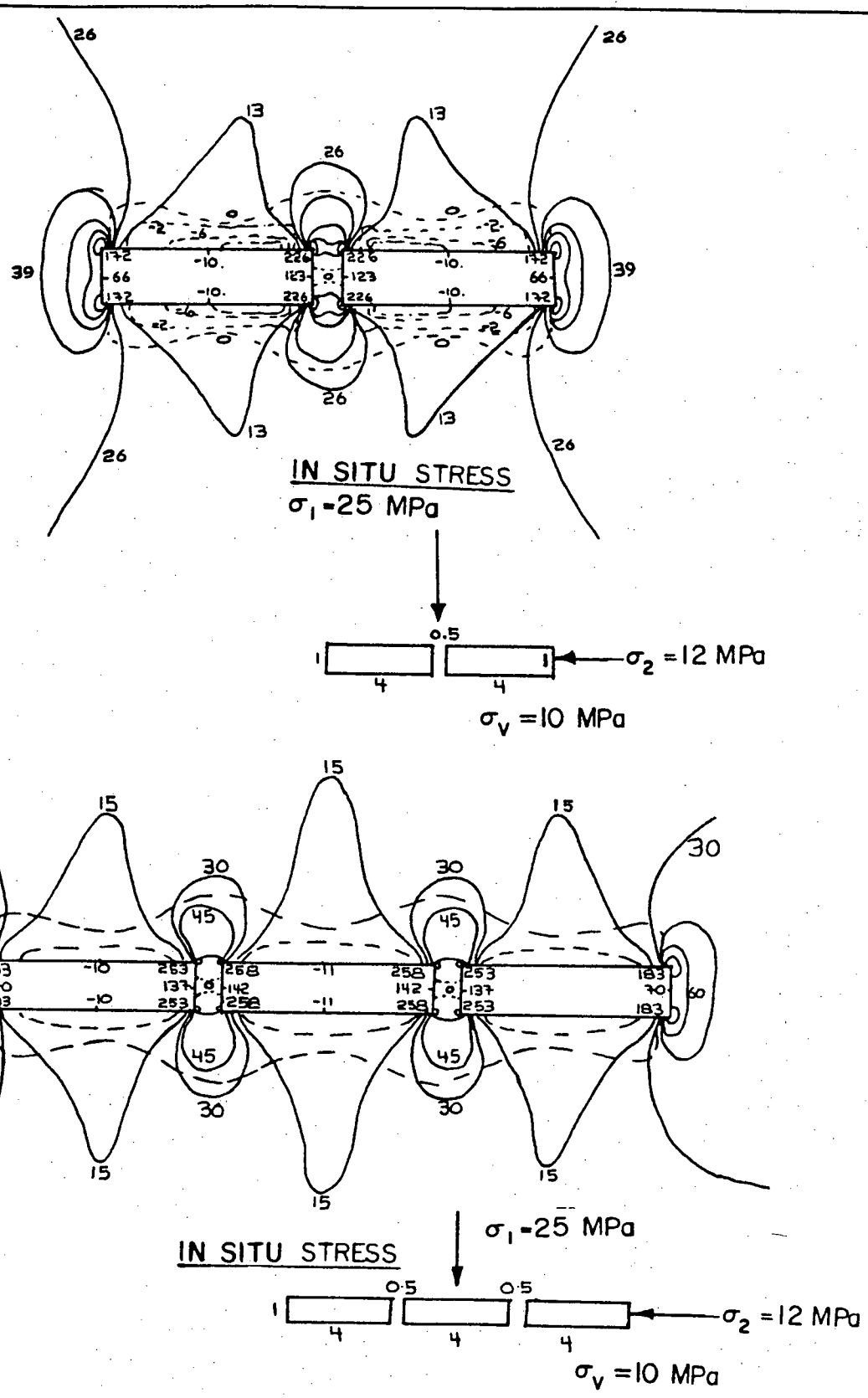

Figure 4.17: Stress Configuration - Rib Stopes

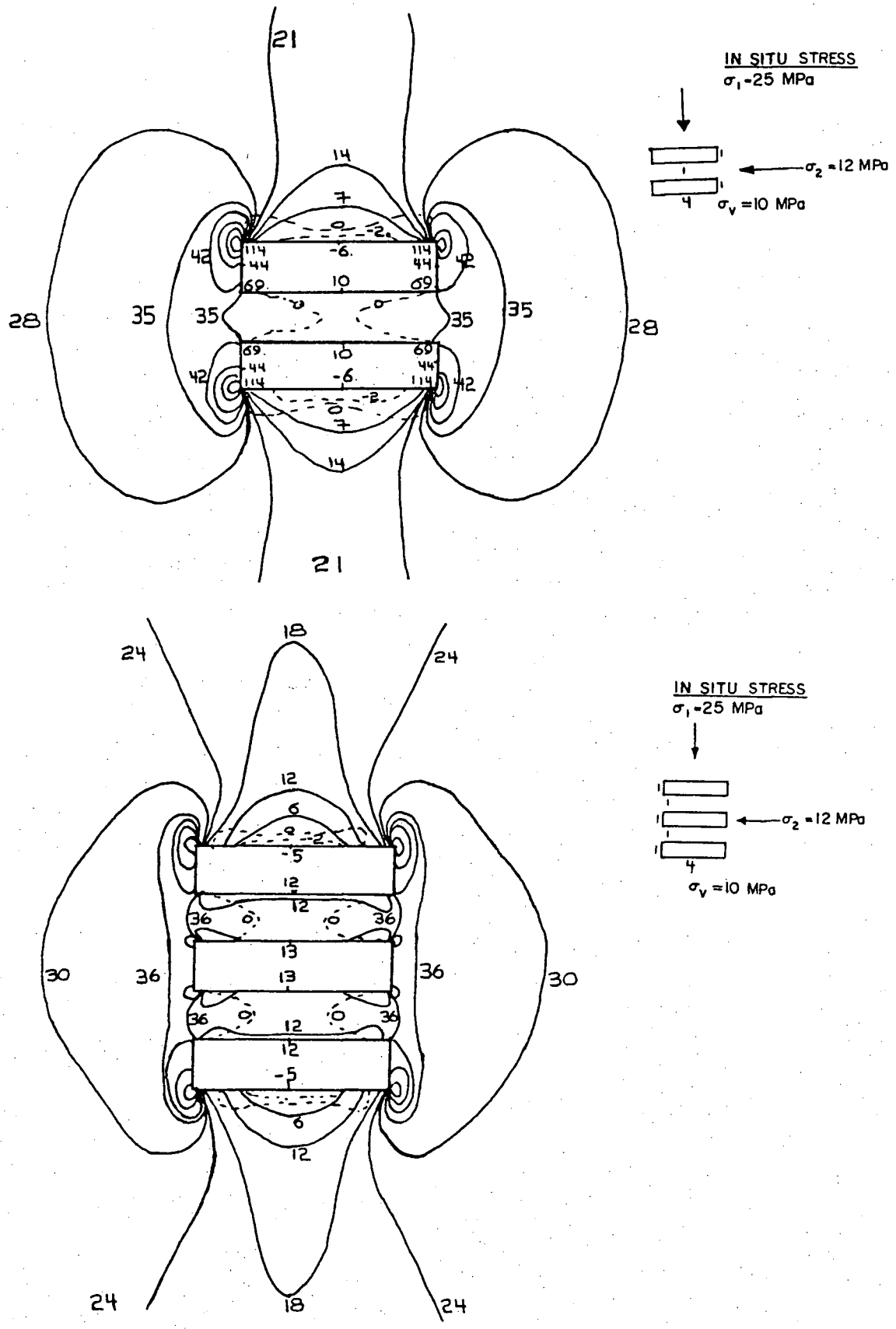

Figure 4.18: Stress Configuration - Echelon Stopes

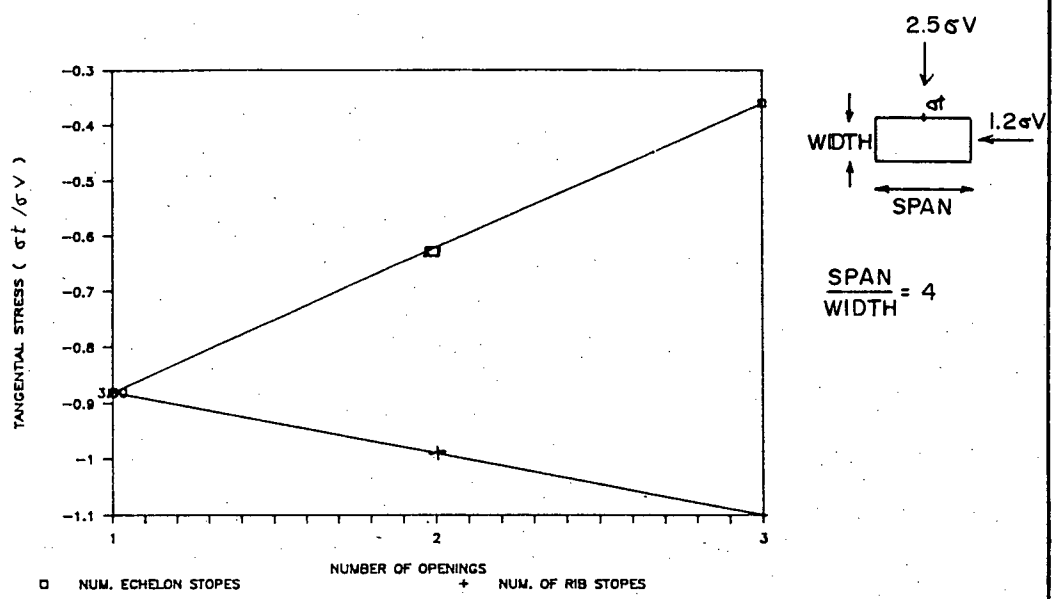

Figure 4.19: Variation of Tangential Stress with Number of Openings

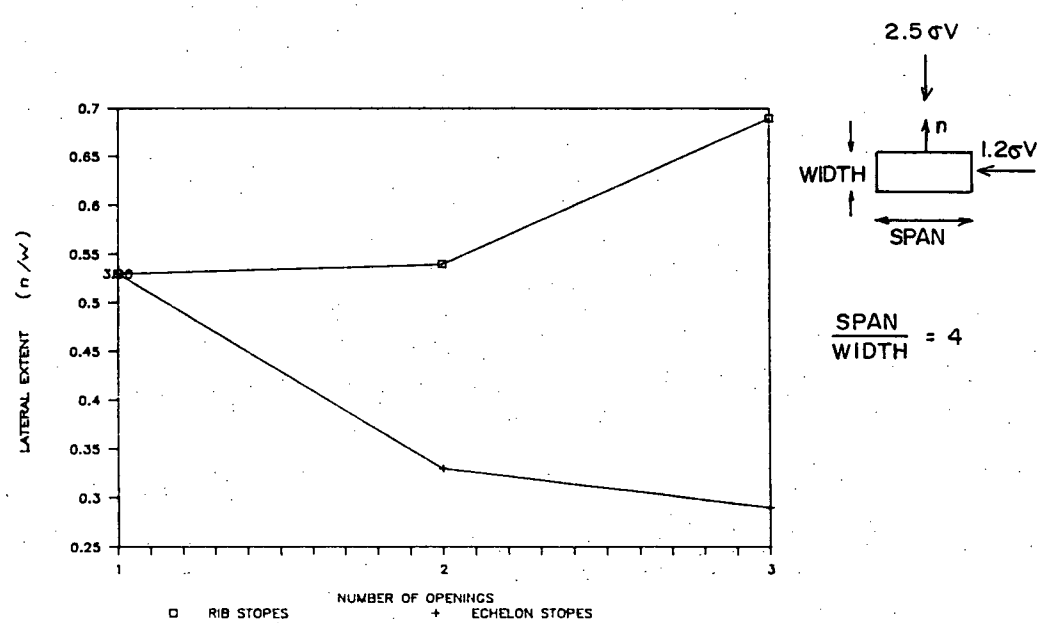

Figure 4.20: Variation of Lateral Extent of Tensile Zone with Number of Openings

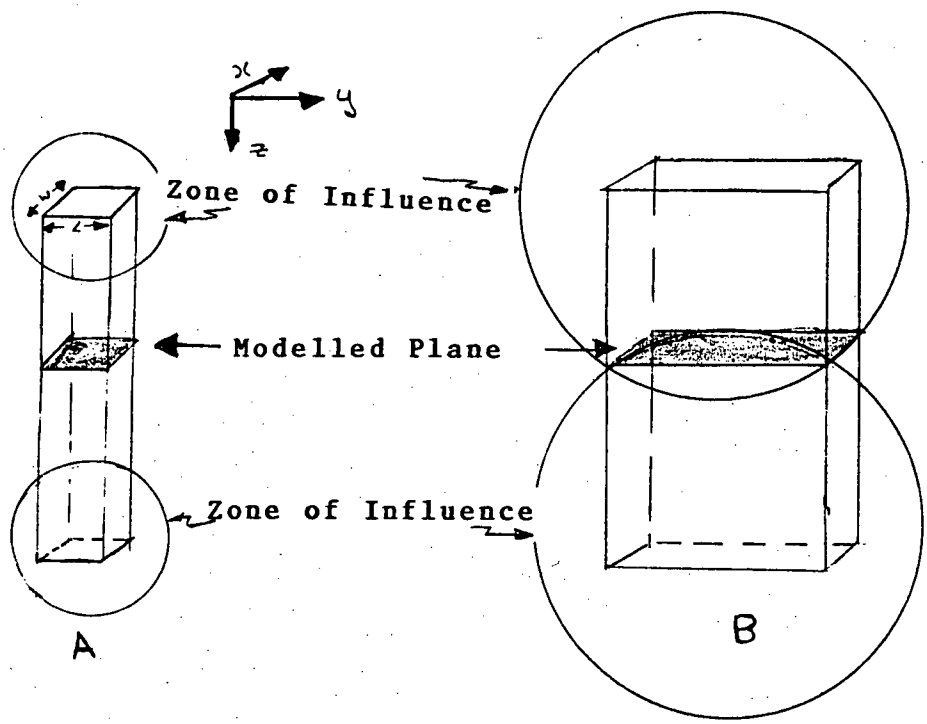

Figure 4.22: Influence of End Effects

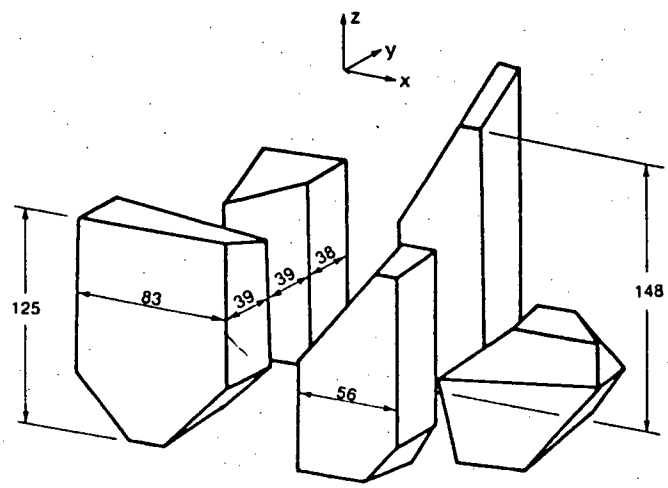

Figure 4.23: Stope Geometry - Mount Isa Mine, analysed by 3D-Boundary Element (Brown, 1985)

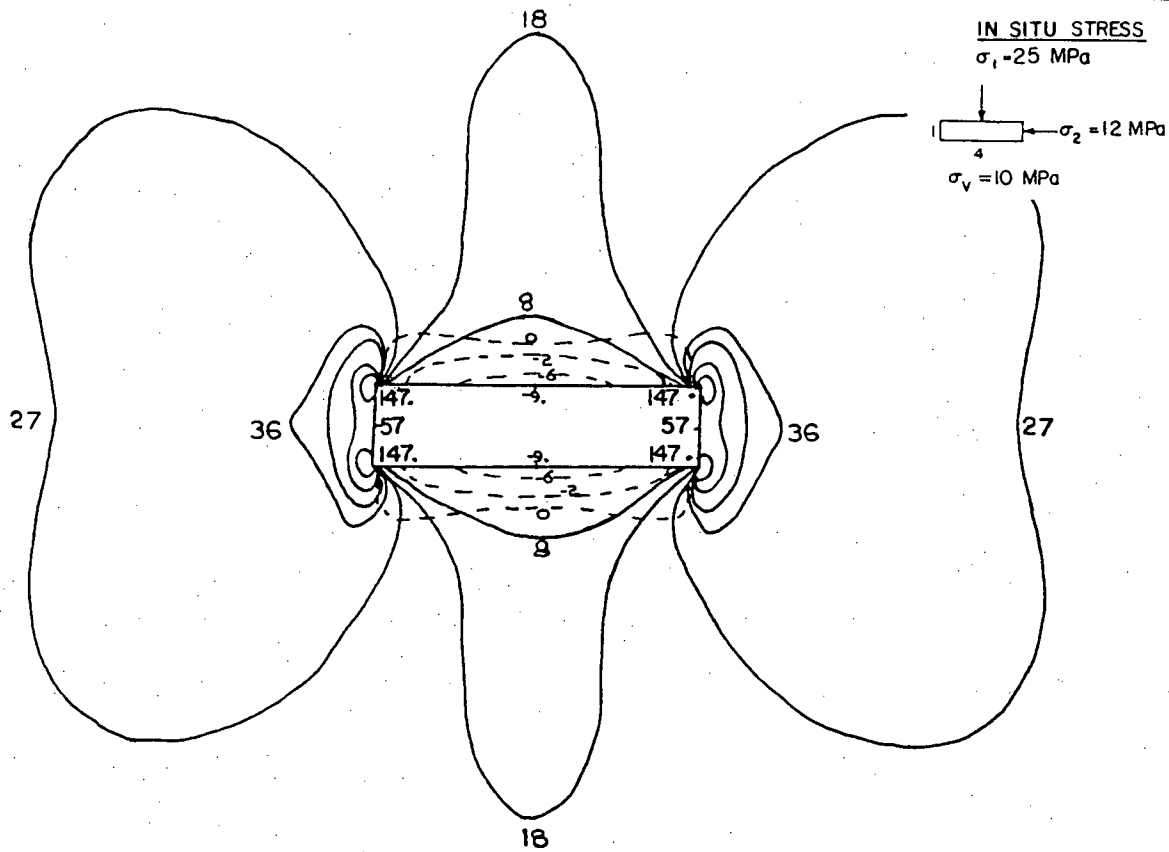

Figure 4.21: Base Case - Stress Configuration

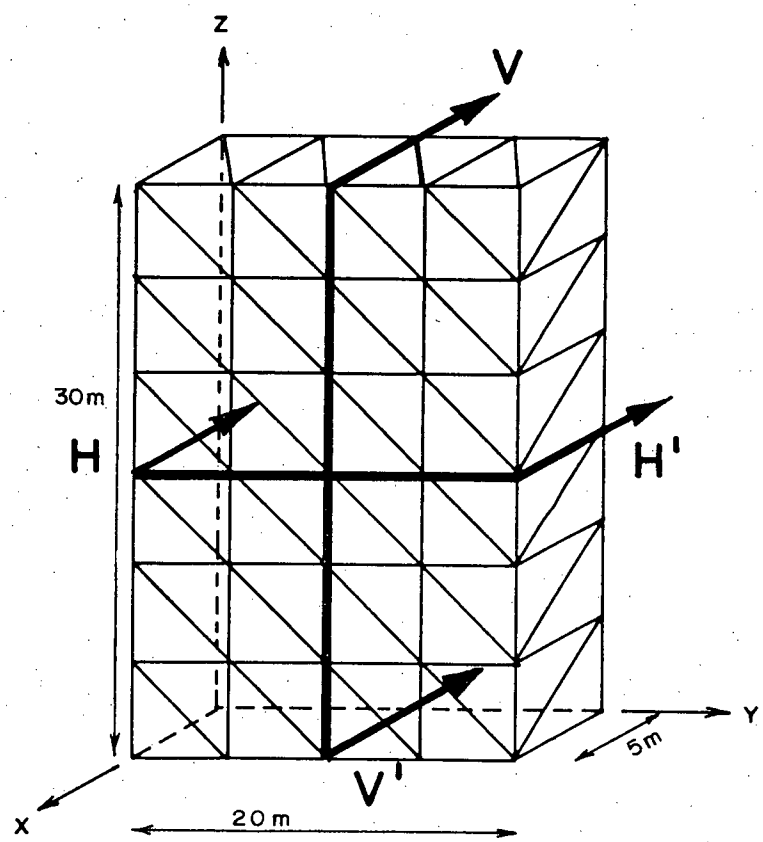

Figure 4.24: 3D Modelled Stope

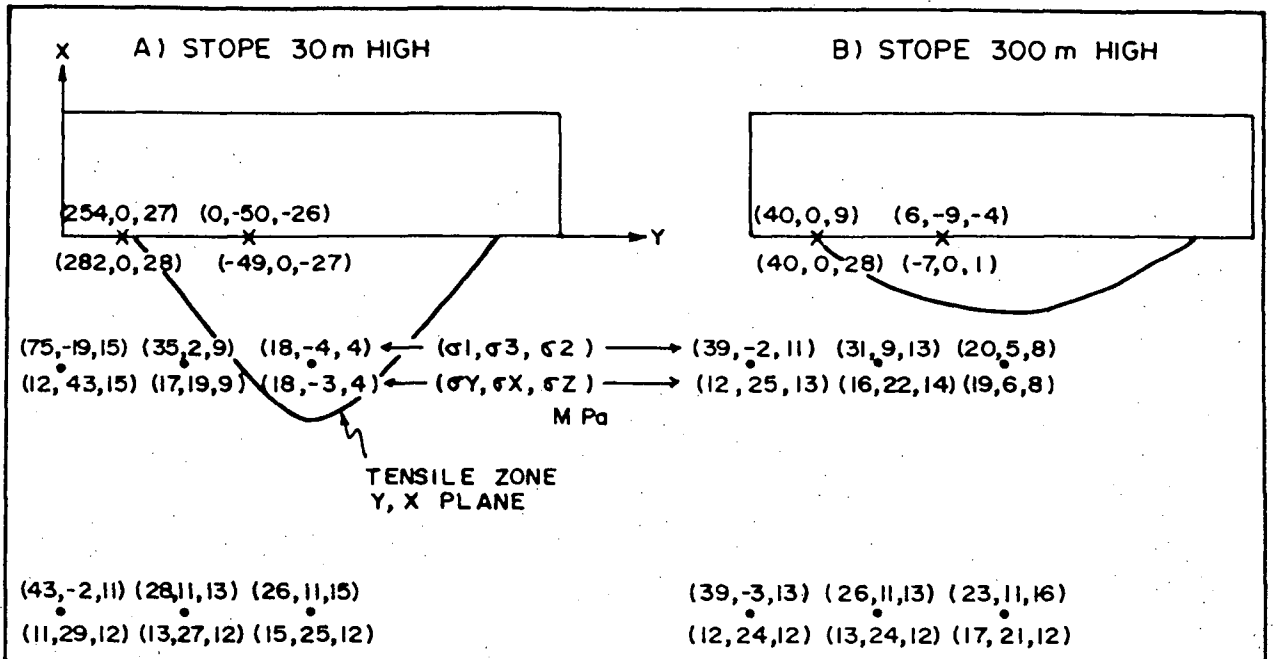

Figure 4.25: Extent of Tensile Zone - horizontal Plane H - H'

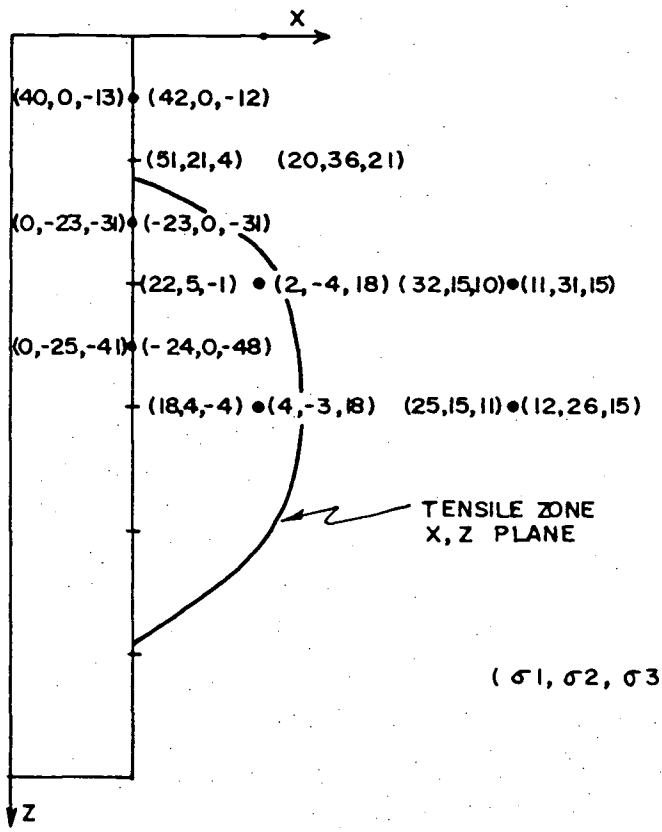

Figure 4.26: Extent of Tensile Zone - Vertical Plane V - V'

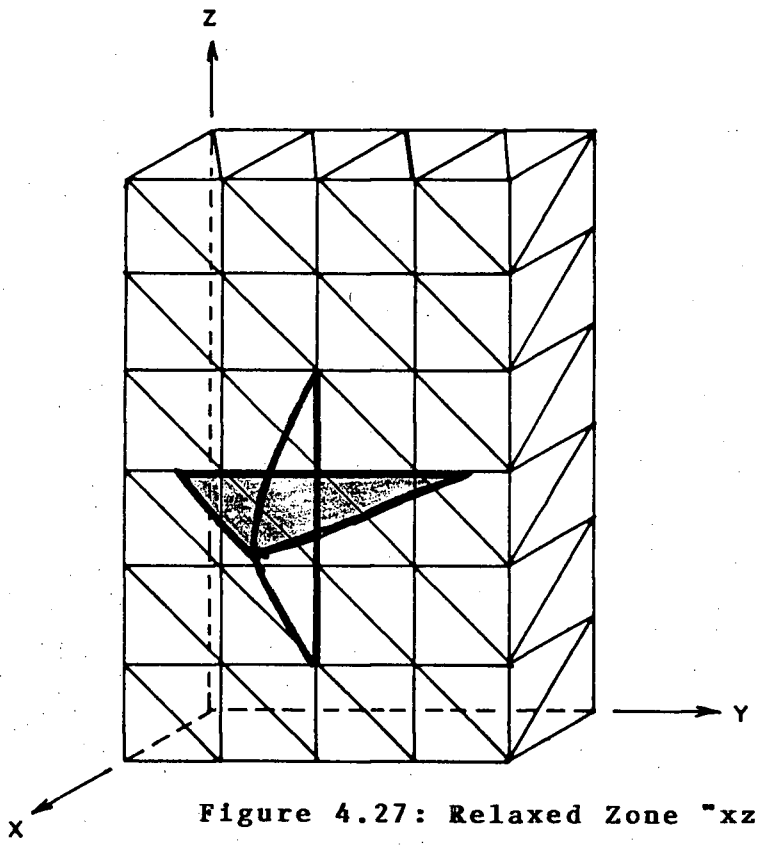

Figure 4.27: Relaxed Zone "xz and xy" plane

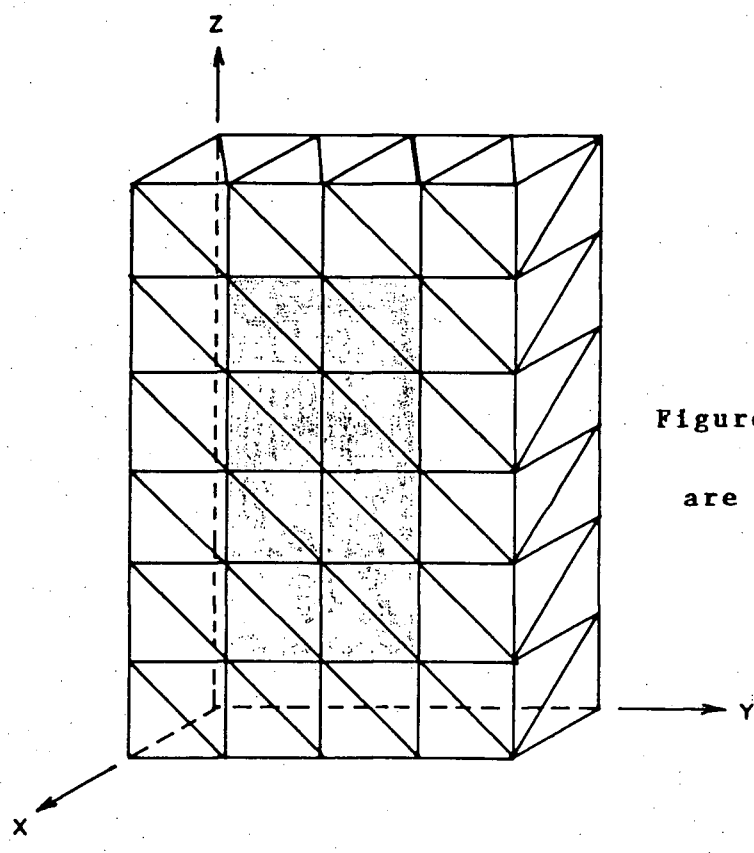

Figure 4.28: Shaded Elements are in a State of Relaxation (All Stresses $\leqslant$ 0)

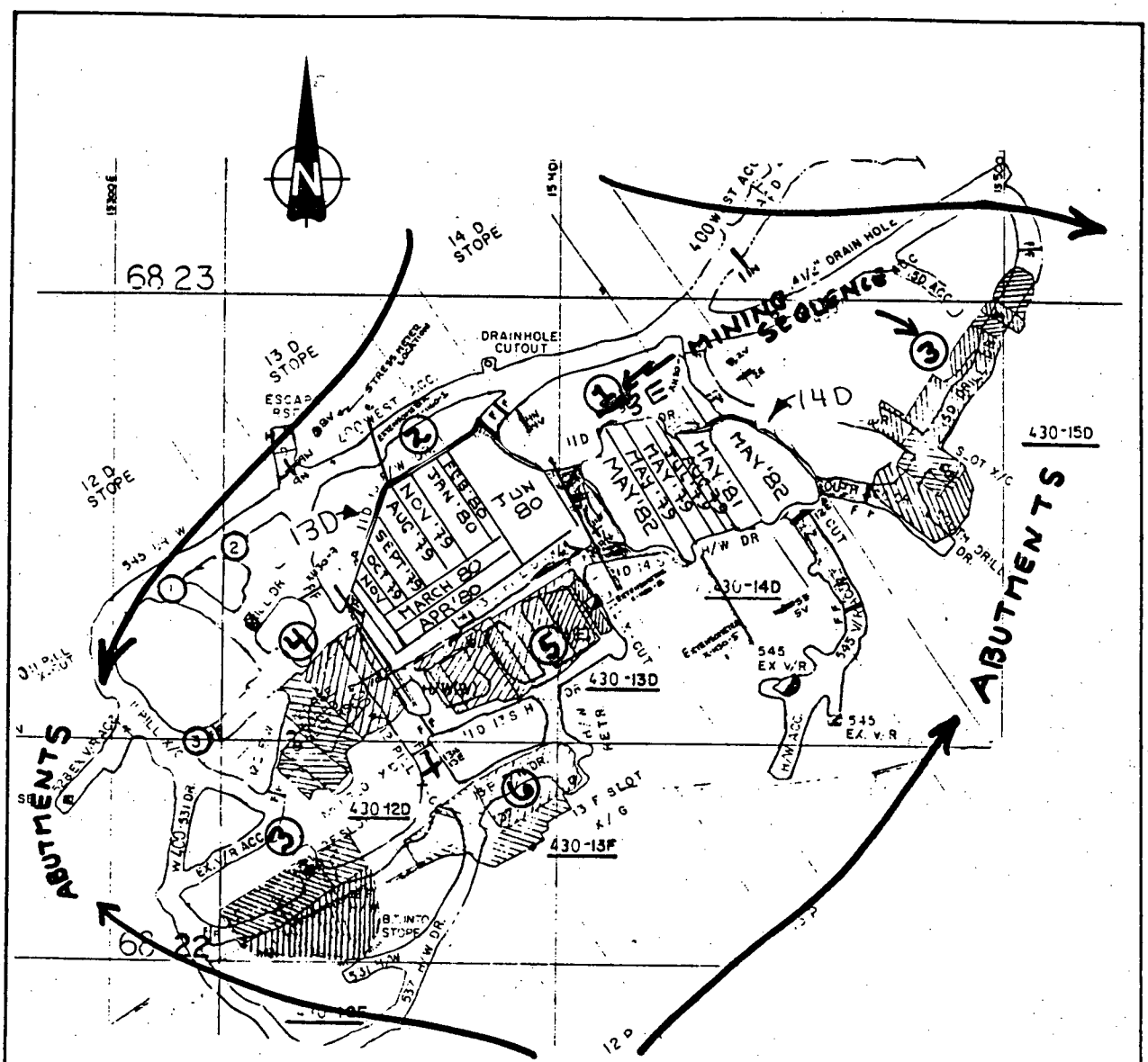

Figure 4.29: Mining Sequence and Instrumentation - 400m Level

STRESS METER LOCATION
— DIRECTION W - E
| DIRECTION N - S
• DIRECTION VERTICAL

———EXTENSOMETER

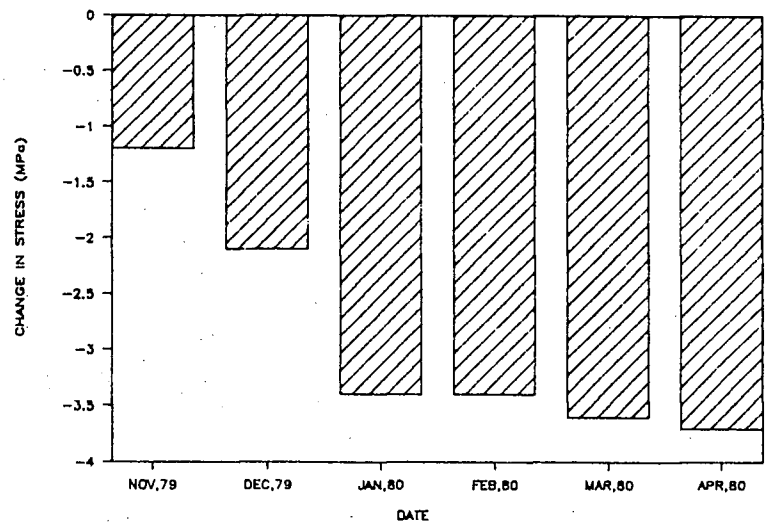

Figure 4.30: Gauge 6NS Located in FW of 19J on 340m Level

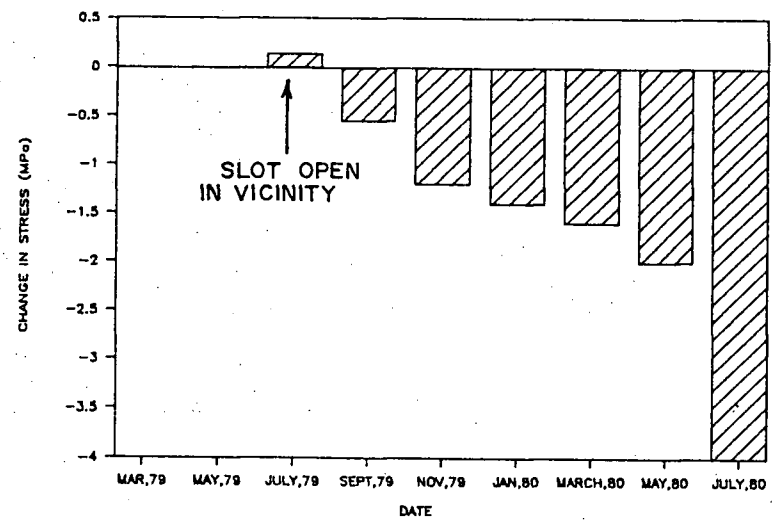

Figure 4.31: Gauge 3EW Located in FW of 14D on 400m Level

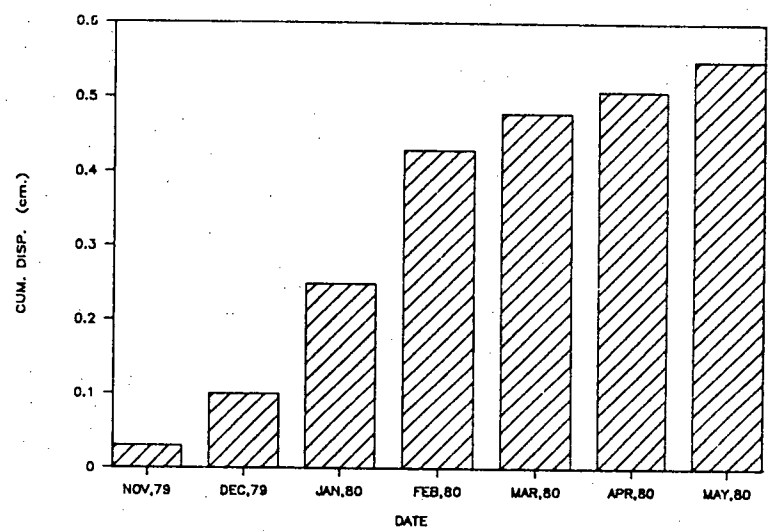

Figure 4.32: Extensometer Located at FW Contact of 13D Stope on 400m Level

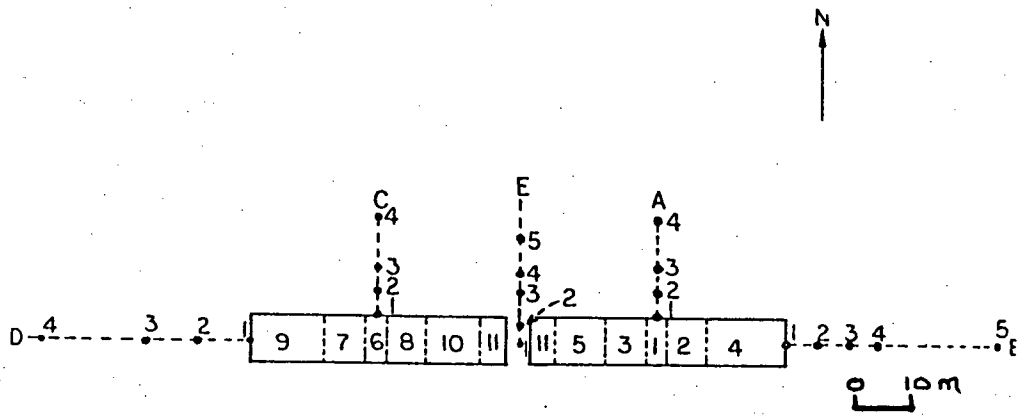

Figure 4.33: Modelled Sequence of Extraction - Plan View

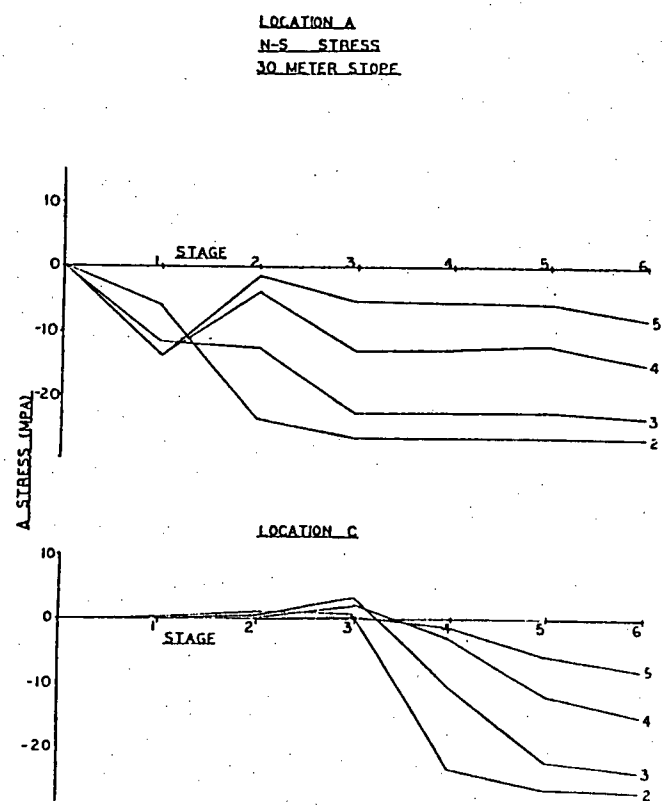

Figure 4.34a: Stress Change Vs Extraction Stage - NS

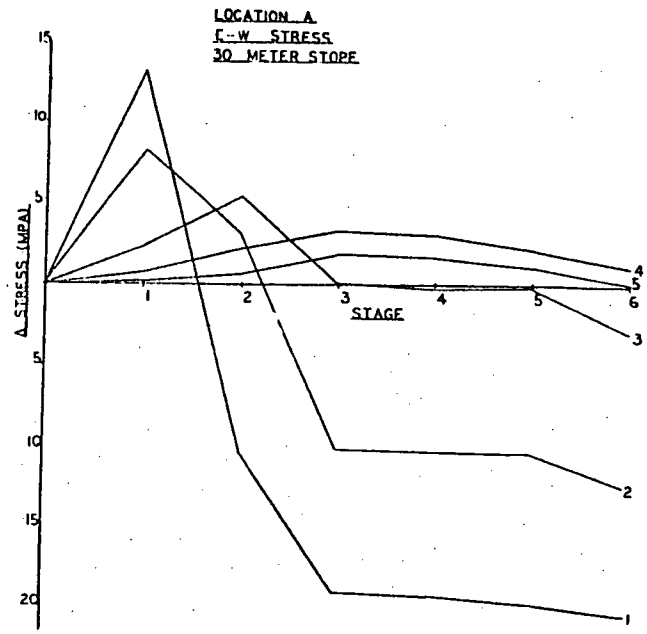

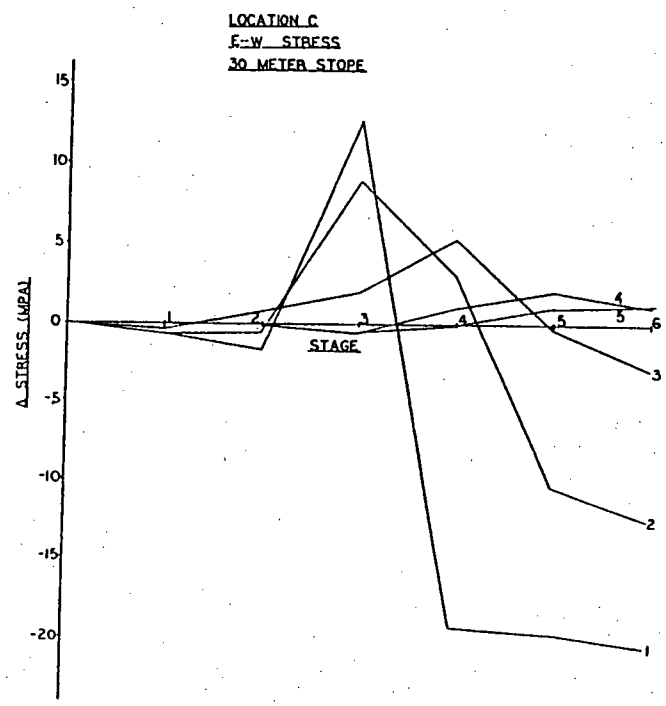

Figure 4.34b: Stress Change Vs Extraction Stage - EW

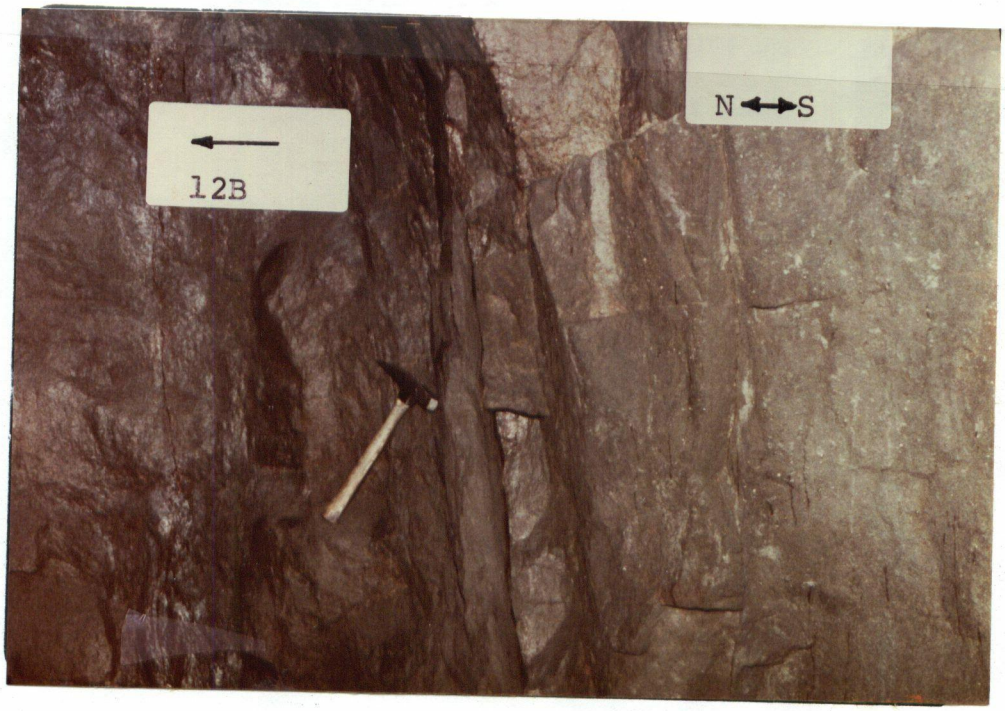

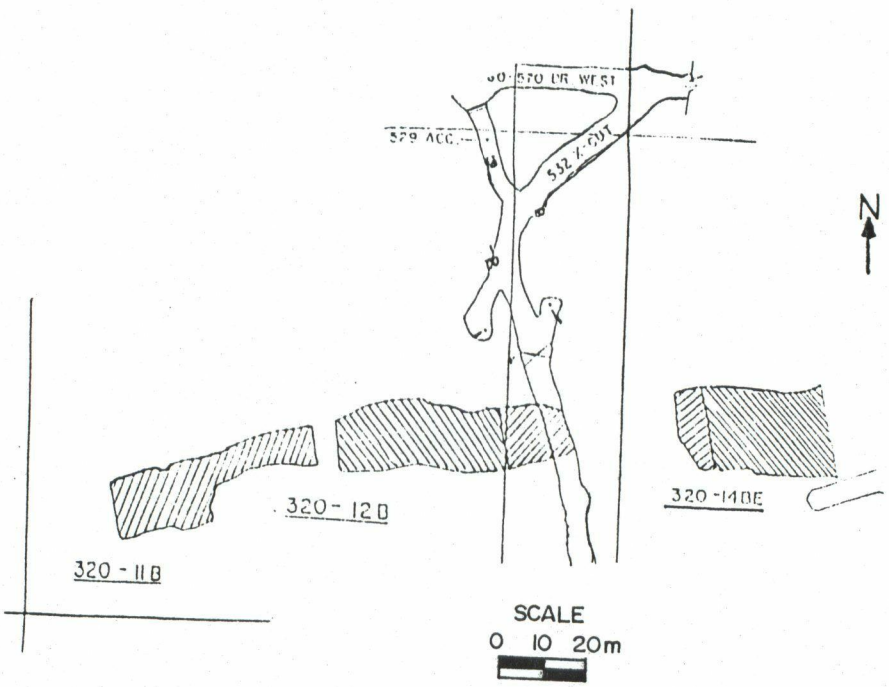

Figure 4.35: Opening of Joint Upon Mining 12B Stope on 240m Level

CHAPTER FIVE

ROCK MASS CHARACTERIZATION

5.1 Introduction

This chapter identifies the parameters describing the rock mass that have the greatest influence upon stope dilution. It begins with a critical evaluation of existing rock mass classification systems. A particular system was selected in order to relate the rock quality of individual stopes at Ruttan to a much larger data base that has been derived throughout the literature. This enables the rock quality to be evaluated quantifiably in terms of existing relationships that have been developed by other investigators. The significance of the parameters incorporated into the classification are subsequently analyzed in order to assess their relative importance in terms of stope design at Ruttan, Chapter 7. A structural assessment, in terms of delineating potential failure modes of individual stope hanging wall and footwall contacts, is presented. A kinematic analysis identifies structure as being a principal factor affecting dilution.

5.2 Rock Mass Classification

Rock mass classification systems have been developed

primarily to assist in recommending support for unerground civil projects. Generally, civil structures are normally isolated from any nearby openings, do not account for the extraction process, are at moderate to shallow depth, and expose a minimum of open ground. These deficiencies do not enable them to be directly applied to the design of underground mining structures. The classifications, although on their own are not adequate to predict mine design requirements, do provide a procedure for investigation. The rock mass classification systems of particular relevance to underground mining applications are the:

- Geomechanical Classification System (RMR) (1973)
- Q System (1974)

These systems have empirically evolved from a large data base. In addition, they not only reflect the experiences of the developers, but also the preceding investigators such as Terzaghi (1946), Lauffer (1958), Stini (1950), Deere (1964), Wickham et al (1972) among others. The systems were primarily derived for the design of civil engineered tunnels. However, they provide the basis for subsequent modifications that enable them to be applied to mining. Laubscher (1976), Mathews et al (1981), Kendorski (1983), and Hoek (1983) have applied adjustments to the existing systems to aid in the design of mining structures.

An ideal mine classification system must have the flexibility that allows it to be used for various mine applications, and it must be simple so that it can be easily assessed and understood. It is only in this manner that it can function as an important tool in the design and operation of a mine. The RMR and Q Systems satisfy the above criteria. Deficiencies do exist with the two classifications, but through adjustments, one is able to overcome the criticisms. In particular the Q System is said to be too rigorous (Kendorski, 1983), has a poorly defined factor that accounts for stress, and does not account for structural orientation. These criticisms are incorporated into adjustments by Mathews (1981) and Kirsten (1983). The RMR system is said to be too simple; it does not account for stress and the input parameters are too qualitative. These limitations are incorporated into adjustments by Laubscher (1976), Kendorski (1983).

A classification system for the Ruttan operation should be patterned after the "Q or RMR" systems with the relevant geotechnical parameters associated with each mining method identified. This requires the generation of a large empirical data base specifically categorized in terms of similarities of applications for open stope design. This data base was equally sparse when Terzaghi proposed his system in 1946. This data base has since expanded and grown and the systems have been refined due to its acceptance among the civil engineering community. This was largely due to the continued success

achieved in tunnel support prediction.

One of the major differences between the civil and mining disciplines is the requirement of mines to generally operate within a rock mass of which the peak strength has been exceeded. In addition, controlled and predicted failure is acceptable in mining which is not the case in civil construction. The temporary requirements of mine openings are generally not reflected within the confines of civil engineering. These factors, plus the geometrical and excavation considerations, require one to modify the existing system through the collection of empirical data relevant to open stope design.

The majority of the classification systems include, either directly or indirectly, an assessment of the following parameters , Table 3.3:

- Intact rock strengths (unconfined compressive strength). It is a necessary parameter since it forms the upper strength limit of a rock mass which is subsequently reduced due to rock defects.

- Rock quality designation (RQD). This parameter is an indirect measure of fracture frequency. It is a quantitative index based on a modified core recovery procedure.

- Spacing of discontinuities.

- Condition of discontinuities. This includes roughness, continuity, separation, joint wall weathering and infilling.

- Orientation of discontinuities.

- Groundwater conditions. This is a measure of inflow rates and water pressures.

- Stress field. This refers to the prevailing in-situ stress environment.

The RMR system was selected as the vehicle for stope wall characterization due to its incorporation of the many variables that are considered to influence the behaviour of a rock mass. The interrelationship between the variables and the constitutive equations linking the different variables to the rock mass behaviour are complex. Therefore, an approach was selected that could be empirically calibrated to the optimum stope design through observed resultant dilution measurements. The RMR system was selected since:

- it incorporates key parameters affecting the rock mass behaviour as defined by the literature.

- the system is simple to employ and is readily

applicable to existing methods of core logging and mapping techniques as practioced at Ruttan, Table 5.1. This is particularly important in relating historic core logs in terms of a rock mass number, since the logs generally form the only available descriptor for a particular stope. This is due to either limited stope wall access and/or the unavailability of drill core due to sampling.

The RMR system was employed in isolated areas of the mine and was found to be a good predictor of mine behaviour. Areas having a low RMR rating were found to have problems with:

- drawpoint plugs due to falls of ground from the FW/HW and from the exposed benched back, Figure 2.15.
- excessive dilution from the FW/HW.
- large amount of re-drills.

This study will be particularly concerned with quantifying the RMR parameter in terms of its effect on dilution. Not all the parameters shown in Table 3.3 are incorporated into the RMR rating and these will be discussed individually in Chapter 7, "Data Base". The individual parameters incorporated into the RMR number will be assessed in terms of their influence on stope design.

5.2.1 Geomechanics Classification (RMR)

A thorough treatise on the RMR system and on its application is found in Appendix II.

5.3 Rock Mass

The data base for this study is comprised of 54 stopes and is distributed as follows:

- 46 stopes mined at the time of completion of this study of which 43 were suitable for subsequent analysis.

- 8 additional stopes mined subsequent to the completion of the study and will be employed to reinforce or disprove the formulating equation.

A detailed structural investigation of the Ruttan operation was conducted by the author in order to identify domains with potentially similar ground behaviour. This, however, is not critical to the formulating hypothesis, since individual stopes will be related to observed dilution upon extraction. In terms of mine design, it is important to identify areas that would exhibit similar rock mass behaviour upon extraction. These would enable a mine plan to be implemented. The concepts of domain analysis were employed (Brady,1985), however, individual stopes were attributed rock mass characteristics and analyzed individually. The reader is referred to a study conducted in cooperation with the author " Determination of Structural Domains and Structural Design Sectors for the Ruttan Mine", Seki (1984).

Histograms have been developed for the Ruttan operation establishing the following parameters for the hanging wall, footwall , and ore zones:

- point load index (Is_{50})
- rock quality designation
- joint spacing
- rock mass rating (RMR)

The intact rock strengths for the main geological units at Ruttan are shown in Table 5.2. The above have been derived for each rock type that forms the individual contact zones. The rock mass information has been compiled from core logs information and has been augmented by structural mapping. The diamond drill core was AQ size(27mm). Figure 5.1 is a stope characterization procedure employed for all stopes at Ruttan. A stope is characterized by two drill holes per section and two sections per stope, Figure 2.11. In essence , four holes are analyzed which are representative of the footwall, ore and hanging wall for a particular stope. Three metres of the immediate hanging wall and footwall were evaluated in addition to the full length of the ore for a particular drill hole. However, the rock quality of the drill core within two stope diameters was studied, but in less detail. Major structures are recorded in addition to the geometry of the proposed stope and its configuration (open ground) at the time of mining. The rock mass rating is further grouped into the following classes:

Class	Rock Mass Rating
A	81 - 100%
B	61 - 80%
C	41 - 60%
D	21 - 40%
E	0 - 20%

Through visual estimates and historic observation, it is generally accepted that wall slough at Ruttan is primarily confined to the hanging wall. This has been determined primarily through visual observation at the drawpoints and the drill levels. It is for this reason, that the rock quality in the vicinity of the hanging wall will be employed in characterizing an individual stope. In certain instances, however, it was found that an assessment of the footwall was more critical when:

- a major fault intercepts the footwall
- the rock mass rating of the footwall was much lower than that of the hanging wall (one class or more difference)

A further practice was reducing the Rock Mass Rating by a single class when a major structure intercepted either of the wall contacts. The RMR system classifies the mean rock mass parameters. A major structure must be treated separately from the adjacent bounding units. This modification was shown to empirically be a good estimator of dilution, Chapter 7. It is

realized that kinematically each major structure should be analyzed in greater detail. However, for purposes of this investigation, it was found that by reducing the RMR value by a class, resulted in statistically higher correlations between the modified RMR and dilution. The orientation of the individual structures was not incorporated into the classification, since structures at Ruttan are generally oriented parallel to the stope contact. The major difference is found in the frequency and strength of the individual jointing. This is described in detail in subsequent chapters. Groundwater was not incorporated into the characterization, Figure 5.1. This is primarily due to the absence of water as evidenced by dip tests conducted on the 430m, 370m, and 260m level. The close diamond drill pattern generally ensures that any trapped groundwater has an access to drain (Pakalnis/Groundwater, 1986).

Figure 5.2a,b,c show the distribution of hanging wall, ore and footwall rock units for the stopes at Ruttan. The rock units can be generalized as follows:

Hanging Wall and Footwall Units

Chlorite Talc Schist (CTC)
Quartzite (QTZ)
Acid Sediments (AS)
Basic Dyke (BD)
Massive Sulphide (MS)

Ore Units

Semi-massive Sulphide with Basic Dyke (SMS-BD)
Semi-massive Sulphide with Quartzite (SMS-QTZ)
Semi-massive Sulphide with Chlorite Talc Schist (SMS-CTC)
Semi-massive Sulphide with Chlorite Schist (SMS-SC)
Massive Sulphide (MS)

The distribution is delineated for stopes located in the west and east lenses respectively. The distribution of rock mass parameters for the immediate hanging wall contact are summarized in Figure 5.3a,b and recorded for the individual FW, ore and HW in Table 5.3. Only minor variations in classification parameters existed when the individual rock units were separated in terms of HW, ore or FW given the same rock type (Pakalnis/Rock Mass,1985). Figure 5.4 shows the distribution of RMR for the hanging wall of all stopes at Ruttan. The east lenses generally exhibit higher RMR values and are normally associated with lower stope dilutions. The average RMR ratings for the individual wall contacts are as follows:

Location	RMR (%)
Footwall(54)	58 ± 18
Ore(54)	63 ± 17
Hanging Wall(54)	60 ± 19

Figure 5.5 and 5.6 show typical RMR sections and plans for the Ruttan operation (Pakalnis/Rock Mass,1985).

5.3.1 Fabric Analysis

A detailed line mapping survey was conducted in the vicinity of the individual lenses. This was supplemented by geologic mapping conducted by Ruttan geologists. The information was compiled onto lower hemisphere stereoplots yielding the following observations:

1) Total Structural Analysis (Figure 5.7a)

This net encompasses all structures for all levels at Ruttan (6717 observations). Three major sets were found throughout the Ruttan Mine:

Most Dominant - Joint set parallel to the orebody having a strike of N50° - 80° E and dipping 75° SE.

Moderately Dominant - Flat joint set dipping at 0° - 20°.

Minor Occurrence - Joint set oriented perpendicular to the orebody having a strike of N0° - 30° E and dipping steeply(80° - 90°).

2) Plot of Faults

The major structures are shown in Figure 2.7 and 5.6 and are summarized below:

North Wall Shear (trending N70°E, dip 80°S)
Art's Fault (trending N45E, dip 30°SE)
East Shear (trending N10°W, dip 85-90°E)

3) Footwall, Ore, and Hanging Wall

Minimal structural information exists for the hanging wall, since most of the stope development is in ore and footwall rocks. In addition, the core was not oriented and consequently makes joint dip determination difficult. Isolated areas where access to hanging wall drives were possible indicated that the hanging wall fabric typified that of the ore and the footwall, Figure 5.8.

4) Dykes and Quartz Veins

Dykes generally trend N20°E and dip 40° - 90° towards the SE.

Veins trend parallel to the ore and plunge 20° - 90° towards the SE.

5) West and East Ore Lenses

No distinct differences exist, however, flatter joints are more dominant in the east than the west.

Stereonets for each ore lens were produced at various levels, Figure 5.9. Figure 5.10 is a photograph identifying the major design sets which are summarized below:

Set 1: Most Dominant - N50-80°E/75°SE
Set 2: Moderate Occurrence - Flat structure 0° - 20° dip.
Set 3: Minor Occurrence - N0-30°E/80° - 90°SE.

The continuity of the stucture was observed as exceeding 200m and 100m respectively for design set one and two. Design set three was disjointed and cut by set "one", it is estimated to be less than 15m in length. The continuity was primarily recorded from pit mapping, Figure 5.11.

5.4 Kinematic Analysis

Residual friction angles on saw-cut joints were performed by Smith (1975) employing direct shear tests on samples of quartz-biotite-chlorite gneiss. The results indicated a residual friction angle of 29° based upon six staged shear tests. Figure 5.12 shows an isometric outlining the potential for failure along the design sets. Employing a simpified analysis, as outlined by Hoek and Bray (1977) and reproduced in Figure 5.13, it is shown that toppling failure of the hanging wall is possible. This is derived from employing a base (b) to block height (h) ratio equivalent to a joint spacing of 3m and a height of 60m. The maximum joint spacing according to Figure 5.3b should not exceed three meters. The footwall is generally more stable than the hanging wall, however, a combination of planar and toppling failure is a possibility. A more rigorous solution is possible, but in the author's opinion not warranted, since it is the purpose of this section to outline that instability due to structure is a possible failure mechanism.

Stereonets of individual stopes indicate that structures exist which would generally yield failure in the footwall as shown in Figure 5.14. Joint set 3 is considered to be a lateral release plane for the failure modes indicated in Figure 5.14. This was also the observed method of slough for the majority of stopes at Ruttan (Pakalnis/Back-Analysis of Stope

Failures,1984).

Toppling or slabbing from the hanging wall is generally the observed method of instability at Ruttan. The parting is along a foliation or joint surface that parallels the ore lens. The observed failure mode is simulated by Figure 5.15. This is a base friction model of which the dimensions and failure geometry typifies the observed conditions for stopes at Ruttan.

5.5 Observations/Conclusions

This chapter summarizes the characteristics of the rock fabric identifying the possible failure modes. Structural instability is evident through toppling on joints sets paralleling the stope contact and resting on flat cross-cutting joints. Further investigations will be based upon the conclusion that:

- the hanging wall and footwall for a particular stope is in a relaxed state
- failure due to structural instability is a possible mechanism

Table 5.1: Core Logging Format - Ruttan

MINERAL TYPE		ROCK TYPE		MINE UNIT		MINERAL DESCRIPTIONS		PRIMARY STRUCTURE	
Quartz	= Q	Footwall Volcaniclastics	=FV	Altered FW Volcaniclastics	=AV	Fine	= F	Very thickly bedded (Thicker than 1 m	= 6)
Plagioclase	= P	Basic Sediments	=BS	Quartzite	=QZ	Medium	= M	Thickly bedded (30-100 cm	= 5)
Orthoclase	= OC	Intermediate Sediments	=IS	Diorite	=DI	Coarse	= C	Medium bedded (10-30 cm	= 4)
Chlorite	= CH	Acid Sediments	=AS	Granite	=GR	Granular	= G	Thinly bedded (3-10 cm	= 3)
Biotite	= BI	Rhyolite	=RHY	Exhalite	=EX	Blebby	= B	Very thinly bedded (1-3 cm	= 2)
Sericite	= SR	Dacite	=DA	HW Sediments	=HWS	Veins	= V	Thickly laminated (0.3-1 cm	= 1)
Talc	= TC	Andesite	=AN	Mineralized Chlorite Schist	=MSC			Thinly laminated (Thinner than 0.3	= 0)
Hornblende	= H	Basalt	=BA						
Carbonate	= CA	Diorite	=DI						
Epidote	= EP	Granite	=GR						
Cordierite	= CD	Chert	=CH						
Andalusite	= AD	Altered FW-Volcaniclastic	=AV						
Staurolite	= ST	Granodrite	=GRD						
Garnet	= GT	Spotted United	=SU						
Tremolite	= TR	Brown Eyes	=BE						
Actinolite	= AC	Quartzite	=QZ						
Anhydrite	= AN	Chlorite Schist	=SC						
Apatite	= AP	Biotite Schist	=BSC						
Gypsum	= GY	Sericite Schist	=SSC						
Magnetite	= MG	Basic Dyke	=BD						
Galena	= GA	Acid Dyke	=AD						
Pyrite	= PY	Quartzview	=QV						
Pryhotite	= PO	Lost Core	=LC						
Chalcopyrite	= CPY	Semimassive Sulfide	=SMS						
Sphalerite	= SPH	Massive Sulfide	=MS						
		Chlorite Talc Schist	=CTC						
		Quartzite - Chlorite	=QZC						
		Quartlite - Sericite	=QZS						
		Quartzite - Biotite	=QZB						
		Tremolite Schist	=TSC						
		Granite with IS	=GIS						
		Granite with BS	=GBS						
		Granite with AS	=GAS						

INTENSITY DESCRIPTORS	
None	= N
Weak	= W
Moderate	= M
Strong	= S
Excessive	= E

GENERAL TEXTURE DESCRIPTORS	
Schistose	= S
Massive	= M
Gnessic	= G

SPECIFIC TEXTURE DESCRIPTORS	
Breccia	= X
Porphyroblastic	= B
Clastic	= C
Porpyritic	= P

SECONDARY STRUCTURE	
Banded	= B
Folded	= F
Faulted	= L
Shear	= S

ORIENTATION
0-10°
10-20°
20-30°
30-40°
40-50°
50-60°
60-70°
70-80°
80-90°

TEXTURAL MINERAL SIZE	
LICH	= 0
1-2 "	= 1
2-3 "	= 2
3-4 "	= 3
4-5 "	= 4
5-6 "	= 5
6-7 "	= 6
7-8 "	= 7
8-9 "	= 8
9-10"	= 9

NUMBER OF BREAKS PER 10 FEET CODE			
0-5	= 0	50-60	= 6
5-10	= 1	60-70	= 7
10-20	= 2	70-80	= 8
20-30	= 3	>80	= 9
30-40	= 4		
40-50	= 5		

Old Format (Prior 1983)

MINERAL TYPE		ROCK TYPE		MINE UNIT		MINERAL DESCRIPTIONS		ORIENTATION
Quarrz	= Q	Footwall Volcaniclastics	= FV	Altered FW Volcaniclastics	= AV	Fine	= F	0 - 10°
Plagioclase	= P	Basic Sediments	= BS	Quartzite	= QZ	Medium	= M	10 - 20°
Orthoclase	= OC	Intermediate Sediments	= IS	Diorite	= DI	Coarse	= C	20 - 30°
Chlorite	= CH	Acid Sediments	= AS	Granite	= GR	Granular	= G	30 - 40°
Biorite	= BI	Rhyolite	= RHY	Exhalite	= EX	Blebby	= B	40 - 50°
Sericite	= SR	Dacite	= DA	HW Sediments	= HWS	Veins	= V	50 - 60°
Talc	= TC	Andesite	= AN	Mineralized Chlorite Schist	= MSC			60 - 70°
Hornblende	= H	Basalt	= BA					70 - 80°
Carbonate	= CA	Diorite	= DI					80 - 90°
Epidote	= EP	Granite	= GR					
Cordierite	= CD	Chert	= CH					
Andalusite	= AD	Altered FW-Colcaniclastic	= AV					
Staurolite	= ST	Granodrite	= GRD					
Garnet	= GT	Sported United	= SU					
Tremolite	= TR	Brown Eyes	= BE					
Actinolite	= AC	Quartzite	= QZ					
Anhydrite	= AN	Chlorite Schist	= SC					
Apatite	= AP	Biorite Schist	= BSC					
Gypsum	= GY	Sericite Schist	= SSC					
Magnetite	= MG	Basic Dyke	= BD					
Galena	= GA	Acid Dyke	= AD					
Pyrite	= PY	Quartzview	= QV					
Pryhotite	= PO	Lost Core	= LC					
Chalcopyrite	= CPY	Semimassive Sulfide	= SMS					
Sphalerite	= SPH	Massive Sulfide	= MS					
		Chlorite Talc Schist	= CTC					
		Quartzite - Chlorite	= QZC					
		Quartzite - Sericite	= QZS					
		Quartzite - Biorite	= QZB					
		Tremolite Schist	= TSC					
		Granite with IS	= GIS					
		Granite with BS	= GBS					
		Granite with AS	= GAS					

PRIMARY STRUCTURE

Rock Quality Designation (RQD)

90 - 100%	= 5
75 - 90%	= 4
50 - 75%	= 3
25 - 50%	= 2
0 - 25%	= 1

RQD = $\frac{\Sigma \text{ Solid} > 10 \text{ cm.}}{\text{Total}}$

(measure centre to centre)

Record under Primary Structure

INTENSITY DESCRIPTORS	
None	= N
Weak	= W
Moderate	= M
Strong	= S
Excessive	= E

GENERAL TEXTURE DESCRIPTORS	
Schistose	= S
Massive	= M
Gnessic	= G

SPECIFIC TEXTURE DESCRIPTORS	
Breccia	= X
Porphyroblastic	= B
Clastic	= C
Porpyritic	= P

SECONDARY STRUCTURE	
Banded	= B
Folded	= F
Faulted	= L
Shear	= S

TEXTURAL MINERAL SIZE	
LICH	= 0
1- 2 LICH	= 1
2- 3 LICH	= 2
3- 4 LICH	= 3
4- 5 LICH	= 4
5- 6 LICH	= 5
6- 7 LICH	= 6
7- 8 LICH	= 7
8- 9 LICH	= 8
9-10 LICH	= 9

NUMBER OF BREAKS PER 10 FEET CODE			
0 - 1	= 0	41 - 60	= 6
2 - 3	= 1	61 - +	= 7
4 - 6	= 2		
7 - 10	= 3		
11 - 20	= 4		
21 - 40	= 5		

New Format (Post 1983)

Point Load Strength Values Recorded on Both Formats

Table 5.2: Intact Rock Strength Parameters

Rock Type	Uniaxial Compressive Strength (MPa)	Poisson's Ratio	Modulus of Deformation (GPa)	Number of Samples
Semi-Massive Sulphide-Chlorite	70 ± 24	0.23 ± 0.05	66 ± 19	13
Massive Sulphide	89 ± 37	0.2 ± 0.08	88 ± 37	39
Basic Dyke	202 ± 66	0.2 ± 0.07	81 ± 14	10
Acid Seds.	135 ± 43	0.19 ± 0.07	77 ± 19	6
Quartzites	113 ± 49	0.12 ± 0.06	54 ± 23	4
Chlorite Schists	49 ± 11	0.34 ± 0.12	50 ± 17	14
Chlorite Talc Schists	25 ± 14	0.33 ± 0.09	39 ± 9	13

Table 5.3: Summary of Rock Mass Parameters

ROCK TYPE	OBSERVATIONS			Is_{50}*	RQD(%)	SPACING (m)
	FW	Ore	HW**			
CTC(7)	5	-	2	<1	25± 8	.16 ± .2
SC(31)	17	-	14	2.1 ± 1.1	47 ± 19	.97± .7
QTZ(34)	16	-	18	4.8 ± 1.9	69 ± 18	1.4 ± .8
AS(8)	1	-	7	3.9 ± 1.8	68 ± 22	1.2 ± .7
BD(6)	3	-	3	5.3 ± 2.6	70 ± 20	1.1 ± .7
MS(63)	12	41	10	2.9 ± .9	82 ± 10	1.7 ± .8
SMS-SC(9)	-	9	-	1.6 ± .6	48 ± 13	.88± .7
SMS-BD(1)	-	1	-	6.0	68	1.3
SMS-QTZ(1)	-	1	-	3.0	70	1.6
SMS-CTC(2)	-	2	-	1.5 ± 1.	44 ± 24	.3 ± .3
	(54)	(54)	(54)			

* Unconfined Compressive Strength Is_{50} x 24 (Smith, 1981)

** Refers to Number of Stope Walls Affected

( ) Sample Size

STOPE : _____

CLASSIFICATION PARAMETERS AND THEIR RATINGS

PARAMETER			RANGE OF VALUES						
1	strength of intact rock material	point load strength index or uniaxial compressive strength	> 8 MPa	4-8 MPa	2-4 MPa	1-2 MPa	for low range, ucs test preferred		
			> 200 MPa	100-200 MPa	50-100 MPa	25-50 MPa	10-25	3-10	1-3MPa
	rating		15	12	7	4	2	1	0
2	drill core quality, RQD		90-100 %	75-90 %	50-75 %	25-50 %	< 25 %		
	rating		20	17	13	8	3		
3	spacing of joints		> 3m	1-3 m	0.3-1m	50-300mm	< 50mm		
	rating		30	25	20	10	5		
4	condition of joints		v rough, not cont. no separ. hrd. jn. wall rock	sli. rough surf. separ < 1mm hrd jn. wall rock	sli rough surf. separ. < 1mm sft jn. wall rock	slk. surf. gouge < 5mm, jn open 1-5 mm, cont jn.	sft gouge > 5mm jn open > 5mm cont jn		
	rating		25	20	12	6	0		

ROCK MASS RATING

	FOOTWALL				ORE				HANGING WALL			
STRENGTH												
R.Q.D.												
SPACING												
CONDITION												
TOTAL												
MAJOR STRUC. COMMENT												
ROCK TYPE												
HOLE NUMBER												
SECTION	e	sec	e	sec	e	sec	e	sec	e	sec	e	sec

CLASSIFY
ISOLATED ___
RIB ___
ECHELON ___

DIMENSIONS

LEVEL	SPAN	WIDTH

HEIGHT: _____

BLASTING : _____

VOLUME, m^3

EXCAV. RATE (≈1000 m^3/mth)	5,000	10,000	20,000	30,000

OPEN GROUND
(sketch/fill)

RATING

F.W.	ORE	H.W.
___	___	___

Figure 5.1: Stope Characterization

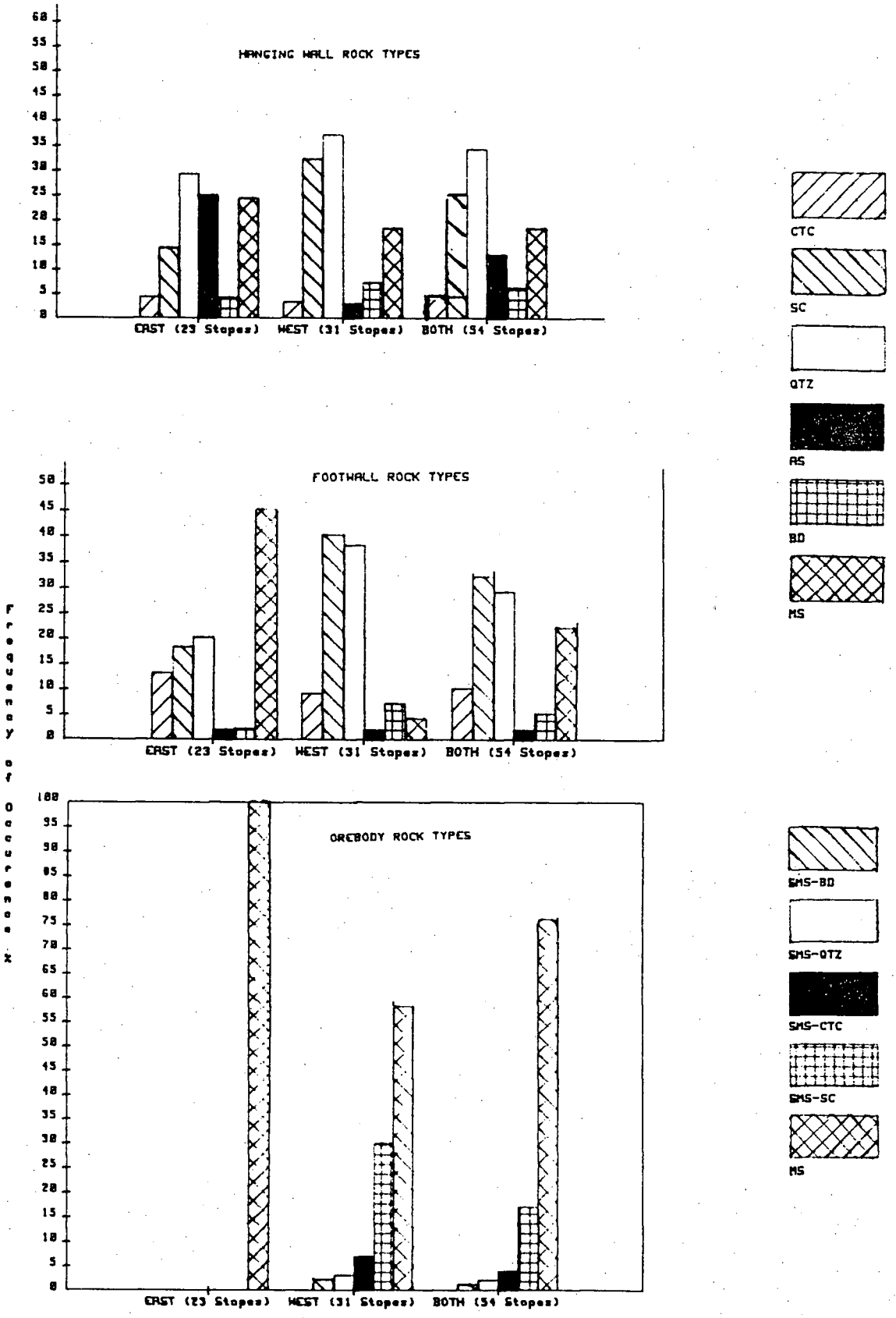

Figure 5.2: Distribution of Rock Types

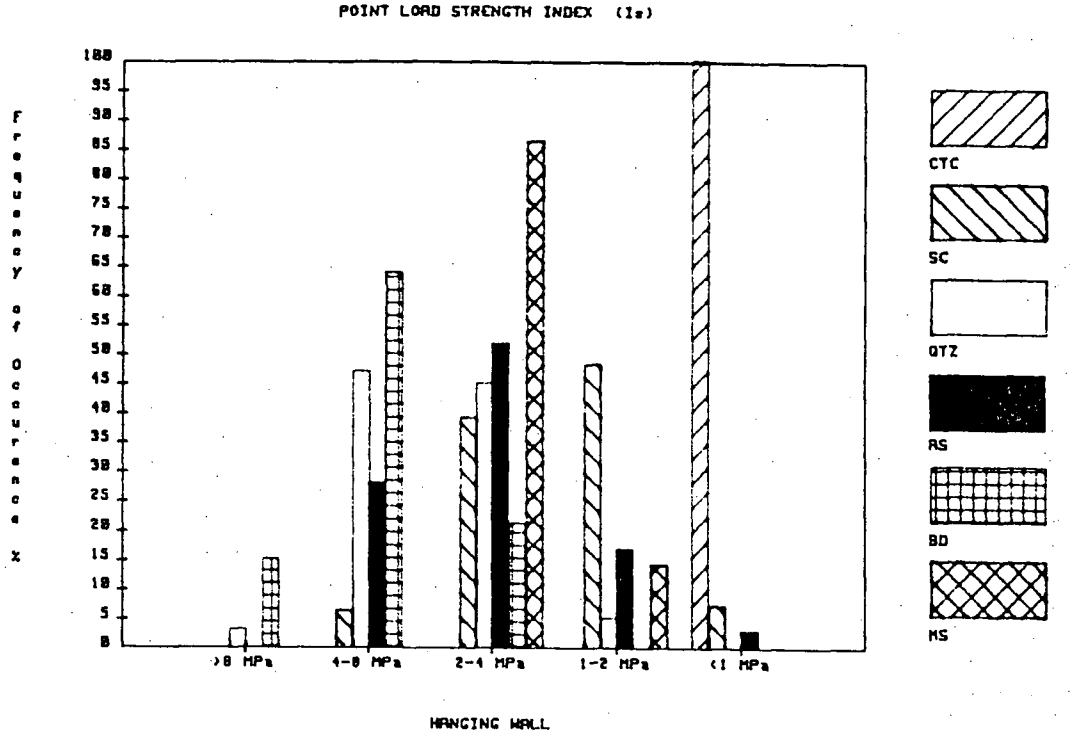

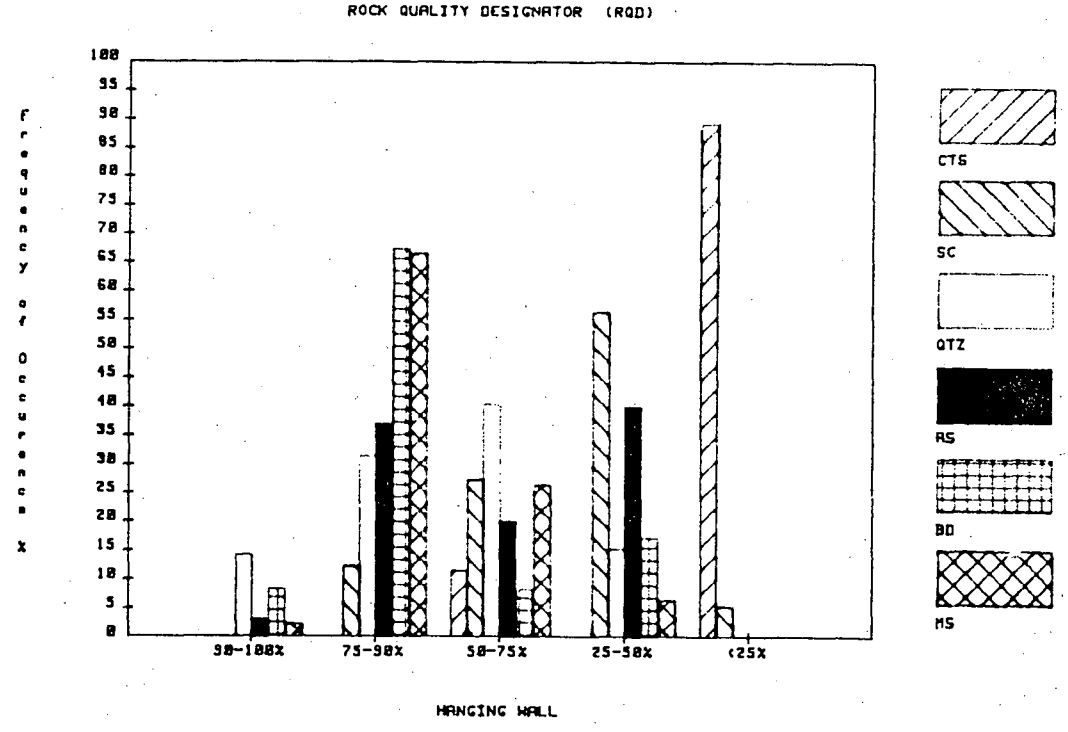

Figure 5.3a: Hanging Wall Rock Mass Parameters

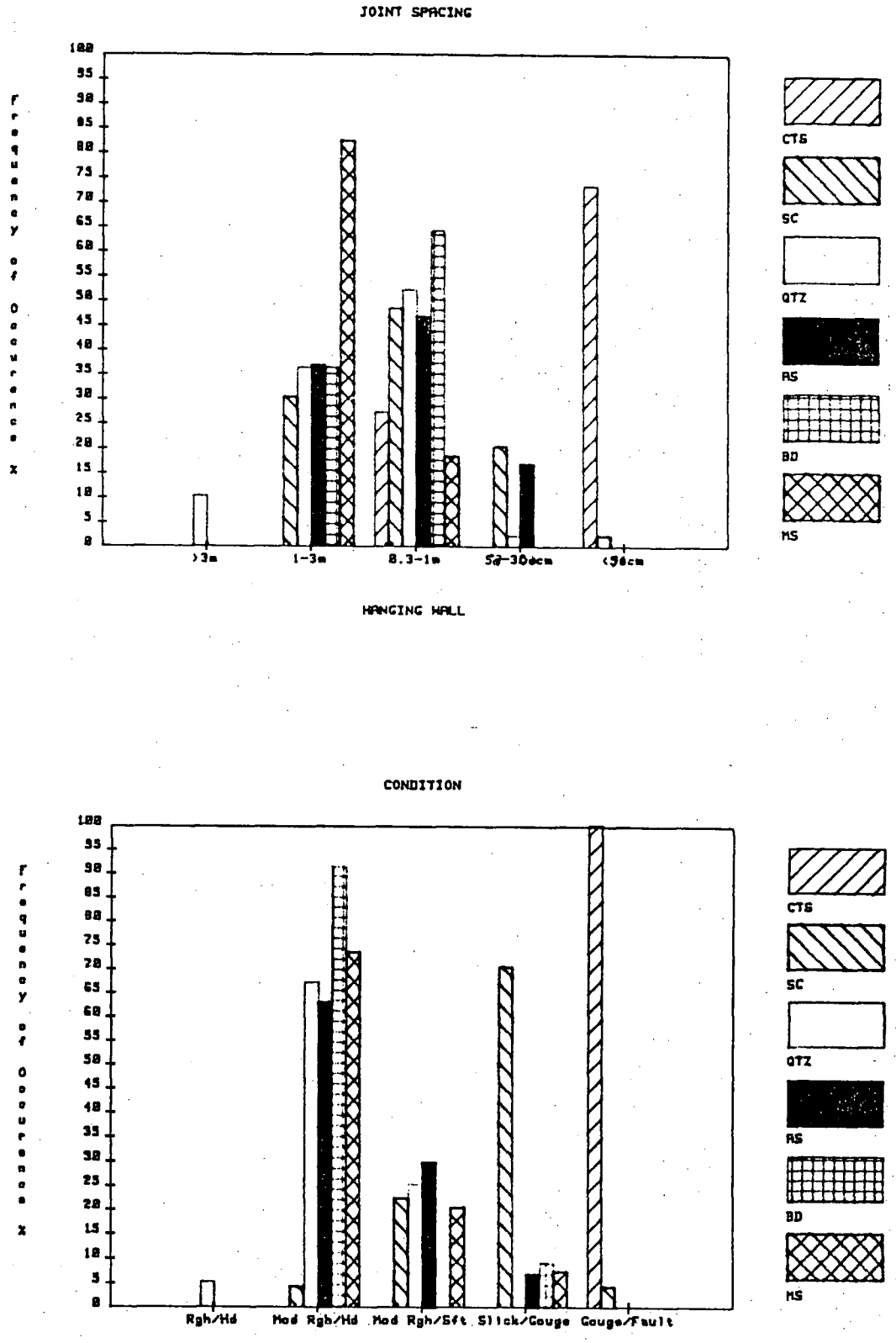

Figure 5.3b: Hanging Wall Rock Mass Parameters

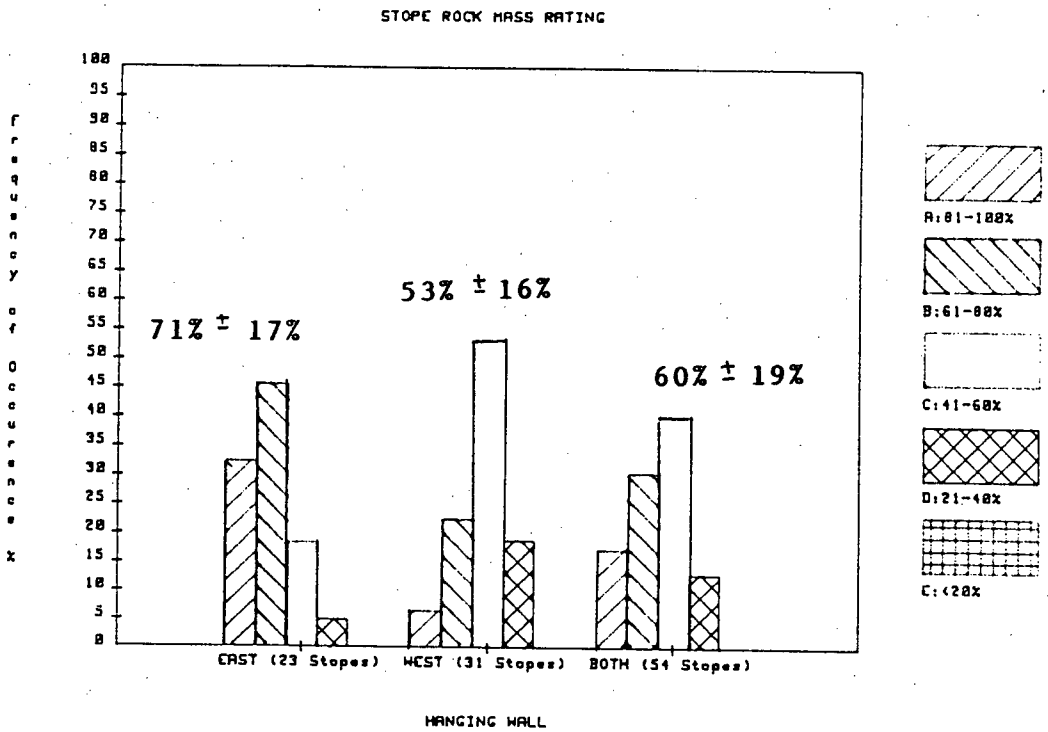

Figure 5.4: Rock Mass Distribution

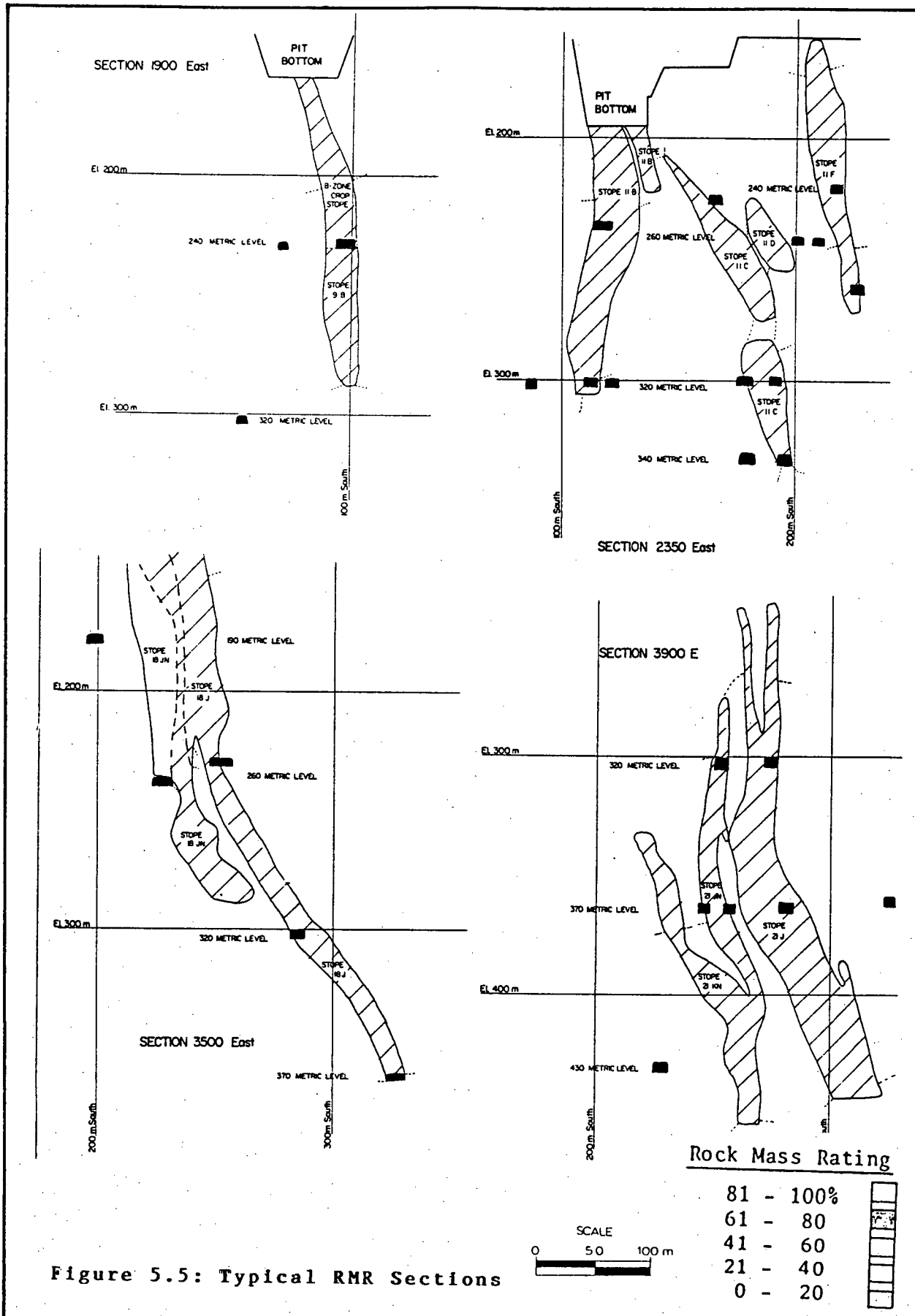

Figure 5.5: Typical RMR Sections

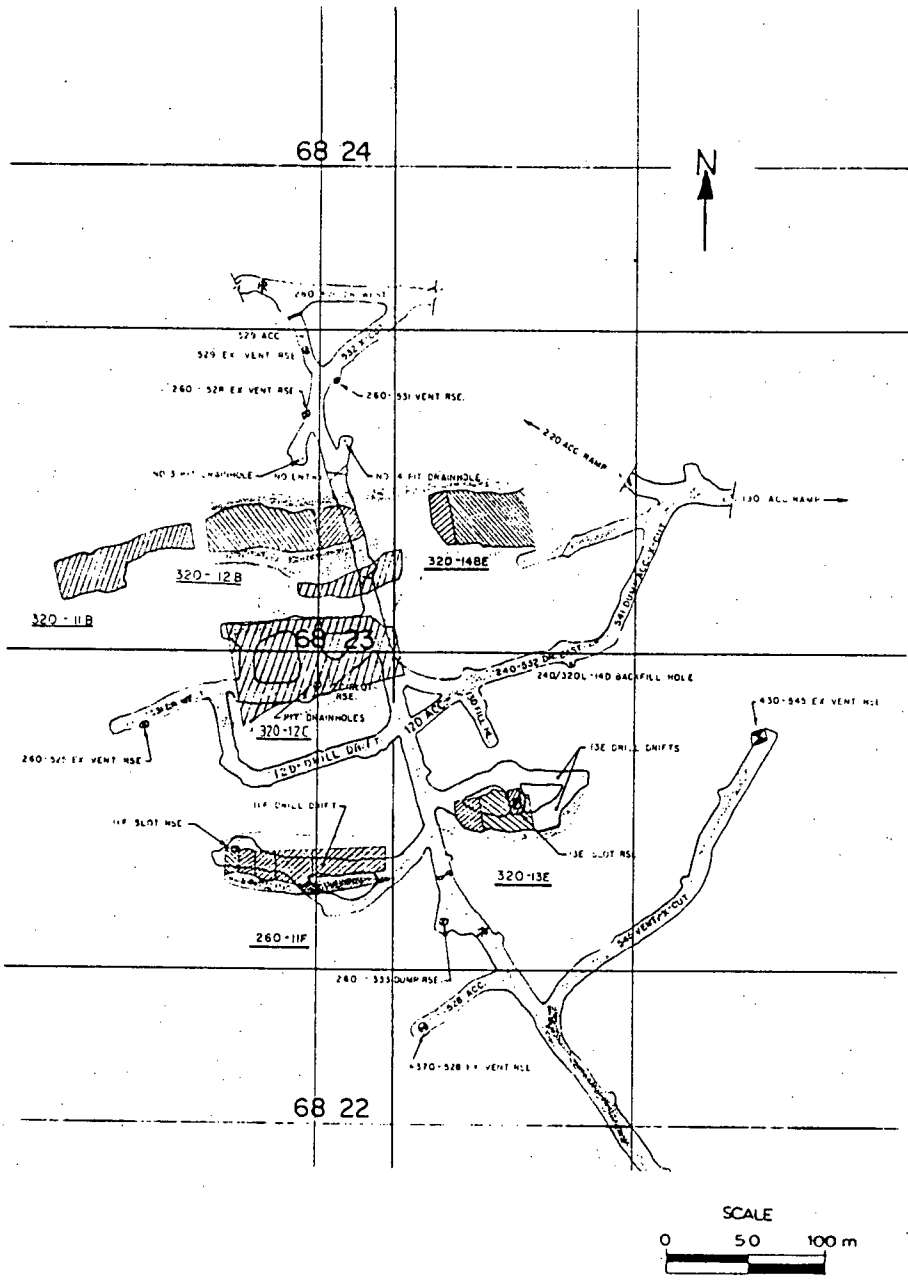

Figure 5.6a: Typical RMR Plan - 240m Level

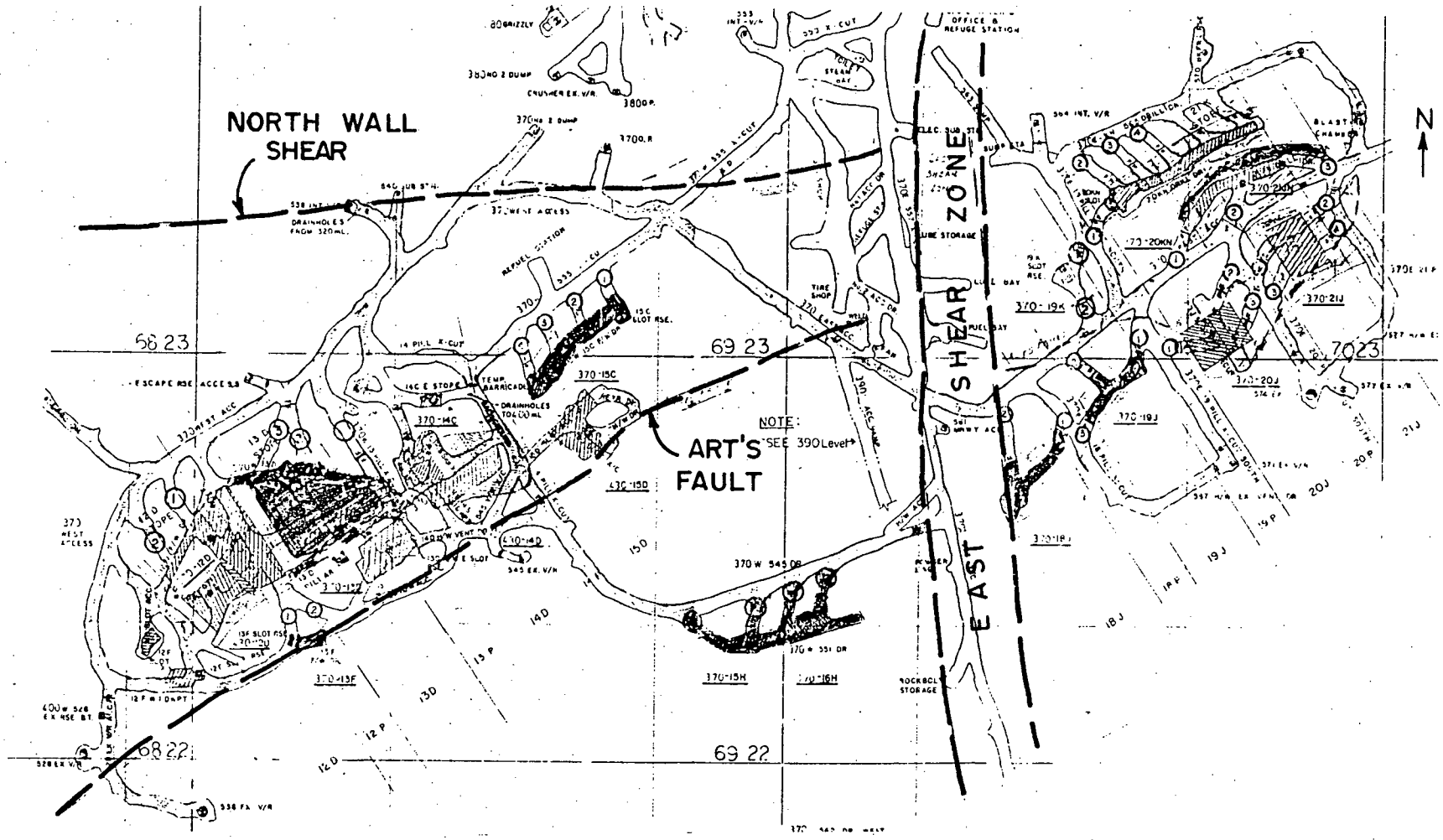

Figure 5.6b: Typical RMR Plan - 370m Level

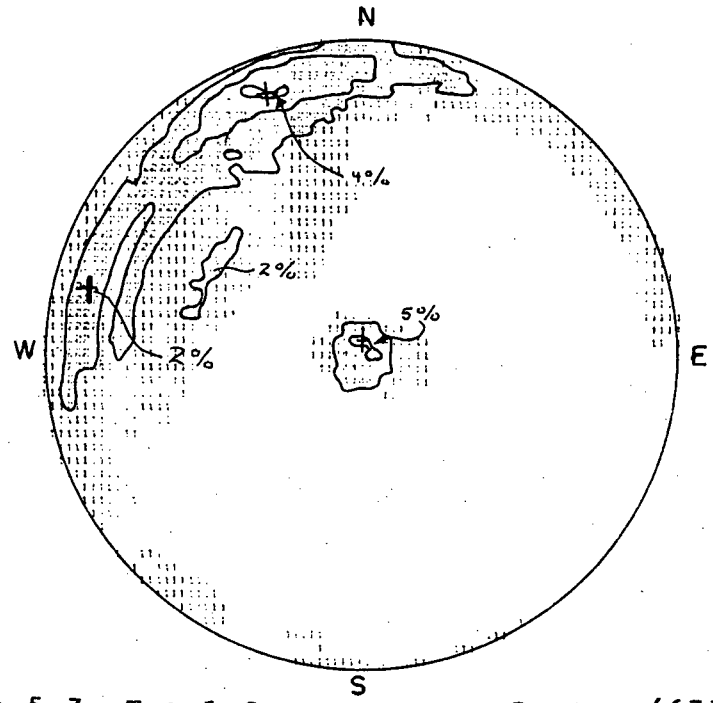

Figure 5.7: Total Structures at Ruttan (6717 obs)

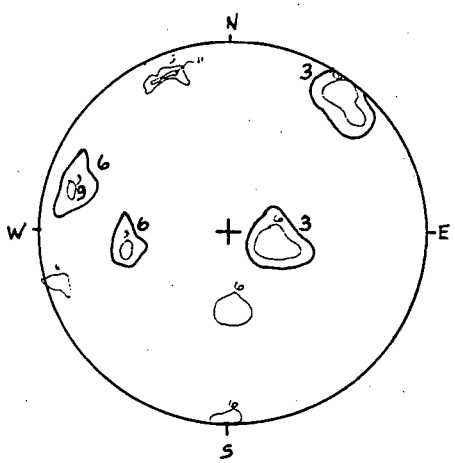

Footwall (33 obs)

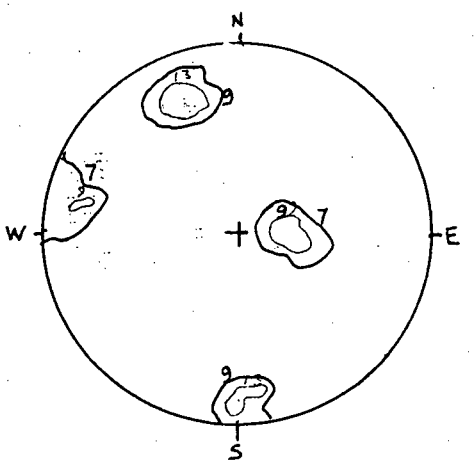

Hanging Wall (22 obs)

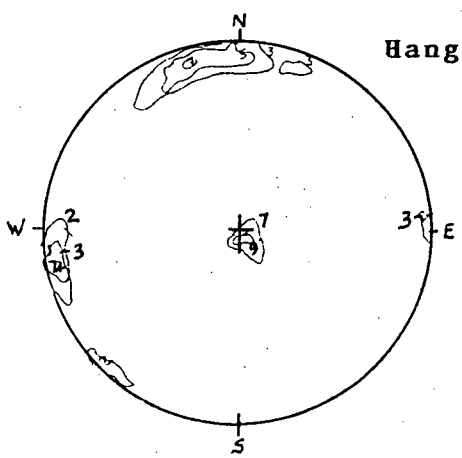

Ore (855 obs)

Figure 5.8: Jointing/Foliation for "C Lens" on 260m Level

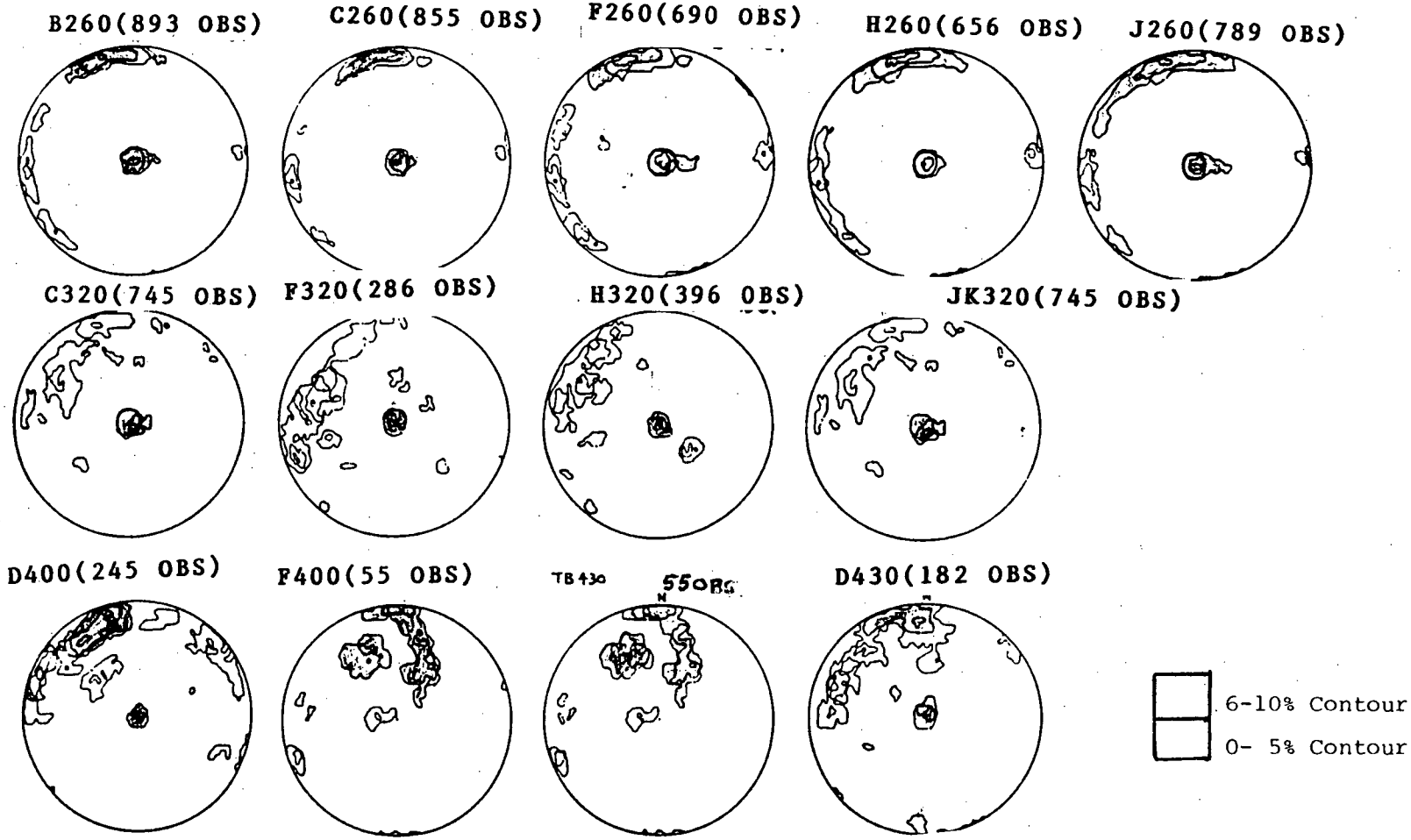

Figure 5.9: Pole Concentrations Including Foliation and Jointing
(ie. "C320" Refers to "C Lens" on 320m Level)

HANGING WALL

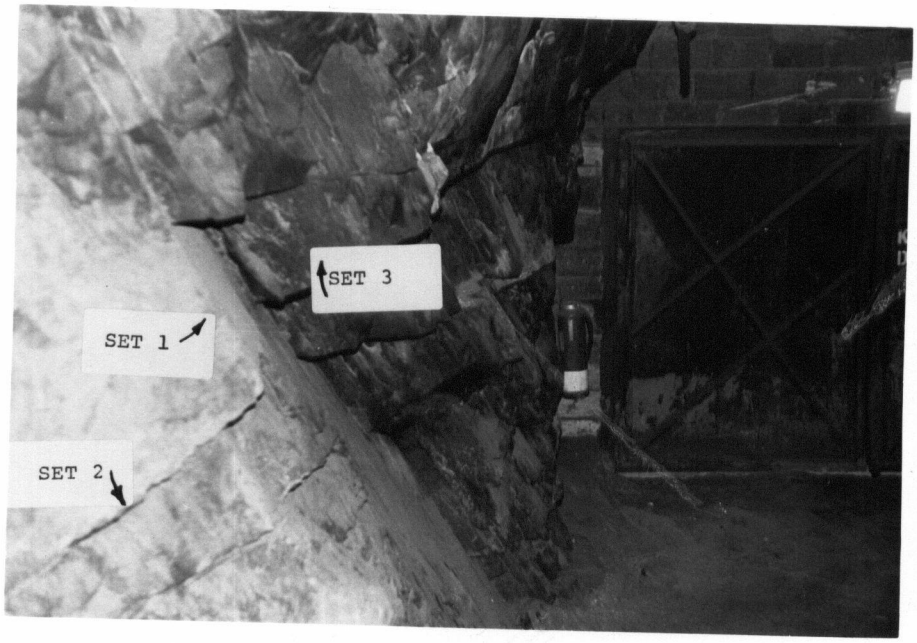

FOOTWALL

Figure 5.10: Photograph Identifying the Major Sets at Ruttan

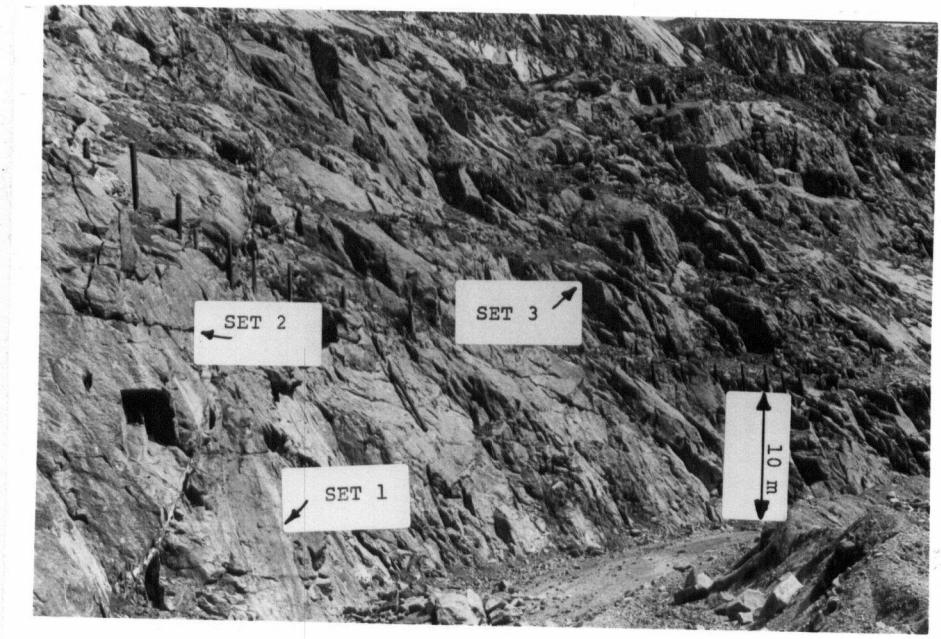

Figure 5.11: Photographs Showing the Continuity of Structure

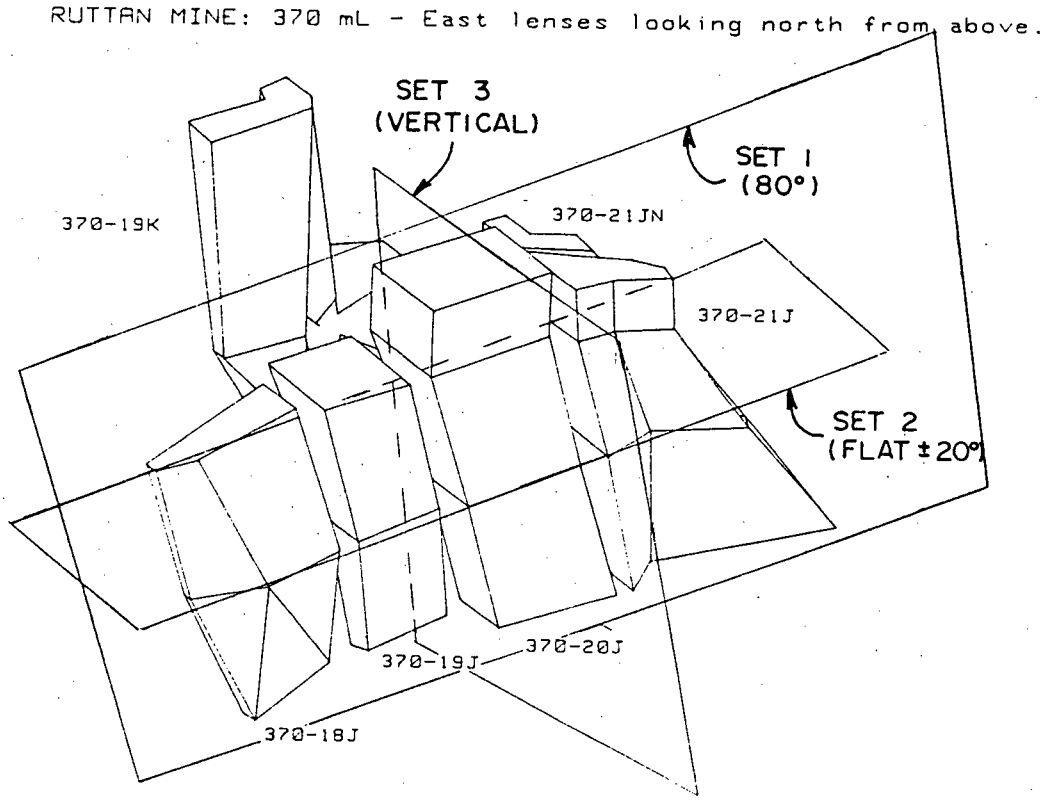

Figure 5.12: Design Sets

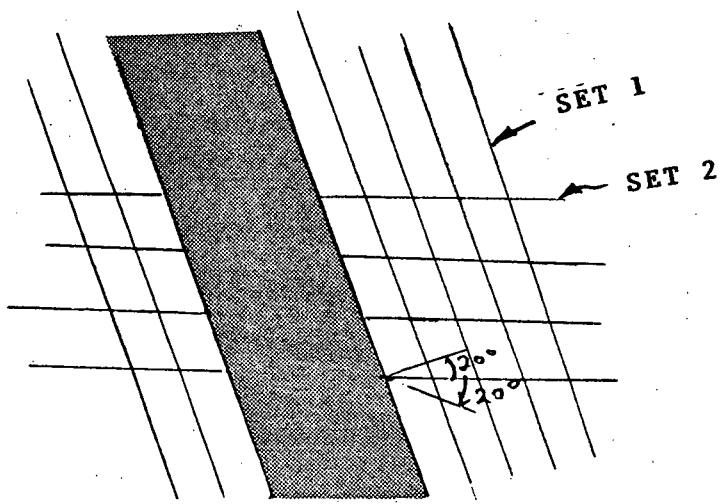

Figure 5.12b: Schematic (section) Identifying Design Set "1 & 2"

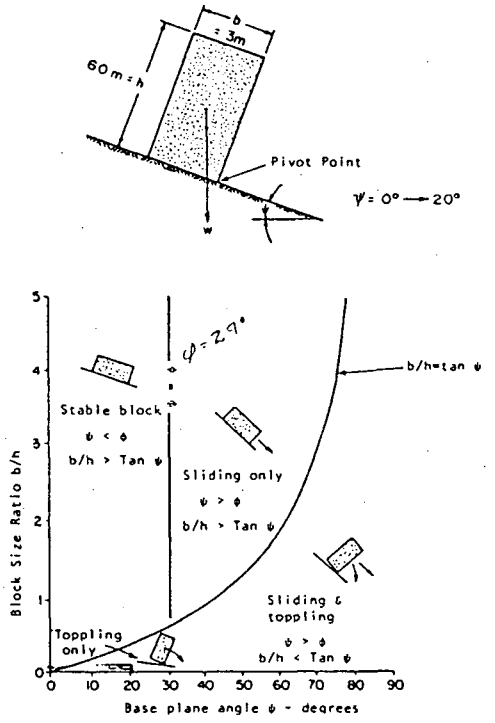

Figure 5.13: Conditions for Sliding and Toppling of a Block on an Inclined Plane (Hoek and Bray, 1977)

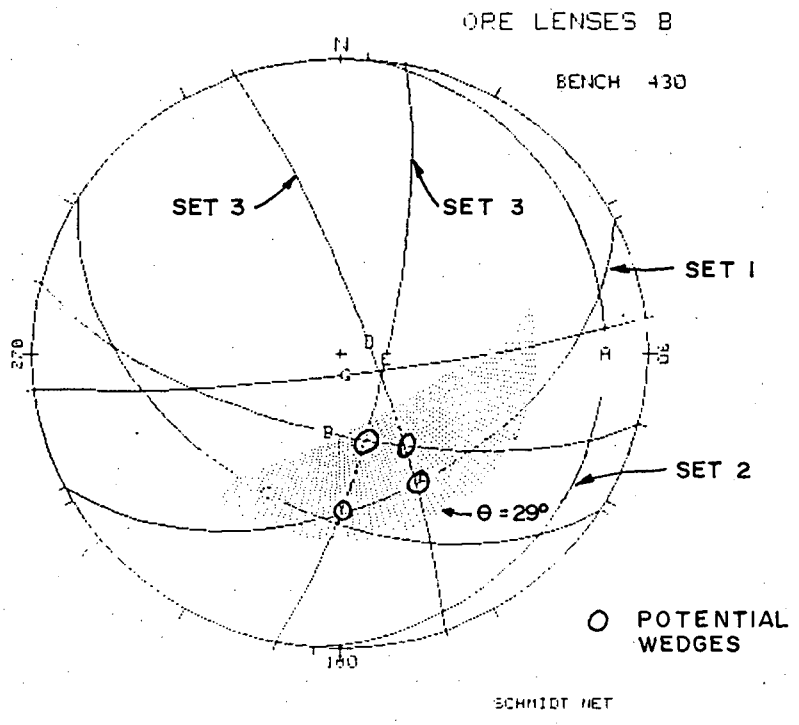

Figure 5.14: Stereonet Showing the Potential for Failure in the FW of the "B Lenses" on the 430m Level

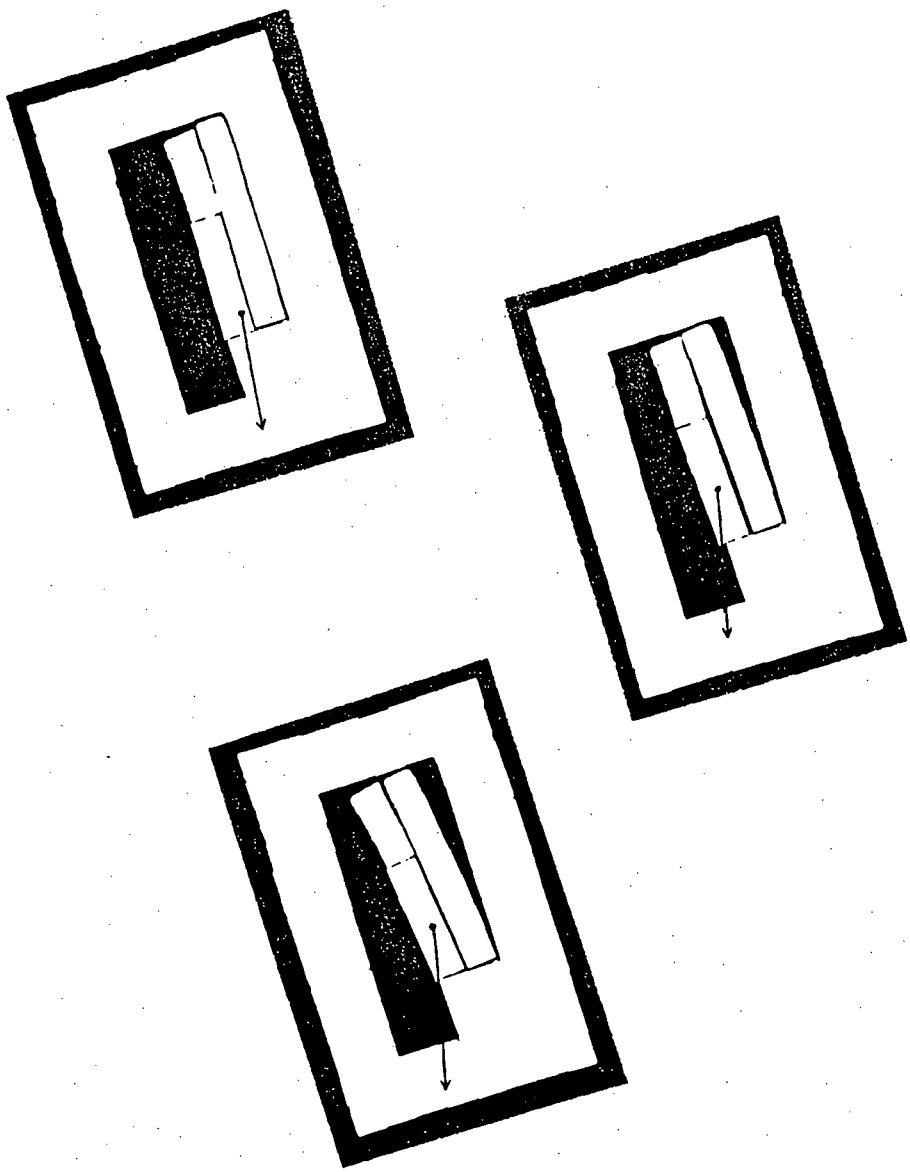

Figure 5.15: Base Friction Model

CHAPTER SIX

DILUTION

6.1 Introduction

This parameter is a measure of the quality of the stope design. Various definitions exist, however, it is a parameter recorded by most open stope operators, Chapter 3.4.3. Dilution will be considered as the dependent control variable. The significance of the individual stope characteristics will be evaluated empirically in terms of dilution. Dilution figures from forty-three stopes will be analyzed at various stages of extraction yielding 432 dilution values. These values are subsequently averaged into 133 observations.

6.2 Definition

Various definitions exist as indicated in Chapter 3.4.3. Dilution has a direct affect on profitability (Kersten,1983) and stope scheduling. The calculation of a diluted geological ore reserve at Ruttan has been historically determined in the following manner. As each mining block is defined, a certain amount of dilution is attributed to the block, this being one meter of the footwall and 1.8 meters in the hanging wall

(historic method). These numbers have no theoretical basis, but reflect the fact that because of the 70 degree dip of the orebody, most of the dilution is attributed to the hanging wall. This width of dilution divided by the width of the ore reserve block gives a volume percentage of dilution. This value is then converted to tonnes dilution which when divided by in-situ tonnes of ore for the block, gives a weight percentage of dilution. This weight percent external dilution is then combined with other blocks forming the reserve for a given stope and an average weight percent dilution is then determined. Consequently, prior to mining, one has an estimated dilution attributed to each stope. At the end of the stope life, an actual dilution figure based on the history of mining of that stope is required in order to properly reconcile it back to the original ore reserve. This is achieved by visual observation of each producing stope on a daily basis by grade control geologists.

A visual interpretation of the volume percentage of massive sulfide, semi-massive sulfide, disseminated material and dilution based on iron content is made for each producing drawpoint. Dilution is classified as anything with less than 10% iron or less than one percent copper. It can be classified as either internal or external to the ore reserve. Based on prior knowledge of the rock types inherent to a particular stope, the size of muck and/or the presence of blast holes within the muck, the geologist can estimate what percentage of

the dilution is internal or external. These visual estimations are compiled at the end of each month and a total average dilution figure for internal and external dilution is derived. The external dilution is converted to a weight percent as follows:

Dilution Weight % = (Dilution Volume % x Tonnage Factor for Ore/Tonnage Factor for Waste)/(100-Dilution Volume % x Tonnage Factor for Ore/Tonnage Factor for Waste)

An average weight percent for the external dilution is determined for a particular stope life. This enables the geologist to reconcile back to the original estimated reserve to determine the accuracy of the original ore reserve estimation and therefore determine subsequent mining losses. This method has been employed at Ruttan since 1979.

The "rule of thumb" quantity of 1m and 1.8m of wall slough is employed irrespective of depth, rock quality, stope configuration or stope width. The dilution, as estimated in terms of ore reserve weight, enables the operator to quickly assess the amount of material mined external to the ore. It is a more meaningful value than a volume dilution in that the variability of ore density is incorporated into the definition. This definition will be employed for purposes of this study.

It is important to comment on the accuracy of the procedure. Dilution is an observed parameter that has been recorded in most instances on a daily basis for each drawpoint.

The frequency of observation and the consistancy of measurement has produced a figure that is a reliable measure of the waste tonnage that comes from a particular stope. In addition to the dilution being observed, the copper and zinc grades are estimated on a monthly basis for each producing stope. They are determined from grab samples, drill hole assays and from the observed dilution. The observed grades were found to be historically within 3% of milled grade (1979 - present). Dilution evaluated solely on a grade basis would yield:

$$\text{Dilution } (\%) = (Go - Gm)/(Gm - Gd)$$

where: Go - is the grade of undiluted ore
Gm - is the grade of tonnage milled
Gd - is the grade of dilution

The problem associated with this method is in determining the value "Go and Gd". Presently work is being conducted in better estimating the two grades on a monthly basis and relating the value to the observed dilution. In addition, sonic probes are being developed by Ruttan/UBC in enabling the operator to profile the void created. It is assumed that the accuracy of grade observation extends to that of dilution estimation since one has an effect on the other. However, the dilution approach at Ruttan is valid for Ruttan and the absolute values must be calibrated for other operations intending to employ this methodology towards stope design.

6.3 Observed Dilution

The following outlines the method employed in determining the resultant dilution at various stages of stope extraction. As mentioned, the observed dilution is a measure of the external waste for a particular stope and can be defined as shown in Figure 6.1. Dilution measurements are recorded daily and tabulated monthly as indicated previously. This is subsequently converted by the author into a given volume of stope excavation exhibiting a particular level of dilution. Monthly tabulations are made and plotted as shown in Figure 6.2 for a particular stope. The cumulative dilution is recorded versus the volume extracted. This volume excavated is determined through recording the trammed tonnes for a particular stope.

The volume drawn is related to the volume excavated since it is general practice at Ruttan to :

- muck evenly from all drawpoints. This is required in order to ensure that the dilution is evenly distributed, ie. the dilution values recorded are representative for the void mined. By shutting down a drawpoint, one would bias the dilution estimates.

- muck all stopes until empty, thereby ensuring a free-face for the subsequent blast. Normally a maximum lag time

between tonnes blasted and mucked is two months. The undercut may be full, therefore the blasted reserves may not exactly be related to the dilutions determined for the tonnes trammed.

The volume associated with the resultant dilution was estimated in this manner rather than employing blasted reserves, in that the dilution estimate is directly related to the tonnes drawn and/or the void created. It is not necessarily related to the tonnes blasted especially if not all the blasted reserves have been trammed.

The incremental dilution (%) is a measure of the amount of wall slough over an increment of excavated volume. Figure 6.2 depicts the resultant incremental dilution for successive mining intervals that are equivalent to 10% of the total stope reserve volume. It graphically shows that as the stope is initially excavated, ie. first 10% of ore volume removed, the dilution is low. However, when the stope is almost completely excavated (80%), for an additional 10% of stope volume removal, the dilution associated with that 10% volume has increased to 16%.

This incremental dilution will be employed subsequently in estimating blast induced damage, error in estimation and other factors that are difficult to quantify.

6.3.1 Volume Trammed Versus Stope Dimensions Mined

Stope span was determined by employing either of two methods:

Method 1: Average span recorded from stope longitudinals, Figure 6.4.

Method 2: Average span back-calculated from the volume trammed, Figure 6.5, whereby:

Inferred Span = (Volume Trammed)/(Vertical Stope Height x Apparent Stope Width), Figure 6.5.

Generally, when intermediate levels are employed, the stope was blasted for the full stope height and width, Figure 2.15. Prior to January, 1983, ITH stopes were benched, Figure 2.16, where after they were blasted for the full stope height. Method 2 would be a poor approximation for benched stopes. It is true that the benched stopes were blasted for the full stope width, however the stope height was variable. In employing method 2, calculation of the span would be underestimating the true span by employing the final stope height. This affected eight (8) stopes in our data base of forty-three(43). The stope extraction profile could not be reproduced for these stopes prior to 1983. These stopes were included within the data base by recording solely the final stope geometry and the resultant overall dilution.

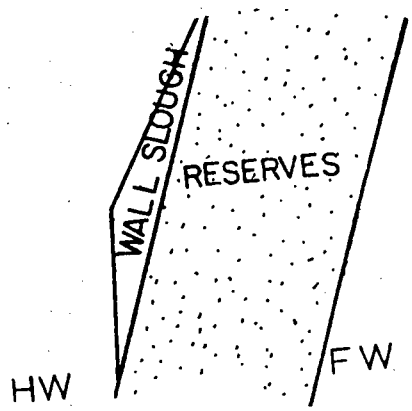

$$\text{Dilution} = \frac{\text{Wt. wall slough}}{\text{Wt. reserves}} \times 100$$

Figure 6.1: Definition of Dilution

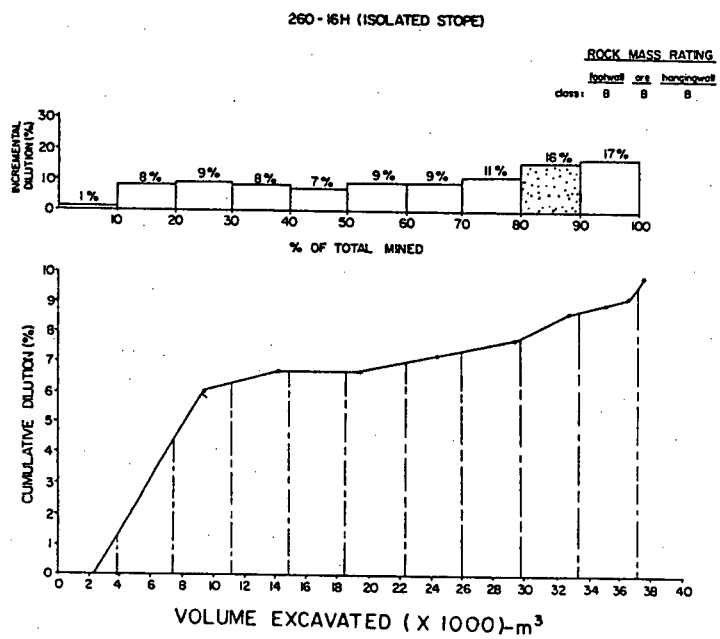

Figure 6.2: Cumulative Dilution VS Volume Excavated

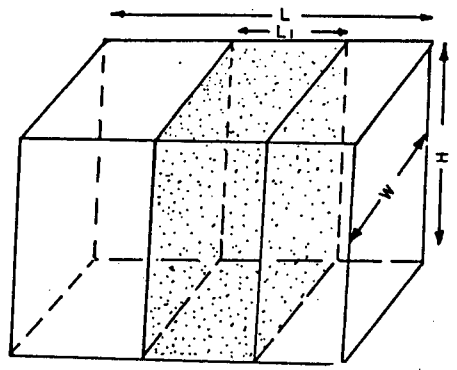

Figure 6.3: Volume Trammed = L1 x W x H

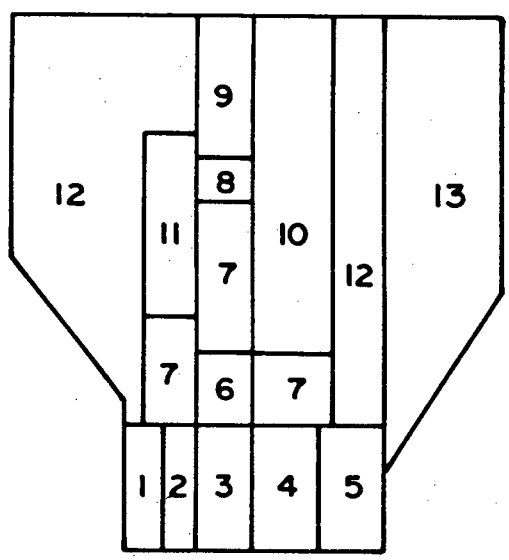

Figure 6.4: Longitudinal Showing A Typical Extraction Sequence

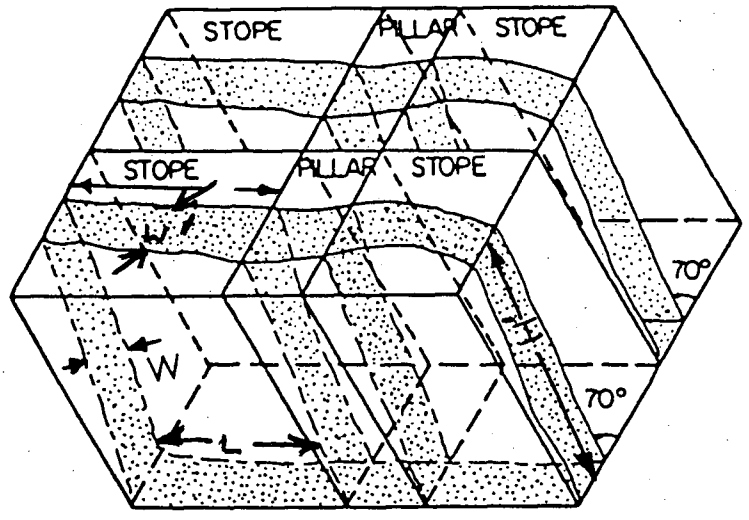

Figure 6.5: Inferred Measurement of Stope Span

Stope Volume = H x W' x L
Stope Volume = H' x W x L

where:

H' = Apparent Stope Height in Plane of Hanging Wall
W = True Stope Width
L = Stope Span
W' = Apparent Stope Width Measured in Horizontal Plan
H = Vertical Stope Height

CHAPTER SEVEN

DATA BASE

7.1 Introduction

This chapter identifies the most critical parameters as determined through single and multivariate statistical analysis. Trend surface analysis has been used to summarize data that is too numerous to be grasped readily by eye. Linear correlations between variables as defined by Spiegel, 1972 were employed initially to determine the relationship between the most critical parameters in order to formulate a governing empirical relationship. A section describing the statistical technique is briefly presented which will outline the general concepts employed in arriving at a statistically significant relationship.

The identification of the parameters formulating the data base are reproduced, which will be subsequently analyzed in determining the most critical parameters in terms of their effect on dilution. The blast correction factor will be discussed in detail since it forms an all encompassing term which will partly compensate for recording error and any blast induced damage. The critical parameters will be subsequently incorporated into a governing equation in Chapter 8 which will analyze further the significance of stope configuration.

7.2 Statistics

In order to assess the suitability of individual sample populations to be described by an appropriate function, multivariate statistical methods were employed. This analysis has been used to describe data that is too numerous to be visually analyzed. This allows values to be predicted along with a quantitative appraisal of the reliability of the prediction.

Koch(1980) suggests that selecting a suitable model depends on "taste, judgement and luck". It is also suggested that the predictive model be chosen in relation to the data base available. A simple model such as a linear or quadratic polynomial is preferred when the data base parameters are not well defined. A more complicated model such as a higher-order polynomial or fourier series may be useful if the data base is well defined and local variability is low and well controlled. A sufficiently complicated function will fit any given set of data, however, this function is not unique (Koch,1980). Therefore, one should not employ multivariate statistical analysis with the hope of generating increasingly more complicated functions with the goal of identifying a "correct" predictive relationship.

This chapter employs multivariate linear correlations

between the control parameter "dilution" and the parameters influencing the control parameter. Initially linear correlations between two parameters, ie. Dilution and Area, will be assessed and subsequently a curve to a plane will be fitted and extended to a linear hyper-surface. This form of expression exhibits a linear variance between the dependent and independent variables employed. They may be reproduced as follows:

$$\text{Dilution}(\%) = A + B(x) \quad \text{line}$$
$$\text{Dilution}(\%) = A + B(x) + C(y) \quad \text{plane}$$
$$\text{Dilution}(\%) = A + B(x) + C(y) + D(w) + \ldots \quad \text{linear hyper-surface}$$

where:
Dilution - Independent parameter
A,B,C,D - Constants
x,y,w - Dependent parameters

The next most complicated expression will be attempted, Chapter 8, which is a quadratic surface. It is expressed as follows:

$$\text{Dilution}(\%) = A + B(x) + C(x^2) \quad \text{quadratic line}$$
$$\text{Dilution}(\%) = A + B(x) + C(x^2) + D(y) + E(y^2) + F(xy) \quad \text{quadratic surface}$$

This section will briefly outline the statistical concepts employed. The reader is referred to Koch(1980) for a more detailed treatise on this topic.

7.2.1 Definition of Statistical Terms

Multivariate analysis attempts to relate independent parameters to the dependent parameters, in terms of a relationship expressed in mathematical form, by determining an equation connecting the variables. A first step is the collection of data showing corresponding values of the variables. Figure 7.1 shows how a curve is fitted to a "scatter diagram" . In order to avoid individual judgement in constructing lines, parabolas, or other approximating curves, it is necessary to agree on a definition of a "best-fitting curve". In Figure 7.1 the independent parameter is "x" and the dependent is "y"(dilution). The goodness of fit is determined by the deviation of the "y predicted" from the "y observed" parameter(y1). Consequently, where the following relation is a minimum, one arrives at the best fit curve defining the relationship between the variables:

$$d1^2 + d2^2 + ... + dn^2 = \text{a minimum}$$

where:

$$dn = (\text{y predicted}) - (\text{y observed})$$

A curve approximating the data in Figure 7.1 is said to fit the data in the least-squares sense and is called a least-squares line,curve or surface. The dependent parameter, in the context of this thesis, is defined as dilution and is

also the control parameter. The independent parameters, among others, are area, rock quality, exposure rate and stope configuration.

The least-squares line approximating the set of points (x1,y1), ..., (xn,yn) has the equation " y = A + Bx " where the constants "A" and "B" are determined by simultaneously solving the equations:

Least Squares Line

$$y = A + B(x)$$
$$\Sigma y = An + B\Sigma x$$
$$\Sigma xy = A\Sigma x + B\Sigma x^2$$

(n = no. of observations)

Similarly, the least squares plane, hyper-surface and quadratic surfaces are also determined from the "normal" equations represented below:

Least Squares Plane

$$z = A + Bx + Cy$$
$$\Sigma z = nA + B\Sigma x + C\Sigma y$$
$$\Sigma xz = A\Sigma x + B\Sigma x + C\Sigma xy$$
$$\Sigma yz = A\Sigma y + B\Sigma xy + C\Sigma y^2$$

Least Squares Quadratic Line

$$z = A + Bx + Cx^2$$
$$\Sigma y = nA + B\Sigma x + C\Sigma x^2$$
$$\Sigma xy = A\Sigma x + B\Sigma x^2 + C\Sigma x^3$$
$$\Sigma x^2y = A\Sigma x^2 + B\Sigma x^3 + C\Sigma x^4$$

Least Squares Hyper-Surface

$$
\begin{aligned}
z &= A + Bx + Cy + Dw + Et \\
\Sigma z &= nA + B\Sigma x + C\Sigma y + D\Sigma w + E\Sigma t \\
\Sigma xz &= A\Sigma x + B\Sigma x^2 + C\Sigma yx + D\Sigma wx + E\Sigma tx \\
\Sigma yz &= A\Sigma y + B\Sigma xy + C\Sigma y^2 + D\Sigma wy + e\Sigma ty \\
\Sigma wz &= A\Sigma w + B\Sigma xw + C\Sigma yw + D\Sigma w^2 + e\Sigma tw \\
\Sigma tz &= A\Sigma t + B\Sigma xt + C\Sigma yt + D\Sigma wt + e\Sigma t^2
\end{aligned}
$$

Least Squares Quadratic Surface

$$
\begin{aligned}
z &= A + Bx + Cy + Dx^2 + Ey^2 + Fxy \\
\Sigma z &= nA + B\Sigma x + C\Sigma y + D\Sigma x + E\Sigma y + F\Sigma xy \\
\Sigma xz &= A\Sigma x + B\Sigma x^2 + C\Sigma xy + D\Sigma x^3 + E\Sigma y^2 x + F\Sigma x^2 y \\
\Sigma x^2 z &= A\Sigma x^2 + B\Sigma x^3 + C\Sigma x^2 y + D\Sigma x^4 + E\Sigma y^2 x^2 + F\Sigma x^3 y \\
\Sigma yz &= A\Sigma y + B\Sigma xy + C\Sigma y^2 + D\Sigma x^2 y + E\Sigma y^3 + F\Sigma xy^2 \\
\Sigma zy^2 &= A\Sigma y^2 + B\Sigma xy^2 + C\Sigma y^3 + D\Sigma x^2 y^2 + E\Sigma y^4 + F\Sigma y^3 x \\
\Sigma zxy &= A\Sigma xy + B\Sigma x^2 y + C\Sigma xy + D\Sigma x^3 y + E\Sigma xy^3 + F\Sigma x^2 y^2
\end{aligned}
$$

A correlation coefficient measures how well a predicted surface will fit the sample data. It is calculated as follows:

$$
r^2 = \frac{\sum(y \text{ est} - \bar{y} \text{ obs})}{\sum(y \text{ obs} - \bar{y} \text{ obs})} = \frac{\text{Explained Variation}}{\text{Total Variation}}
$$

where:

$\underline{y}$ est = predicted value of independent parameter
$\bar{y}$ obs = mean value of the observed independent parameter
y obs = value of the observed independent parameter

The value r^2 can be interpreted as the fraction of the total variation which is explained by the least-squares regression line. "r" measures how well the least-squares regression line fits the sample data. If the total variation is entirely explained by the regression line, ie. r = +1, it is said that there is perfect correlation . If the total variation is entirely unexplained, then the explained variation

is zero and so "r =0". In practice, the quantity "r" lies between "0 and 1". A correlation coefficient of -0.81 indicates that 66% (100 x (-.81)) of the variability of the control (dilution) parameter is explained by the fitted relationship. A correlation of -.27 indicates that only 7% of the variability is explained by the fitted relationship. The deviations "y est- y obs" follow a definite and predictable pattern.

The above concepts can be generalized to more variables. Since the multiple correlation coefficient, as defined previously, is not evaluated in terms of the independent parameters but, only by the control and estimated control parameter.

A further important parameter describing the best fit curve or estimate of the dilution parameter is determining the "confidence levels" for the regression curve. A measure of the scatter of the estimated dilution parameter (y est) for a given value of x1,x2,... xn is determined as follows:

Unbiased Standard Error of Estimate of y on x

$$\hat{S}_{y.x} = \sqrt{\frac{\Sigma(y_{obs} - y_{est})^2}{N}}$$

where:

n = number of sets of observations
N = number of degrees of freedom.
ie. y.x then N = n - 2
y.x.t then N = n - 3

This value is called the standard error of estimate of the predicted dilution given the independent variables from which it was calculated. It is inherent to the definition of the least squares regression curve that the difference between the observed and predicted (z - z est) dilution be a minimum. This will result in the smallest standard error of estimate than for any other possible regression curve.

The standard error of estimate has properties analogous to those of standard deviation. Constructing a pair of lines parallel to the regression line of y on x at respective vertical distances Syx, 2Syx and 3Syx from it, and if "n" is large enough, then there would be included between these pairs of lines about 68%, 95% and 99.7% of the sample points respectively, Figure 7.2. This assumes that the sample population is large and does not require one to estimate the normal distribution of the population by means of the "t" statistic. For sample sizes exceeding thirty(30), it is called a large sample, and can be approximated by a normal distribution and the approximation will improve with increasing "n". For samples of size "n" less than thirty(30), called small samples, this approximation is not as desirable and worsens with decreasing "n". This requires that "small sampling theory" be employed. The above definition for the unbiased standard error of estimate for the population is satisfactory for sample sizes exceeding thirty (Spiegel,1972). This is the situation for the Ruttan data base.

A further statistical test must be introduced - the "level of significance" . This test is required in order to determine that the correlation values that have been calculated, have not done so by chance. This involves hypothesis testing, whereby one is able to determine whether the value of the correlation coefficient found for a sample has arisen from a normal universe. A normal universe is characterized by having a correlation coefficient of zero. Associated with a sample correlation coefficient is a distribution. It is therefore important to determine whether achieving a population correlation coefficient of zero is entirely possible, given the spread of the sample results. This requires that the sample correlation distribution be approximated by a "t" distribution. The probability must then be determined that the standardized distribution, which represents the population correlation coefficient, exceeds zero at a given significance level. Values of correlation coefficients for different levels of significance and degrees of freedom are shown in Table 7.1. This table shows the probability of error in accepting a sample correlation as significant when it should have been rejected. Generally statisticians adopt the terminology that results that are:

(Spiegel, 1972).

- significant at the 0.01 level are "highly significant"
- significant at the 0.05 level but not the 0.01 level are "probably significant"
- significant at levels larger than 0.05 are "not significant"

7.3 Distribution of Data Base

Figure 7.3 shows the distribution of the data formulating the Ruttan data base. Forty-three (43) stopes were assessed from a total of forty-six (46) since the commencement of mining. It was intended to incorporate all stopes at Ruttan and not to bias the results by a selection procedure. The stopes that were not selected were:

- 320 - 19B, a shrinkage-type of stope . ie. entire stope blasted then tramming commenced. Consequently, trammed dilution is not related to void created.

- 370 - 14D, a shrink stope

- 370 - 11D, a mine development problem caused premature stope shut down

Tables 7.2a,b,c identify the individual parameters for each isolated, echelon and rib stope configuration. An observation consists of the following:

1) No. of Observation

2) Stope Name

This is defined by the draw level,the stope number and a lens descriptor (letter)

3) Rock Mass Rating [RMR(%)]

This is defined for the critical wall contact. It normally refers to the hanging wall classification.

4) Stope Height [Ht.(m)]

This is a measure of the apparent stope height (H´) as defined in Figure 6.5.

5) Stope Width [Wdth.(m)]

This is a measure of the true stope width (W) as defined in Figure 6.5.

6) Stope Volume [Vol.(m^3)]

This is a measure of the volume of reserves mined. Observation points were selected at intervals of volume yielding 5000m^3 , 10000m^3 and subsequently in 10000m^3 intervals.

7) Dilution [Dil.(%)]

This parameter was calculated as described in Chapter 6. It was interpolated from plots of "cumulative dilution " versus "volume extracted", Figure 6.2. The interpolation procedure is actually a summary of monthly observations recorded throughout the stope excavation history. For example, the isolated stope data base consists of twenty-two (22) stopes, yielding sixty-one (61) observations which are based upon 200

recordings. This value is recorded as the total cumulative dilution for the stope volume extracted. It has been corrected for the dilution that is recorded at the time of "slot blasting". This will be described subsequently, however, the control parameter has been corrected by subtracting the "blast correction factor" from the observed cumulative dilution. The value recorded in Table 7.2 represents the dilution for a particular volume of mined reserves. The total dilution, however, is actually the recorded value plus the wall slough attributed to slot excavation.

8) Span [m]

This represents the stope span for the volume of reserves removed. It has been determined as outlined in Chapter 6.3.1.

9) Hydraulic Radius [m]

This value has been employed throughout the literature by authors who have conducted work in the field of empirical stope design, Laubscher (1976), Mathews et al (1981). It was employed to determine if it would be a critical parameter in relating the exposed surface area to the conrol parameter. It is a fluid mechanics term (Vennard and Street, 1975) that has been extended to describing the ratio between the exposed surface area/exposed surface perimeter. Mathews has coined this term as the "shape factor" and it is reproduced in Figure 7.4. It is employed to distinguish between one way spanning situations where one

dimension is particularly large with respect to the other. It is shown by this figure that when the long to short span exceeds approximately 4:1, the change in the hydraulic radius is minimal. It is for these geometries that Mathews and Laubsher were particularly trying to distinguish. The initial premise was that a one way spanning situation (ie. tunnel having an exposed surface area of 1000m^2 or 100m long by 10m high) is more stable than a stope wall of which long and short dimensions are similar (32m long by 32m high). This was shown empirically, by both Laubscher and Mathews, to be true. Narrower openings would tend to add a degree of confinement and/or inhibit the occurrence of exposed structures. The hydraulic radius was determined for the Ruttan study in an attempt to relate the results to a wider data base as compiled by previous researchers.It is generally the case for open stoping operations that the hanging wall and footwall surfaces are two-way spanning. It is unlikely that the span ratios would exceed 4:1. This was the case at Ruttan where average span ratios ranged from 1:1 to 3:1. The exposed surface area was also calculated from the span and stope height and correlated to the control parameter.

10) Exposure Rate [m^2/mth]

This value refers to the rate of excavation for a particular stope. It is expressed, initially, as the volume excavated per month, Figure 6.3. The exposure rate is

subsequently calculated as the rate at which the hanging wall or footwall area is exposed. It is expressed as the surface area exposed per month. An example is shown in Figure 6.3 whereby, for the first three months of mining, the shaded area shown in Figure 6.3 has been extracted, consequently:

Rate of Excavation = L1 x H x W/(3 mths) = Volume/ 3 mths

Exposure Rate = L1 x H/(3 mths) = Exposed Surface Area/3mths

or alternatively

Exposure Rate = Rate of Excavation/Width

where width(w) is measured perpendicular to strike and refers to the true stope width.

11) Blast Correction Factor [BCF, %Dilution]

It was found that an initial dilution was present at lower volumes of excavation. This value was higher for stopes exhibiting a lower rock mass quality. Figure 7.5 shows the effect of stope configuration on the extent of the zone of relaxation. A slot is initially excavated from footwall to hanging wall which has the dimensions shown in Figure 7.5. The slot excavated exposes a minimal wall contact under the most favourable confining conditions. Generally the slot is 3.7m x 3.7m for sub-level stopes and 6.1m x 6.1m for ITH stopes, extends for the full stope height and is subsequently slashed for the full stope width. This initial dilution was analyzed

separately from the dilutions observed subsequently. It is generally assumed by Ruttan that dilution in the slot area is negligible and if present, is due to blasting. This dilution is then assumed to be constant over the remainder of the stope life, since the blast practice does not change. Subsequent sections will evaluate the significance of incorporating this correction to the data base. This initial value was subtracted from the subsequent dilution figures recorded to result in a corrected dilution reading. This factor would also tend to compensate for observation error in estimating dilution, since this value should also remain constant for a given stope.

Figure 7.6 shows that the incremental dilution is fairly constant until 30% of the stope has been excavated. The slot generally encompasses a volume of 2500^3- $3000m^3$. The incremental dilution shows that 7% is constant for the first $3000m^3$, after which, it increases and will be subsequently shown to be directily correlated to the enlarged surface area exposed due to mining. Blast damage for 270 Z-Zone is assessed at 7%. This value is generally between 0 - 3%. It has been systematically recorded for the stopes in the calibrated data base as the dilution resulting from the slot area. The slot dilution was calculated as shown above employing incremental dilution estimates and relating the value to the slot area exposed. Figures 7.7,7.8,7.9 summarize the parameter distribution that forms the Ruttan Data Base for the isolated, echelon and rib configurations respectively. A statistical

evaluation for the relevant parameters analyzed for each individual configuration and for the total data base is shown in Table 7.3. A mean and a standard deviation is recorded for each parameter outlined in Figure 7.7,7.8,7.9 and Table 7.3. The average dilution for the forty-three(43) isolated stopes is 10%, whereas the average dilution as derived from the intermediate geometries (133 observations) is only 6%. In order to describe the data base, one has to look at the individual observations for the final and intermediate stope geometries. It is important to know the limitations of any empirically derived formulation, since it is only as accurate as its data base. Extrapolating the observations beyond the observed quantities may have a poorer chance of prediction.

7.4 Identification of Critical Parameters

The observations recorded in Tables 7.2 a,b,c form the basis for the selection of the parameters which have the greatest effect on the control variable "dilution". Initially, dilution was correlated by applying a linear regression analysis to the parameters outlined in Figure 7.10. The dilution sensitive parameters were evaluated with respect to the isolated data base, thereby ensuring that stope configuration would not bias the resulting correlations. The mutual correlations were as follows:

a) Rock Mass Rating

The individual parameters which combine to form the "Rock Mass Rating" were analyzed with respect to the control parameter for the isolated data base. The data base is shown in Table 7.4. A statistically significant correlation coefficient must exceed 0.295 given "n-2" degrees of freedom.(61-2=59). Individually, each coefficient is not statistically significant, Figure 7.11. The highest correlation was obtained between the RQD and dilution (r=-.24). The statistical test is true in the sense that it would select or rank the most critical parameters assuming that the other parameters would not overly bias the correlation. In order to isolate the effect of the other parameters, such as the exposed surface area, multivariate analysis must be employed. This would enable the resultant marginal increase in the overall "best fit" expression to be assessed, Figure 7.10.

Grouping all the parameters that combine to form the "Rock Mass Rating" results in a multiple correlation of 0.3. Relating the RMR value with dilution results in an increased significant correlation of +0.36, Figure 7.10. Consequently, the RMR is selected as a parameter that will reflect the importance of rock quality on dilution. This is not to imply that the NGI system will not be an equal or even better correlative parameter. The RMR was chosen due to its compatibility to the method of data gathering employed at Ruttan. Incorporating "Exposed Surface Area" with the

individual RMR parameters indicates that they would all improve the mutual correlation that exists with dilution and area alone. A third criteria for selection of critical parameters is described. The difference between a correlation of 0.71 and 0.73 is not statistically different at the 95% significance level (Koch,1983) and should be treated jointly. However, in order for the difference to be statistically significant, the correlations would have to generally differ by 0.20 for the isolated data base. The approach taken by the author is to define the most significant parameters "Primary Parameters" and to group the remaining into a linear or quadratic equation that would yield the highest correlation coefficient. A second criteria was the "Criteria for Sensitivity". In order for a parameter to be classified as being dilution sensitive, it must pass the test outlined in Figure 7.12. The governing equation will incorporate the most dilution sensitive and correlative parameters.

b) Stope Dimensions

The best fit parameters were that of exposed surface area, hydraulic radius and span. A mutual correlation between area exposed and hydraulic radius yielded a correlation of +0.96 and the following expression:

$$\text{Area}(m^2) = -460 + 250[\text{Hydraulic Radius}(m)]$$
$$r = +.96 \qquad \hat{s} = \pm 300 m^2$$

Among the three parameters investigated, hydraulic radius and area resulted in higher correlations, Figure 7.10. The primary parameter "Area" will be employed rather than hydraulic radius, due to the high correlation that exists between the two. However, a governing equation in terms of hydraulic radius will also be generated in order for the author to enable comparison of results to other researchers. Figure 7.13 shows the resultant multiple correlations upon combining RMR and stope geometry with that of dilution.

Historically mine operators associated dilution with that of increased span. It was found that for the isolated data base that :

$$\text{Dilution (\%)} = 0.45 + 0.27(\text{span in meters}) \quad r = 0.68 \quad \hat{s} = \pm 3.8\%$$

The governing equation will also be generated in terms of span.

c) Stress

The significance of depth on dilution was assessed in Figure 7.10. It did not yield a statistically significant correlation on its own. Upon combining RMR and "Area", as shown in Figure 7.13, it only marginally increased the combined correlation (.76 to .77). It, however, was not sensitive as per the original definition, Figure 7.12.

The use of fill and no fill was correlated to the

"echelon" data base since fill in adjacent stopes would only affect the echelon and rib configurations. Upon closer examination of the mining sequence and filling cycles, it was concluded that fill was only used as a working platform and not as a means of stabilizing adjacent areas as initially planned. Only five stopes had benefited from having fill in the adjacent stopes, all of them being of the echelon configuration:

320-18J
370-20KN
370-19K
430-12D
430-13D H/W

(19 obs.)

Employing multivariate analysis on the echelon data base does not result in an improvement in either correlation or sensitivity, Figure 7.14. The results were significant at the 99% confidence level, however, it is of the author's opinion that the data base is not sufficiently large to be a reliable estimator.

d) Mining Method

The excavation and exposure rate were mutually correlated to dilution as shown in Figure 7.10. Upon combining RMR and Area, this resulted in multiple correlations as shown in Figure 7.13. The exposure rate was subsequently employed as

augmenting the primary parameters since it yielded an overall higher correlation and sensitivity.

A further analysis was conducted on stopes employing 51mm (conventional) and 151mm (ITH) drilling and their resultant effect on dilution. The 51mm stopes are as follows, refer Table 7.2a:

370-10B
370-15C
370-19J
370-12/13F
430-13D F/W
430-14D
430-12F

no. obs= 29

Multivariate analysis showed that this parameter was not statistically significant, Figure 7.13.

Mine sequence, which refers to the direction of mining, ie. footwall to hanging wall lenses or vice versa, was correlated to the expression shown in Figure 7.14 for the echelon configuration. The following echelon stopes were mined from hanging wall to footwall:

320-18J
370-20KN
370-19K
370-21J
370-21KN
430-21J F/W

no. obs=21

Figure 7.14 indicates that the correlation coefficient

improved upon incorporating mine sequence into the empirical equation and was marginally sensitive. This was further assessed by introducing the "mine sequence parameter" as an option. A mining direction from hanging wall to footwall would dictate that the parameter "opt.=0" otherwise, it would be set to "opt.=1". The following equation was derived:

$$Dil(\%)=7.1 - .12(RMR) + .003(Area) + 1.4(Opt)$$
$$r=\pm.81 \quad \hat{s}=\pm 3\%$$

Upon combining the secondary parameter "Exposure Rate" with the existing governing equation, Figure 7.14, it is determined that the mine sequence does not marginally improve the overall correlation/sensitivity. In addition the partial correlation coefficient (Sect. 7.4.1) for "mine sequence" was found to not be statistically significant, Figure 7.16.

The "Blast Correction Factor" was correlated to the RMR and was shown to be statistically significant at the 99% confidence level. It showed that as the Rock Mass Rating increased, the BCF decreased. Other parameters affecting the BCF were not studied since the factors that would contribute to the BCF were not recorded in the original data base, Chapter 7.3. These factors would be difficult to quantify (other than RMR) since they should include a detailed assessment of blasting/drilling practices, sampling error in dilution estimate and a study of possible stress induced failure that

may exist within the slot area. These, among other factors, should be studied in greater detail in determining the extent of the BCF. Present practice at Ruttan is to reduce the BCF to where the governing equation is able to account for all the dilution that is attributed to a stope.

The governing equation is a combination of the primary parameters :

Area
Rock Mass Rating

and the secondary parameter:

Exposure Rate

A sensitivity analysis was performed on the best fit equation incorporating the relevant parameters for the "total stope " data base (131 obs.), Figure 7.15.

An alternate method of analyzing the above relevant parameters is described in the follows section employing "partial correlation coefficients". This was employed in order to determine the secondary parameters critical to the governing equation.

7.4.1 Partial Correlation (rp)

It is often required to measure the correlation between the dependent variable (dilution) and one independent variable when all other variables involved are kept constant. This can be obtained by defining a coefficient of partial correlation (Spiegel,1973). It is derived as follows:

$$r12.3 = \frac{r12 - r13 \times r23}{\sqrt{(1-r^2 13)\times(1-r^2 23)}}$$

$$r12.34 = \frac{r12 - r13.4 \times r23.4}{\sqrt{(1-r^2 13.4)\times(1-r^2 23.4)}}$$

given: Dil(%) = A + B(Area) - C(RMR) -D(Exp.Rate)
Parameter [1] : [3] [4] [2]

r12.3 = correlation coefficient between parameter [1] and [2] while parameter [3] is constant. In obtaining this coefficient other parameters are not considered.

r12 = correlation coefficient between parameter [1] and [2].

r12.34 = represents correlation coefficient between parameter [1] and [2] while parameters [3] and [4] are constant and others are not considered.

Figure 7.16 shows the partial correlation coefficient (rp) between the secondary parameters and the control parameter keeping "RMR and Area" constant. Similar results to that of Figures 7.13,7.14 are obtained. The only statistically significant secondary parameter being that of "Exposure Rate". Figure 7.10 shows that dilution is largely insensitive to the "stope span/width" ratio when area and rock mass rating are held constant.

7.5 Quadratic/Linear Interpretation

The above analysis was based upon a linear interpretation of variance between parameters. A quadratic expression was also attempted as shown in Figure 7.17. Figure 7.18 compares the correlations as derived between the primary parameters. Table 7.5 compares the predicted dilutions for the best fit linear and quadratic expressions employing the primary parameters. The quadratic equation yields a mean sample difference between the observed and predicted dilution of 2.1%, whereas the linear expression resulted in 2.5%. It is true that the quadratic correlation results in a statistically more significant coefficient than the linear expression, however, upon closer examination of the expression, this is to be expected. The quadratic best fit expression,Figure 7.17, actually incorporates the linear expression and therefore would produce a better fit.

Given "n" observations, a curve having "n" number of parameters would yield a perfect correlation. This of course could be theoretically possible, but practically difficult to employ and understand. Consequently, the additional quadratic surface that would incorporate all the significant primary and secondary parameters would have to be of the form of expression shown in Figure 7.17(3). The marginal increase in predictive accuracy does not warrant the additional complexity inherent to the quadratic equation. Consequently, linear interpretation will be employed since it has produced significant correlations comprised of simply defined relationships.

7.6 Observations/Conclusions

This chapter summarizes the parameters that were found to be particularly significant and sensitive to the control parameter "Dilution". The governing equation will incorporate "Area, Rock Mass Rating and the Exposure Rate" which statistically are significant at a 99% confidence level. The hypothesis at this point concludes that:

DILUTION IS DIRECTLY RELATED TO THE ROCK QUALITY, THE EXPOSED SURFACE AREA AND THE RATE OF MINING GIVEN THE CONDITIONS PREVAILING FOR THE RUTTAN OREBODY.

Table 7.1: Values of Correlation Coefficient for Different Levels of Significance

DEGREES OF FREEDOM	PROBABILITY	
	.05	.01
1	.988	1.00
2	.900	.980
3	.805	.934
4	.729	.882
5	.669	.883
6	.621	.789
7	.582	.750
8	.549	.715
9	.521	.685
10	.497	.658
11	.476	.634
12	.457	.612
13	.441	.592
14	.426	.574
15	.412	.558

DEGREES OF FREEDOM	PROBABILITY	
	.05	.01
16	.4	.542
17	.389	.528
18	.378	.515
19	.369	.503
20	.360	.492
25	.323	.445
30	.296	.409
35	.275	.381
40	.257	.358
45	.243	.338
50	.231	.322
60	.211	.295
70	.195	.274
80	.183	.256
90	.173	.242
100	.164	.230

Table 7.2a: Isolated Stopes Data Base

ISOLATED STOPES DATA BASE — NUMBER OF STOPES = 22

No.	Stope	RMR(%)	Ht.(m)	Wdth.(m)	Vol.(m^3)	Dil.(%)	Span(m)	H.R.(m)	E.R.(m^2/mth)	B.C.F.(%)
1	260 11 F	60	45	8	5000	5	15	6	0.19	3
2	260 11 F	60	45	8	10000	10	53	12	0.23	3
3	260 18 J	51	84	10	5000	3	6	3	0.30	5
4	260 18 J	51	84	10	10000	6	12	5	0.40	5
5	260 18 J	51	84	10	20000	6	24	9	0.40	5
6	260 18 J	51	84	10	30000	9	34	12	0.30	5
7	260 16 H	80	95	13	5000	2	6	3	0.25	0
8	260 16 H	80	95	13	10000	6	15	7	0.36	0
9	260 16 H	80	95	13	20000	7	20	8	0.37	0
10	260 16 H	80	95	13	30000	8	29	11	0.38	0
11	260 16 H	80	95	13	40000	9	46	16	0.21	0
12	270 0 Z	46	48	8	5000	6	13	5	0.15	7
13	270 0 Z	46	48	8	10000	11	26	8	0.09	7
14	320 14 BE	25	105	10	5000	20	44	16	0.21	3
15	320 13 E	79	80	10	5000	6	16	7	0.13	-1
16	320 15 H	66	75	17	5000	0	4	2	0.10	5
17	320 15 H	66	75	17	10000	1	9	4	0.14	5
18	320 15 H	66	75	17	20000	2	17	7	0.22	5
19	320 15 H	66	75	17	30000	3	25	9	0.23	5
20	320 15 H	66	75	17	40000	3	32	11	0.22	5
21	320 18 JN	81	75	13	5000	9	12	5	0.22	-1
22	320 19 J	84	75	25	5000	0	8	3	0.15	0
23	320 19 J	84	75	25	10000	4	16	7	0.18	0
24	320 19 J	84	75	25	20000	6	32	11	0.16	0
25	320 11 B	41	77	9	5000	22	45	14	0.20	-1
26	340 11 C	43	40	8	5000	5	16	6	0.13	10
27	340 11 C	43	40	8	10000	9	42	10	0.14	10
28	370 21 JN	3	52	10	5000	14	37	11	0.32	-1
29	370 15 H	80	76	23	5000	6	23	9	0.09	-1
30	370 10 B	51	63	11	5000	2	8	3	0.12	10
31	370 10 B	51	63	11	10000	3	16	6	0.11	10
32	370 15 C	51	63	9	5000	0	9	4	0.21	29
33	370 15 C	51	63	9	10000	7	19	7	0.19	29
34	370 15 C	51	63	9	20000	11	43	13	0.17	29
35	370 19 J	43	60	23	5000	0	4	2	0.16	2
36	370 19 J	43	60	23	10000	0	8	4	0.19	2
37	370 19 J	43	60	23	20000	5	15	6	0.20	2
38	370 19 J	43	60	23	30000	13	29	10	0.13	2
39	370 16 H	80	76	20	5000	7	27	10	0.12	-1
40	370 12 13F	70	60	10	5000	0	8	4	0.11	0
41	370 12 13F	70	60	10	10000	3	21	8	0.13	0
42	430 13 D F/W	80	60	32	5000	2	3	1	0.08	0
43	430 13 D F/W	80	60	32	10000	4	5	2	0.13	0
44	430 13 D F/W	80	60	32	20000	5	10	4	0.16	0
45	430 13 D F/W	80	60	32	30000	5	16	6	0.16	0
46	430 13 D F/W	80	60	32	40000	5	21	8	0.16	0
47	430 13 D F/W	80	60	32	50000	6	26	9	0.16	0
48	430 13 D F/W	80	60	32	60000	6	31	10	0.16	0
49	430 13 D F/W	80	60	32	70000	7	36	11	0.15	0
50	430 13 D F/W	80	60	32	80000	10	42	12	0.13	0
51	430 14 D	80	60	30	5000	1	3	1	0.06	0
52	430 14 D	80	60	30	10000	3	6	3	0.09	0
53	430 14 D	80	60	30	20000	6	11	5	0.11	0
54	430 14 D	80	60	30	30000	8	17	7	0.03	0
55	430 14 D	80	60	30	40000	9	22	8	0.03	0
56	430 14 D	80	60	30	50000	12	40	12	0.03	0
57	430 21 K	70	52	10	5000	1	10	4	0.21	0
58	430 21 K	70	52	10	10000	1	20	7	0.26	0
59	430 21 K	70	52	10	20000	2	40	11	0.25	0
60	430 12 F	32	85	10	5000	1	6	3	0.11	0
61	430 12 F	32	85	10	10000	25	30	11	0.10	0

BCF = -1 Refers to Benched Stope

Table 7.2b: Echelon Stopes Data Base

ECHELON STOPES DATA BASE — NUMBER OF STOPES = 12

No.	Stope	RMR(%)	Ht.(m)	Wdth.(m)	Vol.(m^3)	Dil.(%)	Span(m)	H.R.(m)	E.R.(m^2/mth)	B.C.F.(%)
1	320 12 BE	47	80	7	5000	11	9	4	0.10	4
2	320 12 BE	47	80	7	10000	12	27	10	0.14	4
3	320 18 J	56	73	9	5000	4	15	6	0.21	9
4	320 18 J	56	73	9	10000	10	35	12	0.10	9
5	370 20 KN	45	64	15	5000	1	6	3	0.09	2
6	370 20 KN	45	64	15	10000	3	11	5	0.12	2
7	370 20 KN	45	64	15	20000	9	22	8	0.15	2
8	370 20 KN	45	64	15	30000	12	46	13	0.13	2
9	370 20 KN	45	64	15	40000	13	49	14	0.13	2
10	370 13 D	49	50	25	5000	1	4	2	0.18	3
11	370 13 D	49	50	25	10000	3	8	3	0.24	3
12	370 13 D	49	50	25	20000	3	16	6	0.20	3
13	370 13 D	49	50	25	30000	7	24	8	0.11	3
14	370 13 D	49	50	25	40000	10	35	10	0.10	3
15	370 19 K	62	115	13	5000	0	3	2	0.18	0
16	370 19 K	62	115	13	10000	1	7	3	0.22	0
17	370 19 K	62	115	13	20000	3	14	6	0.21	0
18	370 19 K	62	115	13	30000	4	21	9	0.22	0
19	370 19 K	62	115	13	40000	5	28	11	0.25	0
20	370 19 K	62	115	13	50000	8	35	13	0.22	0
21	370 21 J	60	65	15	5000	0	5	2	0.23	2
22	370 21 J	60	65	15	10000	1	10	4	0.23	2
23	370 21 J	60	65	15	20000	3	20	8	0.21	2
24	370 21 J	60	65	15	30000	4	30	10	0.19	2
25	370 21 KN	23	44	8	5000	2	16	6	0.28	7
26	370 21 KN	23	44	8	10000	12	30	9	0.28	7
27	370 12 D	26	85	24	5000	2	3	1	0.04	3
28	370 12 D	26	85	24	10000	7	5	2	0.07	3
29	370 12 D	26	85	24	20000	11	10	4	0.08	3
30	370 12 D	26	85	24	30000	15	38	13	0.08	3
31	430 13 F	33	42	10	5000	1	16	6	0.19	8
32	430 13 F	33	42	10	10000	9	35	10	0.28	8
33	430 12 D	26	85	24	5000	2	3	1	0.04	3
34	430 12 D	26	85	24	10000	7	5	2	0.07	3
35	430 12 D	26	85	24	20000	11	10	4	0.08	3
36	430 12 D	26	85	24	30000	15	38	13	0.08	3
37	430 21 J F/W	65	53	24	5000	4	4	2	0.05	2
38	430 21 J F/W	65	53	24	10000	5	18	7	0.04	2
39	430 13 D H/W	52	64	18	5000	2	5	2	0.10	0
40	430 13 D H/W	52	64	18	10000	4	9	4	0.14	0
41	430 13 D H/W	52	64	18	20000	6	19	7	0.16	0
42	430 13 D H/W	52	64	18	30000	7	28	10	0.17	0
43	430 13 D H/W	52	64	18	40000	8	37	11	0.13	0
44	430 13 D H/W	52	64	18	50000	8	40	12	0.11	0

BCF = -1 Refers to Benched Stope

Table 7.2c: Rib Stopes Data Base

RIB STOPES DATA BASE — NUMBER OF STOPES = 9

No.	Stope	RMR(%)	Ht.(m)	Wdth.(m)	Vol.(m^3)	Dil.(%)	Span(m)	H.R.(m)	E.R.(m^2/mth)	B.C.F.(%)
1	320 10 B	34	112	12	5000	0	4	2	0.22	0
2	320 10 B	34	112	12	10000	8	7	3	0.22	0
3	320 10 B	34	112	12	20000	13	15	7	0.25	0
4	320 10 B	34	112	12	30000	16	22	9	0.27	0
5	320 10 B	34	112	12	40000	16	30	12	0.29	0
6	320 10 B	34	112	12	50000	16	37	14	0.30	0
7	320 10 B	34	112	12	60000	16	44	16	0.31	0
8	320 10 B	34	112	12	70000	16	46	16	0.28	0
9	320 12 B	23	106	10	5000	27	20	8	0.24	-1
10	340 12 C	30	40	20	5000	8	6	3	0.12	5
11	340 12 C	30	40	20	10000	10	13	5	0.16	5
12	370 20 J	69	75	22	5000	5	3	1	0.04	1
13	370 20 J	69	75	22	10000	7	6	3	0.08	1
14	370 14 C	47	65	7	5000	8	12	5	0.16	22
15	370 14 C	47	65	7	10000	13	32	11	0.20	22
16	370 18 J	54	75	10	5000	2	7	3	0.20	2
17	370 18 J	54	75	10	10000	9	14	6	0.30	2
18	370 18 J	54	75	10	20000	14	29	11	0.37	2
19	370 18 J	54	75	10	30000	14	43	14	0.31	2
20	370 11 F	57	50	10	5000	9	10	4	0.04	15
21	430 15 D	51	64	15	5000	2	6	3	0.19	0
22	430 15 D	51	64	15	10000	6	11	5	0.23	0
23	430 15 D	51	64	15	20000	9	22	8	0.23	0
24	430 15 D	51	64	15	30000	11	33	11	0.24	0
25	430 15 D	51	64	15	40000	14	47	13	0.15	0
26	430 20 K	74	46	10	5000	1	11	4	0.28	0
27	430 20 K	74	46	10	10000	1	22	7	0.18	0
28	430 20 K	74	46	10	20000	2	38	10	0.21	0

BCF = -1 Refers to Benched Stope

Table 7.3: Data Base - Statistical Summary

PARAMETER	TOTAL	ISOLATED	ECHELON	RIB
No. OF STOPES	43	22	12	9
No. OF OBSERVATIONS	133	61	44	28
Rock Mass Rating (%)	55 ± 19	64 ± 19	47 ± 14	48 ± 16
	(56 ± 20)	(59 ± 22)	(45 ± 15)	(49 ± 17)
EXP. RATE ($^{\circ}$1000m^2/mth)	.18 ± .09	.18 ± .09	.15 ± .07	.22 ± .09
	(.18 ± .08)	(.17 ± .07)	(.15 ± .08)	(.18 ± .09)
HYD. RADIUS (m)	7 ± 4	7 ± 4	7 ± 4	8 ± 5
	(11 ± 3)	(11 ± 3)	(11 ± 2)	(10 ± 4)
SPAN (m)	20 ± 14	21 ± 14	19 ± 14	21 ± 15
	(31 ± 13)	(32 ± 13)	(34 ± 8)	(24 ± 16)
SURFACE AREA (m^2)	1450 ± 1120	1420 ± 1020	1360 ± 1085	1705 ± 1545
	(2250 ± 1120)	(2254 ± 970)	(2360 ± 924)	(2090 ± 1550)
SPAN/WIDTH RATIO	1.6 ± 1.3	1.6 ± 1.5		
	(3.4 ± 1.7)	(3.2 ± 1.8)		
STOPE HEIGHT (m)	71 ± 21	68 ± 15	72 ± 23	78 ± 28
	(68 ± 20)	(68 ± 16)	(68 ± 21)	(70 ± 25)
BCF (%)	3 ± 6	3 ± 9	3 ± 3	3 ± 7
DILUTION (%)	7 ± 6	6 ± 5	6 ± 4	10 ± 7
	(10 ± 6)	(10 ± 6)	(10 ± 4)	(12 ± 7)
STOPE DEPTH (m)	368 ± 54	356 ± 65	385 ± 36	369 ± 47
	(360 ± 48)	(346 ± 55)	(382 ± 40)	(369 ± 40)
STOPE INCLINATION ($^{\circ}$)		67 ± 9		
		(68 ± 9)		
STOPE WIDTH (m)		18 ± 9		
		(15 ± 8)		
LONG SPAN/SHORT SPAN		5.1 ± 5		
		(2.1 ± 1.1)		

( ) Refers to Final Stope Configuration

Table 7.4: Isolated Stopes Data Base

- Typical RMR Classification

ISOLATED STOPES DATA BASE - TYPICAL RMR CLASSIFICATION

No.	Stope	Dil(%)	Stren.	RQD	Spac.	Condit.
1	260 11 F	5	7	8	20	12
2	260 11 F	10	7	8	20	12
3	260 18 J	3	4	8	10	20
4	260 18 J	6	4	8	10	20
5	260 18 J	6	4	8	10	20
6	260 18 J	9	4	8	10	20
7	260 16 H	2	7	17	25	20
8	260 16 H	6	7	17	25	20
9	260 16 H	7	7	17	25	20
10	260 16 H	8	7	17	25	20
11	260 16 H	9	7	17	25	20
12	270 0 I	5	5	10	15	12
13	270 0 I	11	6	10	15	12
14	320 14 BE	20	4	3	10	6
15	320 13 E	6	7	17	25	20
16	320 15 H	0	7	10	21	12
17	320 15 H	1	7	10	21	12
18	320 15 H	2	7	10	21	12
19	320 15 H	3	7	10	21	12
20	320 15 H	3	7	10	21	12
21	320 18 JN	9	12	17	22	20
22	320 19 J	0	12	17	25	20
23	320 19 J	4	12	17	25	20
24	320 19 J	6	12	17	25	20
25	320 11 B	22	7	8	20	6
26	340 11 C	5	2	8	20	6
27	340 11 C	3	2	8	20	6
28	370 21 JN	14	2	3	5	3
29	370 15 H	6	8	17	25	20
30	370 10 B	2	4	8	20	6
31	370 10 B	3	4	8	20	6
32	370 15 C	0	7	8	20	20
33	370 15 C	7	7	8	20	20
34	370 15 C	11	7	8	20	20
35	370 19 J	0	7	8	10	8
36	370 19 J	0	7	8	10	8
37	370 19 J	5	7	8	10	8
38	370 19 J	13	7	8	10	8
39	370 16 H	7	8	17	25	20
40	370 12 13F	0	7	13	20	20
41	370 12 13F	3	7	13	20	20
42	430 13 D F/W	2	7	18	25	20
43	430 13 D F/W	4	7	18	25	20
44	430 13 D F/W	5	7	18	25	20
45	430 13 D F/W	5	7	18	25	20
46	430 13 D F/W	5	7	18	25	20
47	430 13 D F/W	6	7	18	25	20
48	430 13 D F/W	6	7	18	25	20
49	430 13 D F/W	7	7	18	25	20
50	430 13 D F/W	10	7	18	25	20
51	430 14 D	1	7	17	25	20
52	430 14 D	3	7	17	25	20
53	430 14 D	5	7	17	25	20
54	430 14 D	8	7	17	25	20
55	430 14 D	3	7	17	25	20
56	430 14 D	13	7	17	25	20
57	430 21 K	1	4	17	13	6
58	430 21 K	1	4	17	13	6
59	430 21 K	2	4	17	13	6
50	430 12 F	1	5	8	20	3
51	430 12 F	25	5	8	20	3

Table 7.5: Isolated Stopes Data Base - Comparison Quadratic and Planar Surface Empirical Equations

ISOLATED STOPES DATA BASE - COMPARISON QUADRATIC AND PLANAR SURFACE EMPIRICAL EQUATIONS

$$\underline{DIL(\%) = 6 - 8(RMR) + 3.5(AREA)}$$
$$\underline{r = .76 \quad s = \pm 3.4\%}$$

$$\underline{DIL(\%) = 1.1 + 10.3(AREA) - 11.2(RMR) - .7(AREA)^2 + 13.2(RMR)^2 - 7.1(AREA)(RMR)}$$
$$\underline{r = .82 \quad s = \pm 2.9}$$

No.	RMR(%)	AREA (m^2)	Res. Dil(%)	Quad. Dil(%)	Diff.(%)	Lin. Dil(%)	Diff. (%)
1	60	675	5	3	2	4	1
2	60	2385	10	10	0	10	0
3	51	504	3	2	1	4	1
4	51	1008	6	5	1	5	1
5	51	2016	6	9	3	9	3
6	51	2856	9	12	3	12	3
7	80	570	2	3	1	2	0
8	80	1425	6	6	0	5	1
9	80	1900	7	7	0	6	1
10	80	2755	8	8	0	9	1
11	80	4370	9	7	2	15	6
12	46	624	6	3	3	5	1
13	46	1248	11	6	5	7	4
14	25	4620	20	24	4	20	0
15	79	1280	6	5	1	4	2
16	66	300	0	1	1	2	2
17	66	675	1	3	2	3	2
18	66	1275	2	5	3	5	3
19	66	1875	3	8	5	7	4
20	66	2400	3	9	6	9	6
21	81	900	9	4	5	3	6
22	84	600	0	3	3	1	1
23	84	1200	4	5	1	3	1
24	84	2400	6	7	1	8	2
25	41	3465	22	16	6	15	7
26	43	640	5	3	2	5	0
27	43	1680	9	9	0	8	1
28	3	1924	14	18	4	12	2
29	80	1748	6	7	1	6	0
30	51	504	2	2	0	4	2
31	51	1008	3	5	2	5	2
32	51	567	0	2	2	4	4
33	51	1197	7	6	1	6	1
34	51	2709	11	12	1	11	0
35	43	240	0	0	0	3	3
36	43	480	0	2	2	4	4
37	43	900	5	5	0	6	1
38	43	1740	13	9	4	9	4
39	80	2052	7	7	0	7	0
40	70	480	0	2	2	2	2
41	70	1260	3	5	2	5	2
42	80	180	2	1	1	0	2
43	80	300	4	2	2	1	3
44	80	600	5	3	2	2	3
45	80	960	5	4	1	3	2
46	80	1260	5	5	0	4	1
47	80	1560	6	6	0	5	1
48	80	1860	6	7	1	6	0
49	80	2160	7	7	0	7	0
50	80	2520	10	8	2	8	2
51	80	180	1	1	0	0	1
52	80	360	3	2	1	1	2
53	80	660	6	3	3	2	4
54	80	1020	8	5	3	3	5
55	80	1320	9	5	4	4	5
56	80	2400	12	8	4	8	4
57	70	520	1	2	1	2	1
58	70	1040	1	5	4	4	3
59	70	2080	2	8	6	8	6
60	32	510	1	3	2	5	4
61	32	2550	25	15	10	12	13

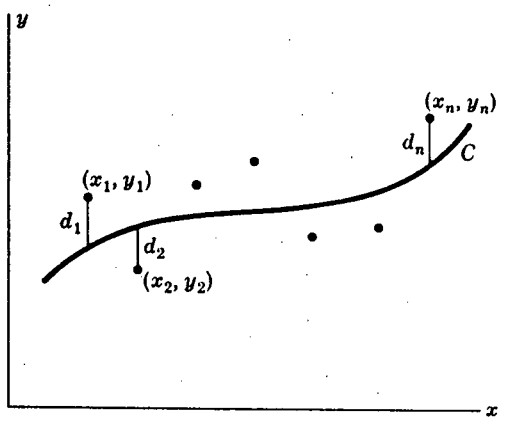

Figure 7.1: Scatter Diagram

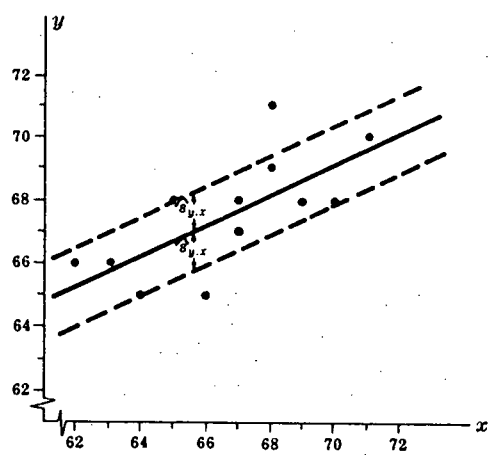

Figure 7.2: Example of Standard Error of Estimate

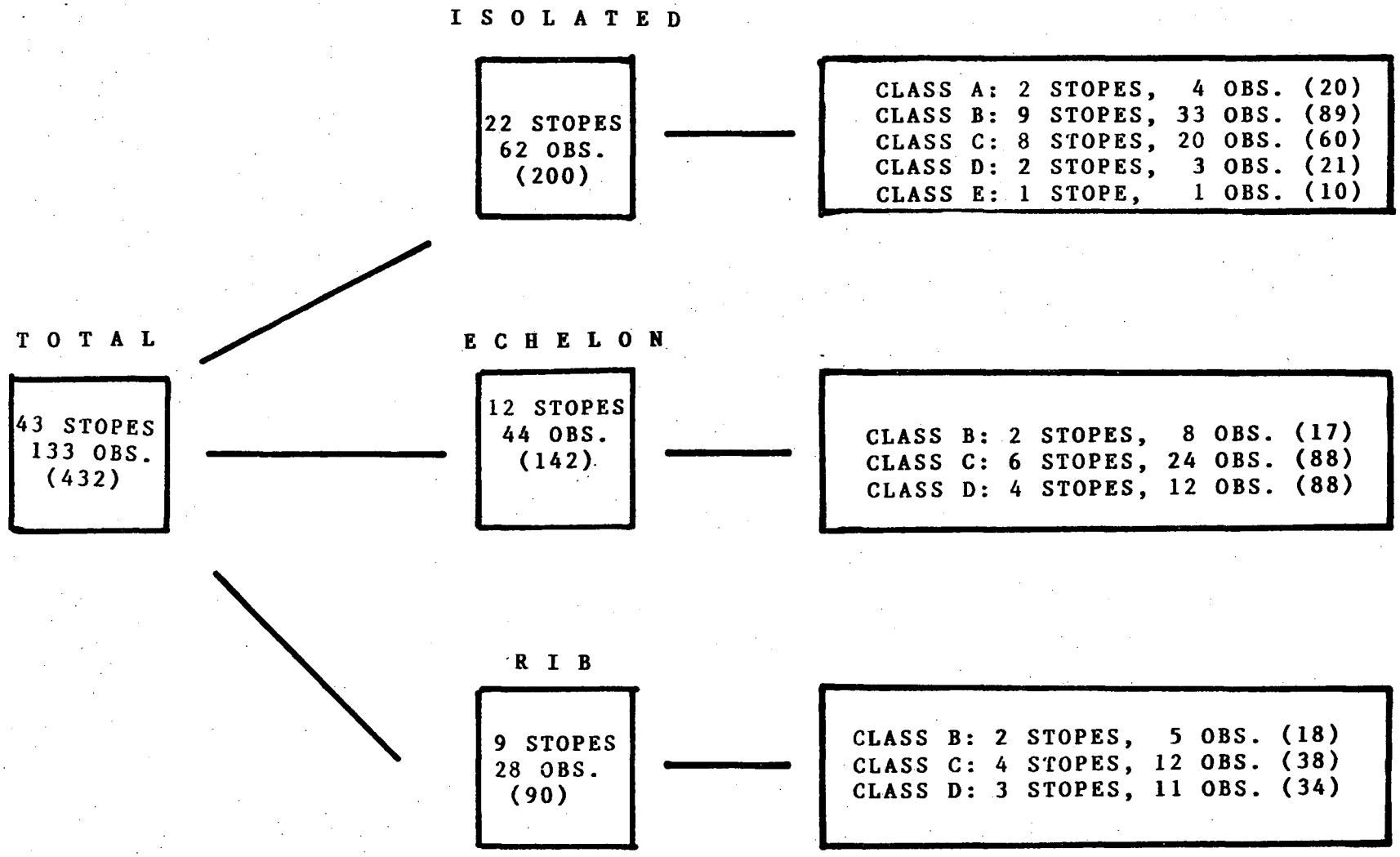

Figure 7.3: Distribution of Stopes - Data Base

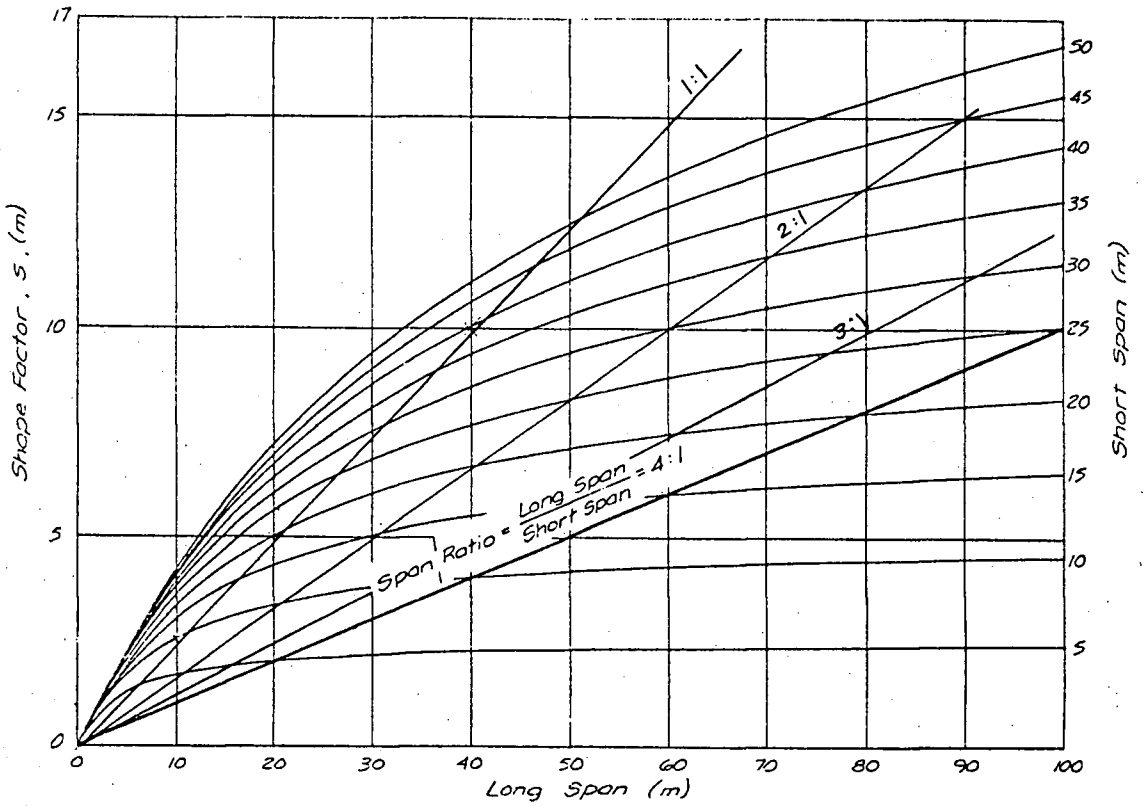

Figure 7.4: Shape Factor (Hydraulic Radius)

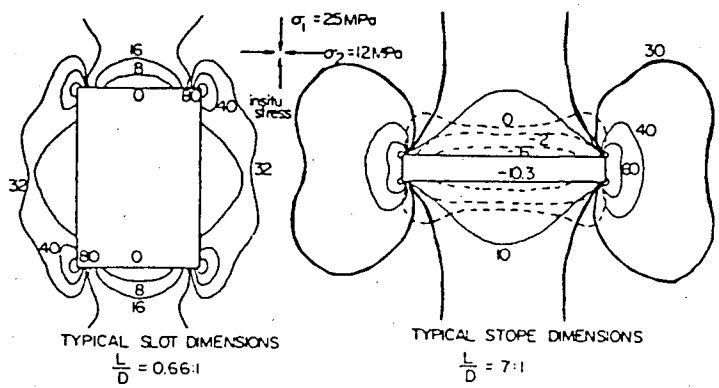

Figure 7.5: Minor (Dashed) and Major (Solid) Stress Contours Surrounding Stopes at Ruttan - Plan View

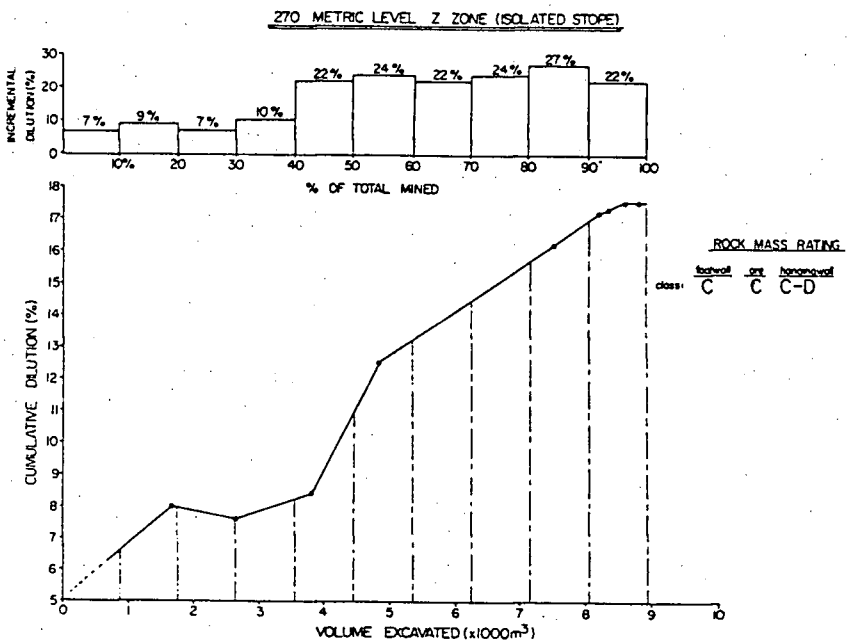

Figure 7.6: Stope Dilution - Blasting

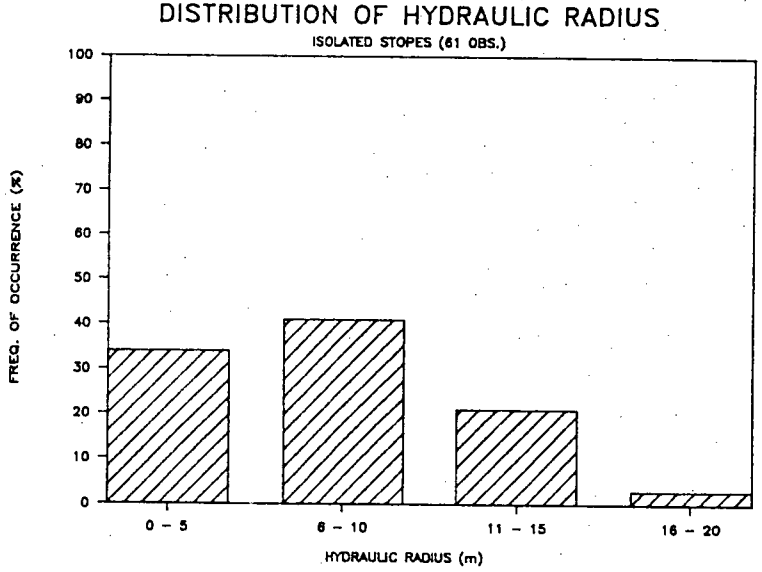

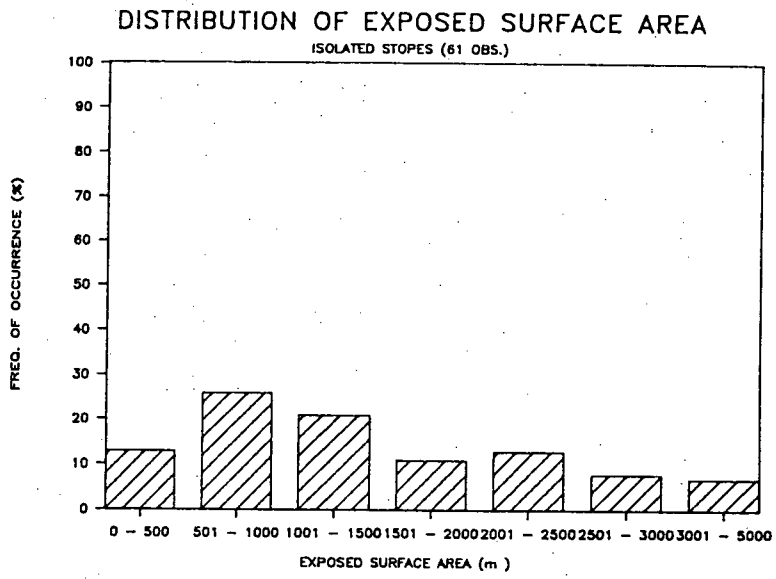

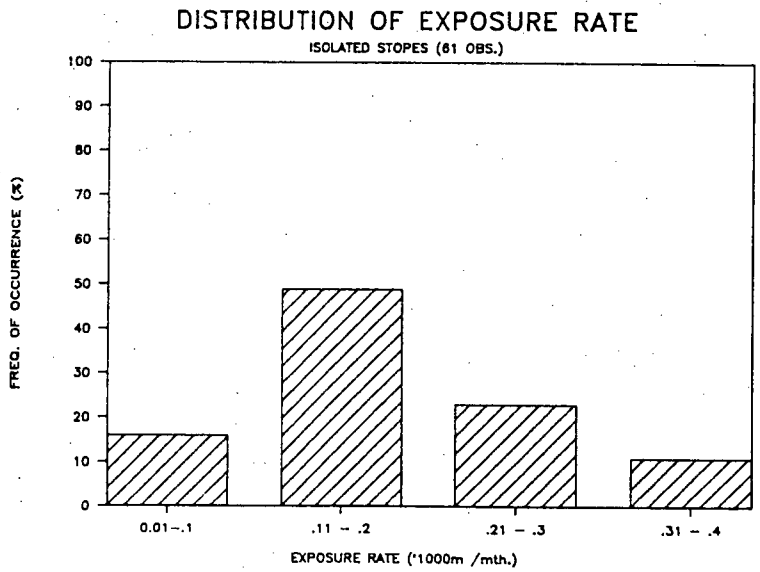

Figure 7.7a: Distribution of Parameters Comprising Isolated Data Base

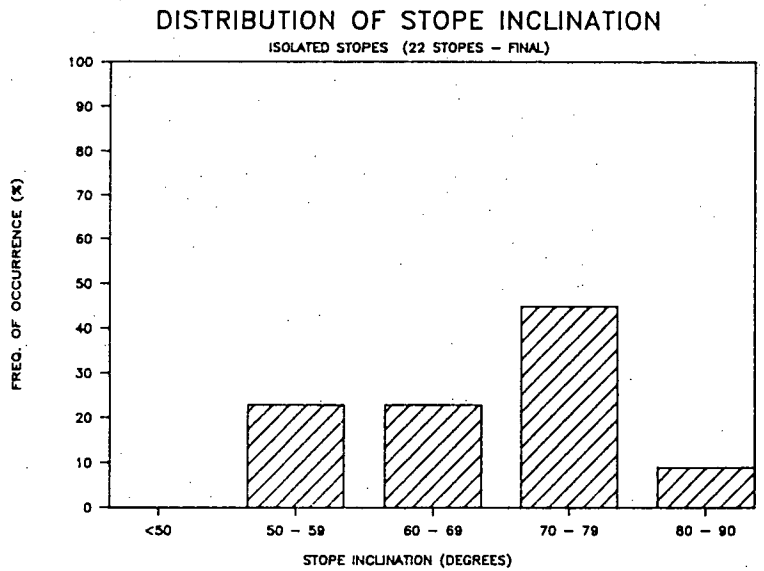

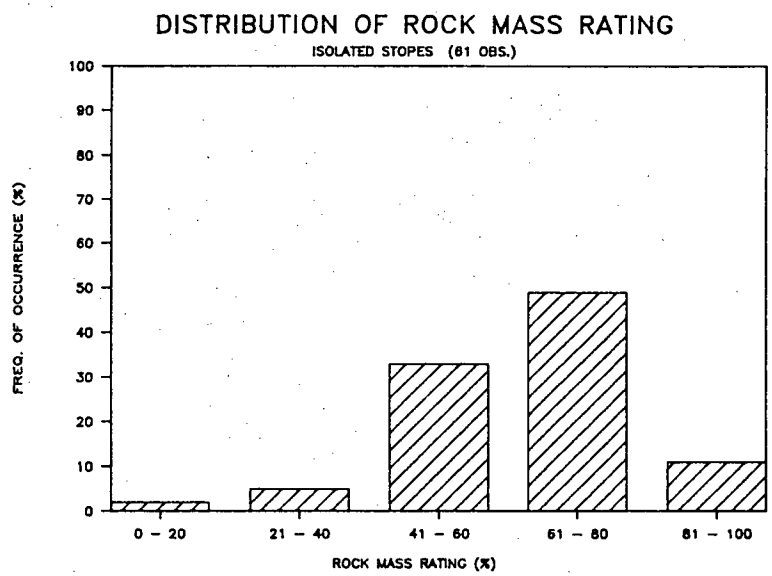

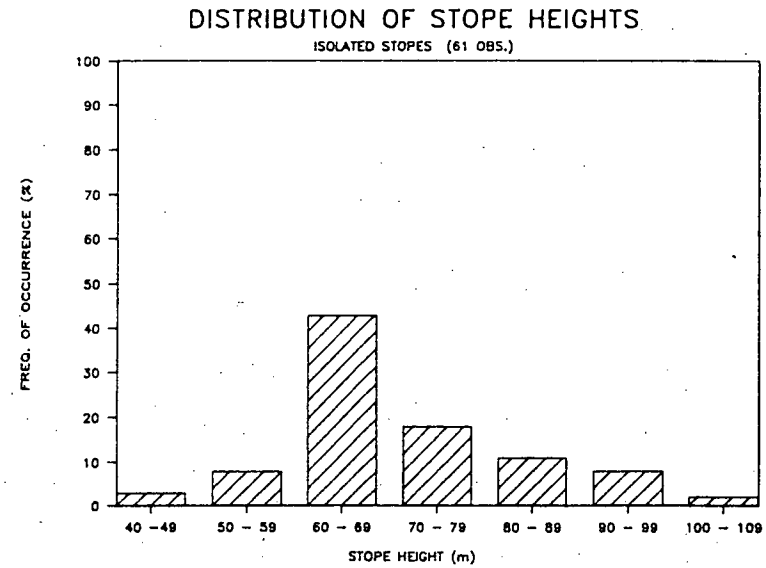

Figure 7.7b: Distribution of Parameters Comprising Isolated Data Base

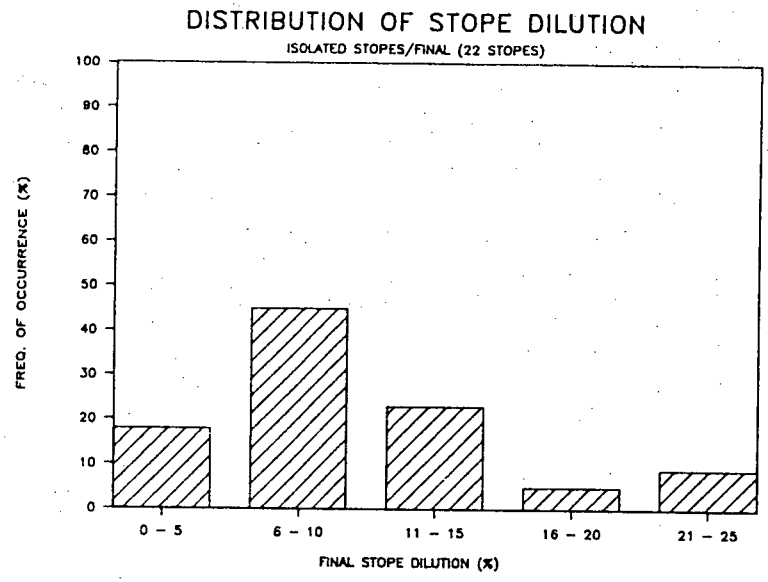

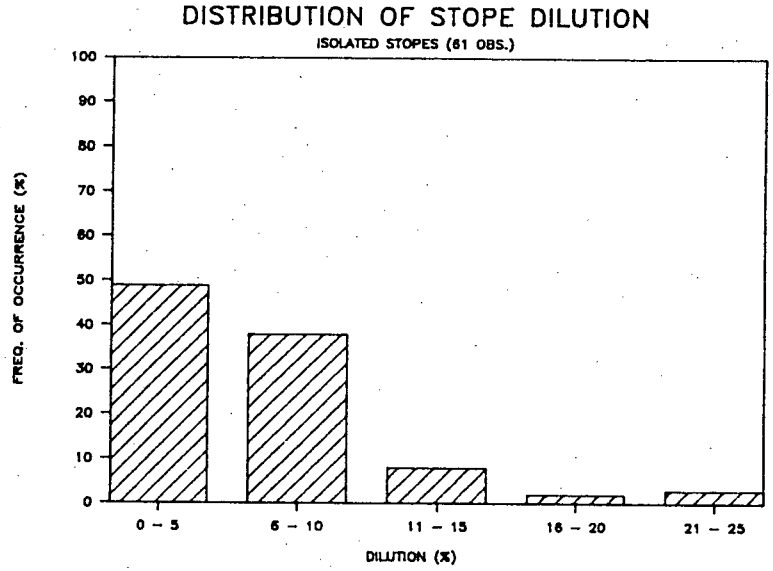

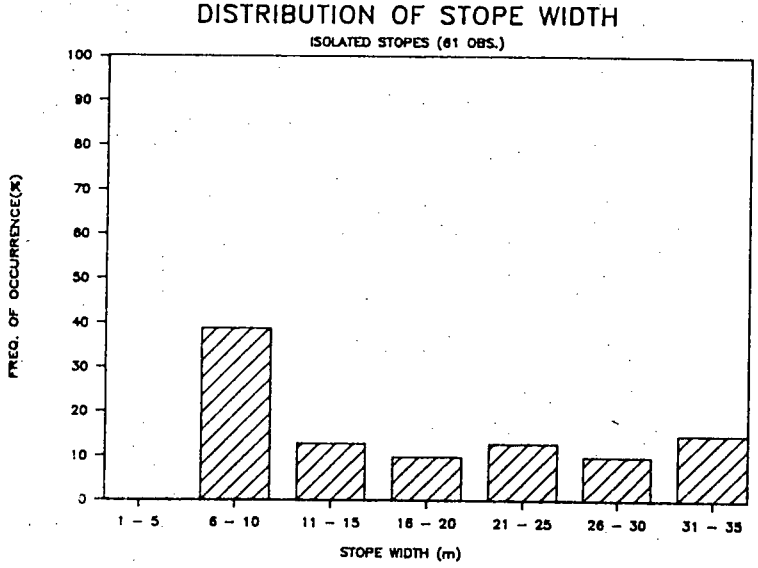

Figure 7.7c: Distribution of Parameters Comprising Isolated Data Base

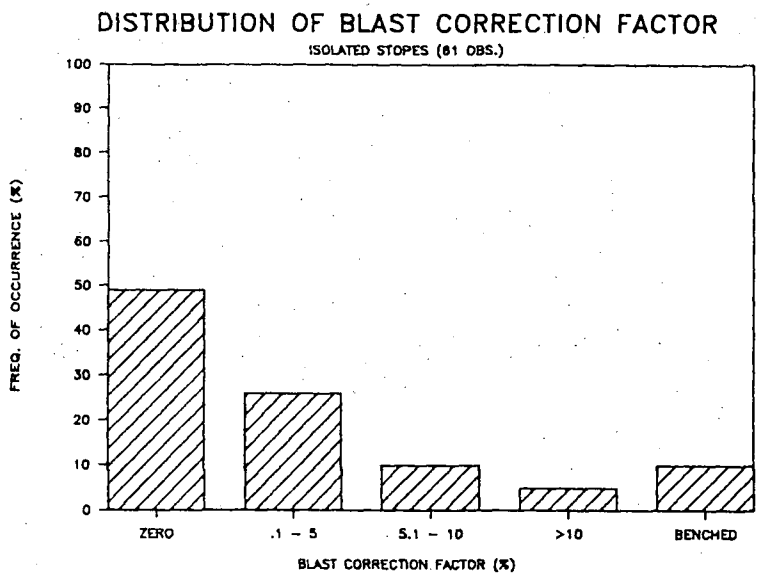

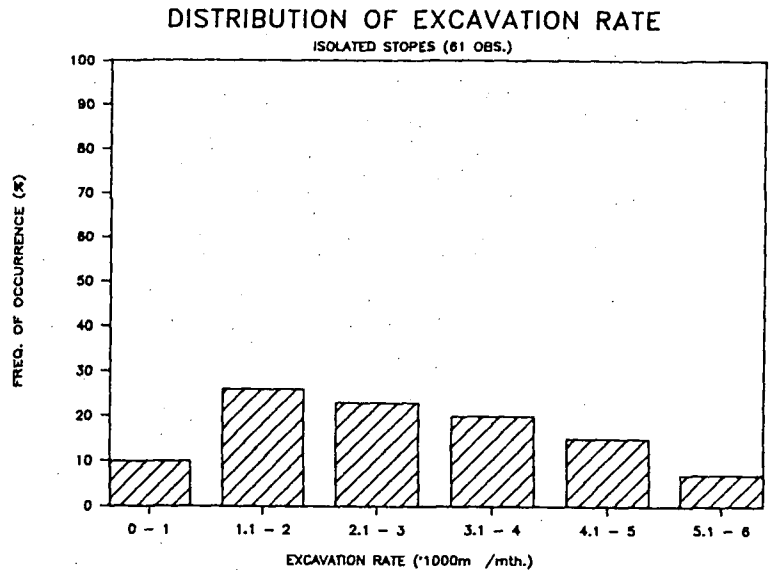

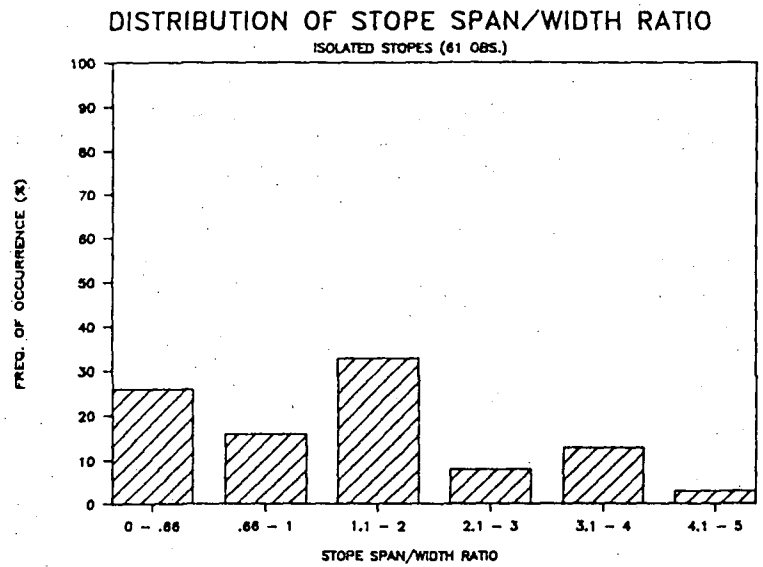

Figure 7.7d: Distribution of Parameters Comprising Isolated Data Base

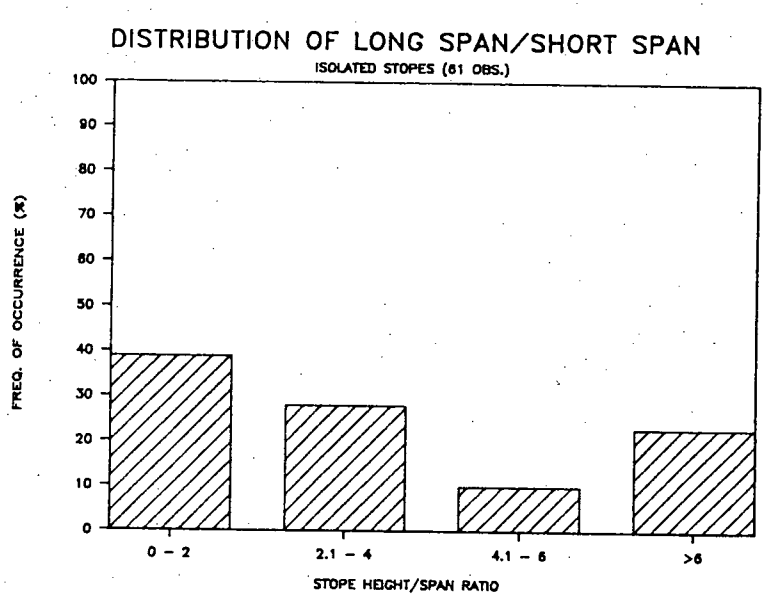

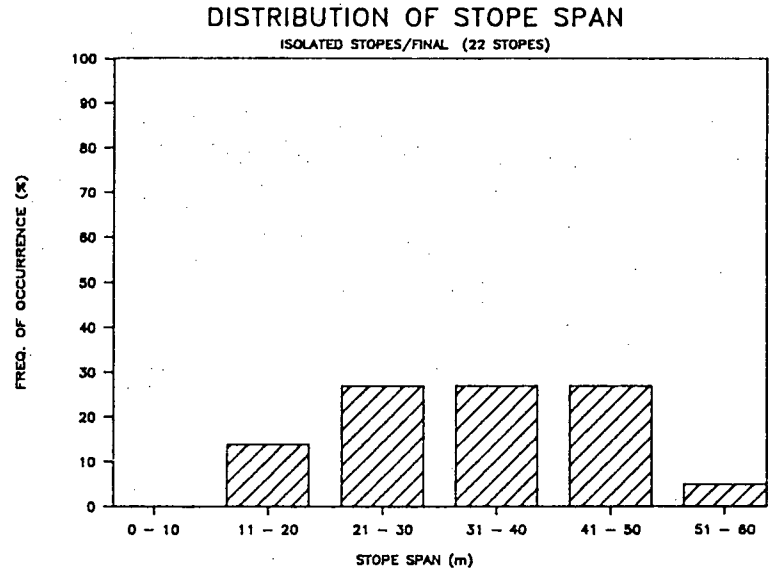

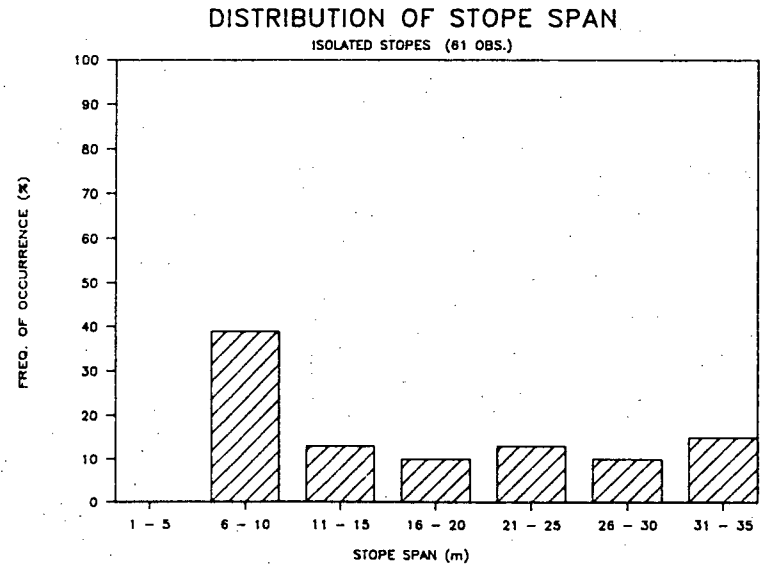

Figure 7.7e: Distribution of Parameters Comprising Isolated Data Base

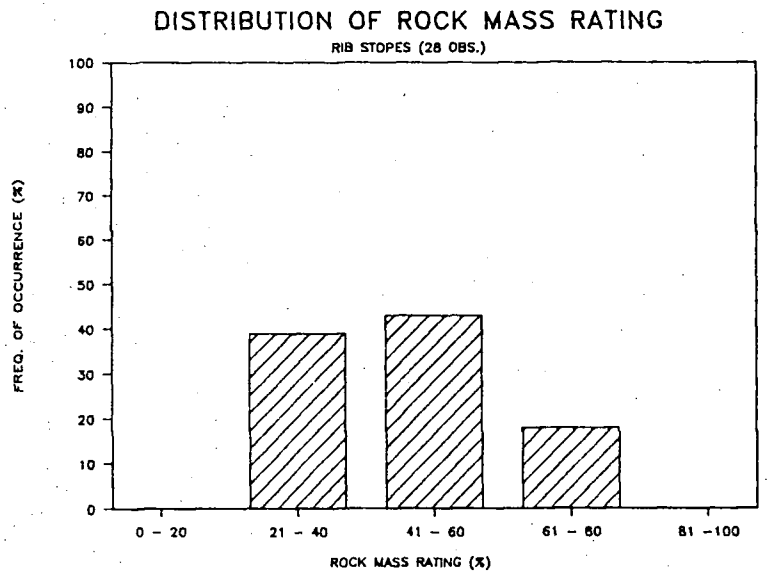

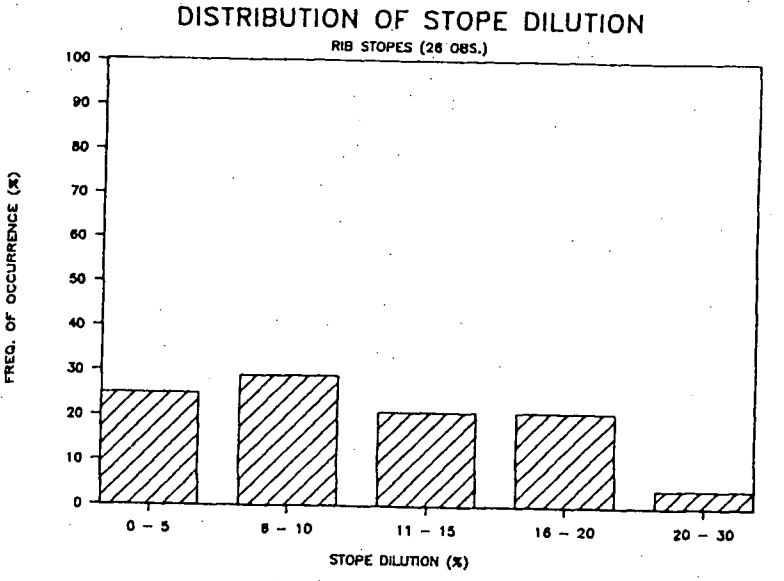

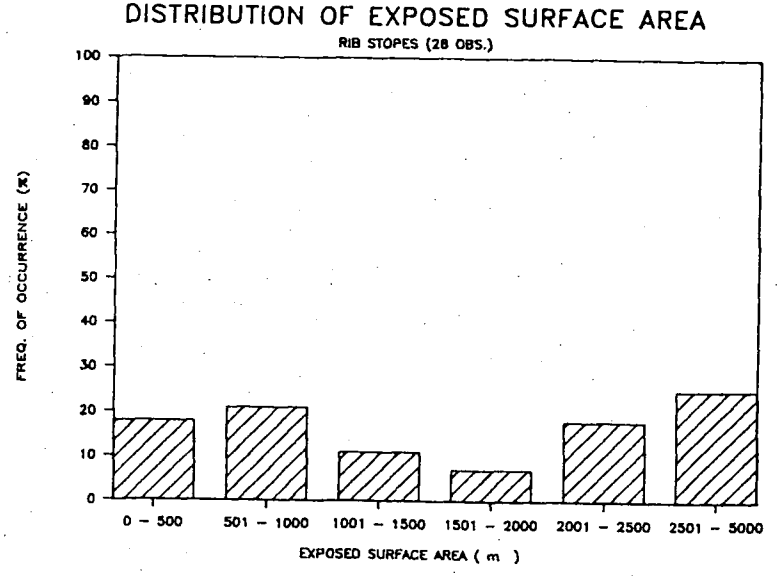

Figure 7.8a: Distribution of Parameters Comprising Rib Data Base

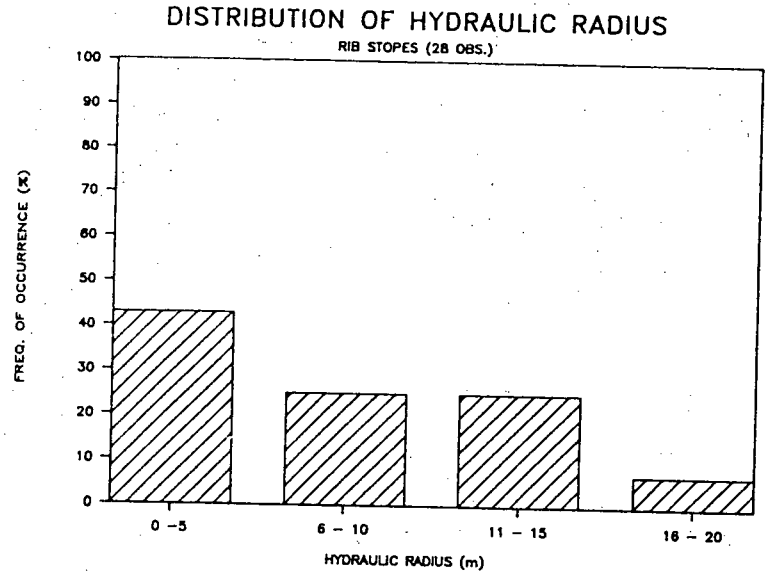

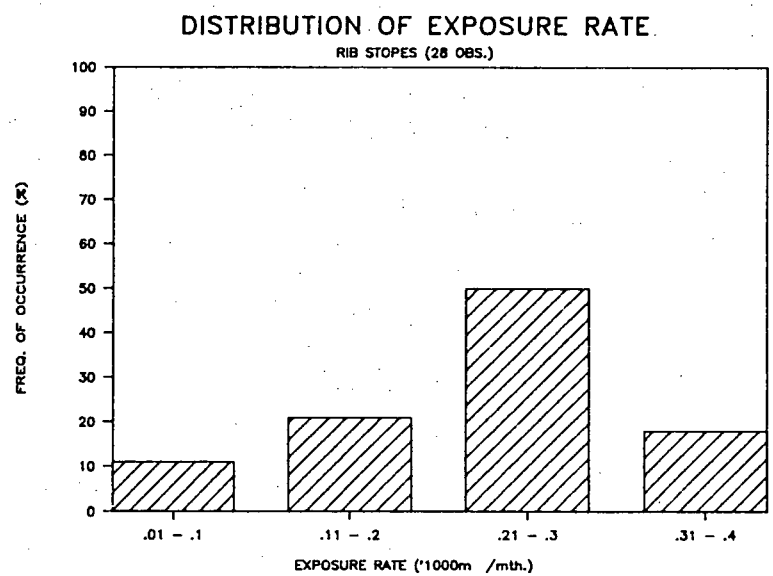

Figure 7.8b: Distribution of Parameters Comprising Rib Data Base

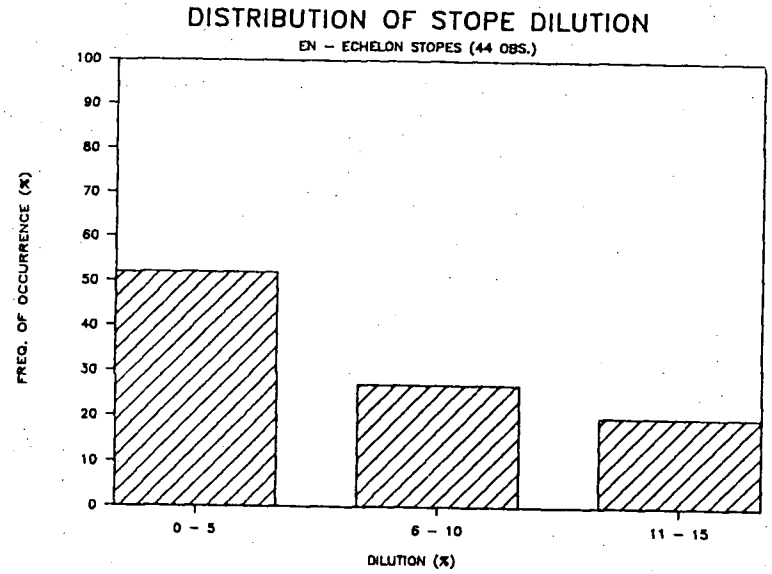

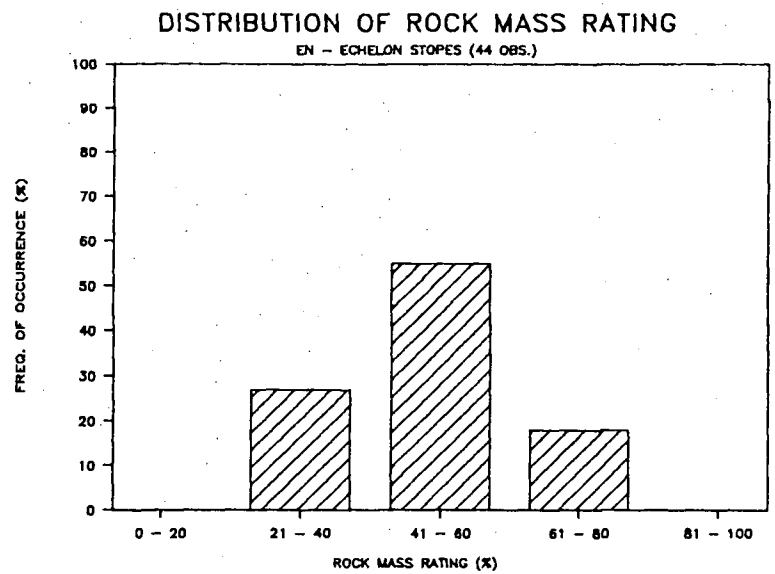

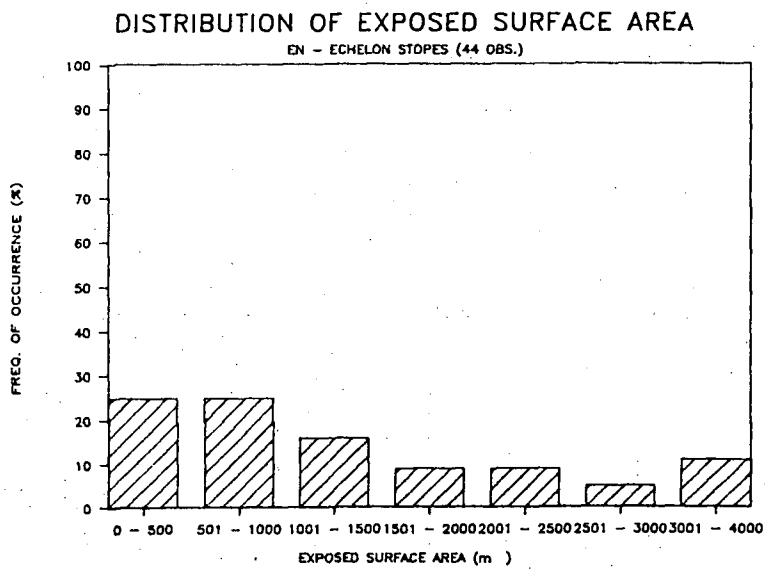

Figure 7.9a: Distribution of Parameters Comprising Echelon Data Base

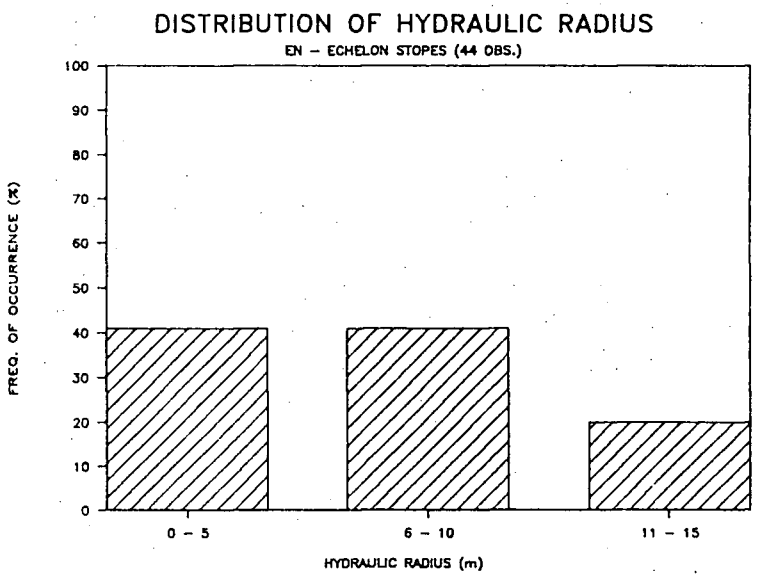

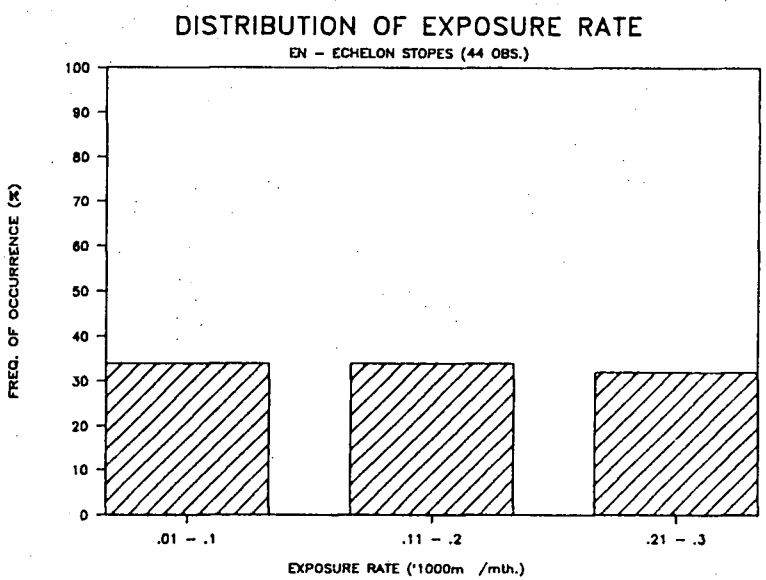

Figure 7.9b: Distribution of Parameters Comprising Echelon Data Base

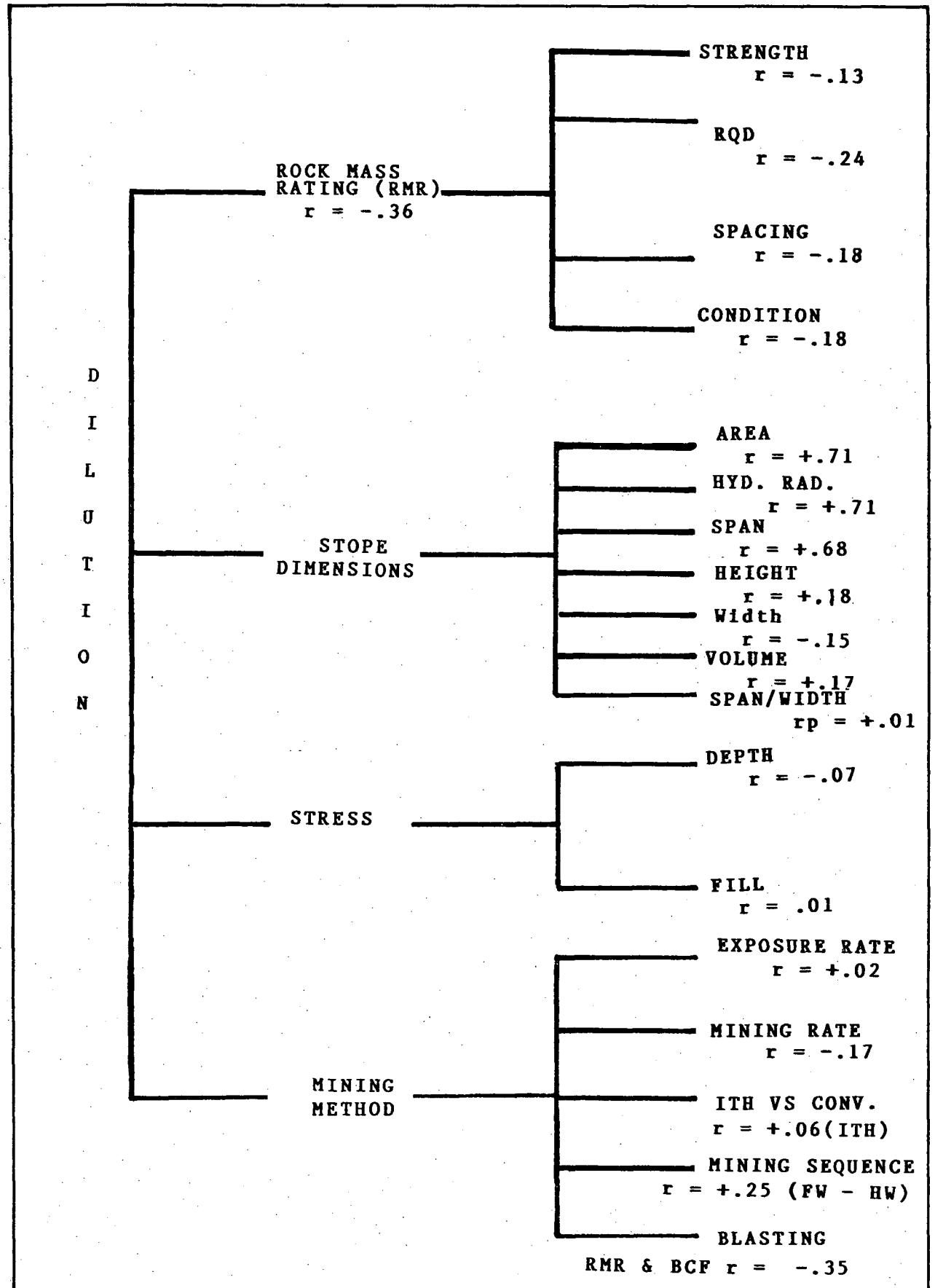

Figure 7.10: Critical Parameters

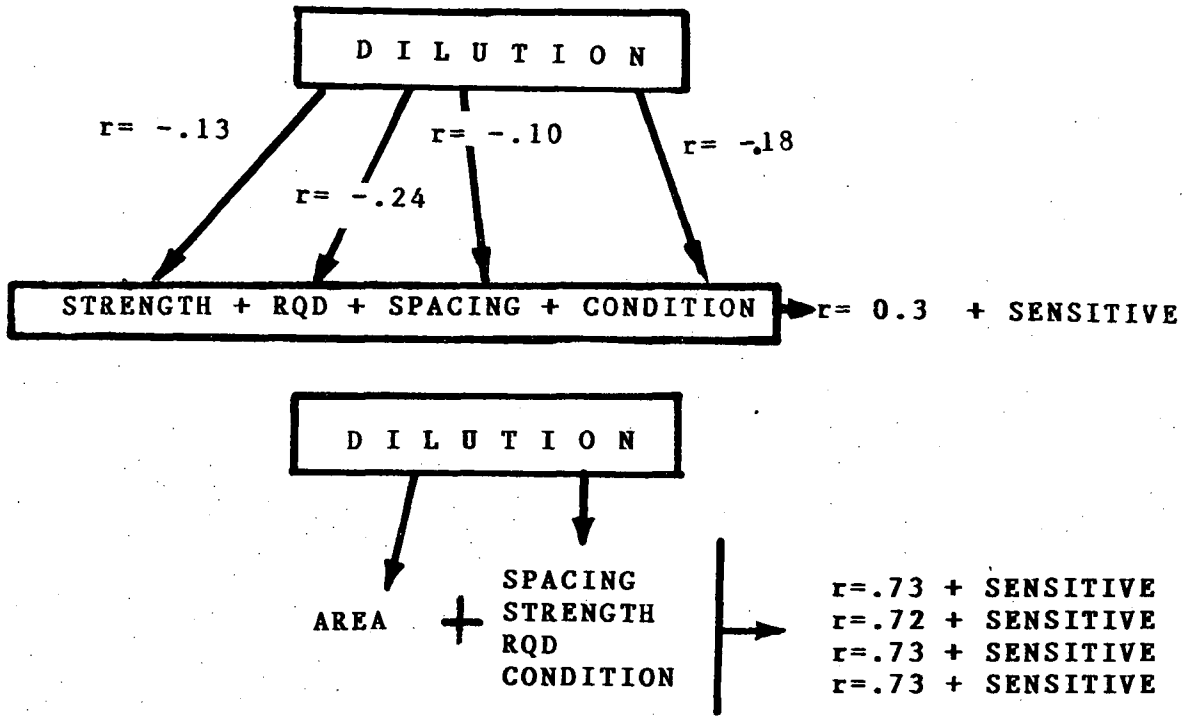

Figure 7.11: Rock Mass Analysis

ACCEPTANCE

100% INCREASE IN THE MEAN VALUE OF A PARAMETER HAS GREATER THAN A 1% (ABSOLUTE) AFFECT ON THE CHANGE IN DILUTION.

EXAMPLE

DILUTION (%) = 1.8 - .08(RMR) + .0037(AREA) + .002(DEPTH)

MEAN AREA = $1418m^2$

MEAN DEPTH = 368m

A) TEST: DEPTH

BASE = |.002*368| = 0.7% DILUTION

SENSITIVITY = |.002*(368*2)| = 1.5% DILUTION

|BASE - SENSITIVITY| $\leq$ 1% "REJECTED"

B) TEST: AREA

BASE = |.0037*1418| = 5.2% DILUTION

SENSITIVITY = |.0037*(1418*2)| = 10.5% DILUTION

|BASE - SENSITIVITY| > 1% "ACCEPTED"

Figure 7.12: Criteria for Sensitivity

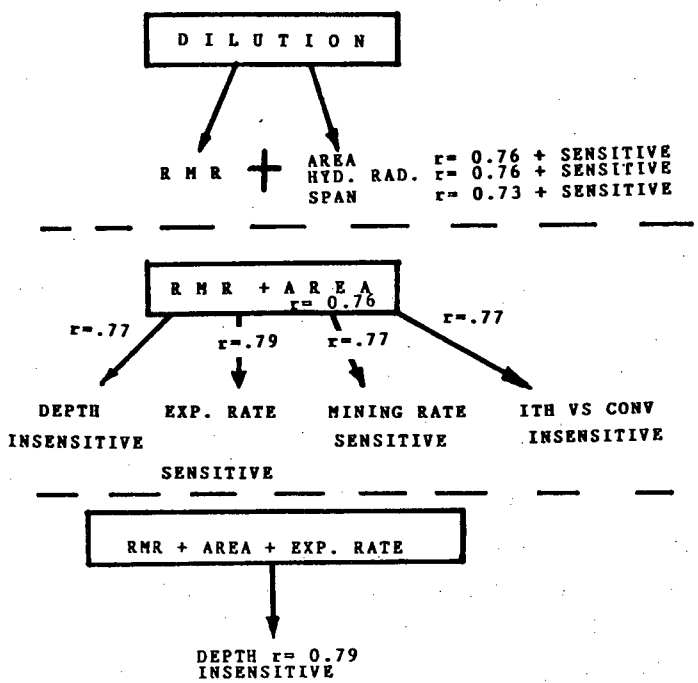

Figure 7.13: Governing Equations - Derivation for Isolated Stopes

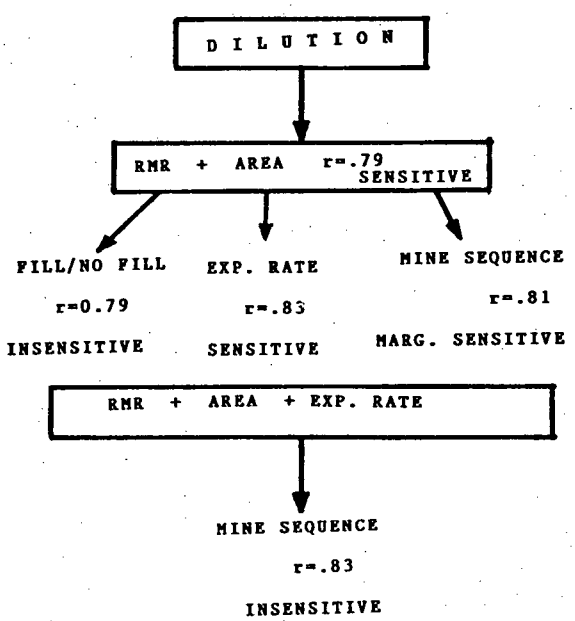

Figure 7.14: Governing Equations - Derivation for Echelon Stopes

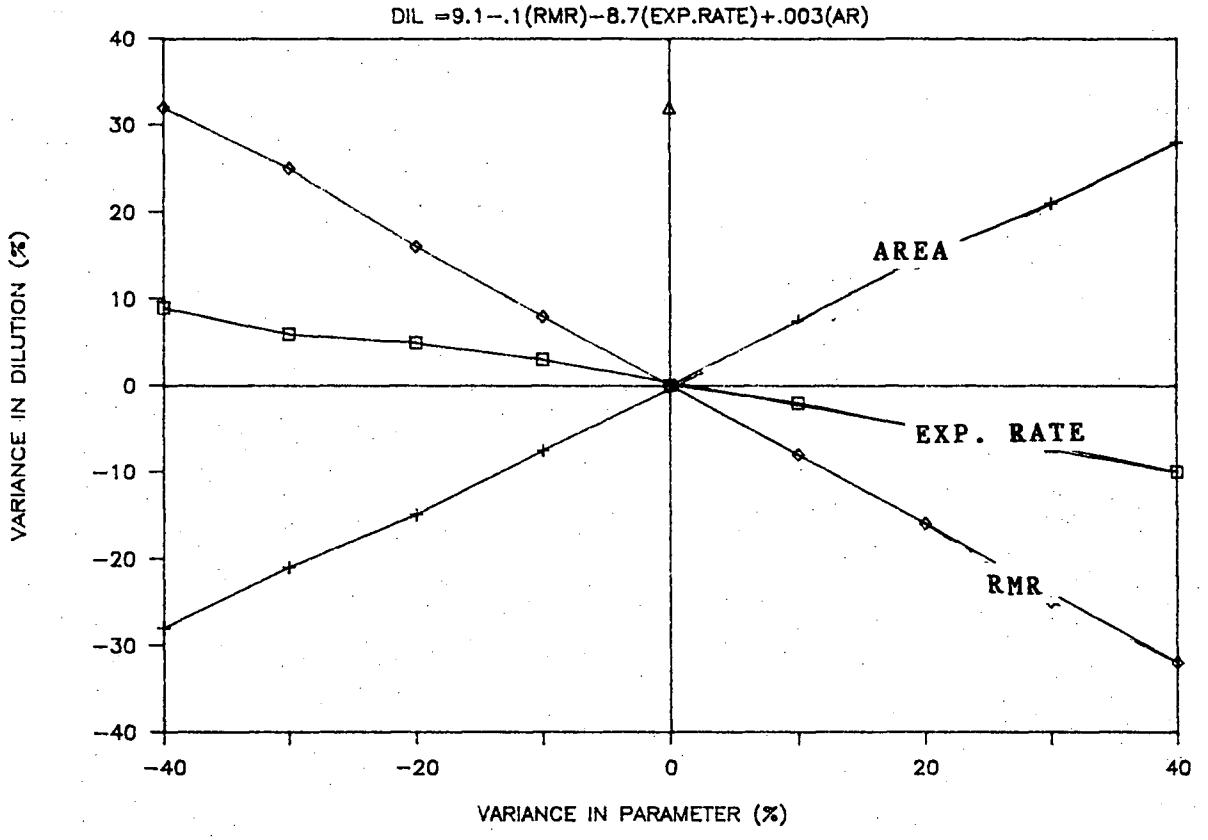

Figure 7.15: Sensitivity Analysis – Data Base = All Stopes

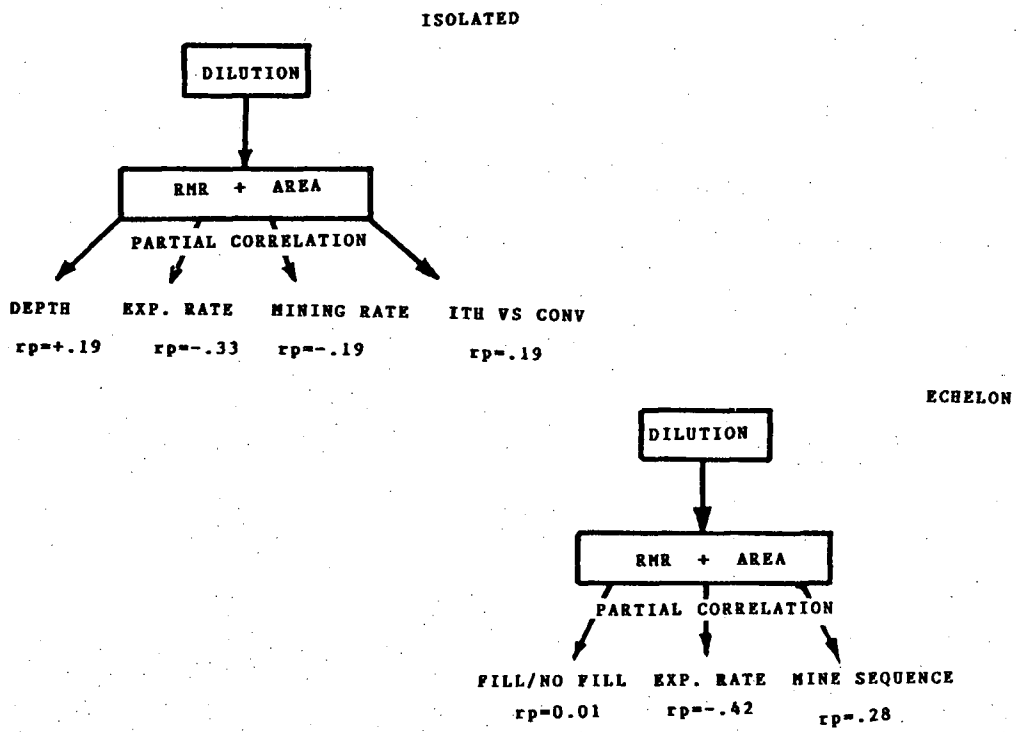

Figure 7.16: Partial Correlation

LINEAR : $Z = a + b(X) + c(Y) + d(W) + ...$

QUADRATIC : $Z = a + b(X^2) + c(X)$

$Z = a + b(X) + c(Y) + d(X^2) + e(Y^2) + f(X)(Y)$

$Z = A + b(X) + c(Y) + d(W) + e(X^2) + f(Y^2) + g(W^2)$
$+ h(X)(Y) + i(X)(Z) + j(Y)(W) + k(X)(Y)(W)$

Figure 7.17: Comparison - Type of Equation (Linear/Quadratic)

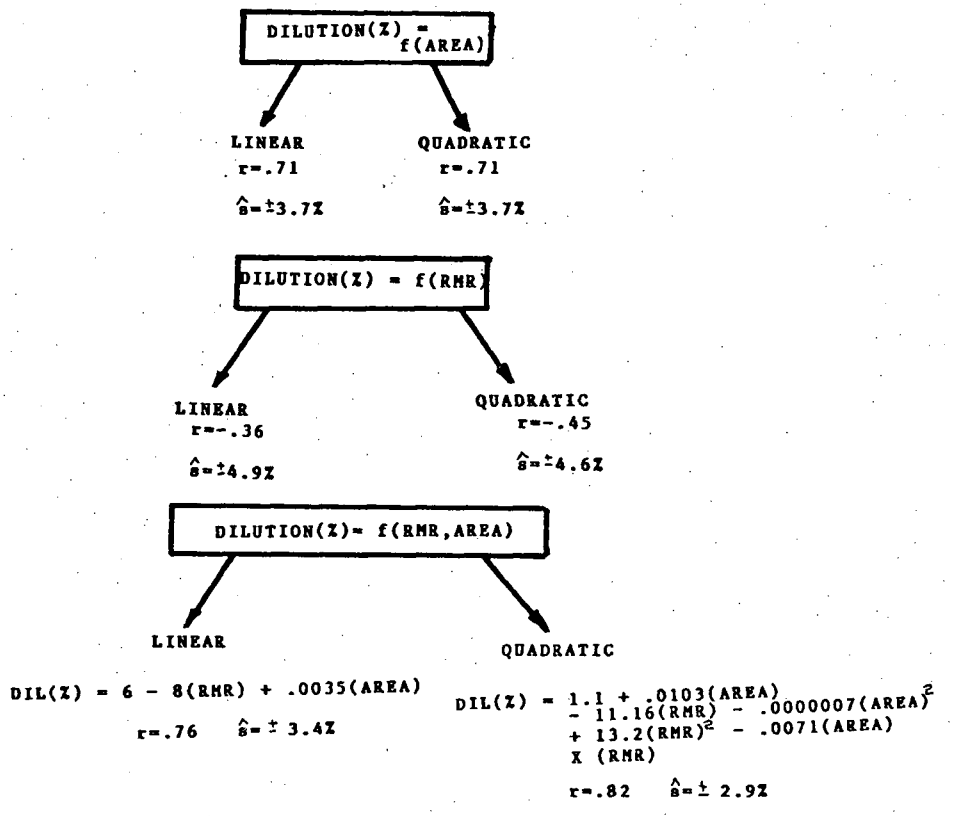

Figure 7.18: Quadratic/Linear Correlation - Isolated Stopes

CHAPTER EIGHT

STOPE DESIGN

8.1 Introduction

This chapter employs the critical parameters "Rock Mass Rating, Area and Exposure Rate" and incorporates them into a governing equation for each individual stope configuration. The influence of stope configuration on the predicted dilution is estimated and the blast correction factor is quantified statistically. This is shown to be an important parameter in establishing an empirical set of equations that would be a reliable predictor of dilution.

8.2 Stope Configuration

The governing equations for the Ruttan data base are shown in Figures 8.1, 8.7a,b,c. They have been determined from a least squares regression analysis and are based upon the observations established in the preceding chapter.

In order to determine the significance of stope configuration, the following analysis was employed:

a) Isolated + Echelon + Rib

A data base incorporating all 133 observations was

employed in generating a best fit hyper-surface. This empirical equation does not distinguish between the different stope configurations. The governing equation is as shown in Figure 8.2. Employing this equation and the observations for the isolated data base results in a correlation coefficient of 0.78. Equally for the echelon and rib observations, the predictive equation would result in correlations of .71 and .72 respectively. In all three situations the correlations and therefore the best fit is lower than that outlined in Figure 8.1. In addition, a further analysis was performed whereby the isolated stopes were designated a value "opt=0" and the remaining observations assessed a value of "opt=1". This resulted in a multiple correlation as shown in Figure 8.2 of 0.77, and a partial correlation of 0.01. In addition, the sensitiviyy of the option parameter is less than 1%. However, the remaining configurations result in significant correlations and sensitivities. This implies that the echelon and rib configurations cannot be incorporated with the remainder of the data base since configuration is a critical parameter.

b) Grouped Stopes

A similar analysis was conducted on the grouped configurations. The isolated and echelon combination, as shown in Figure 8.3, results in a multiple correlation of 0.79 and a partial correlation of 0.3. Similarly, isolated/rib and echelon/rib combinations indicated that the configuration is

significant and sensitive. The grouped empirical equation gave lower correlations for an individual configuration than if a single equation describing that same data base was employed, Figure 8.1. The above indicates that the individual stope configurations are statistically significant and their effect on dilution particularly sensitive. They cannot, therefore, be grouped without employing some parameter (opt) which would account for configuration. Individual governing equations will be employed in relating dilution to the critical parameters for a particular stope configuration. The governing design equations are summarized in Figure 8.1. The equivalent hydraulic radius and span formulation is shown in Figure 8.4. It is interesting to note that a relative comparison of generated dilution can be made from the previous analysis, Figure 8.2. The isolated option would yield approximately 2% more dilution that the echelon and 1.5% less dilution than the rib configuration. The rib would yield approximately 4% more than the echelon. Consequently, the echelon yields the lowest dilution followed by the isolated and rib geometries. This observation has been partly explained by Chapter 4.3.2.

8.3 Blast Correction Factor

This has been previously discussed and will be analyzed in a statistical context in this section.

Figure 8.5 shows the option of incorporating the "BCF"

factor for individual stope geometries. The isolated data base would result in the multiple correlation for the governing equation to be reduced to 0.64 from 0.79. This represents a partial correlation of 0.6. Similarly, significant results are shown for the echelon and rib configurations. Figure 8.6 shows the resultant correlation for a data base, whereby stopes having a BCF value greater than zero are omitted. This would greatly reduce the number of observations, however, they are statistically significant at the 99% confidence level. Obviously, they may pass the test of statistics, but not the test of practical acceptance that is inherent to the study through the experienced observations made by the author.

8.4 Predictive Equations(Governing Equations)

Figure 8.1 shows the governing equations that have been derived from this study and will be subsequently employed in estimating optimum exposed design dimensions. Since area is employed rather than span or hydraulic radius, this would reduce the errors that may occur in estimating the stope dimensions from a given excavated volume, Chapter 6.3.1. Tables 8.1,8.2,8.3 show the critical parameters for the individual stope configurations as identified in the preceding chapters. The governing equations are employed to predict the dilution. These equations are subsequently compared to the observed dilution. The average absolute difference in estimation is 2.4%

for the isolated, 1.8% for the echelon and 2.7% for the rib configurations. These errors of estimation are determined for the sample and for the population estimate, Figure 8.1. Figure 8.7 graphically depicts the predicted versus observed dilution for the individual stope data bases. The upper and lower bounding lines,Figure 8.7, represent a 68% (one standard deviation) confidence that the observed value will fall within the ranges delineated. A further observation is that one is 84% confident that the observed dilution would be less than the mean estimated dilution plus one standard deviation. The above is only true if the sample population can be approximated by a normal distribution. Probability graph paper is employed which plots the cumulative relative frequency of the differences between the estimated and observed dilutions for the isolated case, Figure 8.8. The sample is "normally distributed" since a linear plot is achieved (Spiegel,1973). This is generally the case since it is inherent to the definition of correlation that the predicted dilution is the mean estimate of the best fit expression.

Table 8.1: Comparison Predicted/Observed - Isolated

ISOLATED STOPES DATA BASE — NUMBER OF STOPES=22

EMPIRICAL EQUATION : DILUTION(%) = 8.6 - 0.09(RMR) - 13.2(E.R.) + 0.003B(AREA)

$r = 0.79$, $\hat{S} = 2.1\%$

No.	Stope	RMR(%)	E.R.(ft^2/ath)	Area(ft^2)	Res. Dil(%)	Pred. Dil(%)	Diff.(%)
1	260 11 F	50	0.19	675	5	3	2
2	260 11 F	50	0.23	2385	10	9	1
3	260 18 J	51	0.30	504	5	2	3
4	260 18 J	51	0.40	1008	6	3	3
5	260 18 J	51	0.49	2016	5	6	-0
6	260 18 J	51	0.30	2856	9	11	-2
7	260 16 H	80	0.25	570	2	0	2
8	260 16 H	80	0.36	1425	6	2	4
9	260 16 H	80	0.37	1900	7	4	3
10	260 16 H	80	0.38	2755	8	7	1
11	260 15 H	80	0.21	4370	9	15	-5
12	270 0 Z	46	0.15	624	6	5	1
13	270 0 Z	46	0.09	1248	11	8	3
14	320 14 BE	25	0.21	4620	20	21	-1
15	320 13 E	79	0.13	1280	6	5	1
16	320 15 H	66	0.10	300	0	2	-2
17	320 15 H	66	0.14	675	1	3	-2
18	320 15 H	66	0.22	1275	2	5	-3
19	320 15 H	66	0.23	1875	3	7	-4
20	320 15 H	66	0.22	2400	3	9	-6
21	320 18 JN	81	0.22	900	9	2	7
22	320 19 J	84	0.15	600	0	1	-1
23	320 19 J	84	0.18	1200	4	3	1
24	320 19 J	84	0.16	2400	6	8	-2
25	320 11 B	41	0.20	3465	22	15	7
26	340 11 C	43	0.13	640	5	5	-0
27	340 11 C	43	0.14	1680	9	9	-0
28	370 21 JN	3	0.32	1924	14	11	3
29	370 15 H	80	0.09	1748	6	7	-1
30	370 19 B	51	0.12	504	2	4	-2
31	370 10 B	51	0.11	1008	3	6	-3
32	370 15 C	51	0.21	567	0	3	-3
33	370 15 C	51	0.19	1197	7	6	1
34	370 15 C	51	0.17	2709	11	12	-1
35	370 19 J	43	0.16	240	0	4	-4
36	370 19 J	43	0.13	480	0	4	-4
37	370 19 J	43	0.20	900	5	6	-1
38	370 19 J	43	0.13	1740	13	10	3
39	370 16 H	80	0.12	2052	7	8	-1
40	370 12 13F	70	0.11	480	0	3	-3
41	370 12 13F	70	0.13	1260	3	5	-2
42	430 13 D F/W	90	0.08	180	2	1	1
43	430 13 D F/W	80	0.13	300	4	1	3
44	430 13 D F/W	80	0.16	600	5	2	3
45	430 13 D F/W	80	0.16	960	5	3	2
46	430 13 D F/W	80	0.16	1260	5	4	1
47	430 13 D F/W	90	0.16	1560	6	5	1
48	430 13 D F/W	80	0.16	1860	6	6	-0
49	430 13 D F/W	90	0.15	2160	7	8	-1
50	430 13 D F/W	80	0.13	2520	10	9	1
51	430 14 D	80	0.06	180	1	1	-0
52	430 14 D	80	0.09	360	3	2	1
53	430 14 D	80	0.11	660	6	2	4
54	430 14 D	80	0.03	1020	8	5	3
55	430 14 D	80	0.03	1320	8	5	3
56	430 14 D	80	0.03	2400	12	10	2
57	430 21 K	70	0.21	520	1	2	-1
58	430 21 K	70	0.16	1040	1	3	-2
59	430 21 K	70	0.25	2080	2	7	-5
60	430 12 F	32	0.11	510	1	6	-5
61	430 12 F	32	0.10	2550	25	14	11

Table 8.2: Comparison Predicted/Observed - Echelon

ECHELON STOPES DATA BASE — NUMBER OF STOPES = 12

EMPIRICAL EQUATION : DILUTION(%) = 10.3 -0.13(RMR) - 14.8(E.R.) + 0.003(AREA)

r = 0.83, S^2= 2.4%

No.	Stope	RMR(%)	E.R.(m^2/mth)	Area(m^2)	Res. Dil(%)	Pred.Dil(%)	Diff.(%)
1	320 12 BE	47	0.10	720	11	5	6
2	320 12 BE	47	0.14	2160	12	9	3
3	320 18 J	56	0.21	1095	4	3	1
4	320 18 J	56	0.10	2555	10	9	1
5	370 20 KN	45	0.09	384	1	4	-3
6	370 20 KN	45	0.12	704	3	5	-2
7	370 20 KN	45	0.15	1408	9	6	3
8	370 20 KN	45	0.13	2944	12	11	1
9	370 20 KN	45	0.13	2136	13	12	1
10	370 13 D	49	0.18	200	1	2	-1
11	370 12 D	49	0.24	400	5	2	1
12	370 13 D	45	0.20	800	3	3	-0
13	370 13 D	49	0.11	1200	7	6	1
14	370 13 D	49	0.10	1750	10	8	2
15	370 19 K	62	0.18	345	0	1	-1
16	370 19 K	62	0.22	805	1	1	-0
17	370 19 K	62	0.21	1610	3	4	-1
18	370 19 K	62	0.22	2415	4	6	-2
19	370 19 K	62	0.25	3220	5	8	-3
20	370 19 K	62	0.22	4025	8	11	-3
21	370 21 J	60	0.23	325	0	0	-0
22	370 21 J	60	0.22	650	1	1	-0
23	370 21 J	60	0.21	1300	3	3	-0
24	370 21 J	60	0.19	1950	4	6	-2
25	370 21 KN	23	0.28	704	2	5	-3
26	370 21 KN	23	0.26	1320	12	7	5
27	370 12 D	26	0.04	255	2	7	-5
28	370 12 D	26	0.07	425	7	7	-0
29	370 12 D	26	0.08	850	11	8	3
30	370 12 D	26	0.08	3230	15	15	-0
31	430 13 F	33	0.19	672	1	5	-4
32	430 13 F	33	0.28	1470	9	6	3
33	430 12 D	26	0.04	255	2	7	-5
34	430 12 D	26	0.07	425	7	7	-0
35	430 12 D	26	0.08	850	11	8	3
36	430 12 D	26	0.08	3230	15	15	-0
37	430 21 J F/W	65	0.05	212	4	2	2
38	430 21 J F/W	65	0.04	954	5	4	1
39	430 13 D H/W	52	0.10	320	2	3	-1
40	430 13 D H/W	52	0.14	576	4	3	1
41	430 13 D H/W	52	0.16	1216	6	5	1
42	430 13 D H/W	52	0.17	1792	7	6	1
43	430 13 D H/W	52	0.13	2368	8	9	-1
44	430 13 D H/W	52	0.11	3560	8	10	-2

Table 8.3: Comparison Predicted/Observed - Rib

RIB STOPES DATA BASE — NUMBER OF STOPES = 5

EMPIRICAL EQUATION : DILUTION(%) = 15.8 - 0.18(RMR) - 7.7(E.R.) + 0.005(AREA)

r = 0.80, S^2= 4.0

No.	Stope	RMR(%)	E.R.(m^2/mth)	Area(m^2)	Res. Dil(%)	Pred.Dil(%)	Diff.(%)
1	320 10 B	34	0.22	448	0	9	-9
2	320 10 B	34	0.22	784	8	10	-2
3	320 10 B	34	0.25	1680	13	12	1
4	320 10 B	34	0.27	2464	16	14	2
5	320 10 B	34	0.29	3360	16	16	-0
6	320 10 B	34	0.30	4144	16	18	-2
7	320 10 B	34	0.31	4928	16	20	-4
8	320 10 B	34	0.28	5152	16	21	-5
9	320 12 B	23	0.24	2120	27	15	12
10	340 12 C	30	0.12	240	8	10	-2
11	340 12 C	30	0.16	520	10	11	-1
12	370 20 J	69	0.04	225	5	4	1
13	370 20 J	69	0.08	450	7	4	3
14	370 14 C	47	0.16	780	8	8	-0
15	370 14 C	47	0.20	2080	13	11	2
16	370 18 J	54	0.20	525	2	6	-4
17	370 18 J	54	0.30	1050	9	7	3
18	370 18 J	54	0.37	2175	14	9	5
19	370 18 J	54	0.31	3225	14	12	2
20	370 11 F	57	0.04	500	9	7	2
21	430 15 D	51	0.19	384	2	6	-4
22	430 15 D	51	0.23	704	6	7	-1
23	430 15 D	51	0.23	1408	9	9	0
24	430 15 D	51	0.24	2112	11	10	1
25	430 15 D	51	0.15	3008	14	13	1
26	430 20 K	74	0.28	506	1	2	-1
27	430 20 K	74	0.18	1012	1	4	-3
28	430 20 K	74	0.21	1748	2	5	-3

ISOLATED STOPES (61 OBS)

$$DIL(\%) = 8.6 - 0.09(RMR) - 13.2(EXP.RATE) + .0038(AREA)$$

$$r=\pm 0.79 \quad \hat{s}= \pm 3\%$$

ECHELON STOPES (44 OBS)

$$DIL(\%) = 10.3 - 0.13(RMR) - 14.8(EXP.RATE) + 0.0026(AREA)$$

$$r=\pm 0.83 \quad \hat{s}= \pm 2\%$$

RIB STOPES (28 OBS)

$$DIL(\%) = 15.8 - 0.18(RMR) - 7.7(EXP.RATE) + 0.0026(AREA)$$

$$r=\pm 0.8 \quad \hat{s}= \pm 4\%$$

where:

DIL(%) - DILUTION (%)

RMR - ROCK MASS RATING (%)

EXP.RATE - EXPOSURE RATE (´100m /mth)

AREA - EXPOSED SURFACE AREA (m^2)

Figure 8.1: Governing Equations

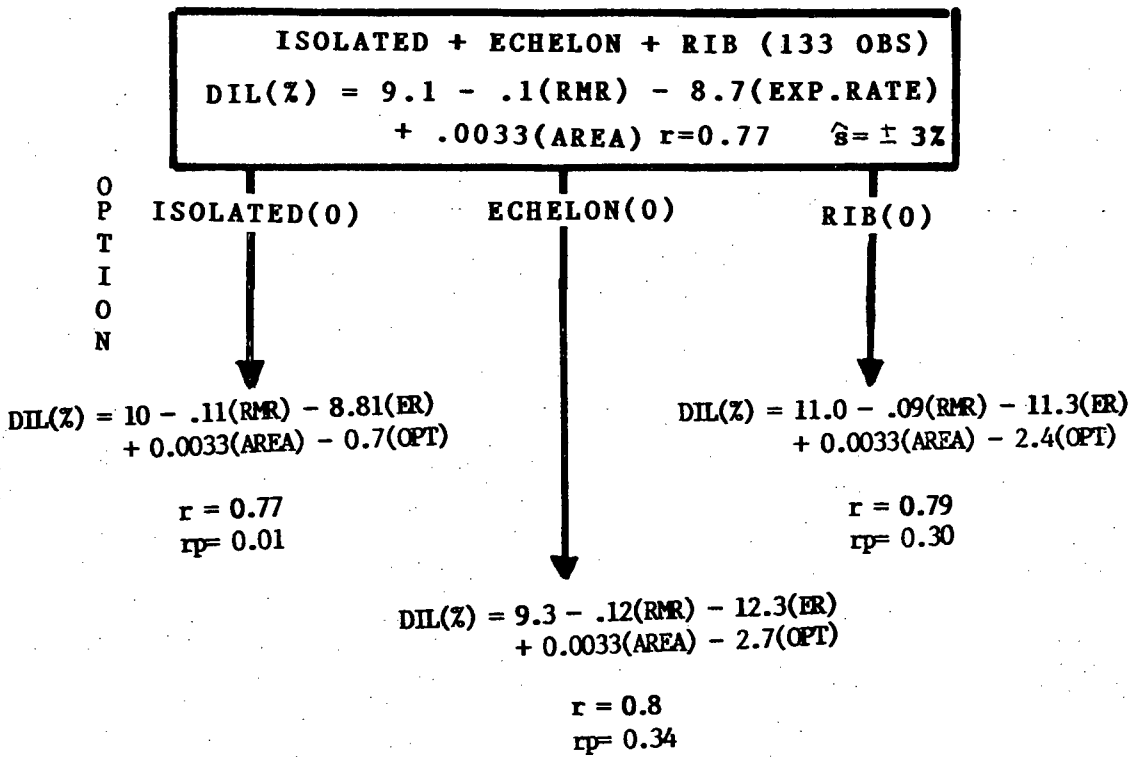

Figure 8.2: Stope Configuration - All Stopes

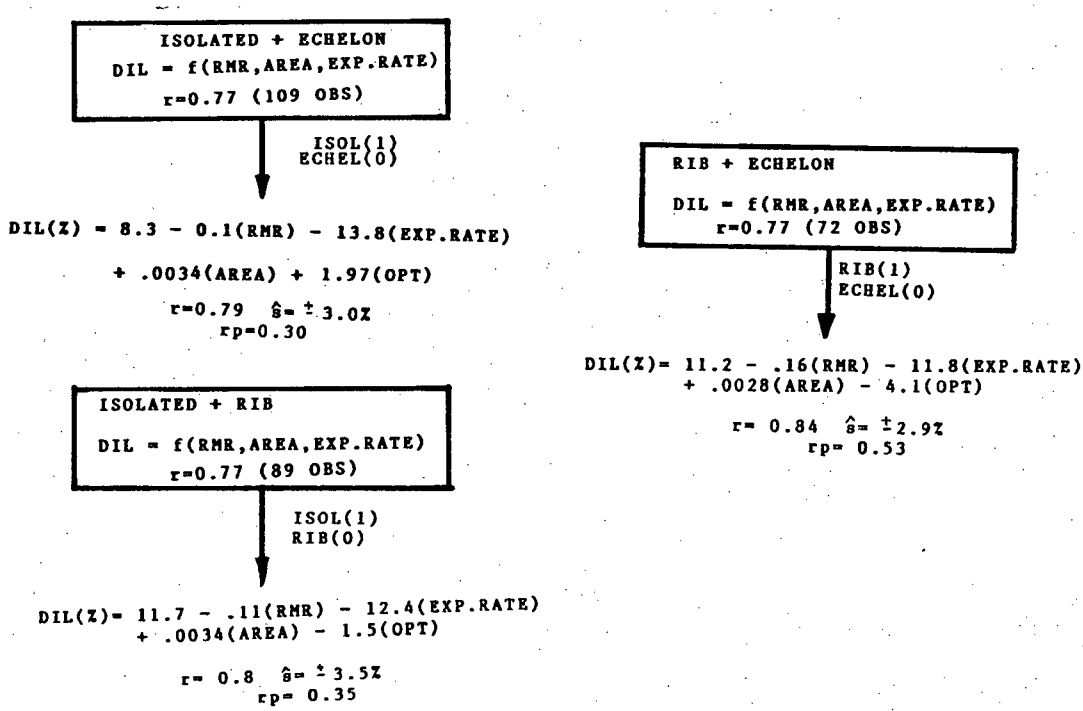

Figure 8.3: Stope Configuration - Combined

ISOLATED STOPES (61 OBS)

DIL(%) = 8.2 - .12(RMR) - 5.3(EXP.RATE) + .9(HYD.RAD) r^2= 0.78 $\hat{s}$ = ± 3.3%

DIL(%) = 7.0 - .08(RMR) - 7.4(EXP.RATE) + .26(SPAN) r^2= 0.74 $\hat{s}$ = ± 3.6%

ECHELON STOPES (41 OBS)

DIL(%) = 8.8 - .12(RMR) - 18.2(EXP.RATE) + .8(HYD.RAD) r^2= 0.83 $\hat{s}$ = ± 2.3%

DIL(%) = 8.8 - .10(RMR) - 17.1(EXP.RATE) + .23(SPAN) r^2= 0.83 $\hat{s}$ = ± 2.4%

RIB STOPES (28 OBS)

DIL(%) = 16.2 - .22(RMR) - 11.4(EXP.RATE) + .9(HYD.RAD) r^2= 0.81 $\hat{s}$ = ± 3.8%

DIL(%) = 17.6 - .25(RMR) - 3.7(EXP.RATE) + .22(SPAN) r^2= 0.79 $\hat{s}$ = ± 4.1%

where:

RMR = ROCK MASS RATING (%)

EXP.RATE = EXPOSURE RATE ($^{\prime}1000m^2$ /mth)

HR = HYDRAULIC RADIUS (m)

SPAN = SPAN (m)

Figure 8.4: Hydraulic Radius and Span Derivation

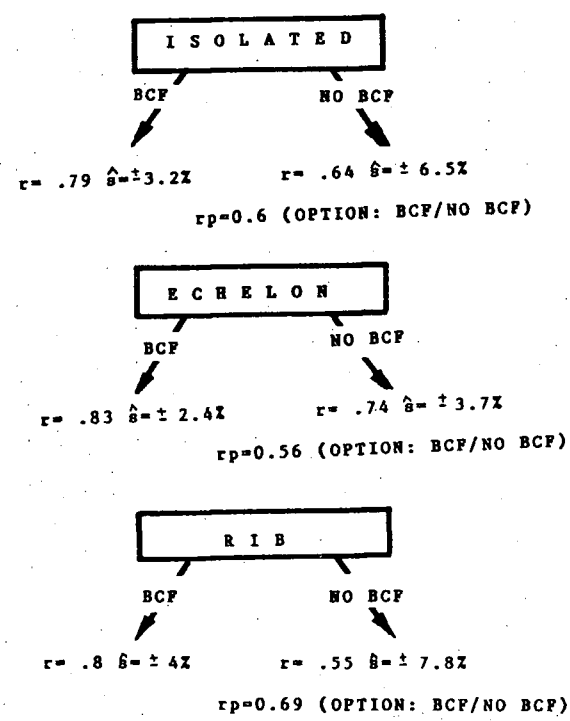

Figure 8.5: Incorporating Blast Correction Factor

I S O L A T E D (13 STOPES, 36 OBS.)	→	DIL(%) = 11.9 - .12(RMR) - 12.8(EXP.RATE) + 0.0035(AREA) r=0.78 $\hat{s}=\pm 3.4\%$
E C H E L O N (2 STOPES, 12 OBS.)	→	r= 0.98 $\hat{s}=\pm 0.69\%$
R I B (4 STOPES, 16 OBS.)	→	r=0.84 $\hat{s}=\pm 4.4\%$

Figure 8.6: Stopes With "BCF > 0" Omitted From Data Base

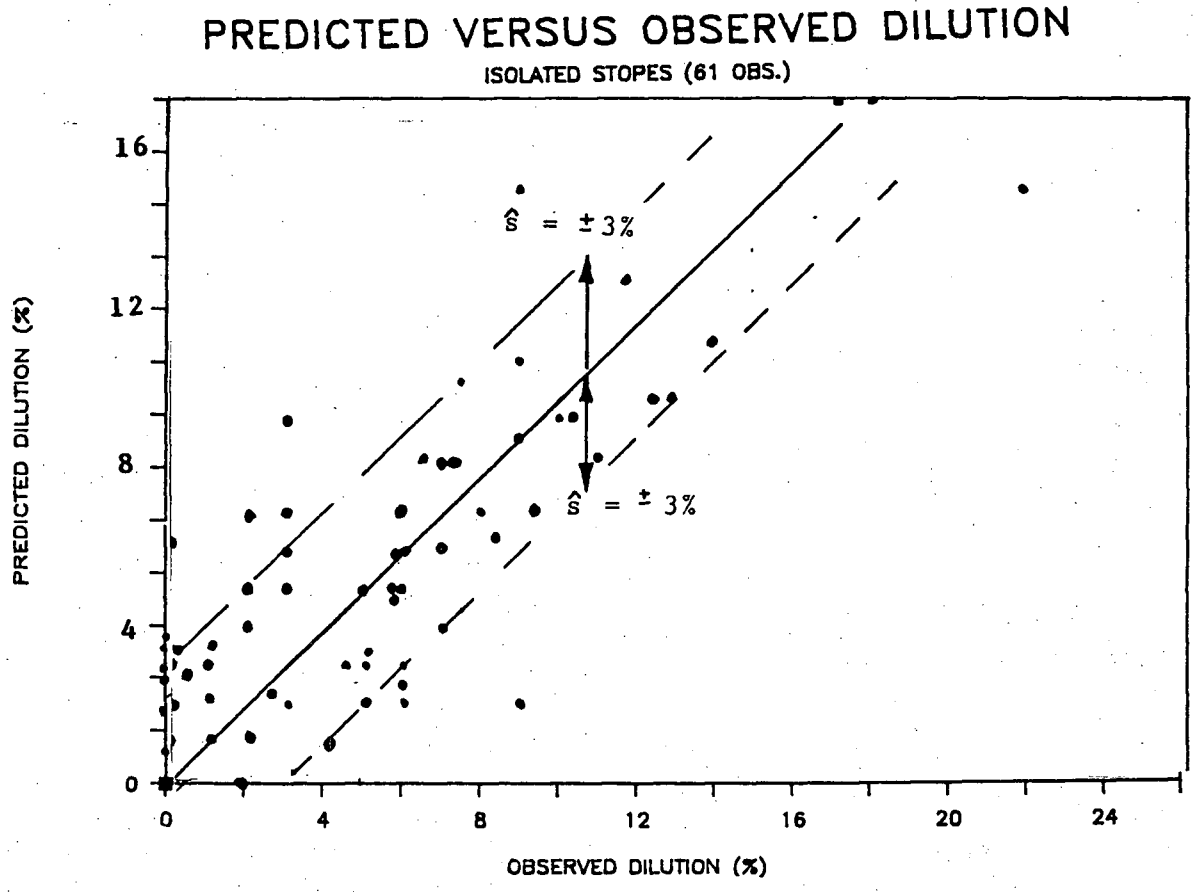

Figure 8.7a: Predicted Vs Recorded Dilution

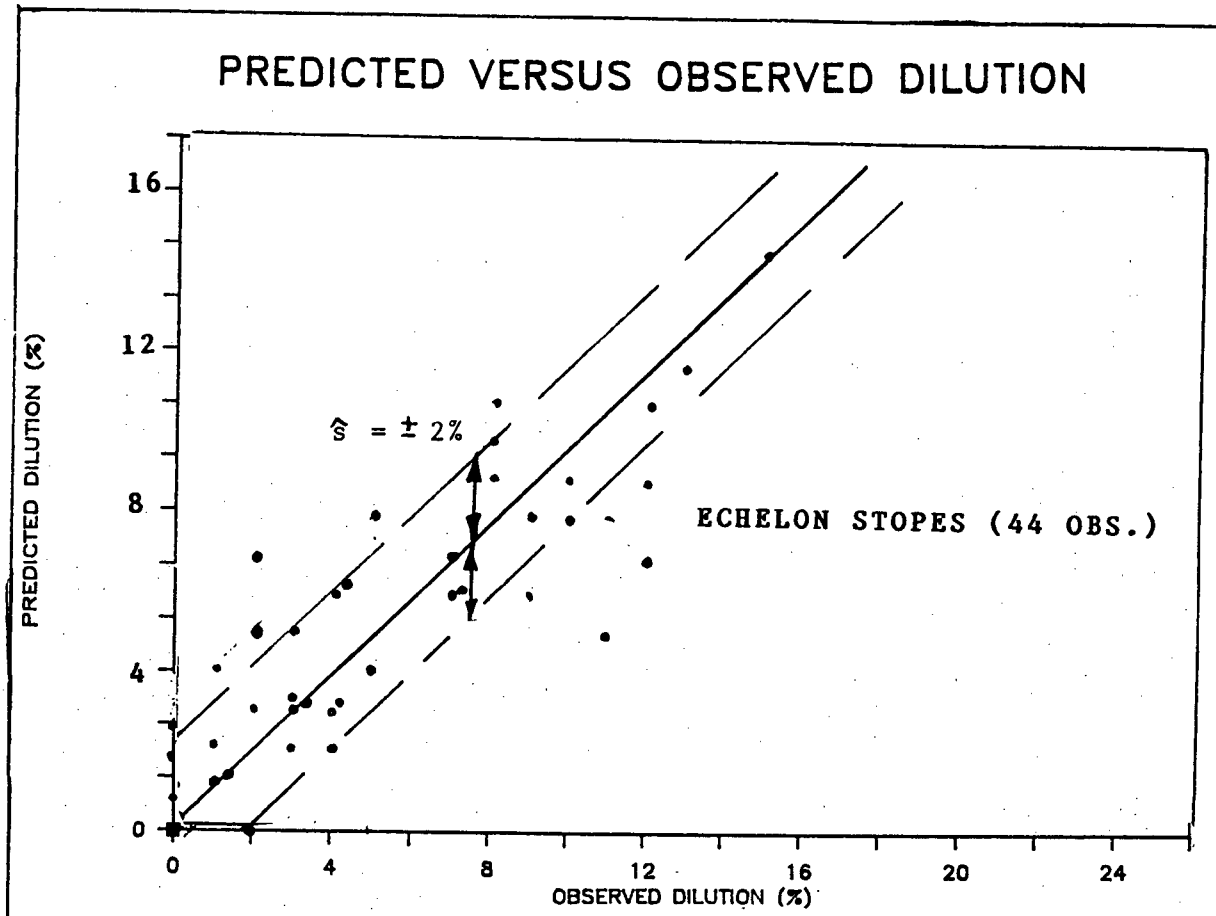

Figure 8.7b: Predicted Vs Recorded Dilution

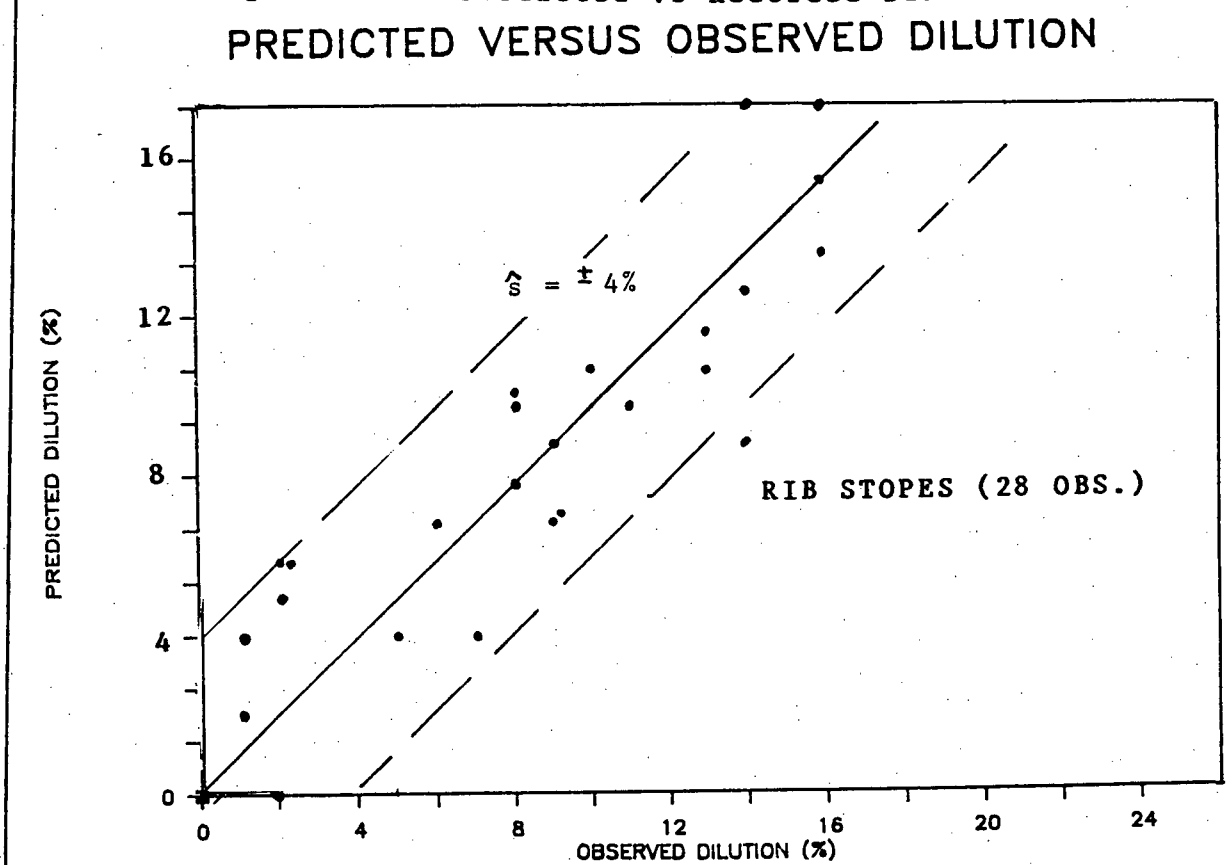

Figure 8.7c: Predicted Vs Recorded Dilution

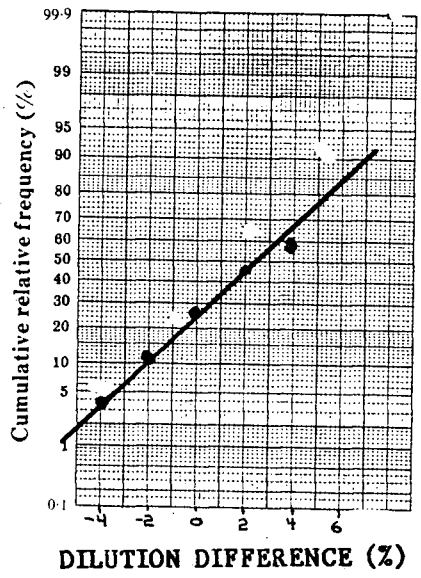

Figure 8.8: Cumulative Relative Frequency VS Dilution Difference

CHAPTER NINE

APPLICATION

9.1 Introduction

The governing equations, Figure 8.1, were employed to estimate dilutions for eight(8) stopes that were mined subsequent to the study. A brief comparison between the most promising methods is also summarized.

9.2 Calibrated Data Base

The stopes that comprise the calibrated data base are shown in Table 9.1. They consist of:

one isolated stope (2 observations)
two echelon stopes (7 observations)
five rib stopes (19 observations)

The governing equations, Figure 8.1, were employed to arrive at an estimated dilution. These results are shown in Table 9.2. An average error of estimate of 2.4% was obtained. The average error of estimate for the final configurations was 3%. The values were tabulated by the Ruttan mine personnel and the "BCF" values were recorded as dilution attributed to the slot removal. The results were subsequently added to the original

data base to arrive at the empirical equations shown in Figure 9.1. The coefficients for the augmented data base are similar to the original governing equations other than for the rib configuration. The difference, however, in the absolute dilution, as derived through the respective equations, does not differ greatly. This was determined by comparing rib data base predicted dilutions for both equations, Tables 9.3,8.3. The results indicated that for the original rib data base, the governing equation results in an estimate of sample error of ±2.7% and the augmented equation would yield an error of ±3.1%. The larger augmented data base similarly showed that the original governing equation yielded an error of ± 2.4% whereas the augmented equation yielded a mean sample error estimate of ±2.6%. The augmented data base will not be incorporated into the predictive solution since these results have been derived by the mine personnel and have not been thoroughly analyzed, as was the case with the original data base.

The calibrated stopes are in close approximation to the predictive dilutions yielded by the governing equations outlined in Figure 8.1.

9.3 Other Methods

The isolated data base was compared to the empirical methods of Mathews et al(1981), Laubscher(1976), Barton(1974) and Bieniawski(1972). It is intended to introduce the methods and

to relate them to that observed at Ruttan. Figure 9.2 shows the relationship that exists between that of Mathews and the observed data base at Ruttan. The reader is referred to Pakalnis/Rock Mass(1985) for a thorough discussion concerning this method. It incorporates the following four parameters, Figure 9.2, into a stability number:

- Barton's Q rating. This value can be derived from the "Rock Mass Rating".

- Stress Factor (A). This factor empirically relates the strength of the intact rock to the induced stress. This value is equated to "1.0" where tensile zones are observed (Ruttan).

- Structure Defect Parameter. This factor relates empirically the orientation of structure with respect to the stope. This factor is equated to "0.5" for structure paralleling the stope walls (Ruttan).

- Stope Inclination Parameter. This factor accounts for the stope inclination. This value is equated to "5.6" for stopes inclined at 70 degrees (Ruttan).

Figure 9.2 shows that the stability number (N), once plotted against the shape factor (hydraulic radius), can be categorized into stable, potentially unstable or potentially caving regions. Observations were plotted in terms of observed dilution, Figure 9.2. The results correlate (visually) well, in that higher dilutions were plotted within zones of instability, whereas lower dilutions were associated with more stable areas.

Figure 9.3a relates RMR to the critical hydraulic radius that would cause instability for an open stope operation as

defined by Laubscher. For rock mass ratings similar to that of Ruttan, Laubscher suggested that the hydraulic radius should not exceed 24m. A stope height of 60m would dictate a maximum stope span of 240m. This method of design is not based upon observations from open stoping, but from caving operations. The exposed surface area in caving operations is gently sloping, whereas in open stope operations, the hanging wall is generally inclined. The author would like to note that the definition as originally stated by Laubscher in describing hydraulic radius for an open stope, is vague since it was derived for caving operations where flat backs are the norm. The hydraulic radius, as defined in Chapter 7 was employed in the author's interpretation of critical span.

Figure 9.3b shows that Barton would design unsupported spans between 10 to 20m for the average rock mass ratings recorded at Ruttan. Bieniawski would predict unsupported spans of between 4 to 9m, Figure 9.3c. This shows the conservatism associated with the individual data bases which were derived primarily from civil projects.

Figure 9.4 shows the method as proposed by Beer and Meek(1982) in terms of predicting stope spans employing Voussoir arch theory. It is particularly applicable in the design of excavations in well-bedded formations where the direction of the bedding planes parallel the long dimension of the opening. It is assumed that the ground above the hanging wall is completely destressed in the direction normal to

bedding. In addition, it assumes that the rock mass has parted along smooth bedding plane breaks, thereby forming a series of "no-tension" beam members. Failure could be by "flexural" or "shear" failure, as indicated in Figure 9.4a. Figure 9.4c shows the suggested critical span given the:

- strata thickness (0.3m - 1m)
- modulus of deformation for the rock mass (8000MPa)
- stope inclination (65°)
- uniaxial compressive strength (100 MPa)

Curve "A" in Figure 9.4c describes the plane strain situation, whereas curve "E" describes that of a square hanging wall. The intermediate curves relate the critical design for the rectangular configurations, Figure 9.4b.

The following parameters are required for input into Figure 9.4c:

- the average joint spacing at Ruttan for the isolated data base is 0.3m to 1m ,Table 7.4

- the in-situ modulus of deformation for an "RMR=64%" is 22GPa, Appendix II. According to Brown(1985), the value should be halved, thereby employing a factor of safety of two. Consequently, the in-situ modulus is 11GPa for the Ruttan data base.

- The unconfined compressive strength is 50-100MPa, Table 7.4.

Employing the curves shown in Figure 9.4c would approximate the critical suggested span given the above input

parameters. This analysis suggests that the critical span should not exceed 20m to 45m. The similarity in the predicted and actual observed spans employed at Ruttan indicate that the Voussoir method does have applications for stope design. The difficulty arises in estimating the strata thickness and in calibrating the strength parameters to that of the mine data base.

The alternative methods were introduced to show that workable solutions can be obtained with the increased application of the individual methods and the subsequent calibration to actual observations. This would result in a more comprehensive method for the design of open stope spans.

Table 9.1: Stopes Mined Subsequent to Study

CALIBRATED DATA BASE - STOPES MINED SUBSEQUENT TO STUDY (8 Stopes)

No.	Stope	RMR(%)	Ht.(m)	Wdth.(m)	Vol.(m^3)	Dil.(%)	Span(m)	H.R.(m)	E.R.(m^2/mth)	B.C.F.(%)
	ISOLATED STOPES									
1	320 0 I	80	125	7	5000	4	6	3	0.21	0
2	320 0 I	80	125	7	10000	5	13	6	0.24	0
	ECHELON STOPES									
3	490 1 D	49	45	23	5000	3	5	2	0.12	3
4	490 1 D	49	45	23	10000	3	10	4	0.13	3
5	490 1 D	49	45	23	20000	3	20	7	0.14	3
6	490 1 D	49	45	23	30000	5	30	9	0.16	3
7	490 1 D	49	45	23	40000	7	40	11	0.16	3
8	370 14 CW	47	50	7	5000	5	15	6	0.15	3
9	370 14 CW	47	50	7	5400	5	25	8	0.15	3
	RIB STOPES									
10	260 17 J	53	25	13	5000	1	15	5	0.21	4
11	260 17 J	53	40	13	10000	2	19	6	0.25	4
12	260 17 J	53	60	13	20000	3	26	9	0.31	4
13	260 17 J	53	60	13	30000	8	40	12	0.33	4
14	260 17 J	53	60	13	36000	12	50	14	0.33	4
15	260 4 /SCROP	67	75	13	5000	3	5	2	0.26	3
16	260 4 /SCROP	67	75	13	10000	3	10	4	0.30	3
17	260 4 /SCROP	67	75	13	20000	4	21	8	0.33	3
18	260 4 /SCROP	67	75	13	30000	5	30	11	0.35	3
19	260 4 /SCROP	67	75	13	40000	5	41	13	0.37	3
20	260 4 /SCROP	67	75	13	44000	6	50	15	0.36	3
21	260 15 H	78	78	12	13600	3	32	9	0.57	0
22	340 9 C	26	28	6	5000	9	30	7	0.35	6
23	340 9 C	26	28	6	7100	14	50	9	0.35	6
24	430 20 J	71	48	17	5000	1	6	3	0.11	0
25	430 20 J	71	48	17	10000	3	12	5	0.13	0
26	430 20 J	71	48	17	20000	4	25	8	0.19	0
27	430 20 J	71	48	17	30000	6	37	10	0.20	0
28	430 20 J	71	48	17	328000	8	40	11	0.21	0

Table 9.2: Calibrated Data Base - Predicted Dilution

CALIBRATED DATA BASE - STOPES MINED SUBSEQUENT TO STUDY (8 Stopes)

No.	Stope	RMR(%)	E.R.(ft^2/mth)	Area(ft^2)	Res. Dil(%)	Pred.Dil(%)	Diff.(%)
ISOLATED STOPE: DIL(%)=8.6 - .09(RMR) - 13.2(E.R.) + .003B(AREA)							
1	320 0 I	30	0.210	750	4	1	3
2	320 0 I	30	0.240	1525	5	4	1
ECHELON STOPES: DIL(%)=10.3 - .13(RMR) - 14.8(E.R.) + .003(AREA)							
3	490 1 D	49	0.120	225	3	3	0
4	490 1 D	49	0.130	450	3	3	-0
5	490 1 D	49	0.140	900	3	5	-2
6	490 1 D	49	0.160	1350	5	6	-1
7	490 1 D	49	0.160	1800	7	7	0
8	370 14 CW	47	0.150	750	5	4	1
9	370 14 CW	47	0.150	1250	5	6	-1
RIB STOPES: DIL(%)=15.8 - .18(RMR) - 7.7(E.R.) + .0026(AREA)							
10	260 17 J	52	0.210	375	1	6	-5
11	260 17 J	53	0.250	760	2	6	-4
12	260 17 J	53	0.310	1560	3	8	-5
13	260 17 J	53	0.330	2400	8	10	-2
14	260 17 J	53	0.330	3000	12	12	0
15	260 4 /SCROP	67	0.260	375	3	3	0
16	260 4 /SCROP	67	0.300	750	3	3	-0
17	260 4 /SCROP	67	0.330	1575	4	5	-1
18	260 4 /SCROP	67	0.350	2250	5	7	-2
19	260 4 /SCROP	67	0.370	3075	5	9	-4
20	260 4 /SCROP	67	0.360	3750	6	11	-5
21	260 15 H	78	0.570	2496	3	4	-1
22	340 9 C	26	0.350	840	9	11	-2
23	340 9 C	26	0.250	1400	14	12	2
24	430 20 J	71	0.110	288	1	3	-2
25	430 20 J	71	0.130	576	3	4	-1
26	430 20 J	71	0.190	1200	4	5	-1
27	430 20 J	71	0.200	1776	6	6	-0
28	430 20 J	71	0.210	1920	8	6	2

Table 9.3: Augmented Rib Data Base

RIB STOPES DATA BASE — NUMBER OF STOPES = 9

EMPIRICAL EQUATION: DIL(%) = 11.2 - .14(RMR) - 2.3(ER) + .0027(AREA)

$r = .76$ $S_e = 4\%$

No.	Stope	RMR(%)	E.R. (ft^2/mth)	AREA(ft^2)	Res. Dil(%)	Pred.Dil(%)	Diff.(%)
1	320 10 B	34	0.220	448	0	7	-7
2	320 10 B	34	0.220	784	8	8	-0
3	320 10 B	34	0.250	1680	13	10	3
4	320 10 B	34	0.270	2464	16	12	4
5	320 10 B	34	0.290	3360	18	15	1
6	320 10 B	34	0.300	4144	16	17	-1
7	320 10 B	34	0.310	4928	16	19	-3
8	320 10 B	34	0.280	5152	16	20	-4
9	320 12 B	23	0.240	2120	27	13	14
10	340 12 C	30	0.120	240	8	7	1
11	340 12 C	30	0.160	520	10	8	2
12	370 20 J	69	0.040	225	5	2	3
13	370 20 J	69	0.080	450	7	3	4
14	370 14 C	47	0.160	780	8	6	2
15	370 14 C	47	0.200	2080	12	10	3
16	370 18 J	54	0.200	525	2	5	-3
17	370 18 J	54	0.300	1050	9	6	3
18	370 18 J	54	0.370	2175	14	9	5
19	370 18 J	54	0.310	3225	14	12	2
20	370 11 F	57	0.040	500	9	4	5
21	430 15 D	51	0.190	384	2	5	-3
22	430 15 D	51	0.230	704	6	5	1
23	430 15 D	51	0.220	1408	5	7	-2
24	430 15 D	51	0.240	2112	11	9	2
25	430 15 D	51	0.150	3008	14	12	2
26	430 20 K	74	0.280	506	1	2	-1
27	430 20 K	74	0.180	1012	1	3	-2
28	430 20 K	74	0.210	1748	2	5	-3

ISOLATED STOPES (63 OBS, 23 STOPES)

$$DIL(\%) = 8.4 - .08(RMR) - 12.6(EXP.RATE) + .0038(AREA)$$

$$r=\pm 0.79 \quad \hat{s}= \pm 3.2\%$$

ECHELON STOPES (51 OBS, 14 STOPES)

$$DIL(\%) = 10.3 - .13(RMR) - 14.8(EXP.RATE) + .0030(AREA)$$

$$r=\pm 0.83 \quad \hat{s}= \pm 2.3\%$$

RIB STOPES (47 OBS, 14 STOPES)

$$DIL(\%) = 11.2 - .14(RMR) - 2.3(EXP.RATE) + .0027(AREA)$$

$$r=\pm 0.76 \quad \hat{s}= \pm 4\%$$

Figure 9.1: Augmented Data Base

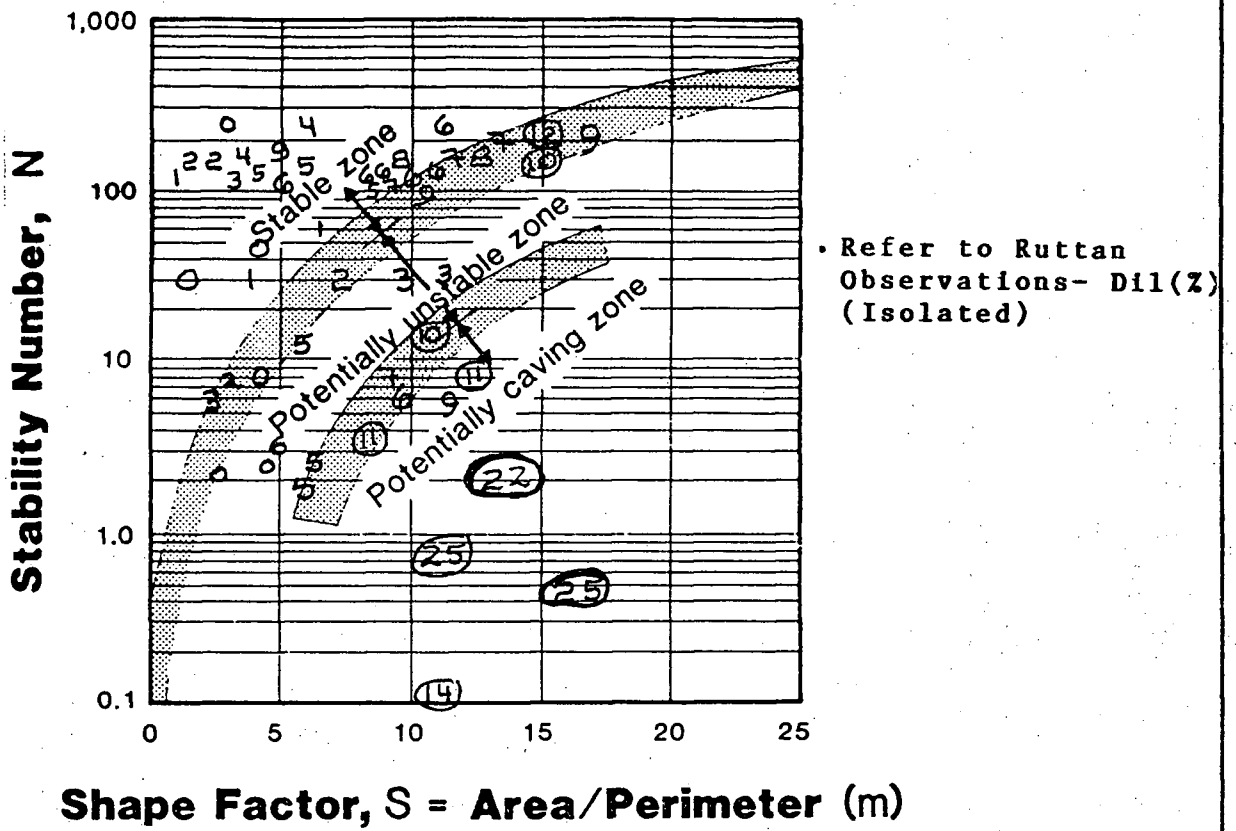

STABILITY NUMBER "N"

The stability number **N** is determined from the following equation:

$$N = Q' \times A \times B \times C$$

where

Q' = modified NGI rock mass rating

A = rock stress factor

B = rock defect orientation factor

C = orientation of design surface factor

Figure 9.2a: Mathews Method of Span Determination (Mathews et al, 1981)

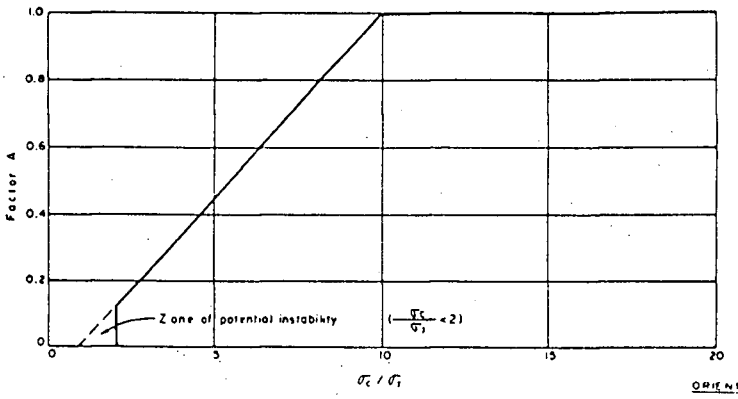

A = ROCK STRESS FACTOR

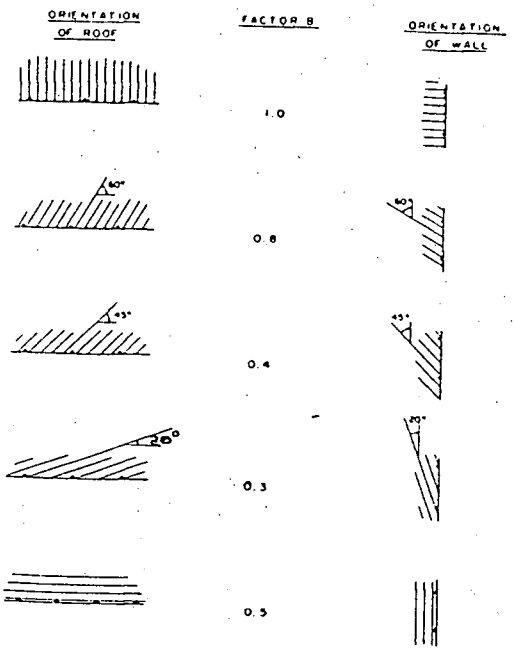

B = ROCK DEFECT FACTOR

C = ORIENTATION FACTOR
= 8 - 7 X COSIN (STOPE INCLINATION)

Figure 9.2b: Design Factors - Mathews Method

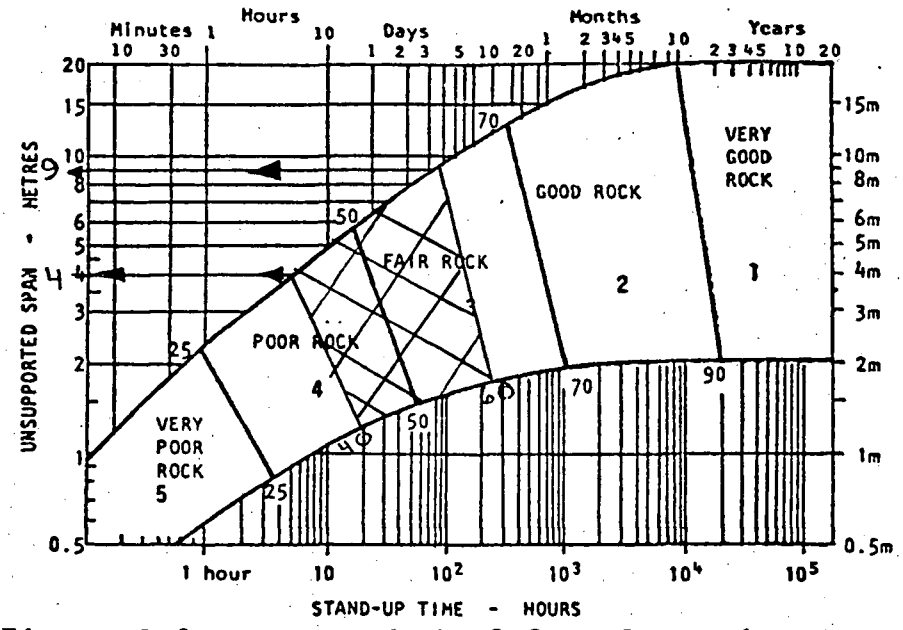

Figure 9.3c: RMR Method of Span Determination

ADJUSTED CLASS RMR %	100 - 80	80 - 60	60 - 40	40 - 20	20 - 0
HYD. RADIUS(m)		24	24 - 16	16 - 6	<6

Figure 9.3a: Laubsher Approach to Span Design (Laubsher, 1976)

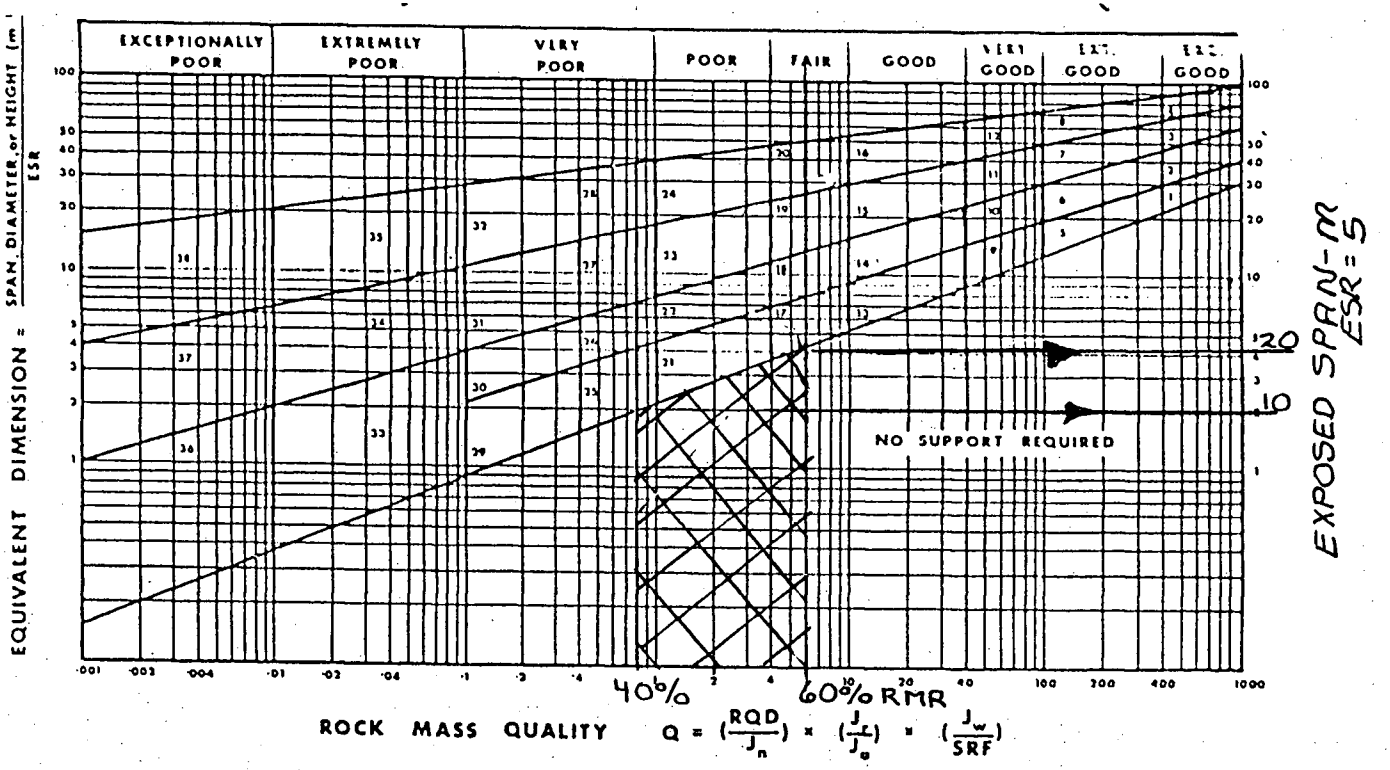

Figure 9.3b: Barton Approach to Span Design (Barton, 1974)

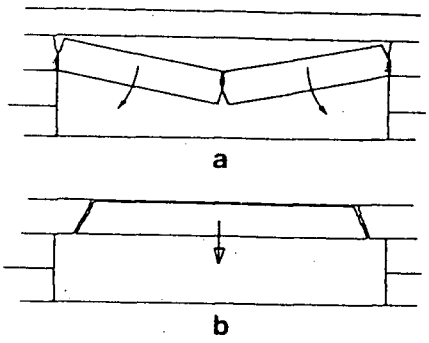

Two Basic Modes of Roof Failure: a) Snap through and b) Shear Failure

Diagram Showing Yield Lines for Rectangular Panel

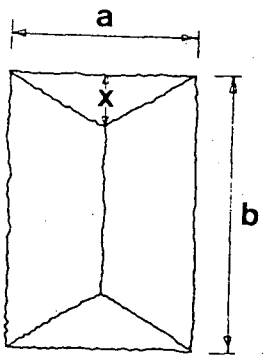

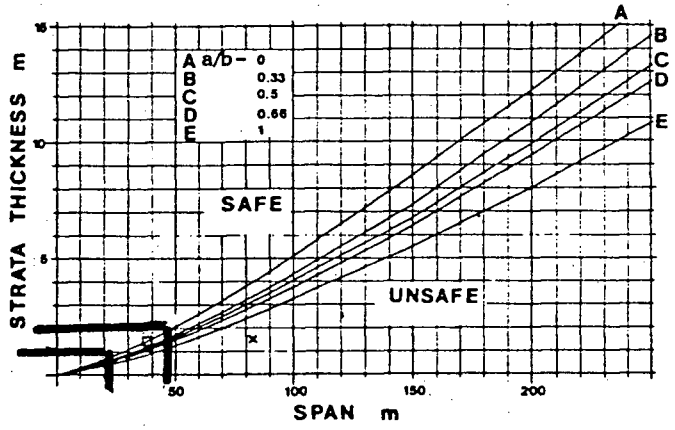

Design Curves for Rectangular Hanging Wall Panel
for Different Values of a/b (E=8000MPa, Dip = 65°)

Figure 9.4 Voussoir Beam Method of Span Determination

(Beer et al, 1982)

CHAPTER TEN

CONCLUSIONS

10.1 Concluding Remarks

The hanging wall and footwall at Ruttan was concluded to be in a state of relaxation, given the prevailing stress conditions and stope configuration. This, coupled with a foliated hanging wall, was determined to be the dominant failure mechanism. Optimum stope geometry was equated to stopes yielding lower observed dilution. The factors that directly contributed to increased wall slough were:

- **the rock quality of the individual critical wall contact**
- **the exposed surface area**
- **the rate at which the wall contact was exposed.**

Figure 8.1 summarizes the empirically derived expressions as quantified through observation(133) recorded for the Ruttan data base. It was concluded through multivariate analyses, that the predictive expressions were highly significant and correlative to the observed dilutions.

Dilution was found to be largely insensitive to the

following factors:

- the stope span/width ratio
- the mining depth
- the method of open stoping ITH versus conventional)
- the mine sequence (FW→ HW)

The predictive equations were defined for the isolated, rib and echelon configurations. Generally, it was found that the echelon geometry yielded the lowest dilution (2% less than isolated) with the rib stopes exhibiting the greatest dilution (1.5% greater than isolated).

Further research should be directed in the following areas:

1) Attempt to develop a more comprehensive predictor for the blast induced dilution.

2) Instrument a test stope in order to reinforce the observations made in this study.

3) Develop alternate methods of recording stope dilution that do not rely solely on visual assessment

4) Augment the present data base by observations made at other mine operations. In particular, attempt to assess the effect of stope inclination, support and groundwater on dilution

The Ruttan operation has adopted the methods proposed in this thesis. It has been able to predict better stope dilutions, design optimum stope spans and to forecast better the mining costs incurred due to wall instability. It is

suggested that the empirical methods of design outlined in this thesis be attempted/calibrated for other operations where similar failure mechanisms prevail. It should be noted that the characteristics unique to the Ruttan operation be assessed prior to extending the study to other operations.

The author's contribution to the existing state of knowledge concerning open stope design is in the empirical approach to the development of a design methodology. That relationship being primarily a function of "exposed surface area, exposure rate and rock mass rating". The governing equations are applicable for the Ruttan operation, however the methodology is valid for all open stoping operations. The absolute magnitudes of stope design are expressed in terms of dilution. This parameter is difficult to assess accurately, however once calibrated, it is a useful indicator of instability for any mine operation. To draw this thesis to a close, the author has selected the following from Terzaghi(1939):

"A good theory is one that works in practice. There is a tendency among the young and inexperienced to put blind faith in formulae forgetting that most of them are based on premises which are not accurately reproduced in practice, and which, in any case, are frequently unable to take into account collateral disturbances which only observation and experience can foresee and common sense provide against".

LIST OF REFERENCES

The following are reports, inter-office memoranda, and published articles that have been generated by the author in order to accomplish the objectives of this thesis. This is followed by a list of references of articles that were related to the thesis topic.

Internal Reports

Miller, H.D.S.M (1982) **Underground Rock Mechanics Investigation at the Ruttan Mine.** Proposal, April, Univ. B.C., pp. 7.

Pakalnis, R.C.T (1982) **Underground Rock Mechanics Investigation at Ruttan Mine-Workscope.** Internal-report, October, Univ. B.C., pp. 4.

Pakalnis, R.C.T (1983) **Bitem Operating Manual-Modifications by R.Pakalnis.** Internal-report, May, Univ. B.C., pp. 160.

Pakalnis, R.C.T (1983) **Plot-Bite. A Post-Processor Program for Bitem.** Internal-report, August, Univ. B.C., pp. 80.

Pakalnis, R.C.T (1983) **CSIRO Overcoring Measurements Conducted At Ruttan:In-Situ Stress Determination ,** Internal-report, November, Univ. B.C., pp. 120.

Pakalnis, R.C.T (1984) **Geo-Numerical Model: An Aid in Mine Design-Thesis Proposal.** Internal-report, August, Univ. B.C., pp.21

Pakalnis, R.C.T and Potvin, Y. (1985) **Review of Rock Mass Classification Systems**,Internal-report, February, Univ. B.C., pp. 140.

Pakalnis, R.C.T (1985) **Comprehensive Research Proposal for The Development of a Geo-Numerical Model as an Aid in Stope Design-Comprehensive.**,Internal-report, February, Univ. B.C., pp. 33.

Pakalnis, R.C.T (1985) **Dilution approach to Stope Design-Progress Report**, Internal-report, July, Univ. B.C., pp. 35.

Pakalnis, R.C.T. (1985) **Rock Characterization-Data Collection at Ruttan.**, Internal-report, May, Univ. B.C., pp. 60.

Pakalnis, R.C.T (1984) **Influence of Groundwater at Ruttan.** Internal-report, August, Univ. B.C., pp. 21.

Pakalnis, R.C.T. and Potvin Y. (1985) **Survey of Open Stope and Room and Pillar Operators**, Internal-report, December, 1985, pp. 30.

B.A.Sc Thesis Supervised by R.Pakalnis

Goldbeck B. (1985) **Analysis of Stress Changes at Sherritt Gordon's Ruttan Mine**, Internal-report, January, Univ. B.C., pp. 50

Green D. (1985) **Pillar Stresses determined by Tributary Area Theory and by Bitem**, Internal-report, April, Univ. B.C., pp. 67

Madsen P. (1985) **The Application of Elementary Beam Theory, Finite Element Analysis and Voussoir Arch Theory to the Design of Underground Openings**, Internal-report, April, Univ. B.C., pp. 110

Seki F. (1984) **Determination of Structural Domains and Design Sectors for the Ruttan Deposit**, Internal-report, February, Univ. B.C., pp. 50

Siu K.K.M. (1985)**Description and Analysis of Common Failure Modes at Ruttan**, Internal-report, April, Univ. B.C., pp. 152

Published Articles

Moss A.E.S., Page C. and Pakalnis R.C.T. (1984) **Rock Mass Classification: A Useful Tool in Planning Open Stopes**, Proc. AIME Fall Mtg.,Denver pp. 10

Pakalnis R.C.T. (1984) **Rock Mass Classification Systems:A Tool in Mine Design**, Crown Pillar Design Workshop (CIMM), Toronto, Ontario, pp. 20

Pakalnis R.C.T., Miller H.D.S., and Madill T. (1985) **Development of a Geo-Numerical Model as an Aid in Stope Design**, 26th U.S. Symposium on Rock Mechanics, A.A. Balkema, Boston pp. 140-148

Pakalnis R.C.T., Miller H.D.S., and Madill T. (1985) **In-Situ Stress Determination at Ruttan Mine, Sherritt Gordon Mines Ltd.**, CIM 87th Annual General Meeting, Vancouver, B.C., April, pp. 18.

Pakalnis R.C.T., Miller H.D.S., and Madill T. (1985) **Open Stope design - A Dilution Approach**, SANGORM Symp. on Rock Mechanics, Randburg, Sth. Africa, November, pp. 93-98

Inter-office Memoranda

Pakalnis R.C.T. (1983) **Rock Mechanics Study at Ruttan-Progress Report**, Inter-office, Univ. B.C., January pp. 5

Pakalnis R.C.T. (1983) **Modelling the Extraction Sequence** ,Inter-office, Sherritt Gordon Mines, March, pp. 10

Pakalnis R.C.T. (1983) **Analysis of Sill Pillar - 20 East Lenses**,Inter-office, Sherritt Gordon Mines, April, pp. 22

Pakalnis R.C.T. (1983) **Rock Mass Classification at Ruttan Mine**,Inter-office, Sherritt Gordon Mines, July, pp. 10

Pakalnis R.C.T. (1983) **Mechanism of Failure at Ruttan Mine**,Inter-office, Sherritt Gordon Mines, July, pp. 10

Pakalnis R.C.T. (1983) **Monitoring of Further 12B F/W Slough on the 260m Level**,Inter-office, Sherritt Gordon Mines, July, pp. 10

Pakalnis R.C.T. (1983) **Stability of Pillar X-Cut 14D and H/W Drive on 370m Level**,Inter-office, Sherritt Gordon Mines, July, pp. 3

Pakalnis R.C.T. (1983) **Degree of Water Entering 320-12B**

Stope,Inter-office, Sherritt Gordon Mines, July, pp. 2

Pakalnis R.C.T. (1983) **Mining Sequence/ Support Methods / Monitoring Program**,Inter-office, Sherritt Gordon Mines, July, pp. 14

Pakalnis R.C.T. (1983) **Proposed Core Logging Format Modification/ Back-analysis of Slough in 370m 14D Stope**, Inter-office, Sherritt Gordon Mines, October, pp. 10

Pakalnis R.C.T. (1984) **Failed Pillar Concept at Ruttan**, Inter-office, Sherritt Gordon Mines, January, pp. 10

Pakalnis R.C.T. (1984) **Numerical Modelling of Mining 320-12BE(Stope) on the 320m Level**, Inter-office, Sherritt Gordon Mines, March, pp. 10

Pakalnis R.C.T. (1984) **Stability Analysis of Sill Pillar Separating Upper and Lower Mine/ Rock Strengths at Ruttan/ Drawpoint Stability**,Inter-office, Sherritt Gordon Mines, April, pp. 30

Pakalnis R.C.T. and Miller H.D.S. (1984) **Guidelines for Designing Mine Layouts**,Inter-office, Sherritt Gordon Mines, June, pp. 37

Pakalnis R.C.T. and Miller H.D.S. (1985) **Dilution Variance with Depth at Ruttan**, Inter-office, Sherritt Gordon Mines, March, pp. 13

References reviewed as part of this study.

Barker,R.M. and Hatt,(1972). **Joint Effects in Bedded Formation for Roof Control**, 14th U.S. Rock Mechanics Symposium, Penn State Univ., June 11-14, pp.10.

Barrett,J.R., Grumitt, B. and Wical, M. (1979). **Arch Formation and Pillar Yield in Jointed Rock**, Int. Cong. on Rock Mech., Proc. 4th, Vol.2, Montreaux,Suisse, pp.10.

Barton, N., Lien, R. and Lunde, J.(1974).**Engineering Classification of Rock Masses for the Design of Tunnel Support**, Rock Mechanics, Vol.6, no.4, pp.183-236.

Beer, G., Meek, J.L. (1982). **Design Curves for Roofs and Hanging Walls in Bedded Rock Based on Voussoir Beam and Plate Solutions.** Trans. Instn. Min. Metall., January, pp.20.

Bieniawski, Z.T. (1983). **Improved Design of Room and Pillar Coal Mines for U.S. conditions**, 1st Int. Conf. on Stability in Underground Mining, AIME, New York, pp. 19-51.

Bieniawski,Z.T. (1973). **Rock Mechanics Design in Mining and Tunneling** A.A. Balkema Publishers, Accord, MA, pp. 272

Blackwood R.L. (1978).**Diagnostic Stress Relief Curves in Stress Measurement by Overcoring**,Int. J. Rock Mech., Min. Sci. & Geomech. Abstr. Vol, pp.205-209.

Brady, B.H.G. and Brown E.T. (1985). **Rock Mechanics for Underground Mining**, Allen and Unwin, Boston, pp. 527.

Brady, B.H.G. (1977). **An Analysis of Rock Behaviour in an Experimental Stoping Block at Mt. Isa Mine**, Queensland, Australia, Int. J. Rock Mechanics, Mng. Sci. Geomech., Vol.14

Bridges, M.C. (1982). **Review of Open Stope Mining in Australia**, 1st Int. Conf. Stability in Underground Mining, AIME, New York, 15pp.

Brown E.T. (1985). **From Theory to Practice in Rock Engineering**, Transactions of Instn. Mining and Metallurgy, April, pp. A67-A83

Chen, D.W., Chen, J.Y. and Zavodni, Z.M. (1983). **Stability Analysis of Sublevel Open Stopes at Great Depth**, Proc. 24th U.S. Rock Mech. Symp.,Texas.

Choquet, P. (1983). **A Method of Estimating Loose Zone Extent Around Mine Openings for Support Assessment**, CNCRM Symp. on Undrground Support Systems, Sept., Sudbury, 16pp.

Deere, D.U., Merritt, A.H. and Coon, R.F. (1968) **Engineering Classification of In-Situ Rocks**, Report by U. of Illinois to AFWL, No. AWFL-TW-67-144, NTIS No. AD848798, pp. 272.

Duvall, W.I (1977). **General Principles of Underground Opening Design in Competent Rock**, Monograph on Rock Mechanics Applications in Mining, AIME, New York. pp.101-111

Elissa E.S. (1980). **Stress Analysis of Underground Excavations in Isotropic and Stratified Rock Using the Boundary Element Method**, Ph.D thesis, University of London

Evans, W.H. (1940). **The Strength of Undermined Strata**, Trans. Instn. Min. Metall., pp. 475-532.

Flint, F. and Skinner B. (1974).**Physical Geology**, Wiley Inc., New York, New York, pp.351-367.

Hedley, D.F. and Grant F. (1972). **Stope and Pillar Design for the Elliot Lake Uranium Mines**, CIM Bulletin, Vol.65, pp.12.

Herget G. (1980). **Regional Stresses in the Canadian Shield - Summary**, CANMET, Division Report MRP/MRL 80-55(op), pp. 7.

Hoek, E. and Brown,E.T. (1980). **Underground Excavations in Rock**, Institution of Mining and Metallurgy, London, pp. 467-492.

Hoek E. (1983). **Strength of Jointed Rock Masses**, Geotechnique 33, No. 3, pp. 187-223.

Irad Gauge Inc. (1977). **Vibrating Wire Stressmeter Instruction Manual**, Lebanon, New Hampshire, pp. 40.

Kendorski, F.S., Cummings, R.A., Bieniawski, Z.T., and Skinner,E.H. (1983. **Rock Mass Classification for the Planning of Caving Mine Drift Supports**, Rapid Excavation and Tunneling Conference, AIME, New York, New York, pp. 28.

Kersten, R.W. (1985). **The Q-System of Tunnel Support Used for Underground Production Excavations**, SANGORM Symposium on Rock Mass Characterization, Randburg,S.A., pp.39-43

Kersten, R.W. (1981). **The Influence of Dilution on the Financial Viability of a Massive Sulphide Deposit**, 24th U.S. Symp. on Rock Mech., pp. 687-690.

Kirsten, H.A.D. (1983). **Combined Q-NATM System: The Design and Specification of Primary Tunnel Support**, South African Tunneling, Vol. 6, No. 1, pp.18-24.

Koch, G. and Link, R.(1980).**Statistical Analysis of Geological Data**, Volume II, Dover Publications Inc., New York, New York, pp.1-152.

Laubscher, D.H. and Taylor, H.W. (1976). **The Importance of Geomechanics Classification of Jointed Rock Masses in Mining Operations**, Exploration from Rock Engineering, ed. Z.T. Bieniawski, A.A. Balkema, Rotterdam. Vol.1, pp. 19-128.

Laubscher, D.H. (1976) **Geomechanics Classification of Jointed Rock Masses - Mining Applications,** Rhodesian Institution of Mining and Metallurgy, No. 86, pp. 8.

Maconochie, D.J, Friday, R.G. and Thompson, R.R (1981). **An Application of Monitoring and Numerical Modelling in Open Stope Mining**, Fourth Australian Tunnelling Conference, Melbourne, Australia, March, pp. 157-170

Mathews, K., Hammett, R.D. and Stewart, S.B. (1983). **Case Examples of Underground Mine Stability Investigations,** Stability in Underground Mining, AIME, New York, pp. 829-846

Mathews, K.E., Hoek, E., Wylie, D.C. and Stewart, S. (1981). **Prediction of Stable Excavation Spans for Mining at Depths Below 1000 Meters in Hard Rock**, CANMET Dept. of Energy, Mines and Resources, Canada, DSS Serial No. 0sQ80-0081DSS File No. 17SQ 23440-0-9020. pp. 80.

Miller H.D.S.,Potts E.L., and Szeki A.(1976).**In-Situ Stress Measurements in Halite in Chesire, Potash in North Yorkshire, and Slate at Dinorwic,Part II**, Proc. Rock Engineering, University of Newcastle-upon-Tyne, England, pp.257-272.

Morrison, R.G.K. (1976). **A Philosophy of Ground Control,** published by Dept. Min. and Metal. Engng., McGill Univ., Montreal, pp. 125-160

Moss, A.E.S and Niemi B. (1985).**Investigation into Mining of a Main Crown Pillar**, District Three Meeting, September, pp.19.

Nicholas, D. (1981)**Method Selection - A Numerical Approach,** Design and Operation of Caving and Sublevel Stoping Mines, eds. D. Stewart, AIME, New York, pp. 39-54.

Ontario Ministry of Labour (1985). **Provincial Inquiry into Ground Control and Emergency Preparedness in Ontario Mines**, Report prepared by 1) Steffen, Robertson and Kirsten and 2) Golder and Assoc., Ontario Ministry of Labour, Sudbury, Ontario.

Page, C.H., Brenner, R.G. (1983). **Stability of Large Open Stopes in Weak Rock**, Stability in Underground Mining, AIME, New York, pp. 336-356

Pariseau, W.G., Fowler, M.E. and Johnson, J.C. (1984). **Geomechanics of the Carr Fork Mine Test Stope**, Geomechanics Applications in Underground Hardrock Mining, SME/AIME, New York, pp. 3-38

Parker J. (1973).**Practical Rock Mechanics for Miners**, EMJ, June, pp.78.

Potts, E.L.J., Szeki, A., Watson, S.H., Mottahed, P. (1979). **The Evaluation of the Design Criteria for an Underground Roof Strata Considered as a Linear Arch Structure**, Intl. congress on Rock Mech., Proc. 4th, Vol.2, Montreaux, Suisse.

Potvin, Y. and Miller,H.D.S (1985). **Pillar Design Methodology**, Presented at AGM-CIM,Vancouver,B.C.

Rotzien, J. and Miller H.D.S (1985). **Report on In-Situ Stress Measurement at McLellan Mine**, Internal Report, University of British Columbia pp. 150.

Smith J.D. (1976-1979). **Progress Report Ruttan Underground Rock Mechanics Study**, Internal Reports. Sherritt Gordon Mines

Speakman, D.,Chornoby,P.,Holmes,G. and Haystead B. (1976). **Geology of the Ruttan Deposit**, Internal Report - Sherritt Gordon Mines, pp.25.

Spiegiel, M. (1972).**Theory and Problems of Probability and Statistics**, Schaum's Outline Series, McGraw Hill Co., pp.72.

St. John, C.M., Christianson, M., Petersen, D.L. (1980). **Evalustion of Mine Parameters for Copper-Nickel Deposits of Northern Minnesota**, U.S. Bureau of Mines, Open File Report No. 10-80, pp.87

Terzaghi K. (1943). **Theoretical Soil Mechanics**, John Wiley, New York, New York, pp. 510.

Vasey, J. (1983). **Design and Support of Excavations subjected to High Horizontal Stresses**, Stability in Underground Mining, AIME, New York, pp.428-449

Vennard, J.K and Street, R.L. (1975). **Elementary Fluid Mechanics**, John Wiley & Sons Inc., Toronto, pp.326-327.

Wang, F.D., Danek, L.A. and Sun, M.C. (1971). **Stability Analysis of Underground Openings Using a Coulomb Failure Criteria**, Trans. Soc. Mining Eng., AIME, Vol. 250 pp. 317-321.

Wardle, L.J. (1980). **Three-Dimensional Boundary Element Program for Mining Applications : MIN3D2 (3DBELM)**, CSIRO Publication, Technical report No. 116, pp. 17.

Watson J.O. and Cowling R. (1985). **Application of Three Dimensional Boundary Element Methods to Modelling of Large Mining Excavations at Depth**, Paper presented to 5th Int. Conf. on Numerical Meth. in Geomech., Nagoya.

Worotnicki, G. and Walton, R.J (1976).**Hollow Inclusion Gauges for the Determination of Rock Stress In-Situ**, Proc. ISRM Symp. on Investigation of Stress in Rock and Advances in Stress Measurement, Sydney, pp. 1-8.

Wright, D.F. (1980). **Roof Control Through Beam Action and Arching** , SME Mining Engineering Handbook, AIME New York, Vol. 13, pp.80-85.

APPENDIX I

QUESTIONAIRE

STOPE & PILLAR DIMENSIONS

- Indicate the stope and pillar dimensions on the sketch or on the "STOPE CHARACTERIZATION" Table (next page).

ROOM & PILLAR MINING

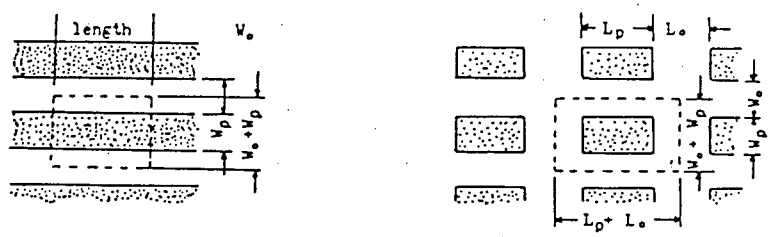

OPEN STOPE MINING

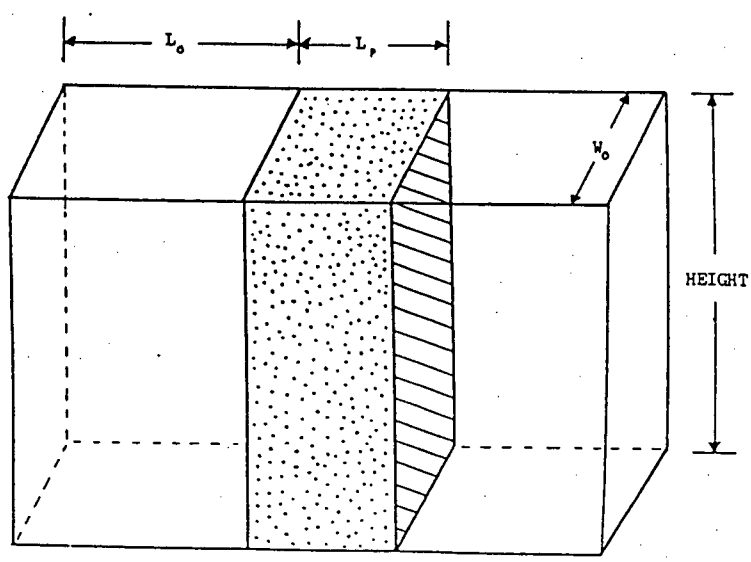

ROCK MECHANIC DATA BASE

Indicate with an "x" which of the following parameters have been estimated at your mine:

1. ROCK STRENGTH PARAMETER	Unit Weight	γ	
	Elastic Mod	c	
	Poisson's Ratio	ν	
2. STRESS INVESTIGATIONS	In-Situ Measurement		
	Photo-Elastic Model		
	Computer Modelling		
3. LABORATORY TEST	Compress. Strength	σ^c	
	Tensile Strength	σ^t	
	Triaxial Strength	$\sigma_1 \mid \sigma_3$	
	Shear Strength	τ	
	Failure Criterion		
4. ROCK MASS CLASSIFICATION	R Q D		
	N G I		
	C S I R		
	Laubscher		
	Structural Mapping		
5. MONITORING	Multi-Wire Extensom.		
	Boroscope Observ.		
	Compression Pad		
	Closure Station		
	Levelling Survey Station		
	Piezometer		

STOPE CHARACTERIZATION

MINING METHOD **	STOPE PLUNGE	DEPTH	FOOTWALL			HANGINGWALL			ORE			OPENING		PILLAR		STOPE HEIGTH	% of DILUTION
			strength	fracture spacing	joints condition	strength	fracture spacing	joints condition	strength	fracture spacing	joints condition	width "W_o"	length "L_o"	width "W_p"	length "L_p"		

** List individual stopes

ROCK STRENGTH

- Indicated by uniaxial compressive strength or as follows:
  - . WEAK: 6000 psi (4)
  - . MODERATE: 6000 - 15000 psi (7)
  - . STRONG: 15000 psi (12-15)

FRACTURE SPACING

	Fracture/m		% RQD
Very Close:	16	(9)	0 - 20
Close:	10 - 16	(17)	20 - 40
Wide:	3 - 10	(32)	40 - 70
Very Wide:	3	(43-50)	70 - 100

GROUNDWATER

Dry (10)

( ) Refers to RMR Rating Equivalent.

JOINTS CONDITION

WEAK: Clean joint with a smooth surface or fill with material whose strength is less than rock mass strength (3)

MODERATE: Clean joint wiyh rough surface (12)

STRONG: Joint is filled with a material that is equal to or stronger than rock mass strength (20-25)

APPENDIX II

RMR SYSTEM OF CLASSIFICATION

Excerpt from **Review of Rock Mass Classification Systems**

Pakalnis (1985)

3.1. DEERE'S ROCK QUALITY DESIGNATION

The concept of the rock quality designation was proposed in 1964 by Deere (1975) and was originally based on fourteen tunnels. It was subsequently expanded and incorporated by numerous classification schemes. (Einstein, 1979).

The RQD is a quantitative index based on a core recovery procedure in which the core recovery is determined incorporating only those pieces of hard, sound core which are 100 mm or greater in length. Shorter lengths are ignored, Figure 14. It can be determined from the following expression:-

$$RQD(\%) = 100 \times \frac{\sum \text{length of core in pieces 100 mm or longer}}{\text{length of core run}}$$

Core of at least 50 mm in diameter should be used. If core of lesser or greater diameters is to be used, the nominal length of 100 mm should be altered to correspond to **two times the core diameter.** The International Society of Rock Mechanics recommends that the length of individual core pieces should be assessed along the centre line of the core, so that the discontinuities that hapen to parallel the drill hole will not unduly penalise the RQD values of an otherwise massive rock mass (Figure 15). It is important to distinguish between mechanical and natural breaks found in the core. A mechanical break caused by handling should not adversely affect the RQD index which is a measure of the in-situ rock quality. The mechanical broken core segments should be approximated into a solid unit of core in order to arrive at a reliable RQD value. Over consolidated gauge is treated as having a core length less than 100mm. This is due to the RQD being a measure of only "hard, sound core." The

RQD should be evaluated over an interval generally not less than .5 m -2 m and is typically between 1.5 m - 6 m. Shear zones or extremely weak zones must be delineated for subsequent analysis. This value will generally be a function of the intactness of the core. The interval evaluated should be of a similar structural design unit.

The RQD procedure is simple, inexpensive and reproductible. The following relationship exists between the numerical values of the RQD and the general quality of the rock for engineering purposes:

RQD	ROCK QUALITY
> 25 per cent	very poor
25 - 50 per cent	poor
50 - 75 per cent	fair
75 - 90 per cent	good
90 - 100 per cent	very good

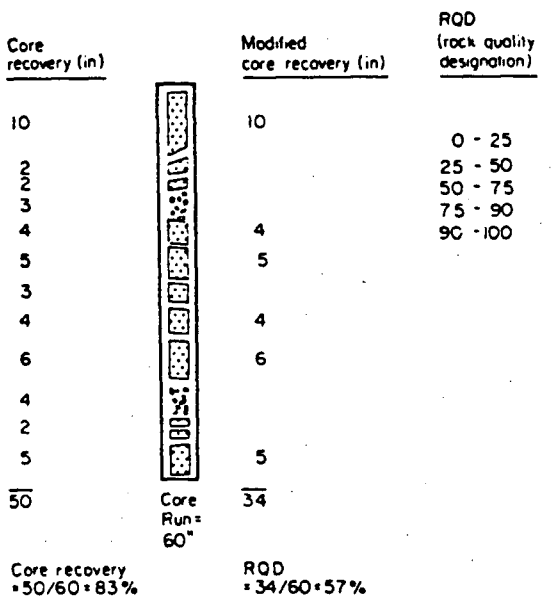

FIGURE 14

MODIFIED CORE RECOVERY AS AN INDEX OF ROCK QUALITY (DEERE,1975).

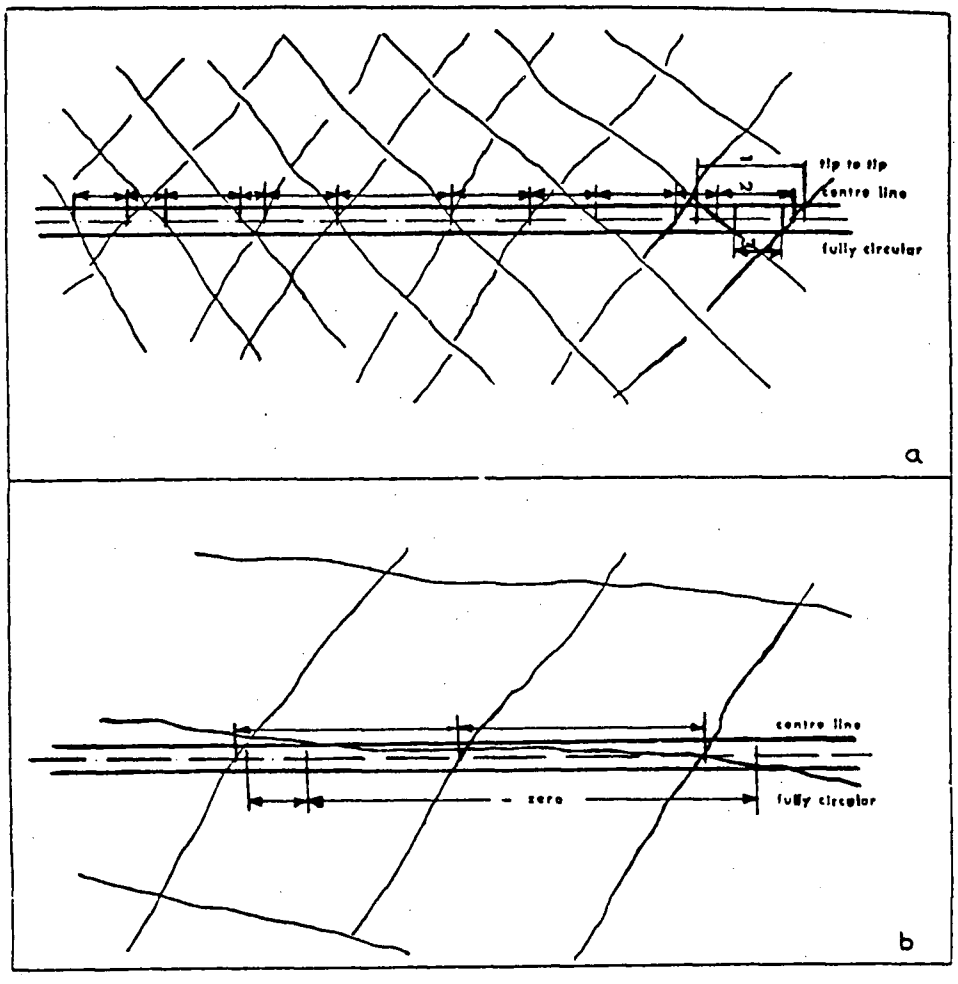

FIGURE 15

Recommended method of measuring fracture lengths: examples of three possible interpretations of the length of core pieces. The centre line length is suggested as the most realistic measurement and is recommended (a). The cylindrical interpretation (b) would unduly penalize the RQD values of an otherwise massive mass.

In order to determine the RQD of rock surfaces a tape is suspended horizontally along the surface and oriented at a right angle to the dominant fracture direction.

In this way, an assessment of the true fracture spacing is obtained. Two metre lengths are assessed. (Laubscher, 1972).

The R.Q.D. is a core recovery technique that can be applied to rock surfaces provided the following points are observed:

a) Experience in determining the R.Q.D.of core is necessary before attempting the R.Q.D. assessments of rock surfaces.
b) Do not be misled by blasting fractures.
c) Weaker bedding planes do not necessarily break when cored.
d) Where a joint (slip) face forms the sidewall, assess the opposite wall.
e) Shear zones greater than two metres in width must be classified separately.

The correlation between core R.Q.D. and rock surface R.Q.D. will be obtained by drilling boreholes parallel to excavations. This wll also give correlation between the other items.

Barton (1983) suggests the following relationship:

- When borehole data is unavailable, RQD can be estimated from the number of joints per unit volume, where the number of joints per meter for each joint are added together. A simple relation can be used to convert this number of joints to RQD. For the results of a clay free rock mass:

$$RQD = 115 - 3.3\ Jv \text{ (approximate)}$$

where Jv is the total number of joint per m^3. (RQD=100 for Jv = 4.5).

Priest and Hudson (1976) developed a chart showing the correlation that exists between RQD and joint spacing, Figure 16.

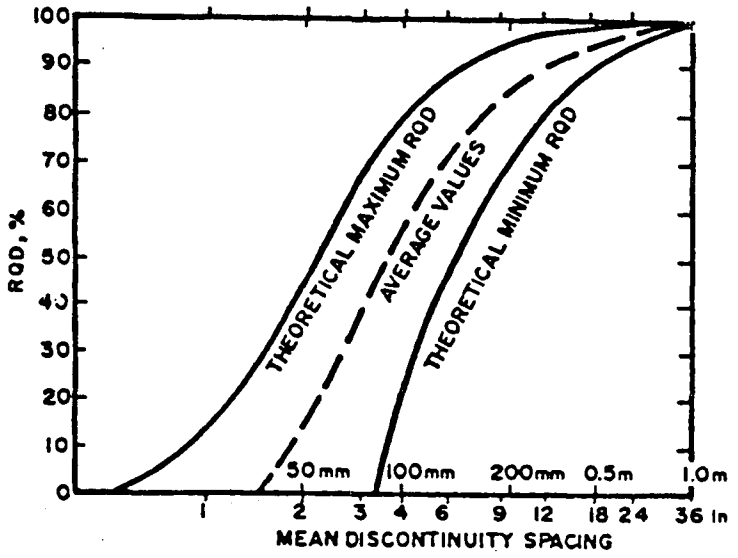

FIGURE 16

THEORETICAL RELATIONSHIP BETWEEN RQD AND DISCONTINUING SPACING. (PRIEST AND HUDSON, 1976)

3.3 GEOMECHANICS CLASSIFICATION (RMR)

This classification system was developed for the South African Council for Scientific and Industrial Research (CSIR) by Bieniawski in 1973. It employs five parameters:

a) the uniaxial compressive strength of intact rock material
b) rock quality designation
c) spacing of fractures
d) condition of fractures i.e. frictional properties and continuity
e) ground water conditions

Each of these parameters is given an importance rating for a particular situation. The ratings were determined from 49 case histories investigated by Bieniawski (1984) and augmented by the work of Wickham et al (1974). The total rating is an indicator or rock quality and ranges from less than 25% (worst rock conditions) to 100% (best rock conditions). The rating is subsequently adjusted to account for the influence of structural orientation on stability. This adjusted rating is used to classify the rock into one of five classes which empirically can be related to the stand-up time of unsupported openings, support requirements, and rock mass strength indices. The classification assesses the typical rather than the worst rock mass conditions.

3.3.1 PARAMETERS

3.3.1.1. UNIAXIAL COMPRESSIVE STRENGTH OF INTACT ROCK MATERIAL

The intact rock strength is the average uniaxial compressive strength of the rock. The strength of the rock material constitutes the highest strength limit of the rock mass for a given confining pressure. The rock mass strength will consequently be lower than the intact rock strength due to alteration, ground water and the presence of discontinuities. A number of strength classifications have been proposed and are compared in Table 12. The RMR system employs the rock strength groupings as derived by Deere (Table 13). Typical rock strengths are summarized in Table 14.

TABLE 12 Classifications for Strength of Intact Rock (Bieniawski, 1973)

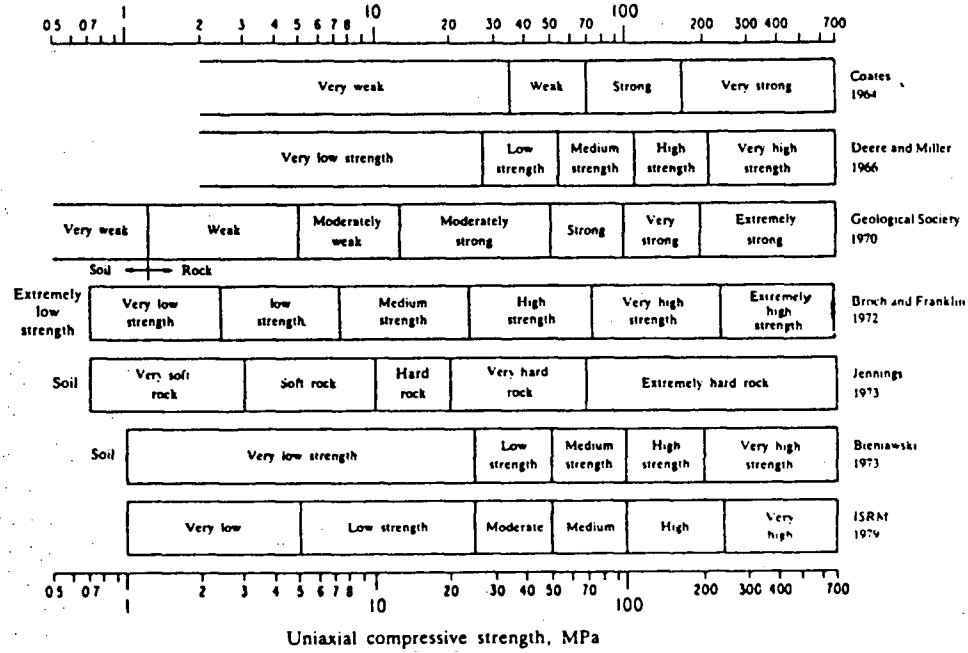

TABLE 13 BIENIAWSKI CLASSIFICATION FOR INTACT ROCK STRENGTH (BIENIAWSKI,1973)

Description	Uniaxial compressive strength,MPa	Examples of rock types
Very low strength	1 - 25	Chalk, rocksalt
Low strength	25 - 50	Coal, siltstone, schist
Medium strength	50 - 100	Sandstone, slate, shale
High strength	100 - 200	Marble, granite, gneiss
Very high strength	> 200	Quartzite, dlerite, gabbro, basalt.

TABLE 14 STRENGTH DATA FOR INTACT ROCK (BIENIAWSKI, 1973)

Rock Type	Uniaxial compressive strength MPa		
	Min.	Max	Mean
Chalk	1,1	1,8	1,5
Rocksalt	15	29	22,0
Coal	13	41	31,6
Siltstone	25	38	32,0
Schist	31	70	43,1
Slate	33	150	70,0
Shale	36	172	95,6
Sandstone	40	179	95,9
Mudstone	52	152	99,3
Marble	60	140	112,5
Limestone	69	180	121,8
Dolomite	83	165	126,3
Andesite	127	138	128,5
Granite	153	233	188,4
Gneiss	159	256	195,0
Basalt	168	359	252,7
Quartzite	200	304	252,0
Dolerite	227	319	280,3
Gabbro	290	326	298,0
Banded ironstone	425	475	450,0
Chert	587	683	635,0

The reasons for these groupings (Table 13) are as follows:

- the classification is widely recognized throughout the world
- groupings are practical and realistic
- easy to remember

It must be noted that a value of 1 MPa is taken as the lowest strength limit for

rock materials and consequently defines the division between soil and rock. Furthermore, the terms of description such as low, medium or high strength are preferred to weak or strong, thus avoiding ambiguity when dealing with weathered rocks. No divisions are given for rock strengths less than 25 MPa other than being classifed as having a very low strength. The reason for this is that rocks exhibiting intact strengths under 25 MPa do not behave drastically different and therefore are grouped as a single unit.

The uniaxial compressive strength, (UCS), can be determined by laboratory techniques or in the field by use of the point load apparatus. Bieniawski (1975) had determined that the point load derived UCS is within 20% of the laboratory derived value. It is recommended to use laboratory procedures to evaluate rock strengths whose values are less than 25 MPa.

3.3.1.2 ROCK QUALITY DESIGNATION (RQD)

Refer to Deere's definition, Section 3.1

3.3.1.3 JOINT SPACING

The term joint means all discontinuities which may be technically joints, faults, bedding planes or other surfaces of weakness. The spacing of joints is the mean distance between the planes of weakness in the rock mass in the direction perpendicular to the joint planes.

The presence of joints reduces the strength of a rock mass and the joint spacing governs the degree of the reduction. The classification of joints based on spacing is derived after Deere as follows:

Description	Spacing of Joints	Rock Mass Designation
very wide	> 3 m	solid
wide	1 - 3 m	massive
moderately close	0.3 - 1 m	blocky/seamy
close	50 - 300 mm	fractured
very close	> 50 mm	crushed

Bieniawski states that the data on spacing of joints must be obtained from a joint survey, for each joint set, and not from borehole logs. It is difficult to distinguish between joint sets from drill cores; however, where possible one should attempt to determine a **mean joint spacing.** It is our experience (Sherritt Gordon Mines) that where site information is restricted to boreholes, a good estimate of joint spacing is derived as follows:

1) choose a borehole interval that exhibits similar rock mass characteristics i.e. RQD, rock type, frequency of fractures, normally between 1.5 to 6 m.

   $$\text{joint spacing} = \frac{\text{logged interval}}{\text{number of joints}}$$

2) an alternative is to group each joint according to its dip, i.e. 0 - 30°, 30 - 60°, 60 - 90°, and determine a spacing for each. Otherwise relative values are obtained for vertical or near-vertical drill holes.

Joints must also be continuous if they are to be included within the definition of "joint spacing". A joint is continuous if its length is greater than one diameter of the excavation or three meters. It is also continuous if it is less than three meters but extends from one joint to another, i.e. define blocks.

The RMR system of importance ratings for joint spacing apply to rock masses having three joint sets. The rating is conservative if only two sets exist. (Bieniawski, 1984).

Bieniawski (1984) has recently applied the work of Priest and Hudson (1976) into developing a single rating incorporating The RQD and joint spacing. In either knowing the RQD or joint spacing one is able to arrive at the RMR rating which sums the two parameters.

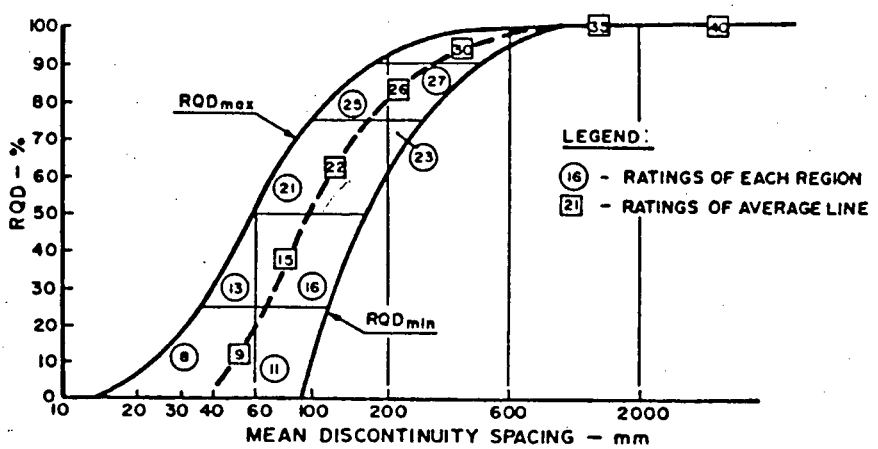

FIGURE 23

CHART FOR CORRELATION BETWEEN RQD AND JOINT SPACING (BIENIAWSKI, 1984)

3.3.1.4 JOINT CONDITION

Condition of joints refers to the separation of joints (distance between joint surfaces), continuity and roughness of joints as well as gouge material. If gouge is present, its type and thickness should be specified. Tight joints with rough surfaces and no gouge have a high strength. Continuous, smooth open joints will facilitate unrestricted in flow of ground water, thus dictating a lower mass rating.

Bieniawski proposed the following descriptions:

ROUGHNESS

- very rough: near vertical steps and ridges occur on the discontinuity surface.
- rough: some ridge and side-angle steps are evident, asperities are clearly visible, and joint surfaces feel very abrasive.
- slightly rough: Asperities on joint surfaces are distinguishable and can be felt.
- smooth: surface appears smooth and feels so to the touch.
- slicken sided: visual evidence of polishing exists.

SEPARATION BETWEEN JOINT WALLS

- very tight < 0.1 mm
- tight 0.1 - 0.5 mm
- moderately open 0.5 - 2.5 mm
- open 2.5 - 10 mm
- very wide 10 - 25 mm

(If separation exceeds 25 mm the joint should be treated as a major discontinuity.)

WEATHERING

a). **Unweathered.** No visible signs are noted of weathering; rock fresh; crystals bright.

b). **Slightly weathered rock.** Discontinuities are stained or discolored and may contain a thin filling of altered material. Discoloration may extend into the rock from the discontinuity surfaces to a distance of up to 20 per cent of the discontinuity spacing.

c). **Moderately weathered rock.** Slight discoloration extends throughout the rock, and the rock material is partly friable. The original texture of the rock has mainly been preserved, but separation of the grains has occurred.

e). **Completely weathered rock.** The rock is totally discolored and decomposed and in a friable condition. The external appearance is that of soil. Internally, the rock texture is partly preserved, but grains have completely separated.

3.3.1.5 GROUND WATER CONDITIONS

Ground water is known to have an important effect on the behaviour of jointed rock masses. The rate of inflow of ground water greatly affects the stability of tunnels. A value of 10 is employed for a completely dewatered situation whereas a rock mass rating of 0 indicates severe water problems.

3.3.2 APPLICATIONS

The above parameters are incorporated into table 15.

The classification parameters discussed previously are to be provided by the engineering geologist from his measurements conducted in the field. One complete set of data is needed for each structural region as encountered along the tunnel route. A structural region is defined as a zone in which similar geotechnical stability can be expected. The geologist should supply any additional information which he considers useful and relevant.

A number of observations should be made with respect to Table 15. It will be

noted that rock parameters and rock masses are grouped into five classes. This is considered sufficient to provide for meaningful discrimination in all the parameters. More classes could be difficult to work with while fewer classes may not offer sufficiently clear distinctions.

In applying various parameters to a rock mass classification, it is necessary to note that different parameters are not equally important for the overall classification of a rock mass. Accordingly, importance ratings are also given in Table 15 for each parameter and its subdivision. These ratings are partly derived from a study by Wickham et al (1974). Two points should be noted in connection with these ratings.

Firstly, the ratings given for joint spacings apply to rock masses having three sets of joints. Thus, when only one or two sets of joints are present, a conservative assessment is obtained. Secondly, some difficulties may be experienced in deciding whether strike and dip orientations are favourable or not in a given tunnel. (Refer to Parameter B, RSR).

Once the importance ratings of the classification parameters are added, giving the total rating for the rock mass, i.e. its structural region under consideration. Note that the higher the total rating, the better the rock mass conditions.

The Geomechanics classification has established itself as a useful and versatile technique for assessing rock mass conditions on engineering projects. The main applications of rock mass classifications have traditionally been in tunnelling. The RMR system has been employed by various authors on rock slopes (Steffen, 1976), dam foundations (Bieniawski for 1976) ground rippability (Kirsten, 1982) coal mining (Bieniawski, 1983) and in metal mining (Laubscher, 1978).

A. Classification parameters and their ratings

PARAMETER			RANGES OF VALUES						
1	Strength of intact rock material	Point-load strength index	> 10 MPa	4 - 10 MPa	2 - 4 MPa	1 - 2 MPa	For this low range - uniaxial compressive test is preferred		
		Uniaxial compressive strength	>250 MPa	100 - 250 MPa	50 - 100 MPa	25 - 50 MPa	5-25 MPa	1-5 MPa	<1 MPa
	Rating		15	12	7	4	2	1	0
2	Drill core quality RQD		90% - 100%	75% - 90%	50% - 75%	25% - 50%	< 25%		
	Rating		20	17	13	8	3		
3	Spacing of discontinuities		>2 m	0.6 - 2 m	200 - 600 mm	60 - 200 mm	60 mm		
	Rating		20	15	10	8	5		
4	Condition of discontinuities		Very rough surfaces. Not continuous No seperation Unweathered wall rock	Slightly rough surfaces Separation < 1 mm Slightly weathered walls	Slightly rough surfaces. Separation < 1 mm Highly weathered walls	Slickensided surfaces OR Gouge < 5 mm thick OR Separation 1-5 mm. Continuous	Soft gouge > 5 mm thick OR Separation > 5 mm. Continous		
	Rating		30	25	20	10	0		
5	Ground water	Inflow per 10 m tunnel length	None	<10 litres/min	10-25 litres/min	25 - 125 litres/min	> 125		
		Ratio $\frac{\text{joint water pressure}}{\text{major principal stress}}$	OR 0	OR 0.0-0.1	OR 0.1-0.2	OR 0.2-0.5	OR > 0.5		
		General conditions	OR Completely dry	OR Damp	OR Wet	OR Dripping	OR Flowing		
	Rating		15	10	7	4	0		

B. Rating adjustment for discontinuity orientations

Strike and dip orientations of joints		Very favourable	Favourable	Fair	Unfavourable	Very unfavourable
Ratings	Tunnels	0	-2	-5	-10	-12
	Foundations	0	-2	-7	-15	-25
	Slopes	0	-5	-25	-50	-60

C. Rock mass classes determined from total ratings

Rating	100 ← 81	80 ← 61	60 ← 41	40 ← 21	< 20
Class No	I	II	III	IV	V
Description	Very good rock	Good rock	Fair rock	Poor rock	Very poor rock

TABLE 15

GEOMECHANICAL CLASSIFICATION SYSTEM

3.3.2.1. SUPPORT, ACTIVE SPAN

The classification has been applied to highway, railroad and water conveyance tunnels as well as to underground caverns for hydroelectric schemes. A total of 49 case histories were compiled which served as the basis for preparing the span versus stand-up time diagram outlined below in Figure 24.

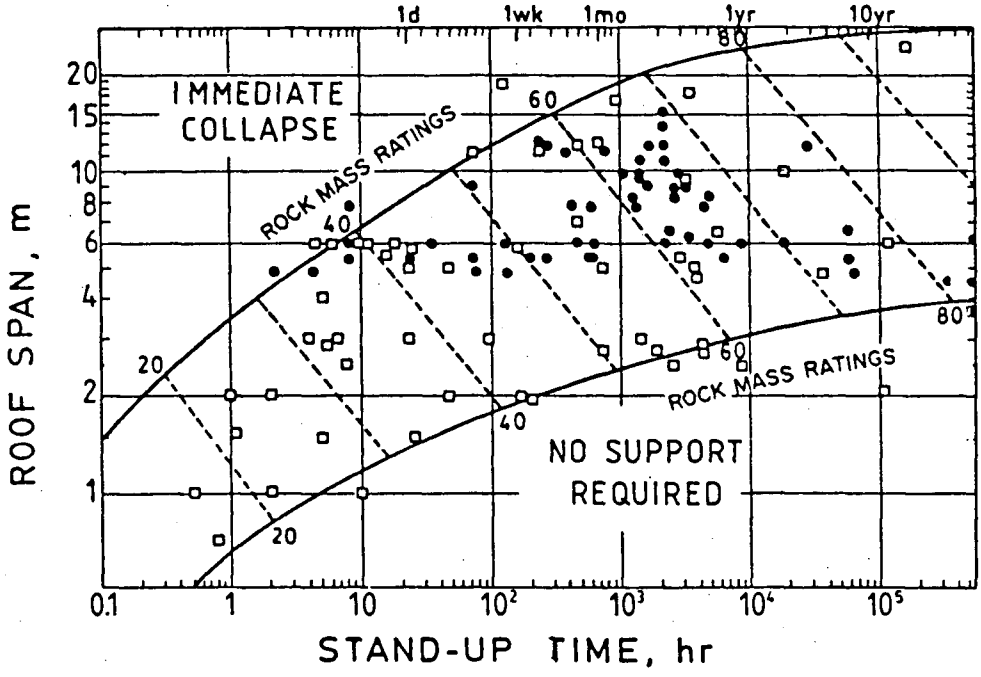

FIGURE 24

GEOMECHANICS CLASSIFICATIONS - Output for mining and tunnelling. Black dots represent mining cases; squares are tunnelling cases. The contour lines are limits of applicability (Bieniawski - 1983)

The above figure gives a relationship between the stand-up time and the roof span for various mass ratings. Span is defined as the distance between the drift walls or distance from the support to the face if this is less than tunnel width.

Example: 1) **Roof strata rating of RMR = 35** means the maximum unsupported span possible in this rock is 5.2 m, however, it will stand unsupportd only for four hours and will subsequently collapse (Figure 24). In order to ensure long term stability, support along the length of the tunnel should be placed. A roof span of 1.5 m and an RMR = 35% will stand indefinitely. 2). A tunnel

required to be 10 m wide and which has an RMR = 50%: It will stay open for six days unsupported; by placing support, (Table 16), at less than 3 m intervals it will remain stable indefinitely. Note that the active span is the distance from the support to the face since it is less than the tunnel width.

Permanent support recommendations are given in Table 16.

TABLE 16 RMR GUIDE FOR EXCAVATION AND SUPPORT IN ROCK TUNNELS (BIENIAWSKI, 1984)

Rock mass class	Excavation	Support		
		Rockbolts (20 mm dia., fully bonded)	Shotcrete	Steel sets
1. Very good rock RMR: 81–100	Full face: 3 m advance	Generally no support required except for occasional spot bolting		
2. Good rock RMR: 61–80	Full face: 1.0–1.5 m advance; Complete support 20 m from face	Locally bolts in crown 3 m long, spaced 2.5 m with occasional wire mesh	50 mm in crown where required	None
3. Fair rock RMR: 41–60	Top heading and bench: 1.5–3 m advance in top heading; Commence support after each blast; Complete support 10 m from face	Systematic bolts 4 m long, spaced 1.5 m–2 m in crown and walls with wire mesh in crown	50–100 mm in crown and 30 mm in sides	None
4. Poor rock RMR: 21–40	Top heading and bench: 1.0–1.5 m advance in top heading; Install support concurrently with excavation–10 m from face	Systematic bolts 4–5 m long, spaced 1–1.5 m in crown and walls with wire mesh	100–150 mm in crown and 100 mm in sides	Light ribs spaced 1.5 m where required
5. Very poor rock RMR: < 20	Multiple drifts: 0.5–1.5 m advance in top heading; Install support concurrently with excavation; shotcrete as soon as possible after blasting	Systematic bolts 5–6 m long, spaced 1–1.5 m in crown and walls with wire mesh. Bolt invert	150–200 mm in crown 150 mm in sides and 50 mm on face	Medium to heavy ribs spaced 0.75 m with steel lagging and forepoling if required. Close invert

3.3.2.2. ROCK LOAD

Unal from Pennsylvania State (Bieniawski, 1984) had correlated support load to the RMR index. The rock load height is given by:

$$ht = \frac{100\text{-}RMR}{100} B$$

Where: ht = rock load height (m)

RMR = rock mass rating

B = tunnel width (m)

The above relationship is presented in Figure 25

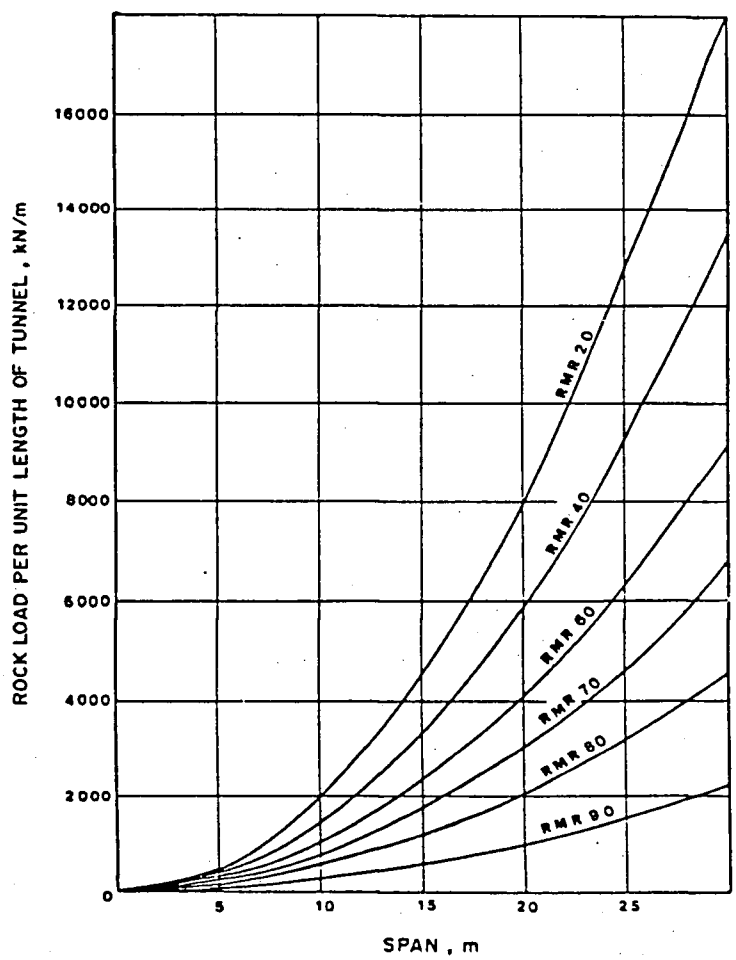

FIGURE 25

VARIATIONS OF ROCK LOAD WITH ROOF SPAN FOR DIFFERENT RMR VALUES (BIENIAWSKI, 1984)

3.3.2.3 MODULUS OF DEFORMATION

The Geomechanics Classification was found to be a useful method of estimating the in-situ deformability of rock masses (Bieniawski, 1978). This is demonstrated by Figure 26, whereby the following correlation was obtained:

$$E_M = 2 \times RMR - 100 \quad \text{(Correlation coefficient = 0.96)}$$

where E_M is the in situ modulus of deformation in GPa.

The above correlation was derived on the basis of 22 case histories involving a wide range of in situ tests conducted in various parts of the world. The accuracy of the modulus prediction by the **Geomechanics Classification** is within 20% (Bieniawski, 1978) which is quite acceptable for rock engineering purposes.

Serafim and Pereira (Bieniawski, 1984) extended the above relationship between E_M and RMR to cover lower values of E_M by adopting a log-linear form:

$$E_M = 10^{(RMR - 10)/40}$$

This was shown to give an improved fit to the lower values of modulus in the range 1 - 10 GPa (Figure 26)

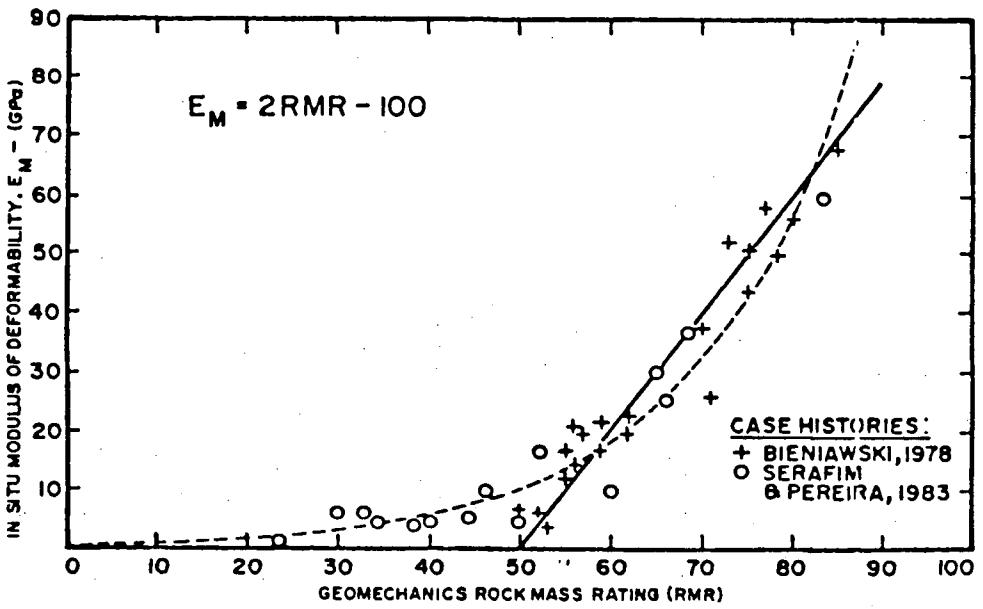

FIGURE 26

CORRELATION BETWEEN THE IN SITU MODULUS OF DEFORMATION AND RMR. (BIENIAWSKI, 1984)

3.3.2.4. ROCK MASS STRENGTH

Serafim and Pereira (1983) utilized Bieniawski's (1979) RMR system to estimate the rock mass cohesive and frictional properties. This was determined through relating the intact strength properties to the mass properties by adjusting for joint condition and ground water. The roughest unweathered joints under dry conditions were assessed a mass friction angle (ϕ) of 45°. Flowing water caused an effective reduction of 8° on - and values for gouge-filled discontinuities were put as low as 10°. The following summarizes the relationship between the shear strength parameters and RMR:

Class No	I	II	III
Average stand-up time	10 years for 15 m span	6 months for 8 m span	1 week for 5 m span
Cohesion of the rock mass	> 400 kPa	300 - 400 kPa	200 - 300 kPa
Friction angle of the rock mass	< 45°	35° - 45°	25° - 35°

Class No	IV	V
Average stand-up time	10 hours for 2.5 m span	30 minutes for 1 m span
Cohesion of the rock mass	100 - 200 kPa	< 100 kPa
Friction angle of the rock mass	15° - 25°	< 15°

3.3.3. LIMITATIONS

- The Geomechanics Classification is a means of identifying the engineering parameters needed to design safe and efficient mine openings.

- RMR is relatively simple to use and repeatable

- The Geomechanics Classification does not account for the virgin stresses which can have an influence on the condition of discontinuities by maintaining them under compression or tensions. (Mathews, 1981)

- The Classification scheme as proposed by Bieniawski is arranged with succesive reductions of roughness as weathering or gouge filling increases. These two processes are not necessarily related. (Barton, 1983)

- The strength of the joints in the ground mass is one of the most important parameters contributing to the stability of a tunnel. In the geomechanics system, this parameter is almost ignored in that the total rating is relatively insensitive to the joint condition. A difference of 15 points in the joint condition rating out of a total of 25 should represent a major difference in the stability of the tunnel. However, the joint condition rating can change by as much as 15 points without changing the overall rock mass class. The insensitivity is partly due to the summation principle on which the system is based. (Kirsten, 1983)

  Bieniawski over-emphaizes joint spacing by employing both an RQD and a joint spacing rating. Rock quality and joint spacing together comprise a measure of block size. By making allowance for these parameters, an unjustified importance is assigned to block size compared to, for example, joint strength. This is the case particularly in view of the fact that together, rock quality and joint spacing represent ratings between two and three times larger than that of any one of the other parameters over most of their respective ranges. (Kirsten, 1983)

- The RMR was based initially on Lauffer (1958) which is generally acknowledged to be excessively conservative. In best qualities of a rock mass, it is extremely conservative in terms of stand-up time.

- The RMR system cannot be employed in the design of structures in rocks containing swelling materials, i.e. shales (Kirsten, 1983)